



HAL
open science

Chemical modification of fluorinated electroactive polymers

Konstantinos Kallitsis

► **To cite this version:**

Konstantinos Kallitsis. Chemical modification of fluorinated electroactive polymers. Polymers. Université de Bordeaux, 2019. English. NNT : 2019BORD0094 . tel-03266621

HAL Id: tel-03266621

<https://theses.hal.science/tel-03266621>

Submitted on 22 Jun 2021

HAL is a multi-disciplinary open access archive for the deposit and dissemination of scientific research documents, whether they are published or not. The documents may come from teaching and research institutions in France or abroad, or from public or private research centers.

L'archive ouverte pluridisciplinaire **HAL**, est destinée au dépôt et à la diffusion de documents scientifiques de niveau recherche, publiés ou non, émanant des établissements d'enseignement et de recherche français ou étrangers, des laboratoires publics ou privés.

THÈSE PRÉSENTÉE
POUR OBTENIR LE GRADE DE
DOCTEUR DE
L'UNIVERSITÉ DE BORDEAUX

École Doctorale des Sciences Chimiques

Spécialité : Polymères

par

Konstantinos Kallitsis

CHEMICAL MODIFICATION
OF FLUORINATED ELECTROACTIVE POLYMERS

Sous la direction de: Prof. Georges HADZIIOANNOU

et la codirection de: Dr. Cyril BROCHON

Soutenue le 21 Juin 2019

Membres du jury:

M. TATON Daniel , Professeur, Université de Bordeaux	Président
M. GEOGHEGAN Mark , Professeur, University of Sheffield	Rapporteur
M. LADMIRAL Vincent , Chargé de Recherche, ENSCM	Rapporteur
M. DOMINGUES DOS SANTOS Fabrice , CEO, Piezotech/Arkema Group	Examineur
Mme STINGELIN Natalie , Professeur, Georgia Institute of Technology	Examineur
M. VINCENT Jean-Marc , Directeur de Recherche, ISM - CNRS	Examineur
M. BROCHON Cyril , Maître de Conférences, Université de Bordeaux	Co-directeur de Thèse
M. HADZIIOANNOU Georges , Professeur, Université de Bordeaux	Directeur de Thèse
M. CLOUTET Eric , Directeur de Recherche, LCPO - CNRS	Invité

Chemical Modification of Fluorinated Electroactive Polymers

Abstract

Organic electronics are a low cost alternative to silicon based electronics that enable the fabrication of flexible devices, broadening the scope of electronics beyond the limitations imposed by silicon. For organic electronics to find wider real world applications, three classes of materials have to be optimized. Those classes are conductors, semiconductors and insulators, which are the three building blocks for any electronic device. While organic conductors and semiconductors have attracted significant attention during the past 40 years, research in high dielectric constant and thus high performance insulators is lagging far behind.

The class of organic insulating materials with the highest dielectric constant are the Fluorinated Electroactive Polymers (FEPs). FEPs can be categorized in two different groups with vastly different electronic properties. Those groups are the ferroelectrics and the relaxor-ferroelectrics. The ferroelectric polymers, with main representative the copolymer P(VDF-TrFE) find application in electronic devices such as sensors, actuators, non volatile memories and energy generators. On the other hand, relaxor-ferroelectric polymers, with main representative the P(VDF-TrFE-CTFE) terpolymer are high performance insulating materials and find application in electronics as dielectric layers, in devices such as capacitors, organic field effect transistors, flexible displays and electrocaloric cooling devices amongst others.

Although the polymers mentioned above are compatible with a large variety of printing techniques, their limited compatibility with photolithography, which is the method of choice for large throughput electronics production limits their potential of realization. One of the main aims of this thesis was to alter the chemistry of such polymers, in a way that would make them directly compatible with photolithography, while maintaining their desirable electronic properties. To do so, a method allowing the introduction of additional functional groups on FEPs had to be developed. However, due to the excellent chemical stability of fluorinated polymers, developing such a method was a challenging task. The methods developed, use nucleophilic

substitution to attach different functional groups on commercially available FEPs by leveraging the existence of groups prone to substitution on the polymer backbone, bypassing the innate chemical stability of such polymers.

First, azido groups, known to cross-link upon irradiation with UV light were attached on relaxor ferroelectric P(VDF-TrFE-CTFE) terpolymers. The terpolymers bearing azido groups were directly used as negative photoresists in conventional photolithography process while maintaining a very high dielectric constant.

Second, due to safety and stability issues, a more general approach was followed, consisting in grafting type II photoinitiators (based on aryl ketones) on the relaxor-ferroelectric P(VDF-TrFE-CTFE) and the ferroelectric P(VDF-TrFE) polymers. In those cases exceptionally stable polymers were obtained, with in some cases improved electroactive properties as compared to the pristine materials.

These chemistries led us to an extraordinary case study, where FEPs bearing unsaturation were showing remarkable enhancement in electroactive properties. This very simple method of functionalizing FEPS paves the way to many more advances in the field.

Keywords

Electroactive, High-k, Ferroelectric, Photolithography

Modification Chimique de Polymères Electroactifs Fluorés

Résumé

L'électronique organique est une alternative peu coûteuse à l'électronique classique (à base de silicium) qui permet la fabrication de dispositifs flexibles, élargissant le champ d'application de l'électronique au-delà des limites imposées par le silicium. Pour que l'électronique organique trouve des applications plus larges dans le monde réel, trois classes de matériaux doivent être optimisées. Il s'agit des conducteurs, des semi-conducteurs et des diélectriques, qui constituent les trois éléments de tout appareil électronique. Alors que les conducteurs et les semi-conducteurs organiques ont attiré une attention particulière au cours des 40 dernières années, la recherche sur des isolants à constante diélectrique élevée et donc de haute performance est en retard.

La famille de matériaux isolants organiques ayant la constante diélectrique la plus élevée sont les polymères électroactifs fluorés (FEPS). Les FEPS peuvent être classés en deux groupes différents avec des propriétés électroniques très différentes. Ces groupes sont les ferroélectriques et les ferroélectriques relaxeurs. Les polymères ferroélectriques, dont le plus connu est le copolymère P(VDF-TrFE), trouvent des applications dans des dispositifs électroniques tels que les capteurs, les actionneurs, les mémoires non volatiles et les générateurs d'énergie. D'autre part, les polymères relaxeurs-ferroélectriques, dont le système le plus connu est le terpolymère P(VDF-TrFE-CTFE), sont des matériaux isolants à haute performance et trouvent, entre autres, une application dans l'électronique comme couches diélectriques, dans des dispositifs tels que les condensateurs, les transistors organiques à effet de champ, les écrans souples et dans des dispositifs de refroidissement électrocaloriques.

Bien que les polymères mentionnés ci-dessus soient compatibles avec une grande variété de techniques d'impression, leur compatibilité limitée avec la photolithographie, qui est la méthode de choix pour la production d'électronique à grande échelle, limite leur potentiel de réalisation. L'un des principaux objectifs de

cette thèse était de modifier la chimie de ces polymères, de manière à les rendre directement compatibles avec la photolithographie, tout en maintenant leurs propriétés électroniques. Pour ce faire, il a fallu mettre au point une méthode permettant d'introduire des groupes fonctionnels supplémentaires sur les FEP. Cependant, en raison de l'excellente stabilité chimique des polymères fluorés, la mise au point d'un tel procédé était une tâche ardue. Pour contourner cette difficulté, l'idée est d'exploiter l'existence de groupes susceptibles de réagir lors d'une substitution nucléophile sur le squelette du polymère, tout en utilisant des FEPS disponibles dans le commerce.

Tout d'abord, des fonctions azotures, connues pour réticuler lors d'une irradiation UV, ont été fixés sur des terpolymères de relaxeur ferroélectrique P(VDF-TrFE-CTFE). Les terpolymères portant ces fonctions ont pu être directement utilisés comme résine photosensible négative dans les procédés de photolithographie classiques et ont conservé une constante diélectrique très élevée. Dans un second temps, pour des raisons de sécurité et de stabilité, une approche plus générale a été développée. Cette approche consiste à greffer des photo-amorceurs de type II (basés sur des arylcétones) sur le relaxeur-ferroélectrique P(VDF-TrFE-CTFE) et le ferroélectrique P(VDF-TrFE). Des polymères exceptionnellement stables ont été obtenus, avec dans certains cas, des propriétés électro-actives bien meilleures que celles des matériaux purs. Ces modifications chimiques nous ont conduits à une étude de cas particulière où des FEP comportant des doubles liaisons (réaction secondaire de la modification chimique) ont montrés une amélioration remarquable des propriétés électro-actives. Cette méthode très simple de fonctionnalisation de FEPS ouvre la voie à de nombreuses avancées dans le domaine.

Mots clés

Electroactif, High-k, Ferroélectrique, Photolithographie

Unité de recherche

Laboratoire de Chimie des Polymères Organiques (LCPO) - UMR5629 Group

4 : "Polymer Electronic Materials and Devices"

16 Avenue Pey-Berland

33607 Pessac Cedex France

List of abbreviations

AFM	Atomic Force Microscope/Microscopy
AQ	Anthraquinone
ATR	Attenuated Total Reflection
ATRP	Atom Transfer Radical Polymerization
BP	Benzophenone
BTFE	Bromotrifluoroethylene
CFE	1-Chloro-1-fluoroethylene
CL	Cross-linked
CTFE	Chlorotrifluoroethylene
D	Displacement
DB	Double Bonds
DHL	Double Hysteresis Loop
DMF	Dimethylformamide
DSC	Differential Scanning Calorimetry
E	Electric field
E2	Bimolecular elimination reaction
Ec	Coercive electric field
eq	Equivalents
FE	Ferroelectric
FEPs	Fluorinated Electroactive Polymers
FT-IR	Fourier-transform infrared spectroscopy
HFP	Hexafluoropropylene
I	Current
K	Dielectric constant
NMR	Nuclear magnetic resonance
OFET	Organic field-effect transistor
P Polarization	Polarization

P(VDF-TrFE)	Poly(vinylidene fluoride-trifluoroethylene)
P(VDF-TrFE-CFE)	Poly(vinylidene fluoride-trifluoroethylene-chlorofluoroethylene)
P(VDF-TrFE-CTFE)	Poly(vinylidene fluoride-trifluoroethylene-chlorotrifluoroethylene)
PE	Paraelectric
PI	Photo initiator
Ppm	Parts per million
Pr	Remnant Polarisation
Psat	Saturation Polarisation
PVDF	Poly(vinylidene fluoride)
RFE	Relaxor ferroelectric
RI	Refractive index
RMS	Root mean squared (roughness)
RT	Room temperature
SAXS	Small Angle X-ray Scattering
SEC	Size-exclusion chromatography
SHL	Single Hysteresis loop
SN2	Substitution nucleophilic (bi-molecular)
T	Temperature
TC	Curie transition temperature
TGA	Thermal gravimetric analysis
TrFE	Trifluoroethylene
UV	Ultraviolet
VDF	Vinylidene fluoride
WAXS	Wide Angle X-ray Scattering
α	Alpha phase
β	Beta phase
γ	Gamma phase
δ	Delta phase

ΔH	Enthalpy
ϵ	Dielectric permittivity
ϵ_0	Vacuum permittivity
ϵ_r	Relative permittivity
ϵ_r'	Real part of the relative permittivity
ϵ_r''	Immaginary part of the relative permittivity

Table of Contents

Chapter 1: Introduction.....	3
1.1) General introduction	3
1.2) State of the Art.....	3
1.2.1) Fluorinated Electroactive Polymers	3
1.2.2) The Basic Physics of Dielectric materials.....	8
1.2.3) Chemical modification of FEPs	11
1.2.4) Cross-linking of Fluorinated polymers	16
1.2) Scope of this Thesis	35
1.3) References	39
Chapter 2: Photopatternable fluoropolymers with pendent azido groups.....	45
2.1) Introduction.....	45
2.2) Results and Discussion	45
2.2.1) Chemical grafting of azido groups on FEPs.....	45
2.2.2) Effect of the grafting on the crystallinity	50
2.2.3) Photochemical cross-linking of FEPs with pendent Azido groups	53
2.2.4) Photolithographic patterning of FEPs with pendent Azido groups.....	55
2.2.5) Blank tests on PCTFE and P(VDF-TrFE)	63
2.2.6) Surface tension characterization	64
2.3) Experimental Part	65
2.4) Conclusions.....	66
2.5) References	67
Chapter 3: Chemical modification of Fluoropolymers via Williamson Ether Synthesis...	71
3.1) Introduction.....	71
3.2) Results and Discussion	72
3.2.1) Chemical modification of P(VDF-TrFE-CTFE) (61.7/28.3/10) terpolymers ..	72
3.2.1.1) P(VDF-TrFE-CTFE) terpolymers functionalized with benzophenone groups	72
3.2.2) Chemical modification of P(VDF-TrFE-CFE) terpolymers with anthraquinone groups	102
3.2.3) Chemical modification of P(VDF-TrFE) copolymers.....	107
3.2.3.2) P(VDF-TrFE) copolymers functionalized with anthraquinone groups ..	114
3.3) Experimental Part	118
3.3.1) Chemical modification of Fluoropolymers	118
3.3.2) Preparation of patterned thin films via photolithography.....	120
3.4) Conclusions.....	121

3.5) References	122
Chapter 4: Unsaturation containing Fluoropolymers	125
4.1) Introduction.....	125
4.2) Results and Discussion	126
4.2.1) P(VDF-TrFE-CTFE) terpolymers containing unsaturation.....	126
4.2.2) P(VDF-TrFE-CFE) terpolymers containing unsaturation.....	142
4.2.3) P(VDF-TrFE) copolymers containing unsaturation	150
4.3) Experimental part	155
4.4) Conclusions.....	156
4.5) References	156
Chapter 5: Electronic Properties and Devices.....	159
5.1) Introduction.....	159
5.2) Results and discussion.....	159
5.2.1) Electronic properties of P(VDF-TrFE-CTFE) terpolymers with pendent Azido groups.....	159
5.2.2) Electronic properties of P(VDF-TrFE-CTFE) terpolymers with pendent benzophenone groups.....	163
5.2.3) Electronic properties of P(VDF-TrFE-CTFE) terpolymers with pendent anthraquinone groups.....	167
5.2.4) Electronic properties of P(VDF-TrFE-CFE) terpolymers with pendent anthraquinone groups.....	172
5.2.5) Electronic properties of P(VDF-TrFE) copolymers with pendent benzophenone groups.	174
5.2.6) Electronic properties of P(VDF-TrFE) copolymers with pendent anthraquinone groups.....	178
5.2.7) Electronic properties of P(VDF-TrFE-CTFE) terpolymers with intrachain double bonds.....	181
5.2.8) Electronic properties of P(VDF-TrFE) copolymers with intrachain double bonds	186
5.3) Experimental part	187
5.4) Conclusions.....	187
5.4)References	188
Chapter 6: Conclusions and Perspectives.....	191
6.1) Conclusions.....	191
6.2) Perspectives.....	192

Chapter 1

Introduction

Chapter 1: Introduction

1.1) General introduction

The motivation behind this work was the introduction of additional functionality and more specifically, photopatternability on high dielectric constant fluorinated electroactive polymers (FEPs). Those polymers find very wide application on electronic devices¹⁻², due to their exceptional dielectric and/or ferroelectric properties. However, the potential of such materials is limited by their non compatibility with photolithographic patterning, which is the method of choice for high throughput electronics production. Another factor limiting the potential of such materials is the lack of a reliable versatile method for the tuning of their electroactive properties, as different kinds of application require vastly different properties. Therefore, the objective of this work was to make fluorinated electroactive polymers compatible with conventional photolithographic patterning protocols, as well as to provide a general methodology for the tuning the electroactive response of such polymers in order to better tackle certain applications.

1.2) State of the Art

1.2.1) Fluorinated Electroactive Polymers

Fluorinated electroactive polymers (FEPs) are maybe the most prominent class of insulating materials, with their properties varying from ferroelectric to relaxor-ferroelectric with exceptional dielectric properties. That variety in terms of electroactive properties allows for a very broad range of application in electronics. Those applications include memories³⁻⁴ sensors², actuators⁵ and energy generators for ferroelectric polymers to capacitors, organic field effect transistors⁶ (OFETs), haptics, flexible displays and electrocaloric cooling devices⁷ for relaxor-ferroelectrics. The dominant polymer in the group of electroactive polymers is polyvinylidene fluoride (PVDF) and its copolymers. The copolymers of vinylidene fluoride with trifluoroethylene (PVDF-TrFE) exhibit exceptional ferroelectric properties and is thus ideal for the corresponding applications. The exceptional ferroelectric properties of those polymers derive from the addition of the trifluoroethylene (TrFE) group, which

forces the polymer to crystallize in the most ferroelectric orientation (all-trans)⁸. On the other hand, when a third comonomer, such as chlorotrifluoro ethylene (CTFE) or 1-chloro-1-fluoroethylene (CFE) is incorporated in the polymer, the electroactive response becomes that of a relaxor-ferroelectric and that due to the introduction of kinks (Gauche type linkages) in the otherwise all-trans orientation of the polymer. That introduction of kinks limits the size of the ferroelectric domains, leading to the relaxor-ferroelectric response and increased dielectric properties in the near room temperature regime.

More specifically, FEPs bear permanent electric dipoles along their polymer chains, due to the difference in electronegativity of the carbon and fluorine atoms. Since those polymers are semi crystalline in nature, the electric dipoles can organize in clusters in the polymer matrix. Depending on the way those dipoles organize in the polymer matrix, those polymers can be categorized in three different groups with vastly different electrical properties.

A) If the dipoles don't organize in any particular way in the polymer matrix, the polymer is called paraelectric. Once an external electric field is applied to a paraelectric polymer, the dipoles will align with the direction of the field and the polymer becomes polarized. When though, the external electric field is removed, the dipoles quickly relax back to random orientation, leaving zero polarization, namely zero remnant polarization see **Figure 1-1**.

B) The second case is one that the dipoles do organize in the crystalline matrix of the polymer in relatively small domains of different sizes. In this case the polymers are called relaxor-ferroelectrics and when an external electric field is applied in such polymer, the dipoles align in the direction of the field, polarizing the sample similarly to the previous case. In contrast to the paraelectric polymers though, once the external electric field is removed in the case of relaxor ferroelectric polymers, the dipoles do not relax back to random positions independently but in clusters with dipoles organized in bigger domains exhibiting more resistance to moving. Thus, the dipoles in bigger domains relax slower while dipoles in smaller domains relax much quicker, leading to the formation of a slim hysteresis loop. This phenomenon leads to the presence of some dipoles aligned with the direction of the field even once this field is removed and is characteristic of relaxor-ferroelectrics (**Figure 1-1**). Relaxorferroelectric polymers are generally insulating materials with high dielectric constant and thus find application as

dielectric layers in electronic devices such as capacitors and organic field effect transistors (OFETs) amongst others.

C) The last case is one that the dipoles organize in the polymer matrix in large domains. In this case, the polymers are called ferroelectrics and their characteristic is that the crystalline domains are so big, that even once the electric field is removed, the dipole domains remain largely unaffected, giving rise to large polarization even at zero electric field, namely large remnant polarization (**Figure 1-1**). Due to this property of ferroelectric polymers to remain polarized even in the absence of electric field, they eventually find application in non-volatile memories, sensors and actuators amongst others⁹.

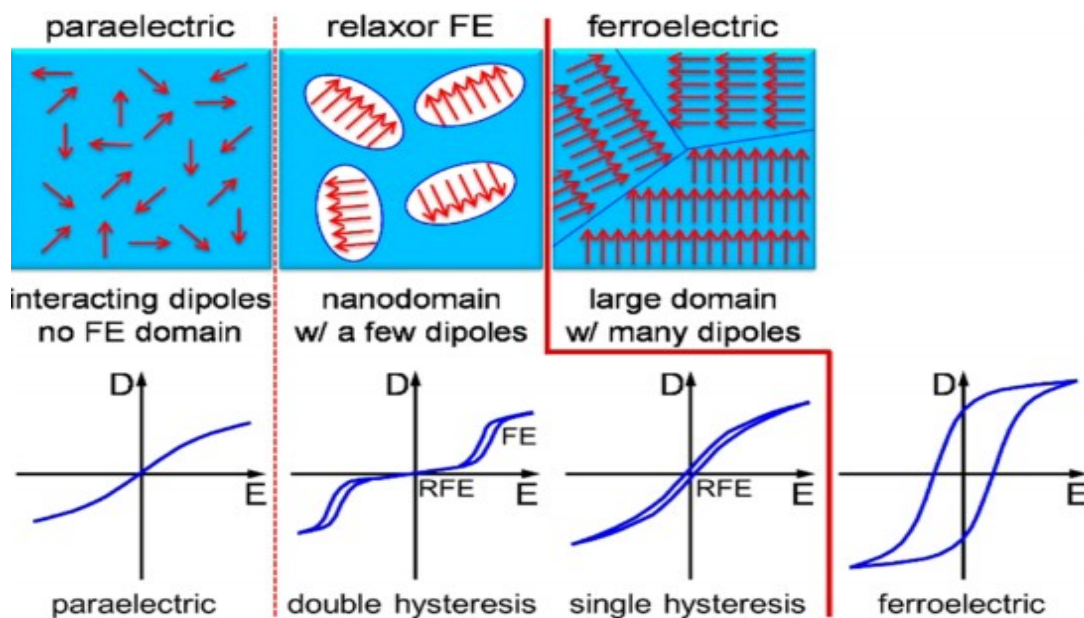


Figure 1-1. Different dipole and FE domain structures with increasing dipole-dipole or domain-domain interactions from left to right (top) and corresponding electroactive responses in D - E loops (bottom)¹⁰.

Electroactivity in FEPs was first demonstrated in 1969 with the discovery of piezoelectricity in PVDF¹¹, initiating the research on the electrical properties of such materials. Later ferroelectric properties of stretched PVDF homopolymer were demonstrated¹². However, all the interesting electrical properties reported on PVDF homopolymers, required that the polymer films were stretched¹³, and that because PVDF can crystallize in different phases of which only two, namely the β and δ phases exhibit ferroelectric properties¹⁴.

Most of the interesting electric properties of PVDF and its copolymers arise from the presence of permanent dipoles in the polymer matrix. Dipoles are generated due to the difference in electronegativity of the carbon and the fluorine groups, which yields a dipole moment of 1.9 D⁸. This dissymmetric structure creates strong dipoles perpendicularly aligned to the long axis of the chains. The alignment of those permanent dipoles to mechanical, thermal, and electrical stimulations gives rise to the electroactivity. The way through that those dipoles organize in the crystalline phase of the polymer can give rise to vastly different dipole moments across different conformations. The most polar conformation is the all-trans conformation and has a dipole moment of 2.1 D. The two other possibilities are the tg+tg- and ttg+ttg- conformations, shown in **Figure 1-2** with their dipole moments varying from 1.0 D to 1.2 D. More specifically, PVDF crystallize in five different polymorphs¹, namely the α , β , γ , δ and ϵ phase. Although the α phase is the most thermodynamically stable and spontaneously formed when PVDF homopolymer crystallizes from the melt, the β phase is the most polar one, due to the all-trans conformation shown in **Figure 1-2**. This very interesting phase is difficult to be formed in PVDF homopolymers and in order to enable its formation stretching and poling of the film are necessary. The polar γ phase with a ttg+ttg- conformation¹⁵ (**Figure 1-2**) can be accessed through annealing at high temperature and pressure. Similarly the δ phase can derive from the α through high electric field poling^{14, 16}.

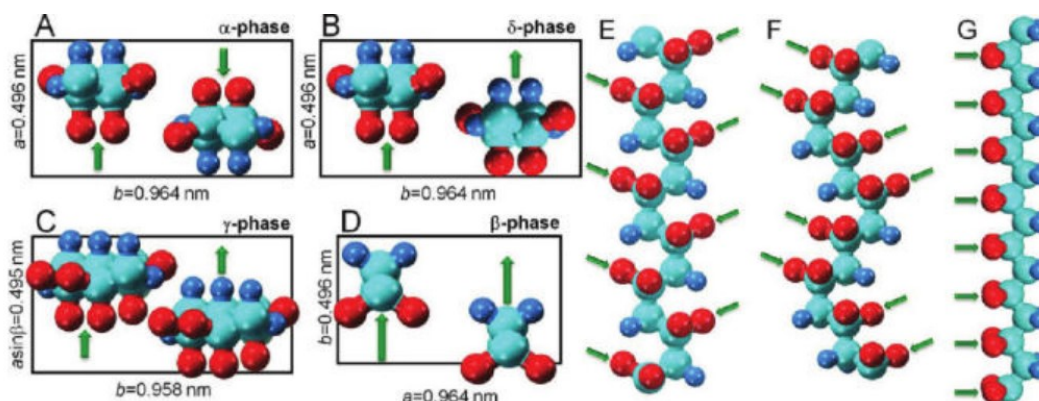


Figure 1-2. Unit cells of (A) α , (B) δ , (C) γ , and (D) β forms of PVDF crystals viewed along the c -axes and schematic chain conformations for (E) TG TG' (α/δ), (F) TTTG TTTG' (γ), and (G) all-trans (β) rotational sequences. Red, cyan, and blue spheres represent F, C, and H atoms. The projections of dipole directions are indicated by green arrows¹⁷.

However in the early 80s it was discovered that copolymers of vinylidene fluoride (VDF) with trifluoroethylene (TrFE), at certain monomer ratios exhibit strong

piezoelectric¹⁸ and ferroelectric¹⁹ properties without the need for stretching the films. Further evidence for the ferroelectric behavior of those copolymers was the presence of a curie transition point²⁰. It was later discovered that PVDF and its copolymers can behave as relaxor ferroelectrics, with slimmer hysteresis loops and enhanced dielectric constant closer to room temperature. Those properties were first demonstrated in electron beam irradiated P(VDF-TrFE) copolymer²¹, by introducing trans-gauche defects to the all-trans conformation and thus reducing the domain size to the nanometer scale. The large lattice strain and dimensional change of such polymers makes them excellent candidates for electromechanical applications. However, irradiation of the copolymers leads to a decrease in the overall crystallinity of the polymer due to the cross-linking side reactions, while the polymer becomes insoluble and thus not processable after irradiation. In 2001 a novel way to achieving the desired relaxor ferroelectric properties was discovered, by introducing a third monomer in the polymerization of VDF and TrFE, the bulkier chloro trifluoro ethylene (CTFE)²²⁻²³. The resulting terpolymers were solution processable materials and showed improved polarization in comparison to the e-beam irradiated copolymer.

Another, more subtle difference arose, when comparing the electroactive response of the e-beam irradiated P(VDF-TrFE), P(VDF-TrFE-CTFE) and P(VDF-TrFE-CTFE). Both e-beam irradiated and P(VDF-TrFE-CTFE) or P(VDF-TrFE-CTFE) exhibit relaxor ferroelectric properties (**Figure 1-3**).

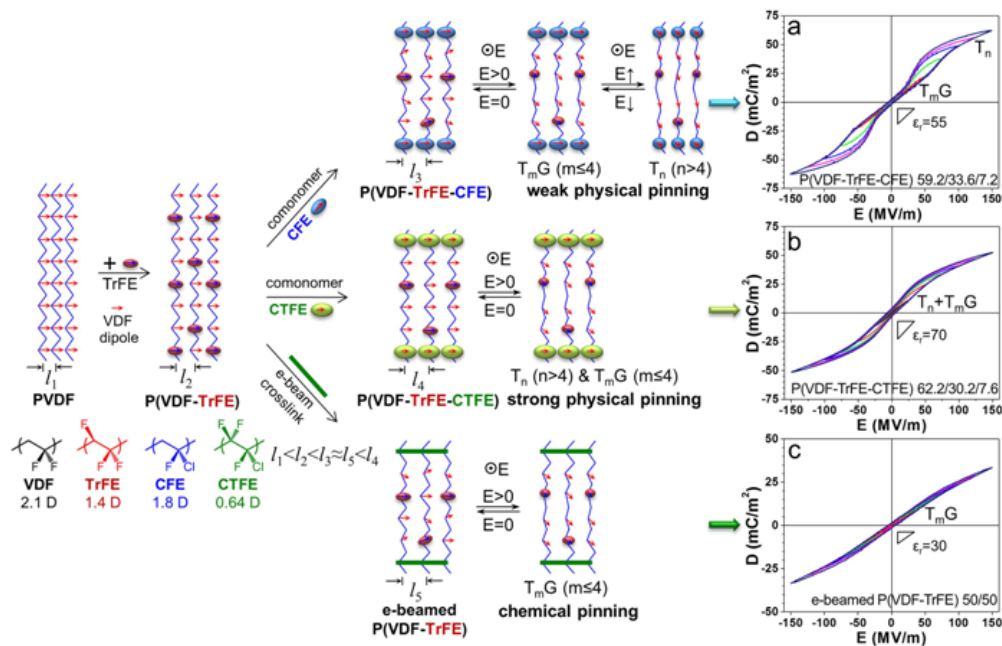


Figure 1-3. Schematic representation of the different types of pinning effect in different cases of PVDF based polymers. From weak physical pinning and DHL behavior to chemical pinning and SHL behavior^{10, 24}.

However, in the case of electron irradiated fluoropolymers, the chemical cross-links act as permanent pinning spots, reducing the crystalline domain size to the nanoscale, leading to slim Single Hysteresis Loop (SHL) behavior (**Figure 1-3**). On the other hand bulky comonomers such as CTFE or CFE act as physical pinning spots, reducing the crystalline domain size as well, but since they are polar groups themselves, they can be polarized under certain electric bias, leading to a field induced relaxor-ferroelectric to ferroelectric transition. However, the CFE and CTFE groups are different, both in terms of size (with the CFE being smaller than CTFE) but also in terms of dipole moment, which is 1.8D for the CFE and 0.64D for the CTFE. That makes the CFE groups more prone to polarization, when the electric field is high enough, leading to the field induced RFE→FE transition and the observed Double Hysteresis Loop (DHL) behavior for the P(VDF-TrFE-CTFE) terpolymers, as shown in **Figure 1-3**. On the other hand the CTFE group, is bigger and less polar than the CFE, which makes its rotation harder and thus the field induced RFE→FE transition much more subtle (**Figure 1-3**).

1.2.2) The Basic Physics of Dielectric materials

At this point, it's worth mentioning the basic principles that govern the behavior of dielectric materials. When an insulating material is placed under an electric field, it gets polarized due to the interaction of its components with the field. Polarization can be caused by one or more of five causes¹⁰:

I) Electronic polarization: This type of polarization derives from the deformation of the electron cloud caused by the electric field.

II) Orientational polarization: Orientational or dipolar polarization is caused by changes in the orientation of electric dipoles caused by the electric field.

III) Vibrational: Vibrational or atomic polarization is caused by changes in the vibrational behavior of atoms caused by the electric field.

IV) Ionic: this kind of polarization is caused by movement of atoms under the applied electric field.

V) Interfacial polarization: This kind of polarization is caused by the accumulation of charges in the interfaces of dielectric materials.

Each kind of polarization though, is associated with dielectric loss at a different frequency range¹⁰ as shown in **Figure 1-4**.

Those types of polarization can be divided in two separate regimes, which occur in

different frequencies. Those regimes are the resonance and relaxation regimes as shown in **Figure 1-4**.

- i. Resonance regime: For polymers the resonance regime includes the electronic and vibrational polarizations which occur at the high frequency range ($>10^{10}$ Hz).
- ii. Relaxation regime: This regime includes the three other kinds of polarization, namely: orientational, ionic and interfacial polarization.

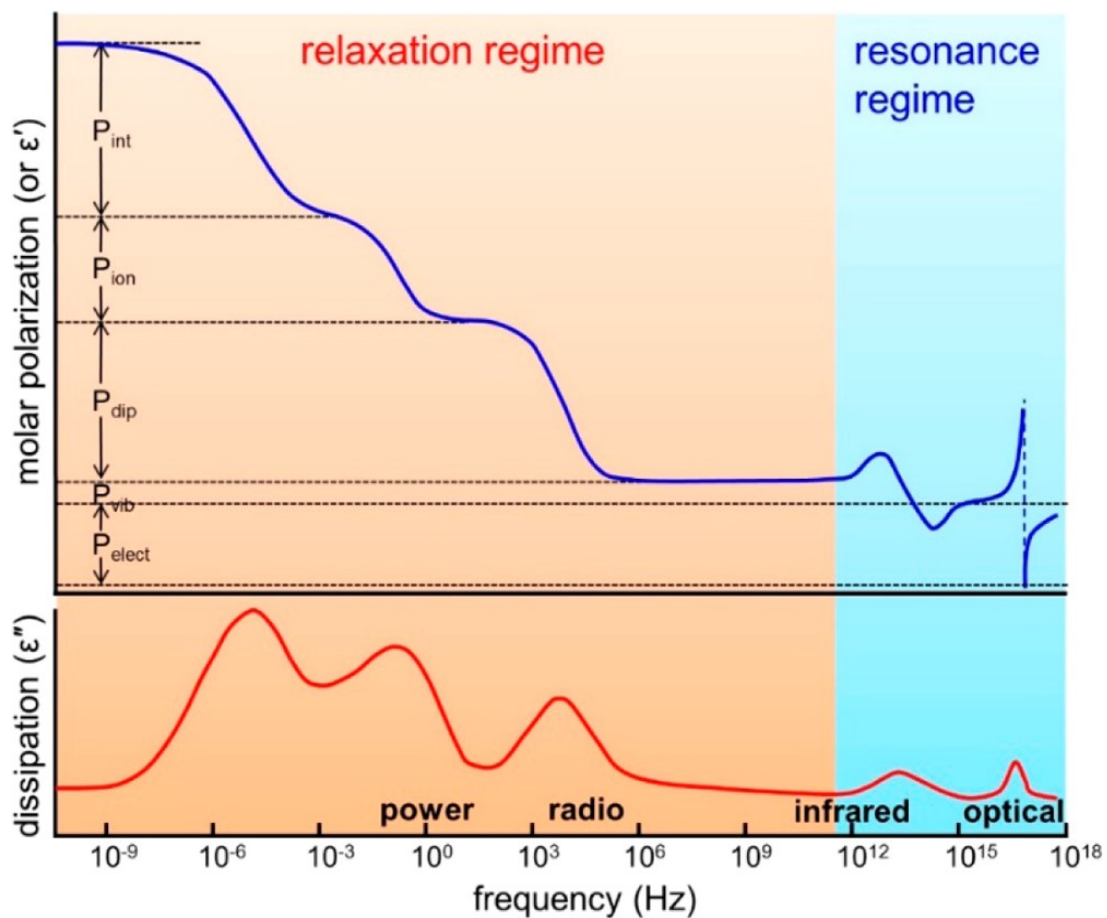


Figure 1-4. Different types of polarization as a function of frequency, where P_{elect} stands for electronic polarization, P_{vib} stands for vibrational (or atomic) polarization, P_{dip} for orientational (or dipolar) polarization, P_{ion} for ionic and P_{int} for interfacial polarization. The top panel shows the real part of permittivity or (or molar polarization) (ϵ'_r), and the bottom panel shows the imaginary part of permittivity (or dissipation factor) (ϵ''_r)¹⁰.

In order to better understand the physics of such phenomena, let's assume a dielectric material, under an external electric field. Then the displacement (D), which is expressed in ($C\ m^{-2}$) and is the field induced separation of electric charges (nuclei and electrons), can be expressed as:

$$D = \epsilon_0 E + P \quad (1)$$

Where ϵ_0 is the vacuum permittivity (or permittivity of free space) and P is the density of the permanent and induced electric dipole moments, called simply polarization P and is expressed in Cm^{-2} . The polarization can be calculated by equation (2):

$$P = \epsilon_0(\epsilon_r - 1) E \quad (2)$$

Where ϵ_r is the relative permittivity (or dielectric constant) of the dielectric material.

Combining (1) and (2) leads to equation (3):

$$D = \epsilon_0 \epsilon_r E \quad (3)$$

However, since materials do not respond instantaneously to a variation of the electric field, contrarily to vacuum, their response depends on the frequency of the field. To represent such behavior, a complex permittivity has to be introduced, as in eq (4):

$$\epsilon_r = \epsilon_r' + i \epsilon_r'' \quad (4)$$

Where ϵ_r' stands for the real part of the relative permittivity and is related to the energy stored in the dielectric material, while ϵ_r'' stands for the imaginary part of the relative permittivity and is related to the energy loss of the material.

A very common way to characterize a dielectric material is the use of D-E loops (displacement – electric field), by varying the intensity of an electric field at a given frequency. The displacement in such loops is calculated as an integration of the current, which results as a contribution of resistivity, capacitance and polarization of a given material. In the same sense, P-E loops can be also recorded indicating the contribution of only the polarization (and not the capacitance as the D-E loops) when varying the intensity of the electric field (**Figure 1-5**).

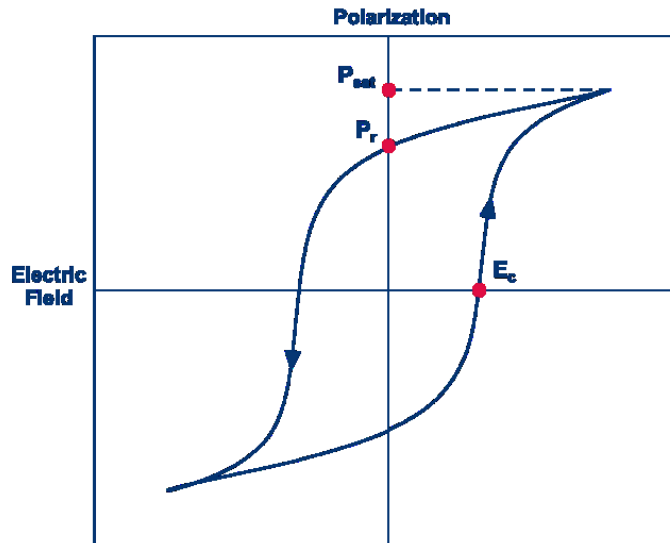


Figure 1-5. Typical hysteresis loop exhibited by ferroelectric (FE) polymers such as $P(VDF-TrFE)$ copolymers. The remarkable values, the saturation polarization (P_{sat}), the remnant polarization (P_r), and the coercive field (E_c), are highlighted (red dots)¹.

Some worth mentioning values that can be extracted from a D-E or a P-E loop respectively are the following:

- i. Saturation polarization or displacement (P_{sat} or D_{sat}): Maximum value of polarization or displacement that is obtained at a given electric field and frequency.
- ii. Remnant polarization or displacement (P_r or D_r): The absolute value of the P-E or D-E curve at zero electric field.
- iii. Coercive field (E_c): The minimum required electric bias allowing the switching of the electric dipoles in order to trigger a ferroelectric response at the material.

1.2.3) Chemical modification of FEPs

Fluorinated electroactive polymers have found very broad application in electronic devices, in part due to their exceptional mechanical and chemical stability. Therefore, when it comes down to tailoring the properties of such polymers to better fit certain applications, the choices are very limited. The most common strategies to alter the chemistry of such polymers are presented below.

1.2.3.1) Fluoropolymer based block copolymers

The most commonly used strategy includes the free radical polymerization of VDF initiated by a chlorine containing derivative of benzoylperoxide, leading to the double

chlorine functionalization of the PVDF chain (**Figure 1-6**). Then the chlorine end groups have been used as initiating points for atom transfer radical polymerization (ATRP) of styrene²⁵ as shown in **Figure 1-6**.

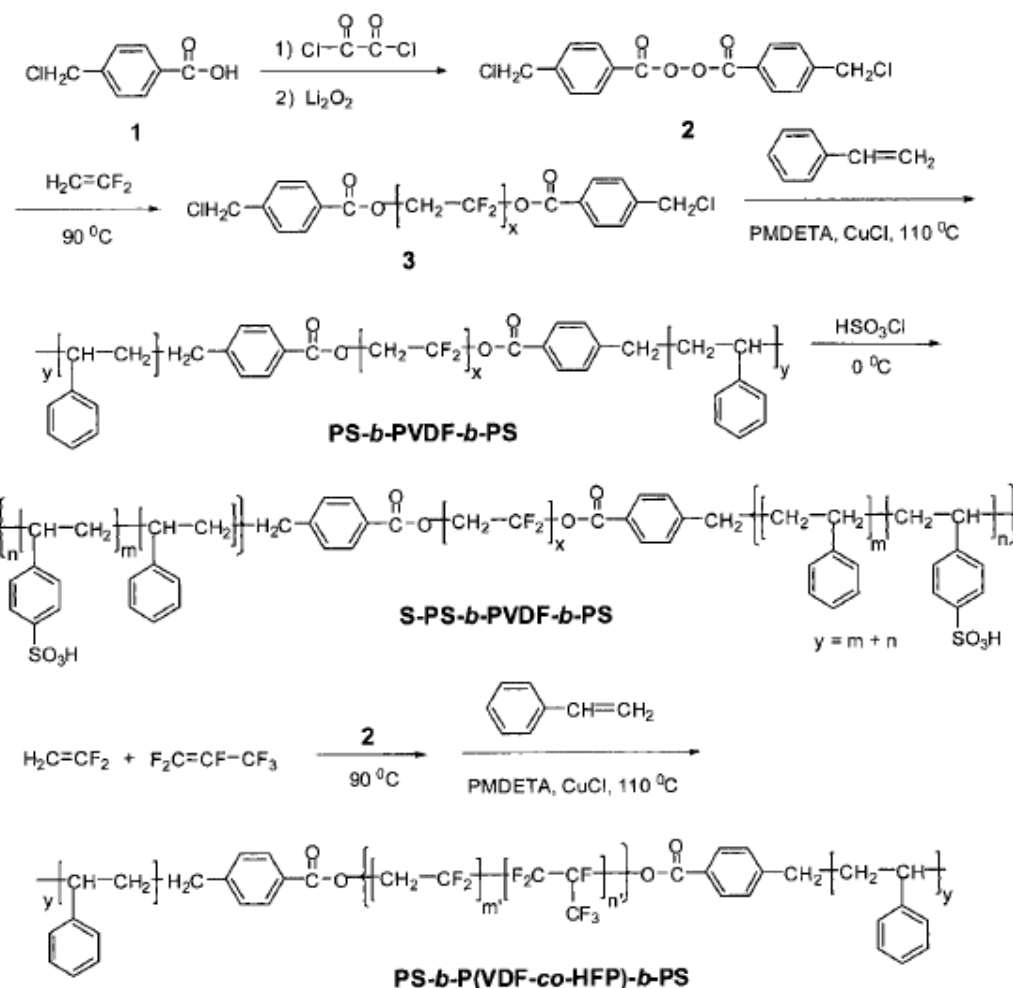


Figure 1-6. Synthesis of chlorine end-functionalized PVDF and subsequent initiation of ATRP polymerization, yielding PVDF based block copolymers²⁵.

Alternatively, PVDF based block copolymers have been synthesized from similar end functionalized PVDF with chlorine, only that in those cases the chlorine was turned into an azide group by an azidation reaction, followed by an alkyne-azide Huisgen cycloaddition in order to attach the desired blocks²⁶. The reaction is shown in detail in **Figure 1-7**.

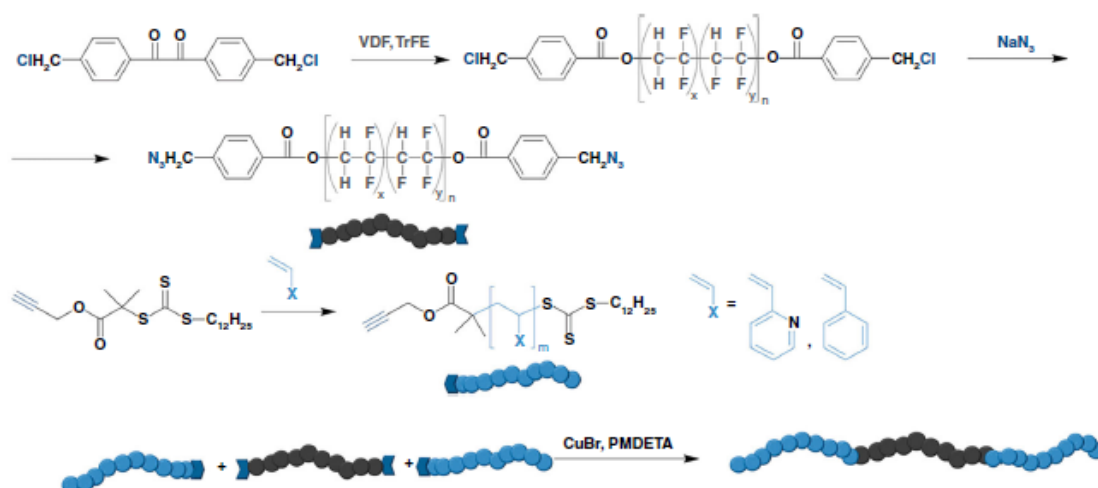


Figure 1-7. Synthesis of various P(VDF-TrFE) based block copolymers via an alkyne-azide cycloaddition reaction²⁶.

A systematic investigation of the electroactive properties of those copolymers has shown that by varying the VDF and TrFE ratio in the synthesized polymers, as well as the attached second block, the ferroelectric response can be tailored from ferroelectric to relaxor-ferroelectric and linear dielectric, see **Figure 1-8**. More specifically, when P(VDF-TrFE) with a 70/30 ratio made in a block with poly(2-vinylpyridine) (P2VP) the electroactive response is that of a ferroelectric, although not a very good one, since the remnant polarization is very low, the coercive field very high and the leakage current very high as well (**Figure 1-8b**). On the other hand, when similar block copolymers are made but with a VDF to TrFE ratio 50/50 the electroactive response is that of a relaxor-ferroelectric (**Figure 1-8d**), as marked by the current peak at zero electric field. The last case is one, where a VDF, TrFE copolymer, with monomer ratio 70/30 is made in a block with polystyrene (**Figure 1-8c**). There, the electroactive response is that of a linear dielectric.

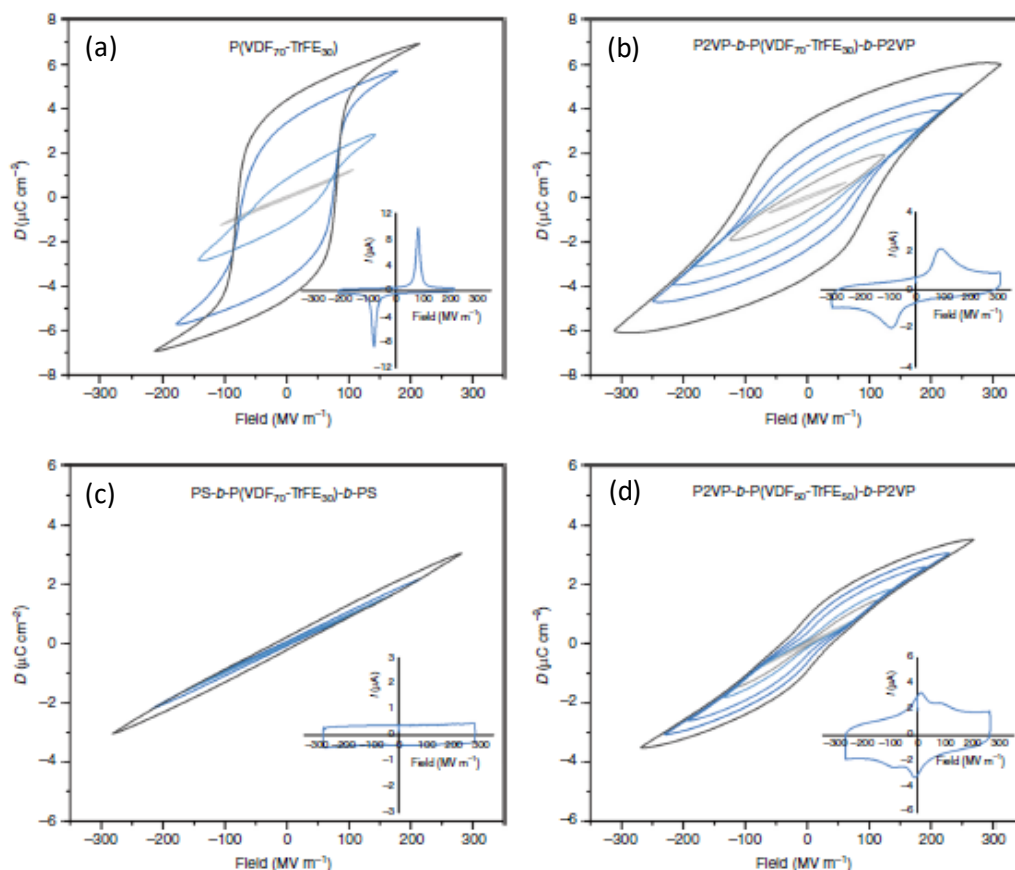


Figure 1-8. Tailoring the electroactive response of FEPs from ferroelectric (a,b) to relaxor ferroelectric (d) and paraelectric (c) by preparation of P(VDF-TrFE) based block copolymers²⁶.

However, it has to be noted that very high leakage currents are observed on those polymers and that is most likely due to the inhomogeneous nature of the self-assembled block copolymers themselves. In addition, both strategies used copper catalysts, either for the atom transfer radical polymerization or for the alkyne azide cycloaddition. Traces of metals however are known to have detrimental effects in organic electronic materials and even more so in insulating materials, where leakage current has to be kept as low as possible.

1.2.3.2) Fluoropolymer based graft copolymers

Alternatively, FEP based graft polymers have been also explored. Those polymers have become an interesting research area since the side chains are expected to modify their electroactive behavior. One strategy to synthesize such graft copolymers, was to use the chlorine groups of the relaxor-ferroelectric P(VDF-TrFE-CTFE) as initiation point for ATRP polymerization of a vinylic monomer, such as styrene, leading to a

fluoropolymer grafted with polystyrene groups (**Figure 1-9**).

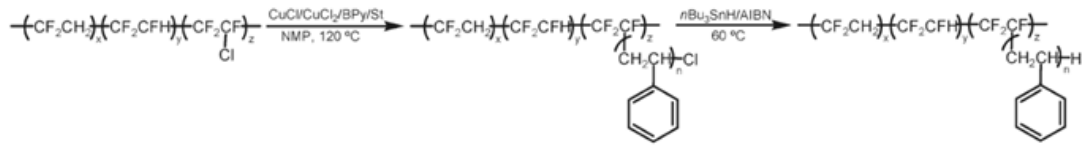


Figure 1-9. Synthesis of *P(VDF-TrFE-CTFE)-g-PS* copolymer by ATRP of styrene with a *P(VDF-TrFE-CTFE)* terpolymer macroinitiator²⁷.

Similar approach was used to initiate the polymerization of ethylene methacrylate from the chlorine groups of *P(VDF-TrFE-CTFE)*. In those cases antiferroelectric like behavior was observed²⁸ as shown in **Figure 1-10**, due to the increase in lateral spacing leading to enhanced confinement effect.

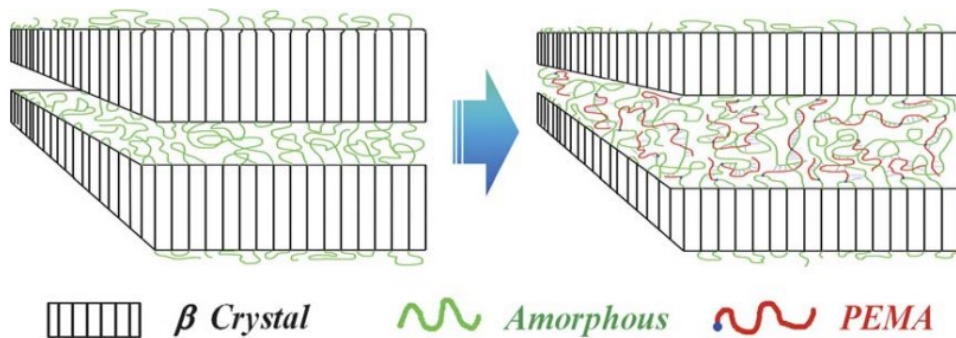


Figure 1-10. Schematic representation of the crystalline structure of *P(VDF-TrFE-CTFE)* grafted with PEMA side chains, leading to increased lateral spacing²⁸.

1.2.3.3) Fluoropolymers containing backbone unsaturation

Fluoropolymers are known to be prone to unsaturation reactions in the presence of bases. Although those reactions have been for long considered undesirable side reactions, recent reports show that they can be used to tune the electroactive response of FEPS²⁹. More specifically, double bonds were inserted on *P(VDF-TrFE)* copolymer in a controllable manner by a copper catalyzed reaction as shown in **Figure 1-11**.

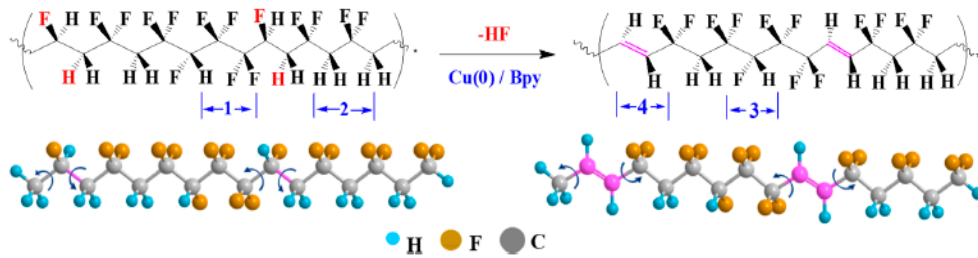


Figure 1-11. Copper catalyzed insertion of unsaturation on P(VDF-TrFE) ²⁹.

Here, the presence of the non-rotatable, non-polarizable double bonds confined the P(VDF-TrFE) domains leading to antiferroelectric like behavior for the non-annealed films. However, when annealed, normal ferroelectric behavior was regained and that was attributed to the thermally induced cross-linking, which consumes the double bonds, giving the fluoropolymer its initial conformation. The effect of the double bonds on the dielectric properties was profound, as 3% of double bonds appeared to shift the ferroelectric to paraelectric transition peak to lower temperature, while increasing the peak of the permittivity. Although, higher double bond content would shift the peak of the permittivity back to higher temperatures and reduce its intensity even lower than the pristine P(VDF-TrFE) peak (**Figure 1-12**)

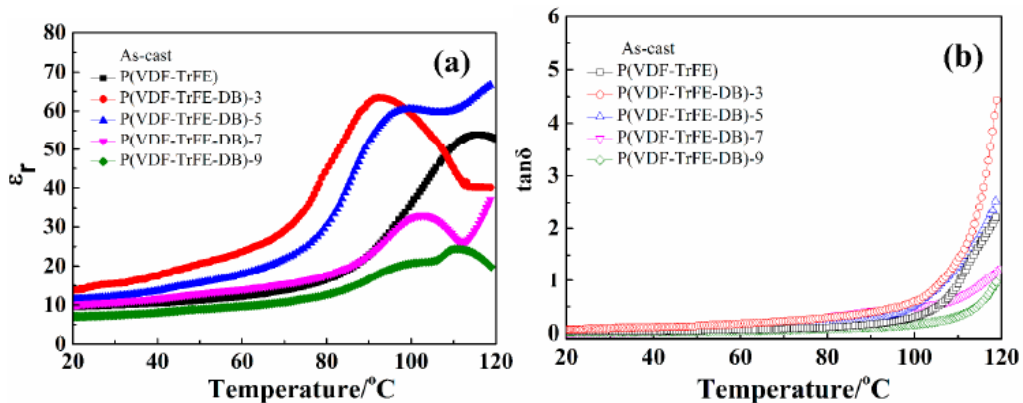


Figure 1-12. Temperature dependence of the dielectric permittivity (a) and the dielectric loss (b) at a frequency of 1kHz.

1.2.4) Cross-linking of Fluorinated polymers

Only a handful of strategies for the cross-linking of FEPs have been proposed in literature and are all mentioned below. However, cross-linking of PVDF based fluoropolymers didn't start with FEPs but rather with PVDF based fluoroelastomers, over half a century ago. Since the chemistry is almost identical in all those cases, we here present a list including all the main strategies reported to date for the cross-

linking of both FEPs and fluoroelastomers based on PVDF.

1.2.4.1) Cross-linking with diamines

The first methodology for the cross-linking of fluoroelastomers was introduced as early as the 1950s³⁰ and it involved the use of diamines. The cross-linking process with this methodology, according to literature takes place in three different steps³⁰⁻³¹.

1. The first step is the dehydrofluorination of the polymer backbone creating unsaturation.
2. Then the nitrogen of the diamine adds on the conjugated double bonds via Michael addition.
3. Finally, further HF is eliminated forming further double bonds.

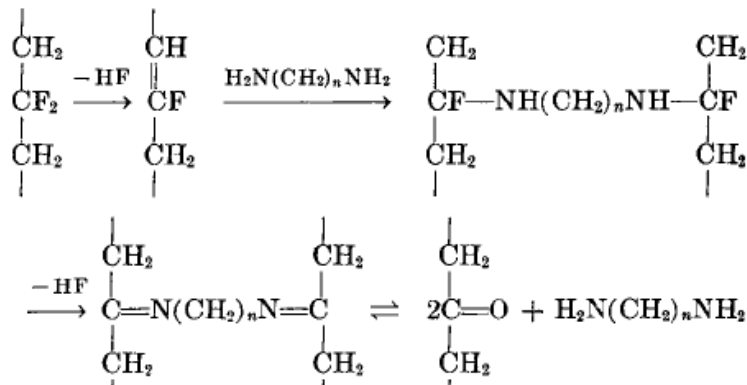


Figure 1-13. Unsaturation creation and subsequent cross-linking via diamines in P(VDF-HFP) copolymer³¹.

More recently the same approach was employed to cross-link P(VDF-HFP). However, the proposed mechanism in those studies was a four step mechanism which still included the Michael addition of a diamine on the double bonds formed on the fluoropolymer, but no mention of conjugated double bonds was made, and rather an addition on a sole double bond appeared to be the case³².

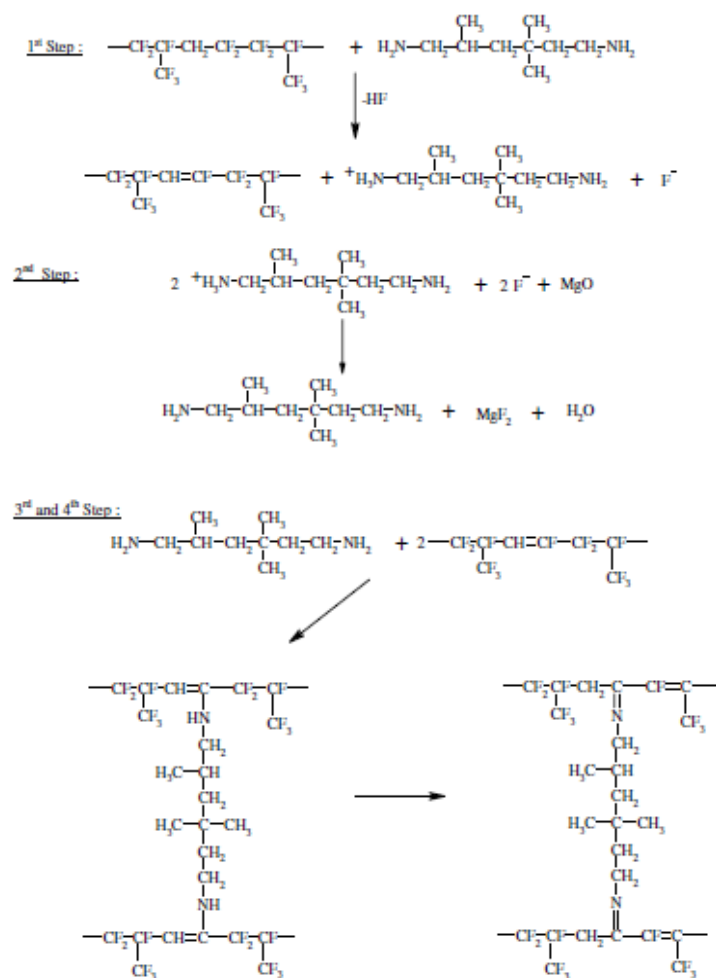


Figure 1-14. Cross-linking mechanism of Kynar® copolymer with diamine cross-linker in the presence of MgO ³².

In the conducted studies, it was found that high cross-linker content would have detrimental effects on the thermal stability of the fluoropolymer with a significant decrease on the initial decomposition temperature of about 200°C (**Figure 1-15**). That was attributed to the formed imide being prone to hydrolysis, leading to backbone cleavage of the fluoropolymer. In addition, coloration of the cross-linked polymer was observed with the amine containing polymer being yellow or even black and inhomogeneous.

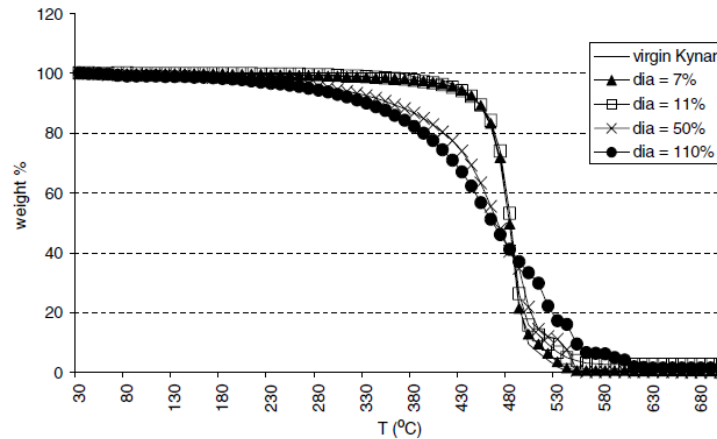


Figure 1-15. TGA thermograms of Kynar® copolymers cross-linked with different amounts of diamine³².

The same cross-linking approach has been more recently applied on P(VDF-TrFE) copolymers for the fabrication on ferroelectric nonvolatile memories, making it easier to use solution processes for the semiconductor deposition due to the solvent resistance of the cross-linked P(VDF-TrFE)³³. A decrease in polarization and an increase in coercive field was observed with increasing the diamine content although the leakage current was reported to be much lower for the cross-linked devices as shown in **Figure 1-16**.

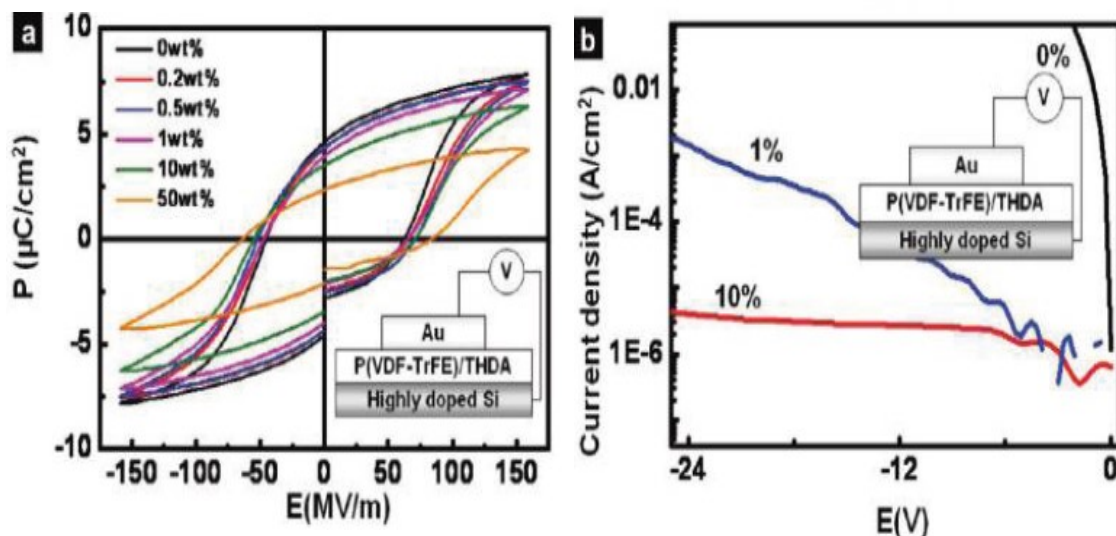


Figure 1-16. a) P-E loops comparing P(VDF-TrFE) copolymers cross-linked with different amounts of diamine. b) Leakage current density versus applied voltage for cross-linked P(VDF-TrFE) copolymers with 1 and 10% of diamine additive respectively³³.

1.2.4.2) Cross-linking with Bisphenols

Bisphenols are the predominant cross-linking agents when it comes to fluorinated elastomers. They were first proposed as alternative to the diamine method to cross-link fluoropolymers³⁴. Cross-linked polymers with this methodology presented improved physical properties as well as processing advantages compared to their amine containing counterparts. The most commonly used cross-linking compound is bisphenol AF (2,2-bis(4-hydroxyphenyl) hexafluoropropane). Others, like hydroquinone, substituted hydroquinones and 4,4'-disubstituted bisphenols appear to work well³⁵. It was observed that bisphenols do not react with the polymer without an accelerator, which could be a phosphonium or tetraalkylammonium salt, combined with a metal oxide. The bisphenol reacts with the metal oxide to give the deprotonated phenolate anion that, in turn interacts with the phosphonium or tetraalkylammonium cation, which acts as the counterion (**Figure 1-17**).



Figure 1-17. Deprotonated bisphenols with I) phosphonium and II) ammonium counter ions³⁵.

The cross-linking of fluoropolymers using bisphenols occurs in three different steps as described below.

1. First HF is eliminated from the polymer backbone in the presence of a base.
2. Then the double bonds reorganize.
3. Finally, the double bond is substituted by the activated bisphenol.

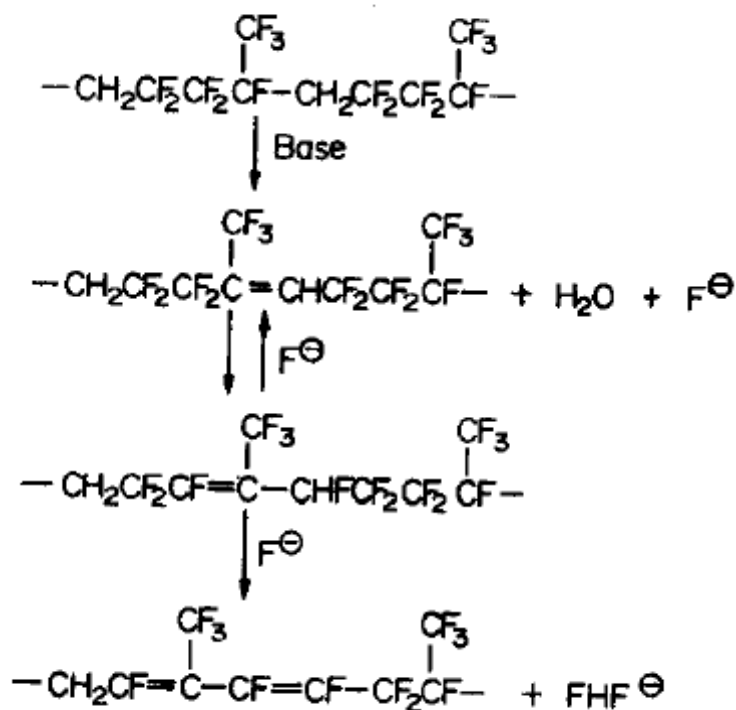


Figure 1-18. Dehydrofluorination reaction of a fluoropolymer in the presence of a base, leading to the formation of *ab* unsaturation³⁵.

Those steps are presented in detail in **Figure 1-18** and **Figure 1-19**. In the first step, the formed phenoxides, which are strong bases, abstract hydrogen fluoride from the polymer backbone (**Figure 1-18**). Then the double bonds rearrange through tautomerism and one more HF molecule is proposed to be abstracted creating a double bond conjugated to the first one. This phenomenon has been reported on the VDF groups and specifically in the HFP-VDF-HFP sequence. The unsaturation formation on the polymer backbone is the rate determining step of the curing reaction. The final step is the addition of the phenoxide on the double bonds via a Michael addition pathway (**Figure 1-19**).

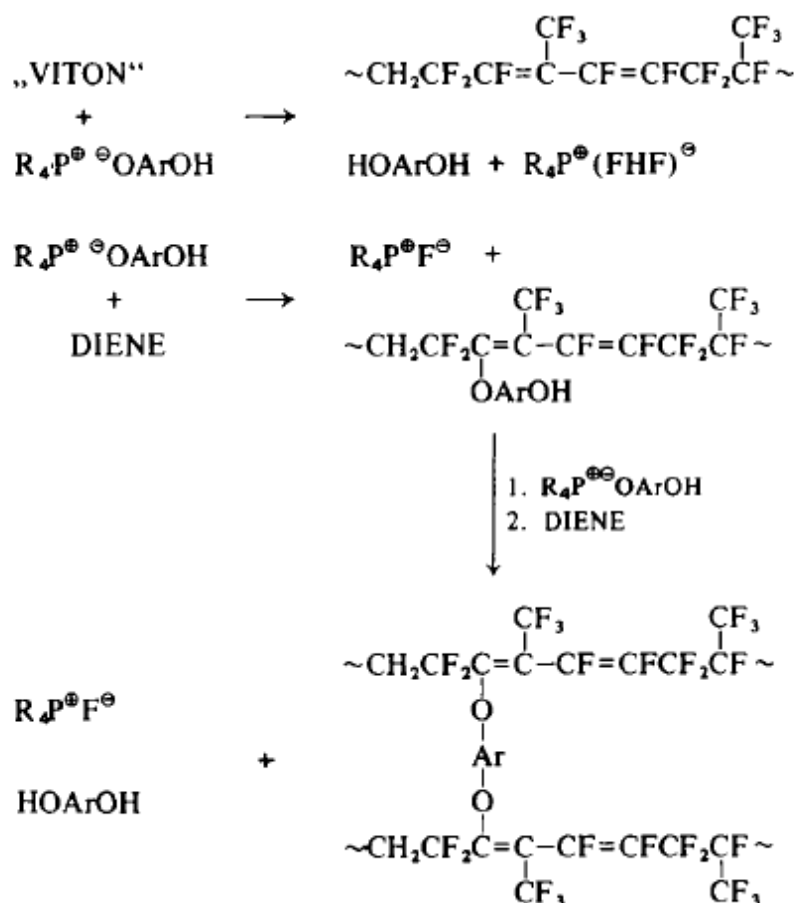


Figure 1-19. Cross-linking pathway of VDF containing copolymers with a bisphenol additive through a Michael addition of the phenoxide on the double bonds³⁶.

The cured compounds show extremely good properties, regarding their oxidative and hydrolytic stability. However, the main drawback of such curing reactions is that large number of volatiles such as HF are produced, which on top of being hazardous, create excessive porosity in the cross-linked films, leading to poor mechanical properties³⁵. Therefore, cross-linking methodologies were developed, in which the fluoropolymers contained cross-linking sites in order to bypass such problems deriving from dehydrofluorination. One such methodology is curing of fluoropolymers with peroxides.

1.2.4.3) Cross-linking with peroxides

Another class of additives that can act as cross-linkers for fluoropolymers are organic peroxides. They were first introduced for the vulcanization of natural rubber³⁷. This cross-linking strategy is somewhat different from the abovementioned cross-

linking strategies, as it requires a cure site on the fluoropolymer backbone susceptible to radical attack³⁵. Therefore fluorolefins containing bromine or iodine groups have been predominantly used for this method³⁸. Examples of such fluorolefins are: Bromotrifluoroethylene, 1-bromo-2,2-difluoroethylene, 4-bromo-3,3,4,4-tetrafluorobutene-1, 3-bromoperfluoropropylene and a large variety of fluorobutylenes³⁹⁻⁴¹.

Many of the abovementioned monomers copolymerize with VDF and other fluorinated monomers giving copolymers containing radical cure sites. Those cure sites can then generate free radicals on the polymer backbone in the presence of a peroxide⁴²⁻⁴³ which in the presence of a radical trap leads to the formation of a cross-linked polymer network. It has to be noted here that coagents such as radical traps are necessary for the efficient cross-linking by trapping the polymeric radicals. Only some examples of the peroxides that have been used in literature include the di-benzoyl peroxide⁴⁴, di-t-butyl peroxide⁴⁴ and the dicumyl peroxide⁴⁴. Such peroxide initiators are presented in **Figure 1-20**.

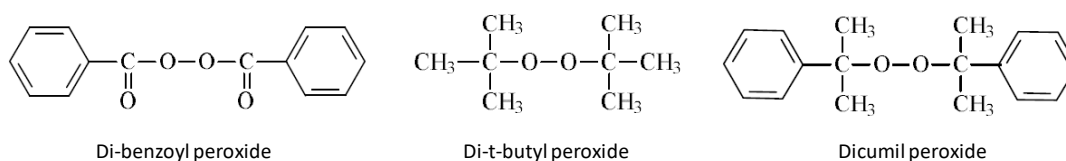


Figure 1-20. Chemical structures and names of some of the peroxides used to cross-link fluoropolymers³⁷.

As mentioned above, another class of additives is also necessary for the efficient formation of cross-linked networks. Such molecules are di- or even trifunctional vinyl compounds including 1,2-polybutadiene⁴⁴, ethylene glycol dimethacrylate⁴⁴, triallyl phosphate⁴⁴ triallylisocyanurate³⁵ and triallylcyanurate⁴⁴. Their chemical structures are shown in **Figure 1-21**.

The triazine groups reinforce the crosslinking due to their thermal stability. So triallyl isocyanurate was proven to be the most efficient co-agent. Also metal oxides have been proposed to be used in such process so as to absorb any HF traces generated during the curing process³⁵. The most widely used of such oxides is magnesium oxide.

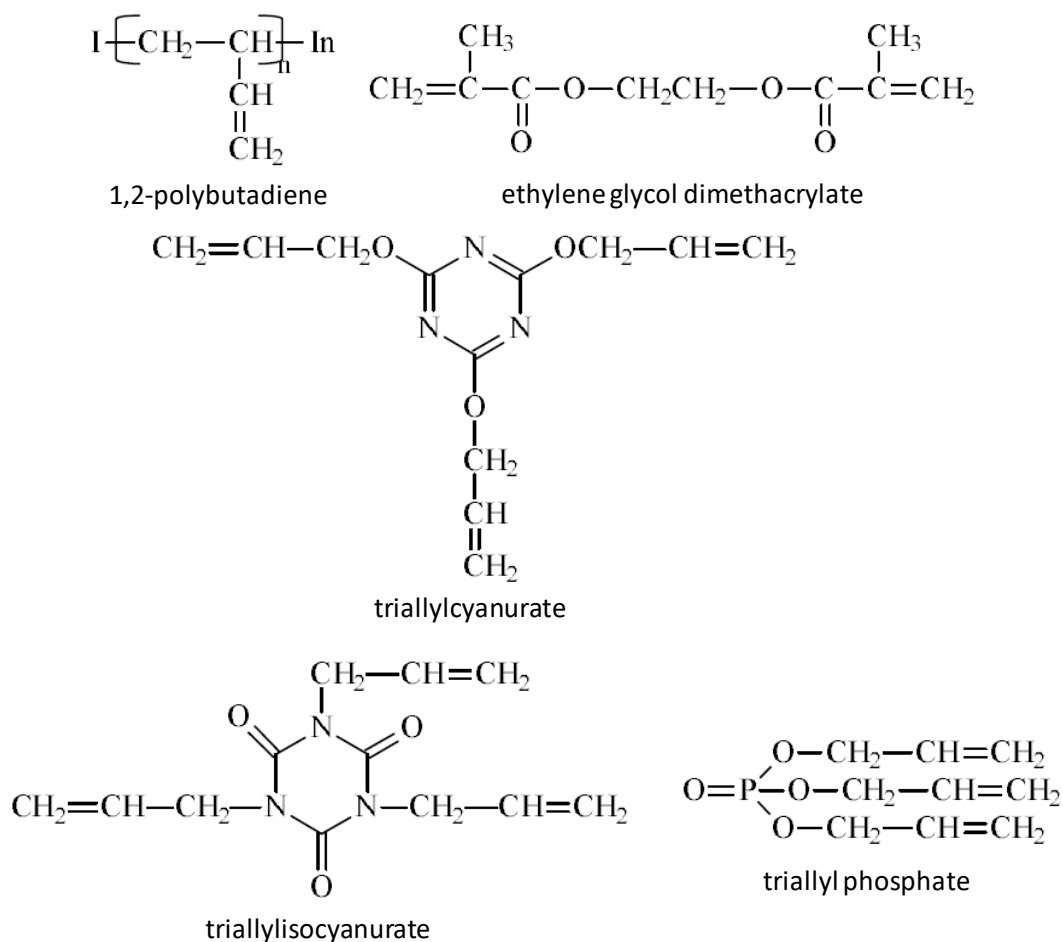


Figure 1-21. Chemical structures and names of some of the coagents used in combination with peroxides to cross-link fluoropolymers.

The curing mechanism through the peroxide/coagent system is vastly different from the two previous cross-linking methodologies. As described in **Figure 1-22**, the first step consists of the homolytic cleavage of the peroxide moieties, yielding two oxy radicals. In the given example, the homolytic cleavage of di-(t-butyl peroxy)-2,5-dimethylhexane leads to the formation of t-butoxy radicals. Subsequently those radicals can abstract a hydrogen in a minor reaction to form t-butanol, while in a major reaction they can decompose, forming acetone and a methyl radical. Then the methyl radical abstracts bromine groups from the cure sites of the fluoropolymer, giving methyl bromine, or alternatively a more stable radical intermediate can be formed by addition of the methyl radical to the coagent. The transfer of the bromine atom from an electron poor fluoropolymer to an electron rich coagent becomes the driving force of the reaction. Since more than one radicals can be transferred to the double bonds of the coagent, that acts as the cross-linker in that process.

1.2.4.4) Cross-linking via thiol-ene systems

Thiol-ene chemistry has also been employed for the cross-linking of fluoropolymers. For that to happen a trifluorovinyl ω -thioacetate monomer was copolymerized with VDF⁴⁶ and after hydrolysis led to fluoropolymers bearing pendant thiol groups. The crosslinking occurs with the thiol-ene reaction of the side groups with dienes under radical conditions as shown in **Figure 1-23**.

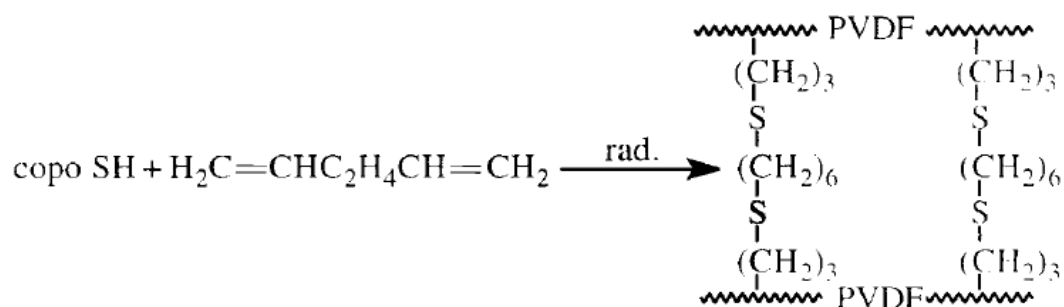


Figure 1-23. Cross-linking reaction of the fluoropolymer bearing side thiol groups through a free radical process⁴⁷.

1.2.4.5) Cross-linking via trialkoxysilanes

Another cross-linking method of fluoropolymers is the one using trialkoxysilanes and in this case of P(VDF-TrFE) involves the sol gel condensation of silanes⁴⁸. In this case a triethoxysilane derivative of benzoyl peroxide was used as an initiator for the polymerization reaction of VDF and TrFE groups, leading to an end-functionalized P(VDF-TrFE) copolymer with triethoxysilane groups on both ends (**Figure 1-24**). Then with thermal treatment of the abovementioned fluoropolymer (120°C), the triethoxysilane groups on both ends react yielding polysilsquioxanes and thus cross-linking the polymer in a very controllable way.

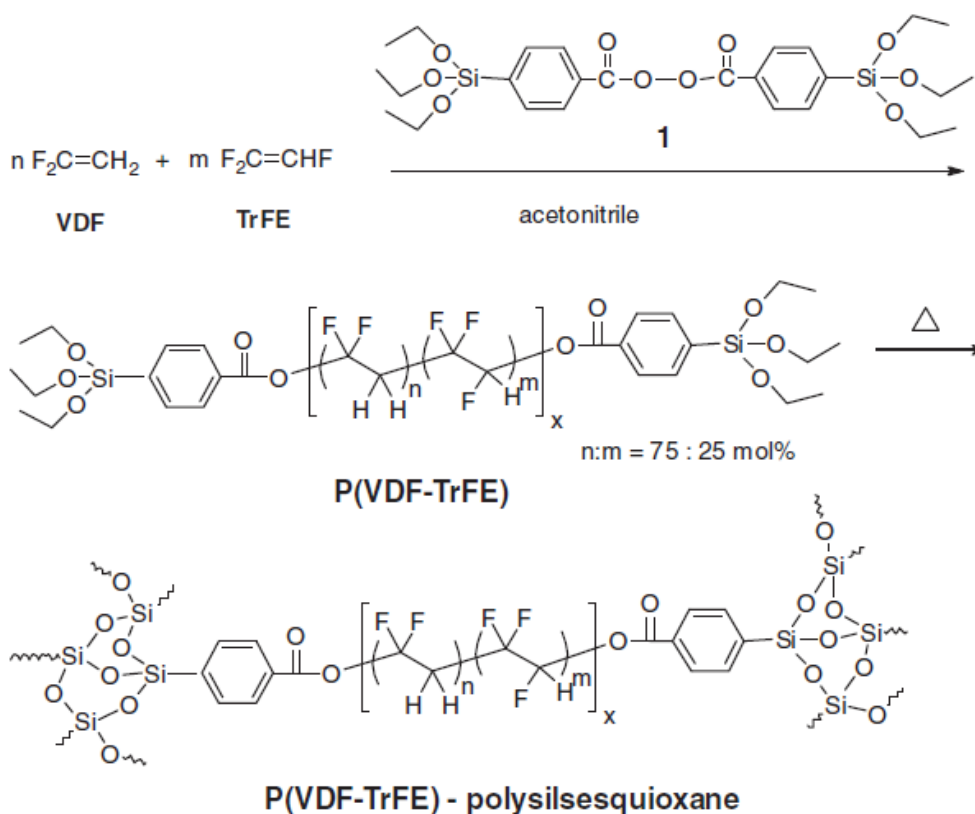


Figure 1-24. Reaction for the synthesis of triethoxysilane end functionalized $P(\text{VDF-TrFE})$ copolymer and the cross-linking reaction leading to the formation of polysilsesquioxanes⁴⁸.

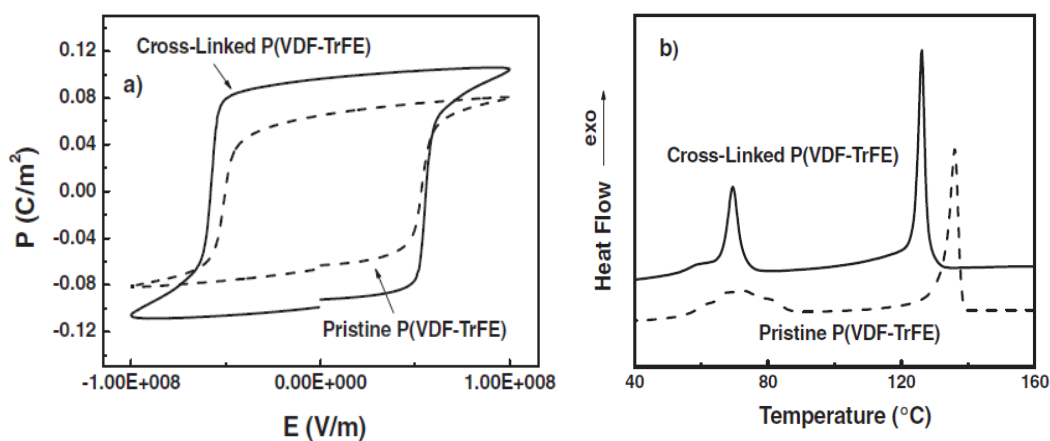


Figure 1-25. a) P - E loops comparing the linear triethoxysilane end functionalized $P(\text{VDF-TrFE})$ copolymer with the crosslinked copolymer after UV irradiation. b) Differential scanning calorimetry comparing the linear triethoxysilane end functionalized $P(\text{VDF-TrFE})$ copolymer with the crosslinked copolymer⁴⁸.

Exceptional ferroelectric properties were observed in such polymers with the polarization of the cross-linked polymer being superior even to the polarization of the pristine polymer, despite the normally negative effect that cross-linking has of such properties. That fact was attributed to the very controllable manner that cross-linking

occurs in such systems only involving the end groups without introducing defects on the main chain, while the polysilsquioxane groups act as nucleating agents enhancing the polymer's crystallinity. The ferroelectric characterization of both the cross-linked as well as the pristine polymer is shown in **Figure 1-25**.

Despite the very interesting properties that such systems exhibit, their application in industrial scale is difficult due to the very demanding anhydrous conditions that such processes require and thus the non compatibility with the existing emulsion and suspension processes with which fluoropolymers are currently produced¹.

1.2.4.6) Cross-linking via Electron irradiation

Another method for the cross-linking of fluoropolymers involves electron beam irradiation. E-beam irradiated P(VDF-TrFE) was shown to exhibit relaxor ferroelectric properties²¹ for the first time (**Figure 1-26**). Similar properties to the ones induced by the electron irradiation have been later achieved by the introduction of a bulkier comonomer such as CTFE or CFE on the P(VDF-TrFE) polymer chain²⁴.

Despite the very interesting properties obtained on polymers cross-linked with such method, application is limited mainly to a) heterogeneous distribution of the irradiation producing non-uniform energy density and b) chain scissions leading to worse mechanical properties of the formed films.

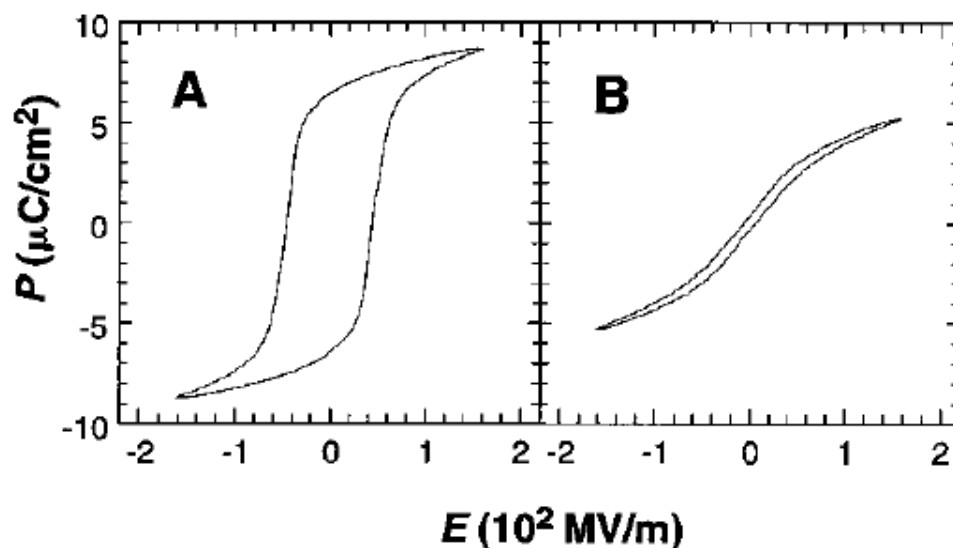


Figure 1-26. Polarization – Electric field (P - E) loop for P(VDF-TrFE) (50/50) before (A) and after (B) electron irradiation. The polymer was exposed at 4×10^5 Gy of electron irradiation at 120°C ²¹.

1.2.4.7) Photochemical cross-linking and Photolithographic patterning

Without any doubt, the most interesting class of cross-linking reactions for the scope of this thesis is the photo-chemical cross-linking. That is because photo cross-linkable polymers can be integrated in a photolithographic process as negative photoresists. Although such processes have only recently been reported on fluoropolymers, a large variety of different chemistries has been developed in different systems due to the emergence of computers in the previous century and the ongoing need for materials to become more efficient and constantly reduce the feature size produced by photolithographic processes, keeping up with Moore's law⁴⁹. The photolithographic patterning of FEPs is of great industrial importance, since that way it will be possible for fluoropolymer based devices to be produced in the established electronics production facilities which are predominantly based on photolithography.

Although there are plenty of reports in literature on the photochemical cross-linking of fluoropolymers or fluorinated oligomers⁵⁰, very little work has been performed in the photochemical cross-linking of FEPs, despite the commercial potential that such materials have. Here we try to summarize the work performed to date on this field presenting the advantages and disadvantages of each approach, although some of the methodologies can be found only in the patent literature and thus less information is available.

1.2.4.7.1) Photochemical cross-linking with additives

Photochemical cross-linking and subsequent photolithographic patterning of FEPs has been demonstrated in literature with the use of additives. In those cases, azide photochemistry was employed, as a bisazide photoinitiator was used as an additive to the fluoropolymer in order to induce photo patternability⁵¹⁻⁵³. Bisazide compounds can act as photochemical cross-linkers for a large variety of polymers, as azides, when exposed to UV light release nitrogen and the remaining radical intermediate, which is called nitrene, can attack a large variety of chemical species, leading to photo induced cross-linking reactions. Therefore, bisazides are called universal cross-linker. Some of the reactions that nitrenes can undergo are described in **Figure 1-27** and include⁵⁴:

- a) The addition to a multiple bond for the formation of aziridines. This reaction occurs to both singlet and triplet nitrenes.

b) The insertion of the nitrene in a C-H bond to form secondary amines, with this reaction occurring only to singlet nitrenes.

c) The hydrogen abstraction reaction at which the nitrene abstracts a hydrogen from a neighboring molecule creating a free radical on this carbon. The protonated nitrene can repeat the hydrogen abstraction process in order to give a primary amine, while creating two carboradicals. Then those radicals can couple with each other, which in the case of polymers would lead to cross-linking. Those reactions predominantly occur in triplet nitrenes and in solutions⁵⁴.

d) The last reaction described in **Figure 1-27** that nitrenes can undergo is the nitrene-nitrene coupling which leads to the formation of azo dyes. It has to be noted that cross-linkers based on organic azides can be activated both with exposure to UV light but also with heating⁵⁵.

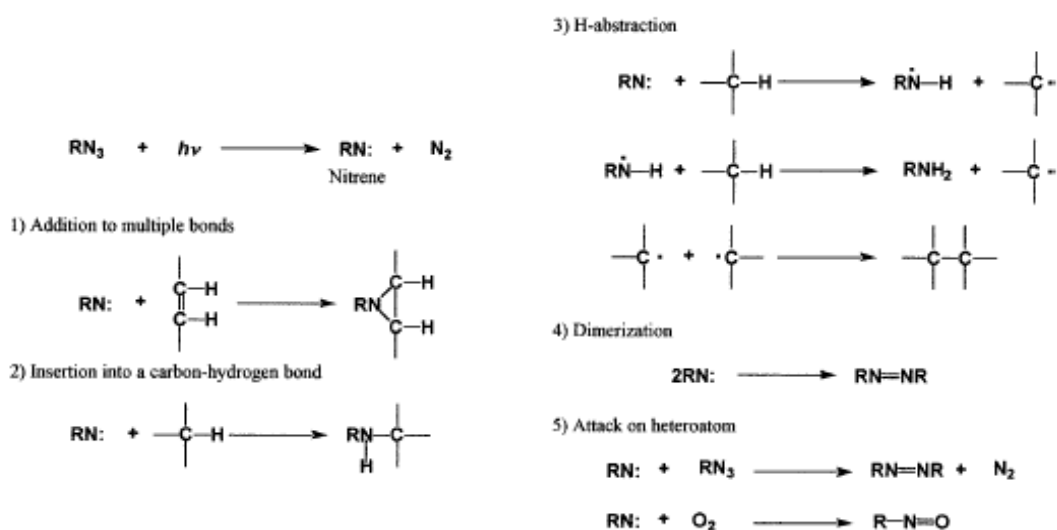


Figure 1-27. Different pathways leading to the photo-induced reaction of azide containing compounds with a large variety of groups⁵⁴.

Such chemistry was first employed in fluoropolymers in 2010, when P(VDF-CTFE) copolymer was photo patterned when mixed with a 2,6-bis(4-azide benzylidene)-4-methylcyclohexanone additive⁵¹ (**Figure 1-28**). Regarding the reactions that can lead to cross-linking only the C-H insertions and hydrogen abstractions are mentioned in this report.

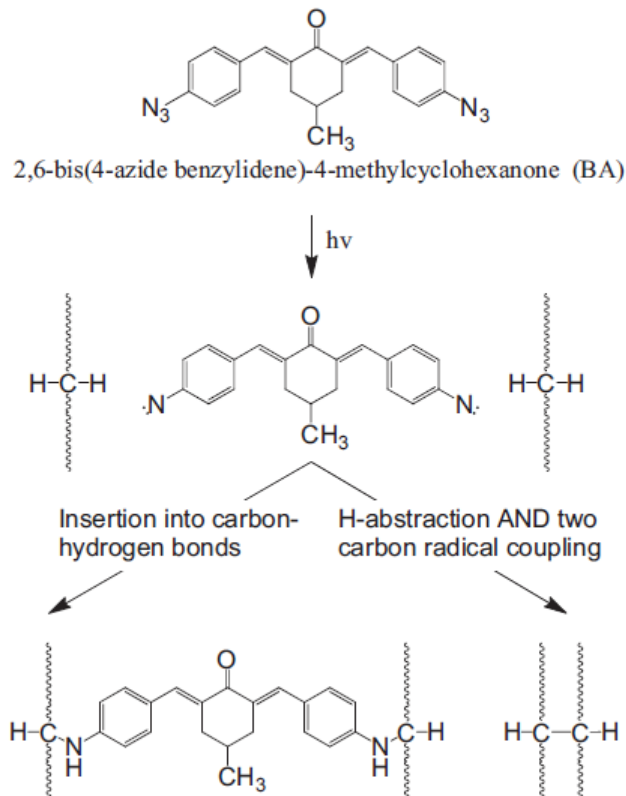


Figure 1-28. Photochemical cross-linking reaction of P(VDF-CTFE) with 2,6-bis(4-azide benzylidene)-4-methylcyclohexanone additive⁵¹.

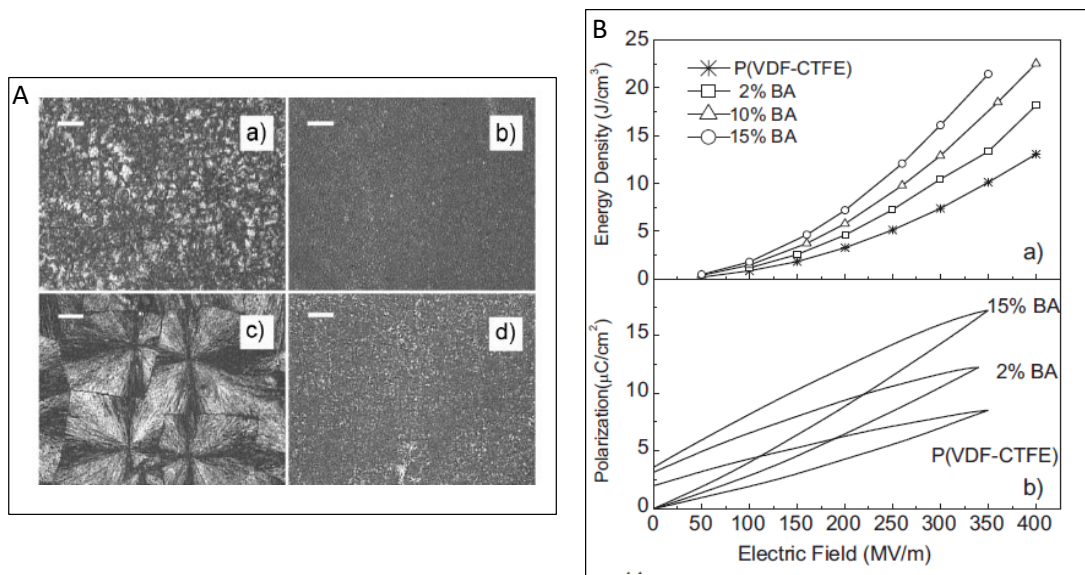


Figure 1-29. A. POM images of pristine P(VDF-CTFE) and the cross-linked sample after their crystallization at a cooling rate of 20°C/min (a) and (b), and after isothermal crystallization at 145°C (c) and (d). The scale bar is 50mm. B. a) Discharge energy density in P(VDF-CTFE) varying by the cross-linker content. b) Example of enhanced polarization in the cross-linked polymers shown by P-E loops at around 350 MV/m⁵¹.

It was observed that when the polymer becomes cross-linked, the maximum energy density of the film increases significantly fact which is closely correlated to higher

achieved polarization for a given field (**Figure 1-29**). Those improvements in the electroactive properties of P(VDF-CTFE) were attributed to the nucleating effects that the cross-linking points have to the film leading to smaller and more homogeneous crystal distribution (**Figure 1-29**) with a larger amount of interfacial areas.

A later report from the same group gives more insights on the influence the cross-linking has on the crystalline phases of the P(VDF-CTFE) copolymer. It was found that the ferroelectric β phase which is not present in the pristine P(VDF-CTFE) appears after crosslinking with increasing amount of bisazide content. Those results were confirmed both by wide angle x-ray diffraction (**Figure 1-30A**), where the 110/200 reflection of the crystalline β phase starts appearing with addition of 2% bisazide and increases with increasing amount of bisazide, to become the predominant phase when bisazide concentration reaches 15%. The same results were confirmed by FT-IR (**Figure 1-30B**), where the absorption bands at 1274, 840, and 1232 cm^{-1} , which correspond to the polar crystalline phases of $T_m \geq 4$ chain conformations and TTTG+TTTG- chain conformations⁵³.

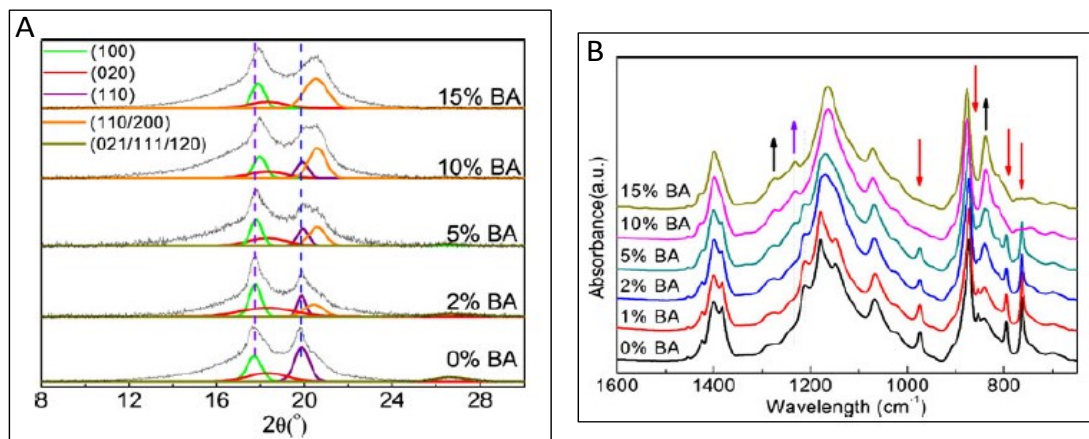


Figure 1-30. A. Room temperature wide-angle X-ray diffraction pattern of the copolymers cross-linked by different contents of bisazide. B. FTIR spectra of the copolymers cross-linked by different contents of bisazide⁵³.

Differential scanning calorimetry comparing the cross-linked copolymer to the pristine showed the appearance of an endothermic peak from 45 to 70°C which resembles the curie peak at ferroelectric polymers and might explain the higher observed polarization for the cross-linked films.

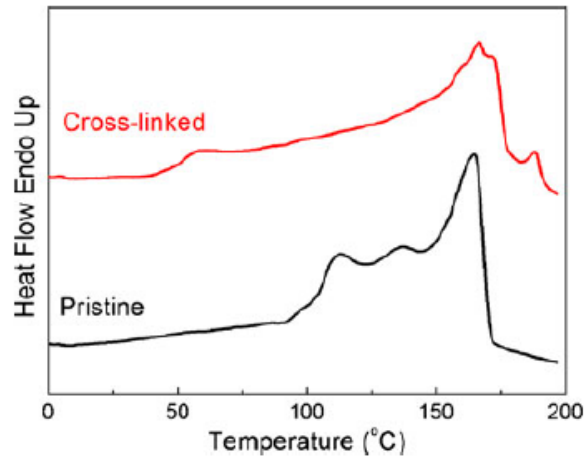


Figure 1-31. DSC thermograms comparing the pristine and the cross-linked P(VDF-CTFE) with 15 wt% bisazide⁵³.

Photolithographic patterning was demonstrated with this mixture of PVDF-CTFE/bisazide acting as a negative photoresist. However, the protocol followed for the patterning to be achieved was rather complicated with a drying step of 24 hours as well an extraction step of 24h in order to remove any residual bisazide. Yet another drying step was used in the end making the process too long to be integrated in a production line^{51, 53}.

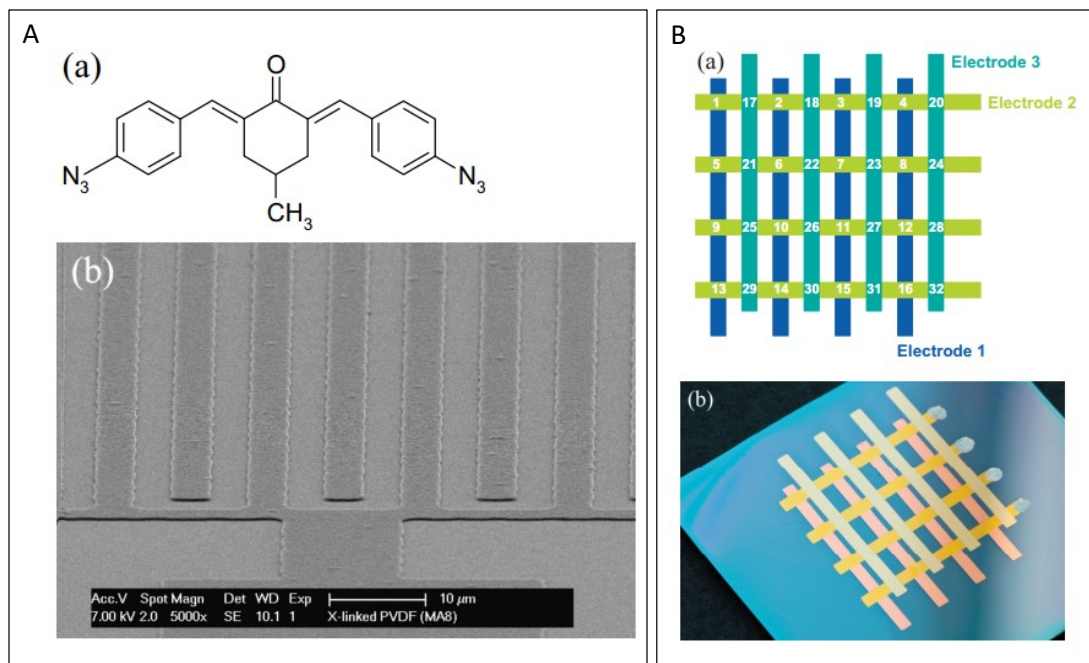


Figure 1-32. A. Chemical structure of the 2,6-bis(4-azide benzylidene)-4-methylcyclohexanone additive (up) and SEM image of the patterned P(VDF-TrFE) films with a 10 µm scale bar. B. Schematic representation of the fabricated non-volatile 3D memory arrays (up) and actual photograph of the fabricated devices (down)⁵⁶.

The same strategy was demonstrated for the photolithographic patterning of the ferroelectric P(VDF-TrFE) copolymers, where it was used for the fabrication of 3D non volatile memory arrays⁵⁶. The same bisazide photoinitiator was used as in the previous case (**Figure 1-32**). This approach presented with two main advantages. First, that the polymers could be selectively patterned only to the intersections of the electrodes and that multilayers could be easily fabricated due to the cross-linked nature of the polymers.

Despite the various advantages of this approach, two major drawbacks would prevent it from reaching large scale production. The first drawback would be the very high cost of the used bisazide photoinitiators, which can cost more than 1000 euros per gram, making the fabrication of the abovementioned devices very cost intensive. The second and most important reason preventing this technology from reaching industrial scale is the high potential risk associated with the use of small organic azides, due to the risk of explosion.

1.2.4.7.2) Photochemical cross-linking without additives

All the previous approaches include the use of additives in order to induce photopatternability in the fluoropolymer. However it has been recently shown that bromine containing fluoropolymers, and more specifically P(VDF-BTFE) (**Figure 1-33a**) can cross-link upon irradiation with UV light without the need for any additives. The cross-linking occurs with the homolytic cleavage of the C-Br bond leading to the formation of free radicals, which can in turn lead to cross-linking reactions⁵⁷. The dielectric constant of the cross-linked fluoropolymers was slightly reduced in respect to the pristine P(VDF-BTFE) but still high for a polymer and equal to 8.4 (1KHz, 20°C). The dielectric constant and dielectric loss at room temperature as a function of frequency are shown in **Figure 1-33b** both for the pristine and the cross-linked P(VDF-BTFE). Since this polymer was cross-linkable upon irradiation with UV light, it could be used as negative photoresist at a photolithographic process. Indeed such patterning was achieved and is shown in **Figure 1-33c**. However, due to the high amount of energy required for such reactions, several hour exposure was needed and the final patterning resolution was poor (**Figure 1-33c**).

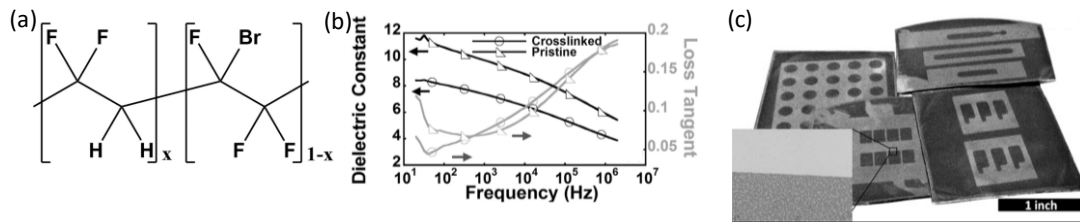


Figure 1-33. (a) Chemical structure of the P(VDF-BTFE) copolymer. (b) Comparison of the dielectric constant and the dielectric loss of the pristine and cross-linked P(VDF-BTFE). (c) P(VDF-BTFE) patterned with a photolithographic process. The scale bar is 1 inch⁵⁷.

The cross-linked P(VDF-BTFE) films shown excellent hole mobility, when used as gate dielectrics in ruberene single crystal OFETs, while keeping a fairly high dielectric constant (**Figure 1-34a**). Indeed those hole mobilities were claimed to be the highest charge mobilities reported to date for devices incorporating high-k ($k > 3$) OFETs⁵⁷. Greatly reduced number of traps was also observed and that was attributed to the elimination of interfacial tensions due to the cross-linking reactions (**Figure 1-34b**).

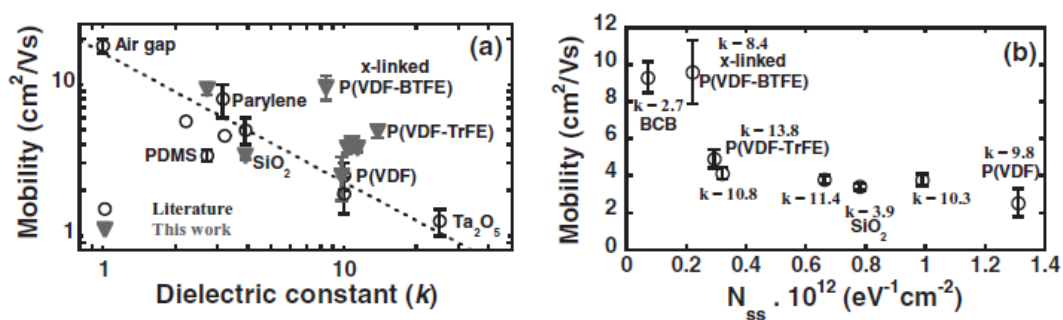


Figure 1-34. (a) Hole mobilities extracted from ruberene single crystal OFETs plotted against the dielectric constant of the gate dielectric. (b) Hole mobilities versus average interfacial trap density for ruberene single crystal OFETs using different materials as the gate dielectric⁵⁷.

Despite the very interesting findings of this study, the required long exposure times would prevent such technology to be incorporated in production lines using photolithography, where the exposure time is limited to a few minutes. In addition, the poor patterning resolution might be an additional issue, although one could argue that this could be improved with process optimization.

1.2) Scope of this Thesis

The objective of this work was to develop Fluorinated Electroactive Polymers (FEPS) that could be incorporated in photolithographic processes as photoresists without the use of any additives, while having excellent dielectric and/or ferroelectric

properties. If that would be made possible it would greatly broaden the scope of FEPs as it would make them compatible with the method of choice for high throughput electronic production processes.

The requirements for such materials would be the following:

1. The photo patternable polymers should exhibit excellent dielectric ($k > 10$) and/or ferroelectric properties.
2. Photolithographic patterning should be achieved at low UV dose ($< 3 \text{ J/cm}^2$).
3. The processes used should be easy to scale up, involving as low number of steps as possible.

Additionally, since the scope of application of FEPs gets increasingly broader, the need emerges for tailoring the properties of those polymers to better tackle certain applications. Therefore, the crude difference between ferroelectric and relaxor-ferroelectric polymers is not sufficient to tackle those vastly different fields of application. A way to better understand this is if we consider temperature sensors, electrocaloric cooling devices and OFETs for flexible displays. Despite the fact that all three classes of devices would make use of relaxor-ferroelectric polymers, the two former classes of devices would require strong temperature dependence of the dielectric constant, while the latter class of devices would ideally require no temperature dependence of the dielectric constant. This and many other examples highlight the need for tailoring the response of FEPs, much more precisely than it is now done and will be discussed in detail in following chapters.

In order to tackle both issues mentioned above, we designed processes that would allow us to alter the chemical structure of FEPs in order either to induce photopatternability or to tune their electroactive response.

In order to induce photopatternability to FEPs, we developed processes allowing the grafting of photoinitiator groups on the fluoropolymer backbone, making them cross-linkable upon irradiation with UV light. Those materials were subsequently used in photolithographic patterning processes as negative photoresists. First, the relaxor-ferroelectric P(VDF-TrFE-CTFE) polymer was functionalized with azido groups, which made the final polymer photo cross-linkable without the use of any additives. That was achieved by converting the chlorine groups of P(VDF-TrFE-CTFE) into azide groups, by a single step substitution reaction with sodium azide. The synthesized polymers

became indeed photo cross-linkable and photolithographic patterning processes allowing excellent quality patterning at low UV dose were developed. The dielectric constant of those polymers was up to 25 at 20°C and 1kHz, which was the highest dielectric constant reported to date for a photo cross-linkable polymer. Despite those dielectric constant values being very high, they were still slightly reduced with respect to the pristine polymer, which had a dielectric constant of 35 at the same conditions. This approach is discussed in detail in **Chapter 2**.

Despite all the advantages of this approach, it came with some serious limitations, which are listed below:

1. The electroactive properties were degraded after the modification, with the degree of degradation being strongly dependent on the reaction conditions.
2. The azide containing polymers had to be handled and stored with great care, since azide groups are very sensitive to heat (60°C) and UV light, causing the polymers to cross-link in bulk.
3. This method was very specific, both regarding the grafted group (azide) and the polymer (P(VDF-TrFE-CTFE)), allowing for no flexibility in either of the above.

We were therefore looking for an alternative method to the abovementioned, that would allow for more flexibility regarding both the grafted groups but also not limited by the presence of the chlorine groups in P(VDF-TrFE-CTFE). Ideally, that method would address some of the other drawbacks of the azide approach such as the reduced electroactive properties and the stability issues.

Knowing that substitution reactions are possible in FEPs, we designed a Williamson etherification reaction that would allow the grafting of a huge variety of groups on FEPs. In order for the fluoropolymers to become photo cross-linkable, two Type II photoinitiators were grafted on FEPs using that process. The two grafted photoinitiators were benzophenone (BP) and anthraquinone (AQ). Grafting was made possible not only on relaxor-ferroelectric polymers such as P(VDF-TrFE-CTFE) and P(VDF-TrFE-CFE) but also on the ferroelectric P(VDF-TrFE). The electroactive response of the relaxor-ferroelectric terpolymers functionalized via this method was greatly dependent on the photoinitiator (PI) loading. When the PI loading was low, the polymers had relaxor-ferroelectric response with even improved dielectric properties in respect to the pristine polymer, but with increasing the PI loading the polymers would behave more like linear dielectrics with lower dielectric constant. In all cases,

the polymers would become photo patternable with excellent thermal stability.

As mentioned above, P(VDF-TrFE) ferroelectric copolymers were also grafted with the same PI groups. Here again the polymers maintained their ferroelectric character even after being cross-linked with light. However, their ferroelectric properties, which are measured from the remnant polarization and the coercive bias, were always reduced in respect to the pristine polymers.

As the developed methodology involving Williamson ether synthesis on fluoropolymers was making use of bases, which would lead to the formation of unsaturation on the polymer backbone, assessing when the difference in properties is due to the grafted group or the formed double bonds was rather complicated. To do so FEPs containing unsaturation were synthesized and studied in terms of their electroactive response. In many cases, the double bonds appeared to improve the electroactive response of FEPs, as measured by the dielectric constant and the obtained displacement at a given field.

All the materials synthesized in the context of this thesis were characterized in terms of their electronic properties, such as their dielectric constant and electroactive response. Those characterizations are extensively discussed in **Chapter 5**, where the impact of each modification on the electroactive and dielectric response of FEPs is better understood. The highest performing materials were integrated in Electrocaloric Cooling devices, where improved performances with respect to the pristine materials were also observed.

In summary, the initial objective of this work was to induce photopatternability in FEPs. However, in the process of achieving that, a general methodology for the functionalization of FEPs was developed, allowing for the tuning of their electroactive properties in order to better suit certain applications. Furthermore, the fact that the developed methodologies would introduce unsaturation on the polymer backbone as a side reaction led us to the detailed investigation of the effect of unsaturation on FEPs. Contrarily to the consensus view, the impact of the unsaturation was shown to be beneficial for both the electroactive and the dielectric properties of relaxor-ferroelectric polymers. All the above broaden the scope of application of FEPs, by either improving their performance or by making them compatible with the patterning processes currently used in the semiconductor industry.

1.3) References

1. Soulestin, T.; Ladmiral, V.; Dos Santos, F. D.; Améduri, B., Vinylidene fluoride- and trifluoroethylene-containing fluorinated electroactive copolymers. How does chemistry impact properties? *Progress in Polymer Science* **2017**, *72*, 16-60.
2. Stadlober, B.; Zirkl, M.; Irimia-Vladu, M., Route towards sustainable smart sensors: ferroelectric polyvinylidene fluoride-based materials and their integration in flexible electronics. *Chemical Society Reviews* **2019**, *48* (6), 1787-1825.
3. Hwang, S. K.; Bae, I.; Kim, R. H.; Park, C., Flexible Non-Volatile Ferroelectric Polymer Memory with Gate-Controlled Multilevel Operation. *Advanced Materials* **2012**, *24* (44), 5910-5914.
4. Naber, R. C.; Tanase, C.; Blom, P. W.; Gelinck, G. H.; Marsman, A. W.; Touwslager, F. J.; Setayesh, S.; De Leeuw, D. M. J. N. M., High-performance solution-processed polymer ferroelectric field-effect transistors. *Nature materials* **2005**, *4* (3), 243.
5. Choi, S. T.; Lee, J. Y.; Kwon, J. O.; Lee, S.; Kim, W., Varifocal liquid-filled microlens operated by an electroactive polymer actuator. *Optics letters* **2011**, *36* (10), 1920-1922.
6. Li, J.; Sun, Z.; Yan, F., Solution processable low-voltage organic thin film transistors with high-k relaxor ferroelectric polymer as gate insulator. *Advanced Materials* **2012**, *24* (1), 88-93.
7. Ma, R.; Zhang, Z.; Tong, K.; Huber, D.; Kornbluh, R.; Ju, Y. S.; Pei, Q., Highly efficient electrocaloric cooling with electrostatic actuation. *Science* **2017**, *357* (6356), 1130-1134.
8. Lovinger, A. J., Ferroelectric Polymers. *Science* **1983**, *220* (4602), 1115-1121.
9. Stadlober, B.; Zirkl, M.; Irimia-Vladu, M., Route towards sustainable smart sensors: ferroelectric polyvinylidene fluoride-based materials and their integration in flexible electronics. *Chemical Society Reviews* **2019**.
10. Zhu, L., Exploring Strategies for High Dielectric Constant and Low Loss Polymer Dielectrics. *The Journal of Physical Chemistry Letters* **2014**, *5* (21), 3677-3687.
11. Heiji, K., The Piezoelectricity of Poly (vinylidene Fluoride). *Japanese Journal of Applied Physics* **1969**, *8* (7), 975.
12. Tamura, M.; Ogasawara, K.; Ono, N.; Hagiwara, S., Piezoelectricity in uniaxially stretched poly(vinylidene fluoride). *Journal of Applied Physics* **1974**, *45* (9), 3768-3771.
13. Tamura, M.; Ogasawara, K.; Yoshimi, T., Piezoelectricity in uniaxially stretched poly(vinylidene fluoride) films and its applications. *Ferroelectrics* **1976**, *10* (1), 125-127.
14. Li, M.; Wondergem, H. J.; Spijkman, M.-J.; Asadi, K.; Katsouras, I.; Blom, P. W. M.; de Leeuw, D. M., Revisiting the δ -phase of poly(vinylidene fluoride) for solution-processed ferroelectric thin films. *Nature materials* **2013**, *12*, 433.
15. Weinhold, S.; Litt, M. H.; Lando, J. B., The Crystal Structure of the γ Phase of Poly(vinylidene fluoride). *Macromolecules* **1980**, *13* (5), 1178-1183.
16. Jr., W. M. P.; Luca, D. J., The formation of the γ phase from the α and β polymorphs of polyvinylidene fluoride. *Journal of Applied Physics* **1978**, *49* (10), 5042-5047.
17. Zhu, L.; Wang, Q., Novel Ferroelectric Polymers for High Energy Density and Low Loss Dielectrics. *Macromolecules* **2012**, *45* (7), 2937-2954.
18. Higashihata, Y.; Sako, J.; Yagi, T., Piezoelectricity of vinylidene fluoride-trifluoroethylene copolymers. *Ferroelectrics* **1981**, *32* (1), 85-92.

19. Hiroji, O.; Keiko, K., Ferroelectric Copolymers of Vinylidene fluoride and Trifluoroethylene with a Large Electromechanical Coupling Factor. *Japanese Journal of Applied Physics* **1982**, *21* (8A), L455.
20. Yagi, T.; Tatemoto, M.; Sako, J.-i., Transition Behavior and Dielectric Properties in Trifluoroethylene and Vinylidene Fluoride Copolymers. *Polymer Journal* **1980**, *12*, 209.
21. Zhang, Q. M.; Bharti, V.; Zhao, X., Giant Electrostriction and Relaxor Ferroelectric Behavior in Electron-Irradiated Poly(vinylidene fluoride-trifluoroethylene) Copolymer. *Science* **1998**, *280* (5372), 2101-2104.
22. Chung, T. C.; Petchsuk, A.; Taylor, G. W., Ferroelectric polymers with large electrostriction; based on semicrystalline VDF/TrFE/CTFE terpolymers. *Ferroelectrics Letters Section* **2001**, *28* (5-6), 135-143.
23. Chung, T. C.; Petchsuk, A., Synthesis and Properties of Ferroelectric Fluoro-terpolymers with Curie Transition at Ambient Temperature. *Macromolecules* **2002**, *35* (20), 7678-7684.
24. Yang, L.; Li, X.; Allahyarov, E.; Taylor, P. L.; Zhang, Q. M.; Zhu, L., Novel polymer ferroelectric behavior via crystal isomorphism and the nanoconfinement effect. *Polymer* **2013**, *54* (7), 1709-1728.
25. Xu, K.; Li, K.; Khanchaitit, P.; Wang, Q., Synthesis and Characterization of Self-Assembled Sulfonated Poly(styrene-*b*-vinylidene fluoride-*b*-styrene) Triblock Copolymers for Proton Conductive Membranes. *Chemistry of Materials* **2007**, *19* (24), 5937-5945.
26. Terzic, I.; Meereboer, N. L.; Acuautla, M.; Portale, G.; Loos, K., Electroactive materials with tunable response based on block copolymer self-assembly. *Nature Communications* **2019**, *10* (1), 601.
27. Guan, F.; Wang, J.; Yang, L.; Tseng, J.-K.; Han, K.; Wang, Q.; Zhu, L., Confinement-Induced High-Field Antiferroelectric-like Behavior in a Poly(vinylidene fluoride-co-trifluoroethylene-co-chlorotrifluoroethylene)-graft-polystyrene Graft Copolymer. *Macromolecules* **2011**, *44* (7), 2190-2199.
28. Li, J.; Tan, S.; Ding, S.; Li, H.; Yang, L.; Zhang, Z., High-field antiferroelectric behaviour and minimized energy loss in poly(vinylidene-co-trifluoroethylene)-graft-poly(ethyl methacrylate) for energy storage application. *Journal of Materials Chemistry* **2012**, *22* (44), 23468-23476.
29. Zhang, Y.; Tan, S.; Wang, J.; Wang, X.; Zhu, W.; Zhang, Z., Regulating Dielectric and Ferroelectric Properties of Poly (vinylidene fluoride-trifluoroethylene) with Inner CH=CH Bonds. *Polymers* **2018**, *10* (3), 339.
30. Dixon, S.; Rexford, D. R.; Rugg, J. S., Vinylidene Fluoride - Hexafluoropropylene Copolymer. *Industrial & Engineering Chemistry* **1957**, *49* (10), 1687-1690.
31. Smith, J. F.; Perkins, G. T., The mechanism of post cure of viton A Fluorocarbon elastomer. *Journal of Applied Polymer Science* **1961**, *5* (16), 460-467.
32. Taguet, A.; Ameduri, B.; Dufresne, A., Crosslinking and characterization of commercially available poly(VDF-co-HFP) copolymers with 2,4,4-trimethyl-1,6-hexanediamine. *European Polymer Journal* **2006**, *42* (10), 2549-2561.
33. Shin, Y. J.; Kang, S. J.; Jung, H. J.; Park, Y. J.; Bae, I.; Choi, D. H.; Park, C., Chemically Cross-Linked Thin Poly(vinylidene fluoride-co-trifluoroethylene) Films for Nonvolatile Ferroelectric Polymer Memory. *ACS Applied Materials & Interfaces* **2011**, *3* (2), 582-589.
34. Schmiegel, W. W., Vulcanizable fluoroelastomer composition. US387265A: **1973**
35. Logothetis, A. L., Chemistry of fluorocarbon elastomers. *Progress in Polymer Science* **1989**, *14* (2), 251-296.
36. Schmiegel, W. W., Crosslinking of elastomeric vinylidene fluoride copolymers with nucleophiles. *Die Angewandte Makromolekulare Chemie* **1979**, *76* (1), 39-65.

37. Taguet, A.; Ameduri, B.; Boutevin, B., Crosslinking of vinylidene fluoride-containing fluoropolymers. In *Crosslinking in Materials Science*, Springer: 2005; pp 127-211.
38. Ameduri, B.; Armand, M.; Boucher, M.; Manseri, A., Bromosulphonated fluorinated cross-linkable elastomers based on vinylidene fluoride having low T_g and processes for their preparation. US20030181615A1: **2003**.
39. Souzy, R.; Ameduri, B.; Boutevin, B., Synthesis of functional polymers—Vinylidene fluoride based fluorinated copolymers and terpolymers bearing bromoaromatic side-group. *Journal of Polymer Science Part A: Polymer Chemistry* **2004**, *42* (20), 5077-5097.
40. Bowers, S., Fluoroelastomer composition having excellent processability and low temperature properties. US6329469B1: **2001**.
41. Staccione, A.; Albano, M., Curable fluoroelastomers. Google Patents: 2003.
42. Apotheker, D.; Finlay, J.; Krusic, P.; Logothetis, A., Curing of fluoroelastomers by peroxides. *Rubber Chemistry and Technology* **1982**, *55* (4), 1004-1018.
43. Arthur, J. C., *Polymers for fibers and elastomers*. ACS: 1984.
44. Ogunniyi, D. S., Peroxide vulcanization of rubber. *Prog. Rubb. Plast. Technol.* **1999**, *5*, 95.
45. Apotheker, D.; Finlay, J. B.; Krusic, P. J.; Logothetis, A. L., Curing of Fluoroelastomers by Peroxides. *Rubber Chemistry and Technology* **1982**, *55* (4), 1004-1018.
46. Améduri, B.; Boutevin, B.; Kostov, G., Fluoroelastomers: synthesis, properties and applications. *Progress in Polymer Science* **2001**, *26* (1), 105-187.
47. Boutevin, B.; Kostov, G. K.; Petrova, P., Synthesis and polymerization of fluorinated monomers bearing a reactive lateral group. Part 10. Copolymerization of vinylidene fluoride (VDF) with 5-thioacetoxy-1,1,2-trifluoropentene for the obtaining of a novel PVDF containing mercaptan side-groups AU - Améduri, Bruno. *Designed Monomers and Polymers* **1999**, *2* (4), 267-285.
48. Jin, J.; Lu, S.-G.; Chanthad, C.; Zhang, Q.; Haque, M. A.; Wang, Q., Multiferroic Polymer Composites with Greatly Enhanced Magnetoelectric Effect under a Low Magnetic Bias. *Advanced Materials* **2011**, *23* (33), 3853-3858.
49. Moore, G. E., Cramming more components onto integrated circuits. *Proceedings of the IEEE* **1998**, *86* (1), 82-85.
50. Vitale, A.; Bongiovanni, R.; Ameduri, B., Fluorinated Oligomers and Polymers in Photopolymerization. *Chemical Reviews* **2015**, *115* (16), 8835-8866.
51. Chen, X.-Z.; Li, Z.-W.; Cheng, Z.-X.; Zhang, J.-Z.; Shen, Q.-D.; Ge, H.-X.; Li, H.-T., Greatly Enhanced Energy Density and Patterned Films Induced by Photo Cross-Linking of Poly(vinylidene fluoride-chlorotrifluoroethylene). *Macromolecular Rapid Communications* **2011**, *32* (1), 94-99.
52. Van Breemen, A.; Van der Putten, J.; Cai, R.; Reimann, K.; Marsman, A.; Willard, N.; De Leeuw, D.; Gelinck, G., Photocrosslinking of ferroelectric polymers and its application in three-dimensional memory arrays. *Applied Physics Letters* **2011**, *98* (18), 86.
53. Chen, X.-Z.; Cheng, Z.-X.; Liu, L.; Yang, X.-D.; Shen, Q.-D.; Hu, W.-B.; Li, H.-T., Evolution of nanopolar phases, interfaces, and increased dielectric energy storage capacity in photoinitiated cross-linked poly (vinylidene fluoride)-based copolymers. *Colloid And Polymer Science* **2013**, *291* (8), 1989-1997.
54. Yasuda, N.; Yamamoto, S.; Wada, Y.; Yanagida, S., Photocrosslinking reaction of vinyl-functional polyphenylsilsesquioxane sensitized with aromatic bisazide compounds. *Journal of Polymer Science Part A: Polymer Chemistry* **2001**, *39* (24), 4196-4205.

55. Bräse, S.; Gil, C.; Knepper, K.; Zimmermann, V., Organic azides: an exploding diversity of a unique class of compounds. *Angewandte Chemie International Edition* **2005**, *44* (33), 5188-5240.
56. Breemen, A. J. J. M. v.; Putten, J. B. P. H. v. d.; Cai, R.; Reimann, K.; Marsman, A. W.; Willard, N.; Leeuw, D. M. d.; Gelinck, G. H., Photocrosslinking of ferroelectric polymers and its application in three-dimensional memory arrays. *Applied Physics Letters* **2011**, *98* (18), 183302.
57. Adhikari, J. M.; Gadinski, M. R.; Li, Q.; Sun, K. G.; Reyes-Martinez, M. A.; Iagodkine, E.; Briseno, A. L.; Jackson, T. N.; Wang, Q.; Gomez, E. D., Controlling Chain Conformations of High-k Fluoropolymer Dielectrics to Enhance Charge Mobilities in Rubrene Single-Crystal Field-Effect Transistors. *Advanced Materials* **2016**, *28* (45), 10095-10102.

Chapter 2

Photopatternable Fluoropolymers with pendent azido groups

Chapter 2: Photopatternable fluoropolymers with pendent azido groups

2.1) Introduction

Photolithographic patterning of FEPs and more specifically of P(VDF-TrFE)¹ and P(VDF-CTFE)² has been reported in literature. In both cases, azide photo-chemistry was applied. In order to make the FEPs photo cross-linkable and thus photo-patternable an expensive bis-azide photoinitiator was used as an additive. Another report suggests that P(VDF-BTFE) with a dielectric constant (k) of 8.4 can be patterned with a photolithographic process, with the addition of radical photoinitiators in the spin-cast blend, and exposure of the film under UV light for several hours⁴. The patterned fluoropolymer film is then integrated in OFETs as gate dielectric and charge mobilities exceeding $10 \text{ cm}^2 \text{ V}^{-1} \text{ s}^{-1}$ were observed, which are the highest charge mobilities reported to date for transistors using high- k polymer dielectrics⁴⁻⁶.

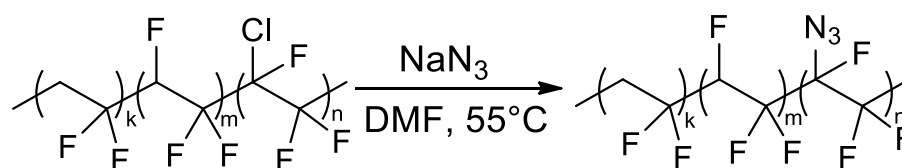
Our challenge was therefore to develop fluorinated electroactive polymers bearing photo sensitive groups on the polymer backbone and thus be compatible with photolithographic patterning techniques without the use of any additives. P(VDF-TrFE-CTFE) is one of the most interesting FEPs, mostly due to its high dielectric constant and its electroactive properties which make it ideal for a large variety of electronic devices.

2.2) Results and Discussion

2.2.1) Chemical grafting of azido groups on FEPs

In order to enable the photocrosslinking of the P(VDF-TrFE-CTFE) terpolymer (61.9, 29.9, 8.2), azidation of the CTFE groups was attempted, as polymers bearing azide side groups are known to act as negative photoresists⁷⁻⁹. Initially the polymer was modified with sodium azide, substituting the chlorine groups on the polymer backbone with azido groups. Different modification conditions were tested by varying the sodium azide feeding ratio in respect to the total number of repeating units as well as the reaction temperature and solvents. The products were characterized by infrared spectroscopy, following the characteristic azide band at 2100 cm^{-1} . The reaction is shown in **Scheme 2-1**, where the chlorine of the P(VDF-TrFE-CTFE) terpolymer is used

as a leaving group.



Scheme 2-1. Single step azidation reaction of the P(VDF-TrFE-CTFE) terpolymer (for 100% conversion of the chlorine group).

The infrared spectroscopy of the P(VDF-TrFE-CTFE) terpolymer modified with various amounts of sodium azide is shown in **Figure 2-1**, where two new peaks appear. The first peak is at 2100 cm^{-1} that corresponds to the desired azido groups, while the second is at 1680 cm^{-1} and corresponds to backbone unsaturation. The equivalents of NaN_3 mentioned below correspond to the total number of repeating units of the fluoropolymer.

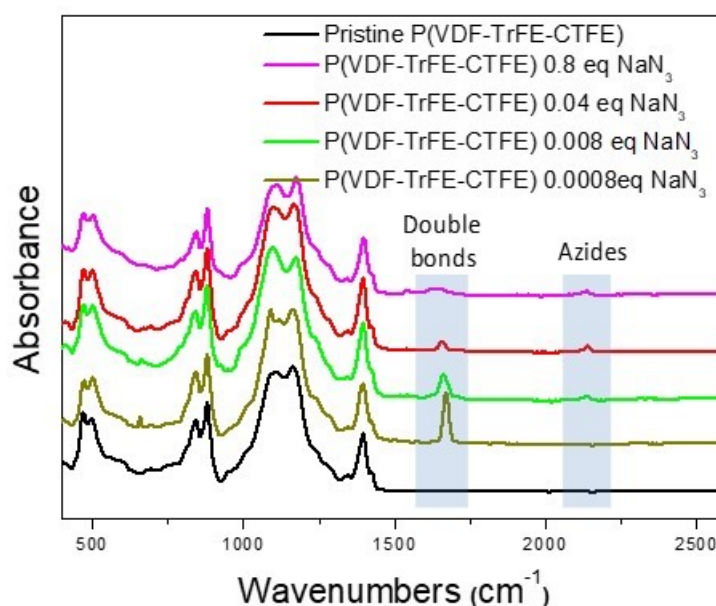
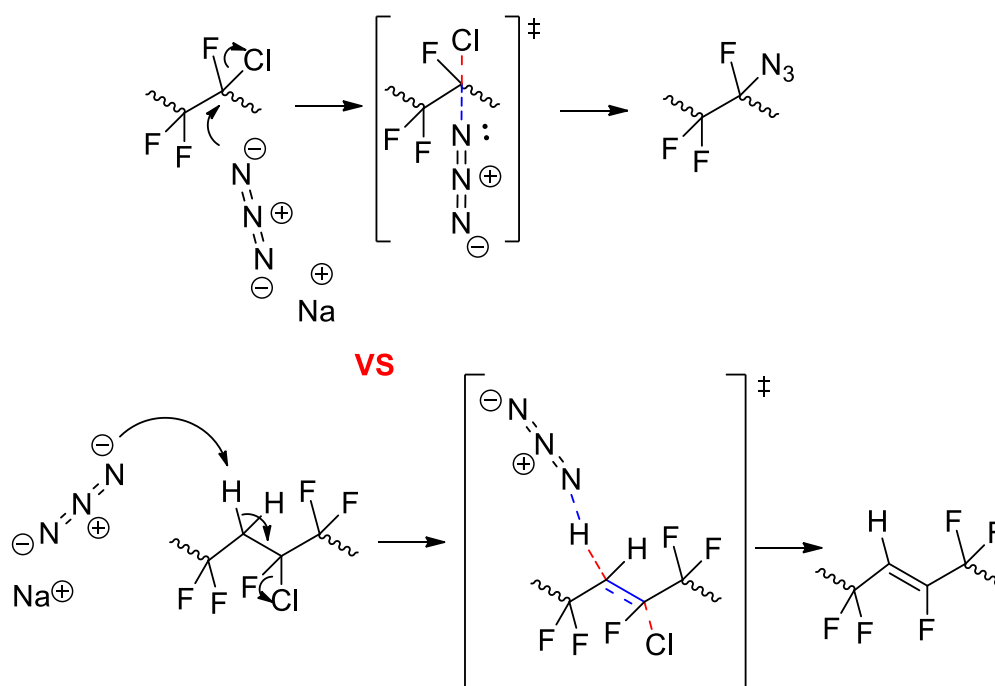


Figure 2-1. ATR FT-IR spectra of P(VDF-TrFE-CTFE) (61.8/30.4/7.8) mol before reaction with sodium azide (black) and after reaction with different amounts of sodium azide with respect to the total number of repeating units.

As mentioned above, except for the expected substitution reaction that leads to azide functionalization of the polymer an additional band at 1680 cm^{-1} appeared due to double bond formation on the polymer backbone. That indicates the competition between the substitution reaction leading to the desired azido functionalized polymer through an $\text{S}_{\text{N}}2$ mechanism, and the elimination reaction leading to the formation of

double bonds on the polymer backbone through an E2 mechanism, due to the basic nature of the used sodium azide. Both pathways are shown in **Scheme 2-2**.



Scheme 2-2. Mechanism of the substitution (up) and the elimination reaction (down) reaction of sodium azide with P(VDF-TrFE-CTFE) terpolymer.

In order to confirm our hypothesis about the existence of the competing pathways we used Nuclear magnetic resonance (NMR) spectroscopy. That because the IR peak at 1680cm^{-1} could also be due to a variety of other reasons such as residues of the solvent used for the modification reaction (DMF) which contains carbonyl groups. The ^1H NMR spectra of the pristine and the azide modified P(VDF-TrFE-CTFE) terpolymer is shown in **Figure 2-2**. The double bonds appeared on the azide modified polymer, with a signal at 6-6.5 ppm. The other signals on the ^1H NMR spectra, which appeared both for the pristine and the modified polymer are the following:

1. The protons of the trifluoroethylene group at 5-5.7 ppm
2. The protons from the regular VDF-VDF additions at 2.5-3.5 ppm
3. The protons from the inverse VDF-VDF additions at 2.2-2.5 ppm

It was observed that the shoulder at 3.3ppm, which corresponds to the VDF-CTFE sequences greatly decreases in intensity after the azide modification (**Figure 2-2**), which shows the consumption of the CTFE groups.

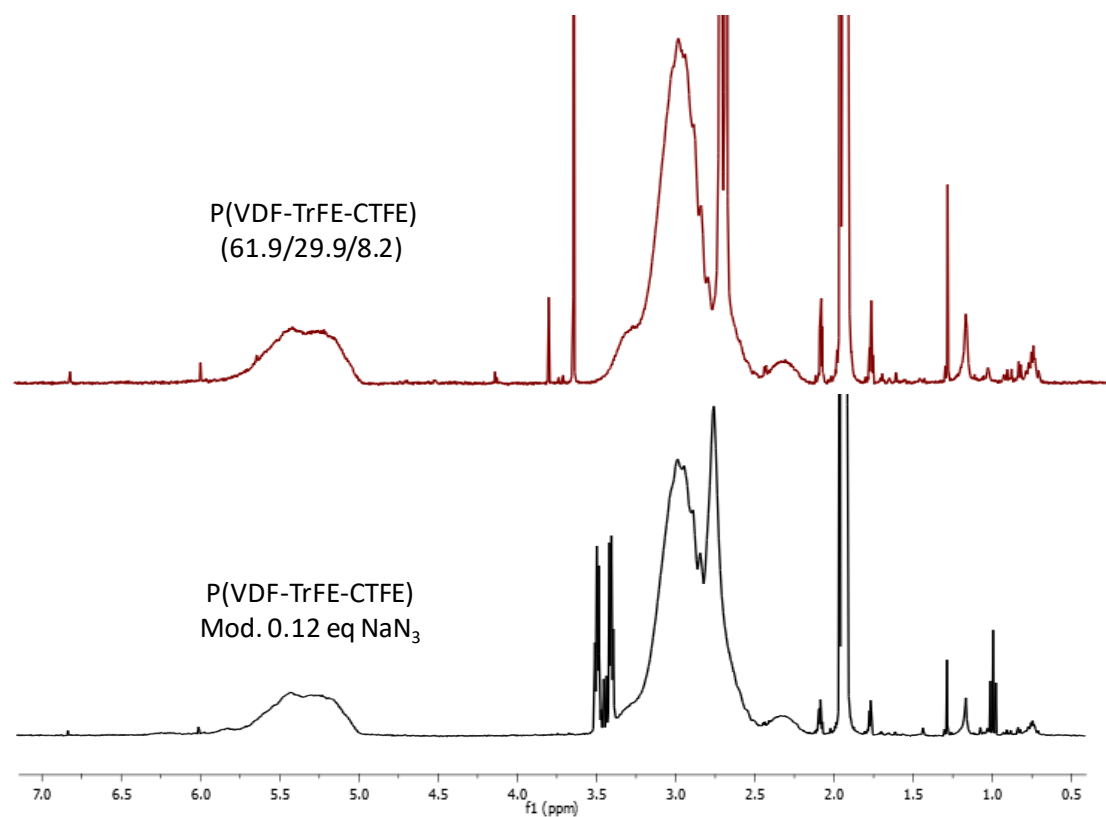
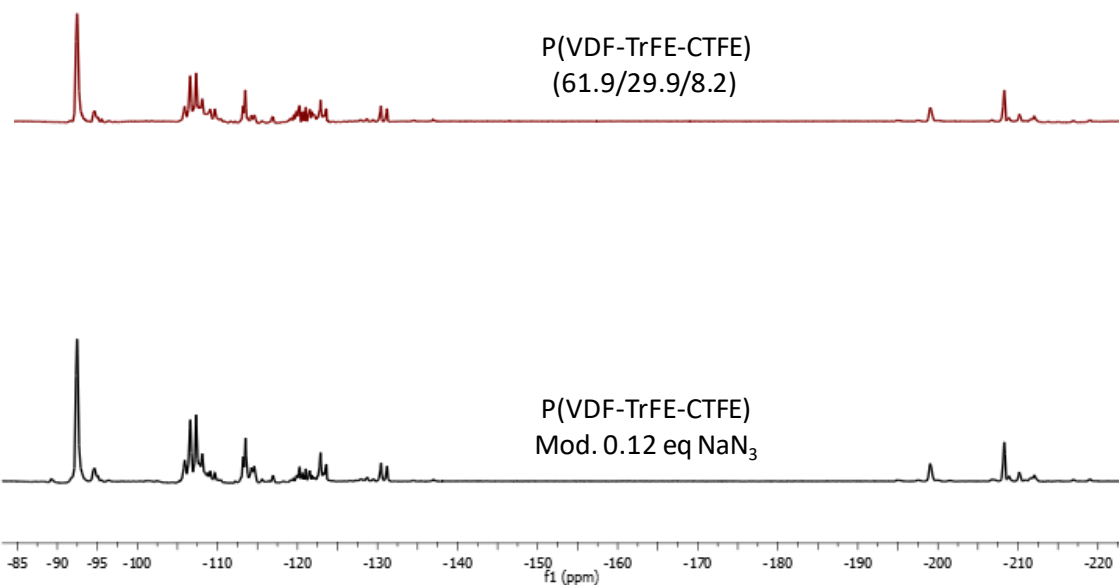


Figure 2-2. ¹H NMR spectra (in acetone D₆) of the P(VDF-TrFE-CTFE) (61.9/29.9/8.2) mol before and after reaction with sodium azide.

The same materials were also characterized by ¹⁹F NMR, where more information can be obtained. The created double bonds after the azide modification appeared at -89 ppm as shown in **Figure 2-3** and **Figure 2-4**, but since the spectra were rather complex tables from literature were used for the interpretation of the signals. Such table is presented in **Table 2-1**.

Table 2-1. Assignment of ^{19}F NMR signals for $P(\text{VDF-TrFE})$ in 3C and 5C sequences¹⁰.

3C Sequence	5C Sequence	Designation	Chemical Shift (ppm)
	$\text{CF}_2\text{CH}_2\text{CF}_2\text{CH}_2\text{CF}_2$	<u>VDF</u> -VDF, H-T	-92.4
<u>CH₂CF₂CH₂</u>	$\text{CH}_2\text{CH}_2\text{CF}_2\text{CH}_2\text{CF}_2$	VDF- <u>VDF</u> -VDF, T-T / H-T TrFE-	-94.9 to -97.1
	$\text{CHFCH}_2\text{CF}_2\text{CH}_2\text{CF}_2$	<u>VDF</u> -VDF, H-T / H-T	-93.8 to -94.9
<u>CH₂CF₂CHF</u>	$\text{CF}_2\text{CH}_2\text{CF}_2\text{CHFCH}_2$	<u>VDF</u> -TrFE H-T	-107.0
<u>CH₂CF₂CF₂</u>	$\text{CF}_2\text{CH}_2\text{CF}_2\text{CF}_2\text{CHF}$	VDF- <u>VDF</u> -TrFE, H-T / H-H	-113.5
	$\text{CH}_2\text{CH}_2\text{CF}_2\text{CF}_2\text{CH}_2$	VDF- <u>VDF</u> -VDF, T-T / H-H	-116.6
	$\text{CF}_2\text{CH}_2\text{CF}_2\text{CF}_2\text{CH}_2$	VDF- <u>VDF</u> -VDF, H-T / H-H	-120.4
<u>CHFCF₂CHF</u>	$\text{CF}_2\text{CHFCF}_2\text{CHFCF}_2$	<u>TrFE</u> -TrFE, H-T	-122.9
	$\text{CH}_2\text{CHFCF}_2\text{CHFCF}_2$	VDF- <u>TrFE</u> -TrFE, T-T / H-T	-123.7
<u>CHFCF₂CF₂</u>	$\text{CH}_2\text{CHFCF}_2\text{CF}_2\text{CH}_2$	<u>TrFE</u> -VDF, H-H	-130.4
	$\text{CHFCF}_2\text{CHFCF}_2\text{CHF}$	<u>TrFE</u> -TrFE, T-H	-210.1 to -212.1
<u>CF₂CHF</u> CF ₂	$\text{CF}_2\text{CF}_2\text{CHFCF}_2\text{CHF}$	<u>TrFE</u> -TrFE, H-H / T-H	-199.0
	$\text{CH}_2\text{CF}_2\text{CHFCF}_2\text{CH}_2$	<u>TrFE</u> -VDF, T-H	-200.3
<u>CF₂CHF</u> CHF	$\text{CF}_2\text{CF}_2\text{CHFCF}_2\text{CHFCF}_2$	VDF- <u>TrFE</u> -TrFE, H-H / T-T	-216.9 to -218.9

**Figure 2-3.** ^{19}F NMR of the $P(\text{VDF-TrFE-CTFE})$ (61.9/29.9/8.2) mol before and after reaction with sodium azide.

Since the differences before and after the modification are quite subtle in the ^{19}F -NMR, the area of interest from **Figure 2-3** is enlarged and presented in **Figure 2-4**, where the changes upon modification become more apparent. A new peak appears at the -90 ppm regime, which corresponds, to the newly formed double bonds.

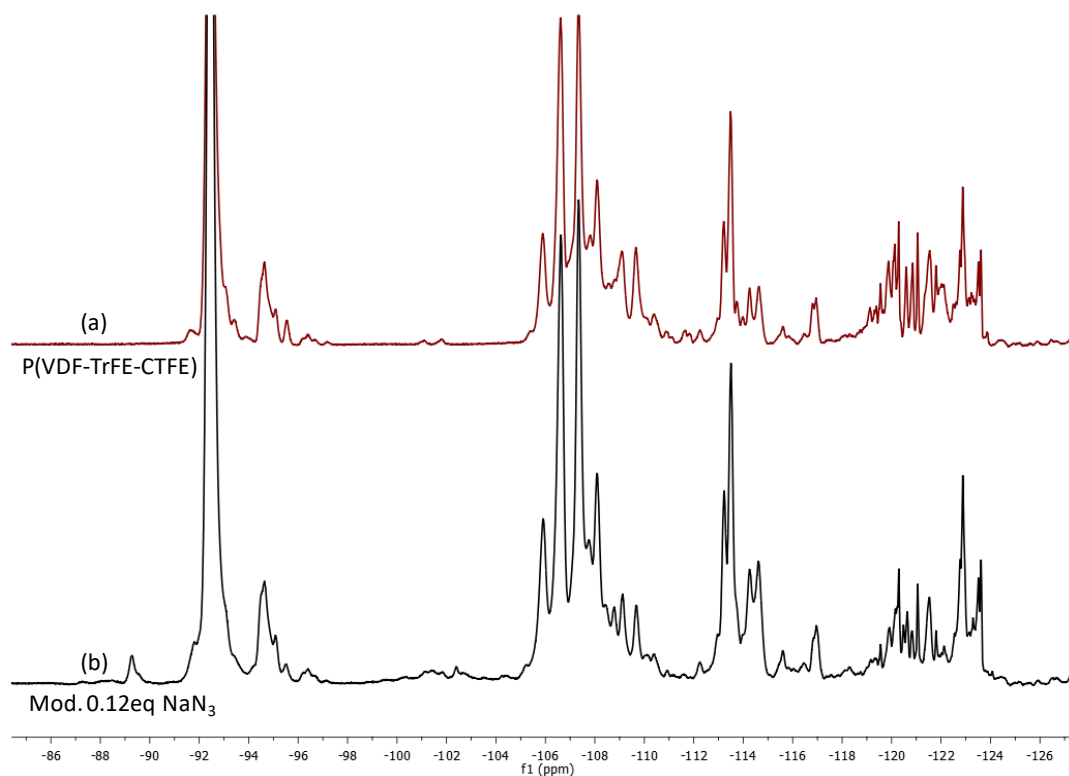


Figure 2-4. Amplification of **Figure 2-3**, ^{19}F NMR of the P(VDF-TrFE-CTFE) (61.9/29.9/8.2) mol before and after reaction with sodium azide.

2.2.2) Effect of the grafting on the crystallinity

In a first approach, the azide modified terpolymers were thermally cross-linked. Therefore differential scanning calorimetry (DSC) was employed in order to evaluate the effect that the modification and the subsequent cross-linking have on the polymer crystallinity (**Figure 2-5**). As expected, the cross-linking broadens the melting and crystallization peaks, shifting them at lower temperatures and at the same time decreases their intensity, while at a certain feeding ratio of sodium azide (0.8 eq, **Figure 2-5**), the polymer loses its semicrystalline nature as neither melting nor crystallization peaks can be observed. These results indicate that cross-linking leads to the lowering of the total crystallinity of the modified polymers, while broadening the crystal size distribution. The reaction conditions had to be fine-tuned in order to

induce photopatternability through the azido groups all in maintaining the relaxor ferroelectric and dielectric properties of the terpolymer.

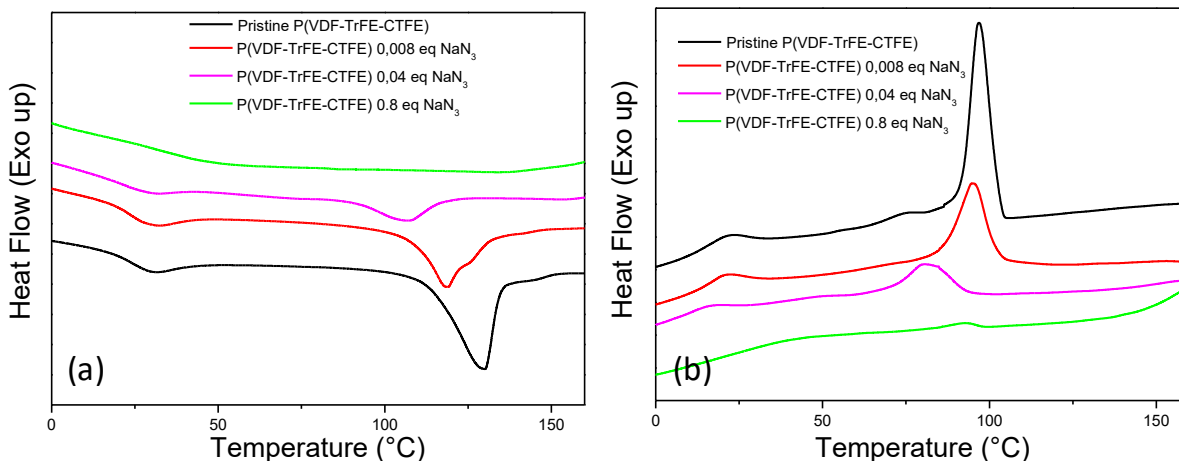


Figure 2-5. Differential scanning calorimetry thermograms comparing the pristine P(VDF-TrFE-CTFE) terpolymer with terpolymers modified with different amounts of sodium azide after thermal cross-linking at 80°C for 30 min. (a) 2nd heating, (b) 1st cooling.

Table 2-2. Melting temperature and the corresponding enthalpies calculated from the DSC thermograms (**Figure 2-4**) for thermally cross-linked terpolymers modified with different amounts of sodium azide.

	Melting transition	
	T (°C)	ΔH (J/g)
Pristine terpolymer	127.3	12
Terpolymer mod 0.008eq NaN₃	109.0	8
Terpolymer mod 0.04 eq NaN₃	107.1	4
Terpolymer mod 0.8 eq NaN₃	-	-

Since the azide groups can be activated either photochemically or thermally, an attempt was made to monitor the thermal cross-linking during a DSC ramp. To do so, the pristine and modified polymers were casted directly on the DSC capsule in order to ensure good contact and then the first heating was monitored for those polymers. As we can see in **Figure 2-6** the thermal cross-linking becomes apparent as an exotherm peak, however no quantitative conclusions could be drawn, since there is overlapping of the cross-linking exotherm and the melting endotherm peaks. It is nevertheless apparent that the polymer modified with 0.04 eq NaN₃ contains much more azido groups than the polymer modified with 0.008 eq of NaN₃, since the cross-linking

exotherm is much more pronounced.

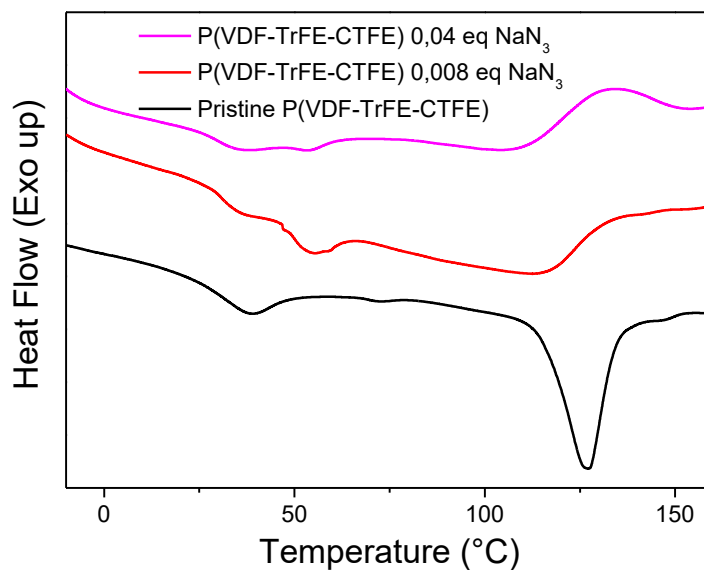


Figure 2-6. Differential scanning calorimetry thermograms comparing the first heating of THF casted films of the pristine P(VDF-TrFE-CTFE) terpolymer with terpolymers modified with different amounts of sodium azide.

Films of the azide modified terpolymer were compared to films of the pristine terpolymer by Atomic Force Microscopy (AFM) in tapping mode. The large crystal grains of the pristine P(VDF-TrFE-CTFE) (**Figure 2-7a, b**) disappear for the azide modified terpolymer (**Figure 2-7c, d**), making the surface of the latter considerably smoother.

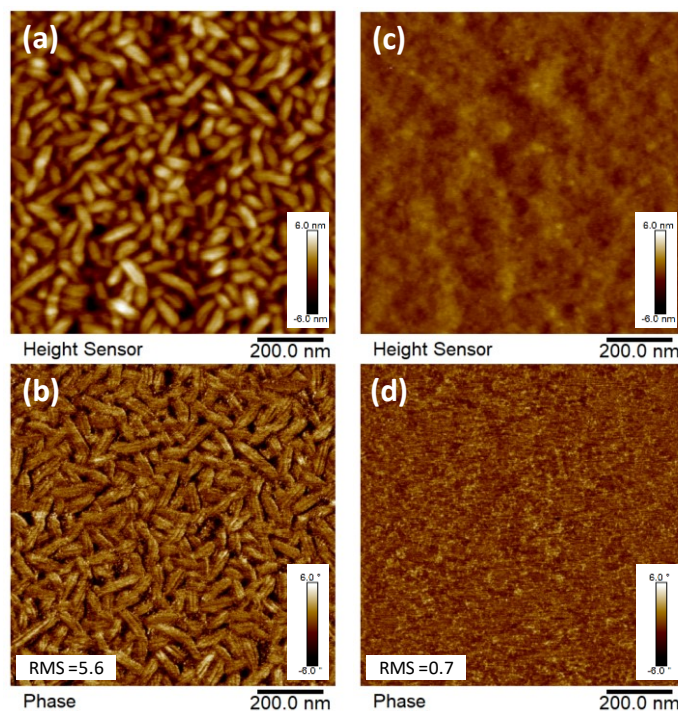


Figure 2-7. AFM images of the height (a, c) and phase (b, d) comparing the pristine terpolymer (left) to the azide-grafted terpolymer with 0.06 eq NaN_3 (right).

The root mean squared roughness (RMS) of the two polymers was reduced from 5.6 nm to 0.7 nm, as calculated from 50 μm AFM scans, which are shown in **Figure 2-8**.

Such feature makes the azide modified polymers better candidates for gate dielectrics in OFETs, as smoother interface between the gate dielectric and the organic semiconductor leads to better performing OFETs¹¹⁻¹².

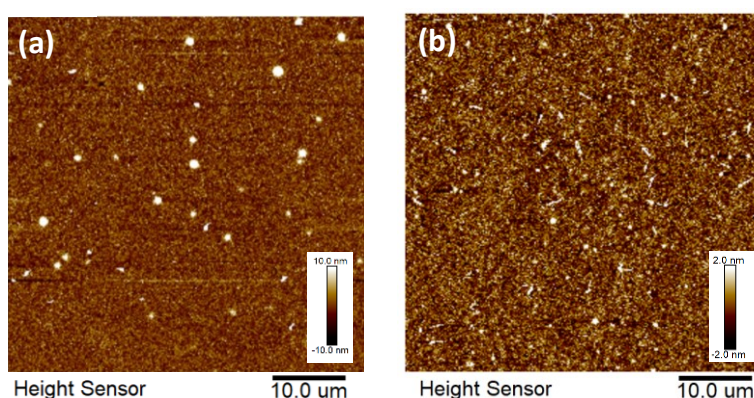
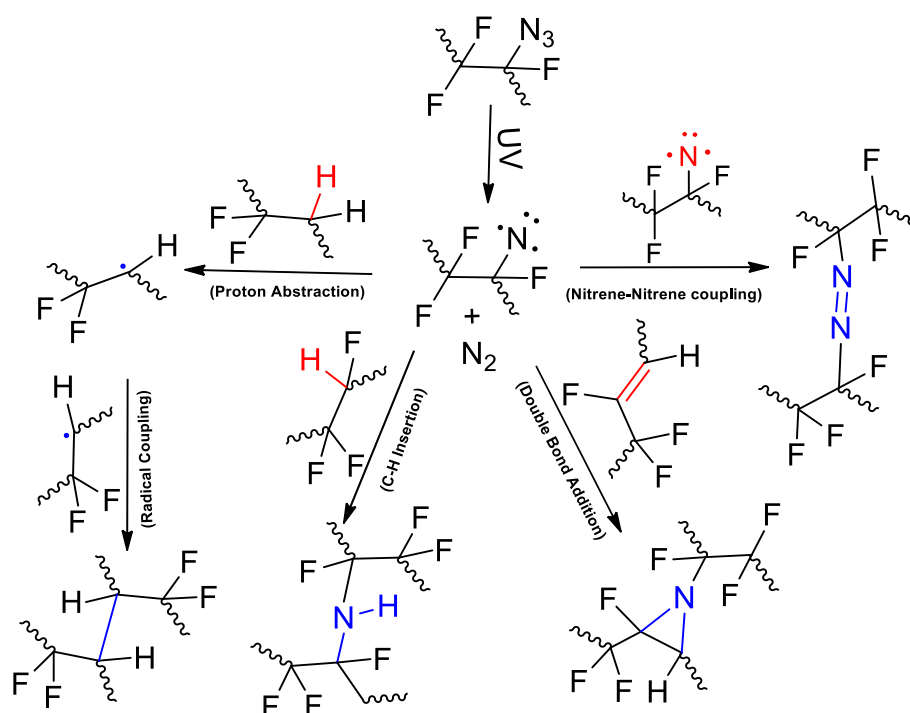


Figure 2-8. Height AFM images comparing the pristine terpolymer (left) to the azide-grafted terpolymer with 0.06 eq NaN_3 (right).

2.2.3) Photochemical cross-linking of FEPs with pendent Azido groups

As mentioned before, the reason azido groups were grafted on the P(VDF-TrFE-

CTFE), was to make the terpolymer cross-linkable upon irradiation with UV light in order to make it possible to use such materials as negative photoresists in photolithographic processes. When a polymer containing azide groups is either exposed at UV light or heated at high temperatures, the azido groups release nitrogen and form some very reactive free radical intermediated that are called nitrenes (**Scheme 2-3** middle). Those nitrenes can then react almost with any chemical species that exists in their surroundings, with some of the reactions leading to cross-linking of the polymer and that is why azide groups are generally called universal cross-linkers. Those reactions are described in **Scheme 2-3** and the most favorable of them is the addition of nitrenes on double bonds, since double bonds are known to act as radical traps as described in the introduction of this thesis. However, there are two other very likely pathways, such as the hydrogen abstraction caused by the nitrene, leading to a free radical formation on the polymer backbone with neighboring free radicals being able to recombine leading to cross-linking reaction. The other very likely pathway is the C-H insertion reactions that nitrenes can cause, leading to direct cross-linking of the polymer with the formation of secondary amines. The last and much less likely pathway is the nitrene-nitrene coupling that can also lead to cross-linking, however the chance that two activated nitrenes will be in special proximity is very low, making that reaction very unlikely to occur.



Scheme 2-3. Reaction pathways that lead to the cross-linking of the azide modified terpolymer upon UV irradiation.

The UV-Vis absorption of the azide modified polymers was also investigated. In order to avoid substrate resonance at the deep UV regime, self standing films of the azide modified terpolymer were prepared and the absorption spectrum is shown in **Figure 2-9**. The polymer absorbs strongly in deep UV with absorption up to 300nm.

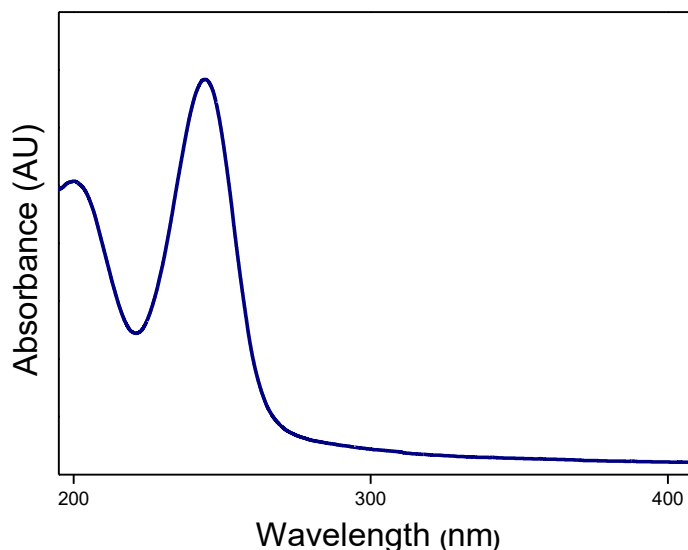


Figure 2-9. UV-Vis absorption spectra of P(VDF-TrFE-CTFE) terpolymer film functionalized with azido groups.

2.2.4) Photolithographic patterning of FEPs with pendent Azido groups

In order to use the synthesized polymers in a photolithographic process, the design of appropriate protocols was necessary. A large number of parameters had to be carefully tuned in order to obtain good quality patterning, with low thickness loss and at low UV dose. The different steps for a photolithographic process are described in **Figure 2-10** and are:

1. Spin coating of the azide grafted P(VDF-TrFE-CTFE) on a substrate such as a silicon wafer.
2. Soft Bake (SB) in order to remove residual solvent.
3. Selective exposure at UV light with a photolithographic mask under constant nitrogen flow.
4. Post Exposure Bake (PEB) for cross-linking propagation.
5. Development of the desired pattern by selective dissolution of the non exposed parts.
6. Rinsing with isopropanol in order to exchange the development solvent with a bad solvent for the polymer.

7. Air drying.

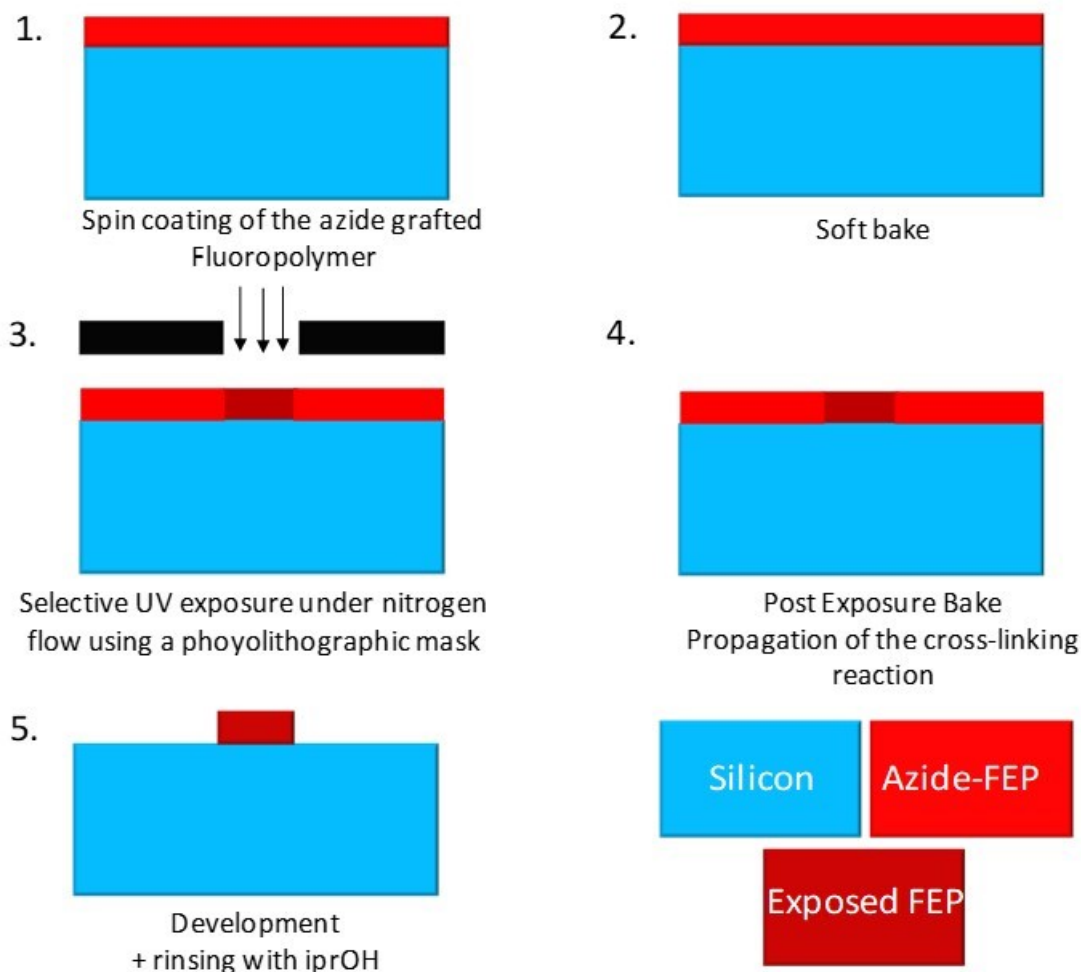


Figure 2-10. Schematic representation of the photolithographic patterning process step by step.

In order to develop appropriate protocols for the patterning of the azide modified P(VDF-TrFE-CTFE) we started from the simplest protocol possible. First, we baked the spin-coated polymers in different temperatures for 5 minutes and discovered that once the polymer is baked at temperature above 60°C the polymer becomes thermally cross-linked and it's impossible to be removed. That set the baking temperature at 60°C. Then different solvents were screened as shown in **Figure 2-11**. Those solvent were acetone, cyclopentanone and 2-butanone (MEK), which are known to be good solvents for the P(VDF-TrFE-CTFE) terpolymer. The UV doses that had been used at this stage were extremely high, since no patterning could be achieved at doses below 6J/cm². That was a very important step as it showed that photo-patterning was possible using those polymers, but the quality of the patterned films was very poor (**Figure 2-11**) with signs of overexposure in almost all films.

A. Effect of the dose and the developing solvent

Protocol (I)

- 1) Spincoating 4% solution of azide modified polymer @ 1000 rpm
- 2) Soft baking @ 60°C for 5 min
- 3) Exposure @ different doses from 6 J/cm² to 20 J/cm²
- 4) Developing @ RT for 1 min in different solvents

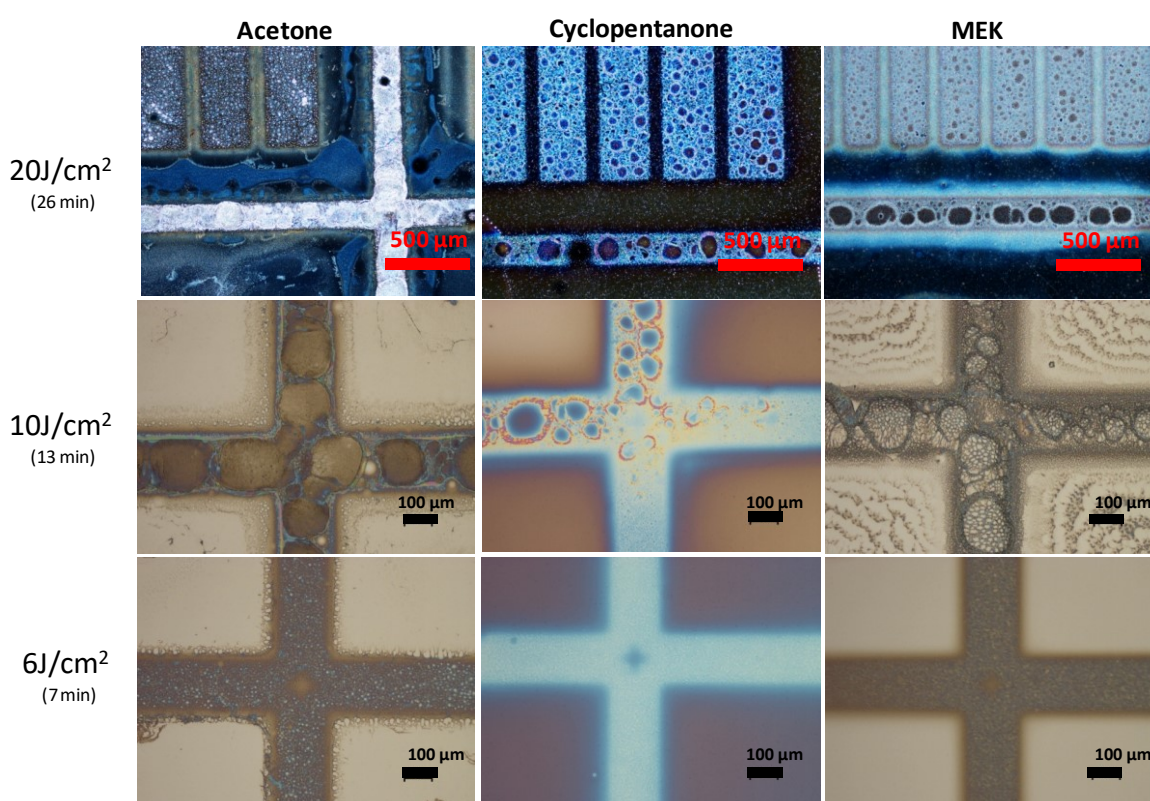


Figure 2-11. Effect of various UV doses and development solvents on the quality of films of azide modified P(VDF-TrFE-CTFE) patterned on silicon substrate by a single photolithographic step, following Protocol (I).

From the general screening of different development solvents and different UV doses it was found that cyclopentanone is the most appropriate of the development solvents screened above and with lowering of the UV dose the film quality tends to improve. It has to be noted that at this point no air drying at the end of the process was possible since the swollen films would get totally detached from the silicon substrates.

B. Effect of the isopropanol rinsing after the development step

In order to be able to stop the development process instantly one more step was added to the above protocol, which was the rinsing with isopropanol of the film directly after the development step. In fact, isopropanol was chosen for its miscibility with cyclopentanone and its precipitating effect on fluoropolymers. By adding this step, the quality of the patterned films was significantly improved as shown in **Figure 2-12**.

Protocol (II)

- | | |
|----|--|
| 1) | Spincoating 4% solution of azide modified polymer @ 1000 rpm |
| 2) | Soft baking @ 60°C for 5 min |
| 3) | Exposure @ different doses |
| 4) | Developing with cyclopentanone @ RT for 1 min |
| 5) | Rinsing with isopropanol |

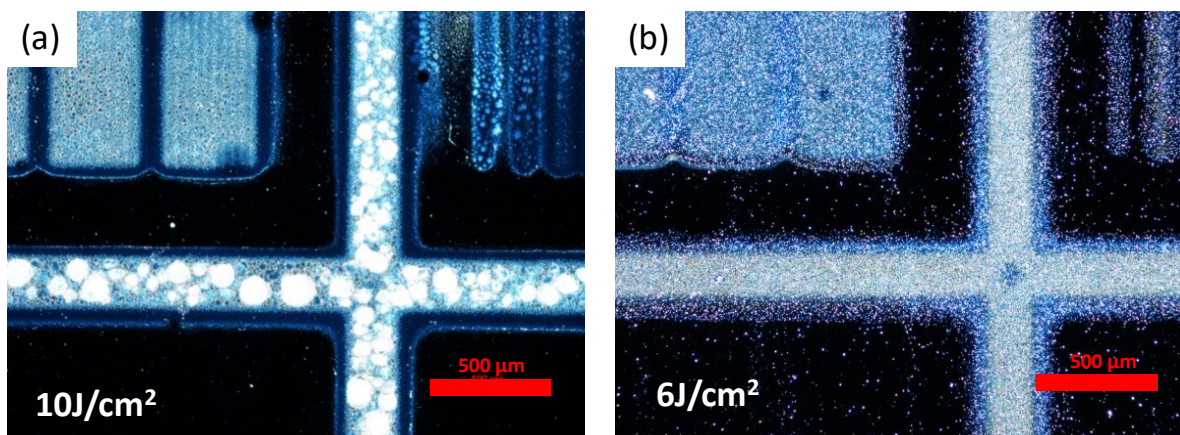


Figure 2-12. Azide modified P(VDF-TrFE-CTFE) on silicon substrate patterned through a single photolithographic step, following Protocol (II) for 2 different UV doses, 6J/cm² and 10J/cm².

C. Effect of the Nitrogen purging during exposure

The next parameter investigated in our protocol optimization process was to do the exposure in UV light under constant nitrogen flow, with the double objective to prevent side reactions of the formed nitrene with oxygen from the atmosphere and to prevent the formation of ozone due to the exposure of oxygen in UV light. That improved the patterning quality even further and at this point, we were able to get the profile of the patterned films (**Figure 2-13c, f**). Except for the fact that the films were extremely

rough, the thickness loss was also very high, with more than 85% of the initial thickness lost during the development process.

Protocol (III)

- 1) Spincoating 4% solution of azide modified polymer @ 1000 rpm
- 2) Soft baking @ 60°C for 5 min
- 3) Exposure @ different doses under nitrogen flow
- 4) Developing with cyclopentanone @ RT for 1 min
- 5) Rinsing with isopropanol

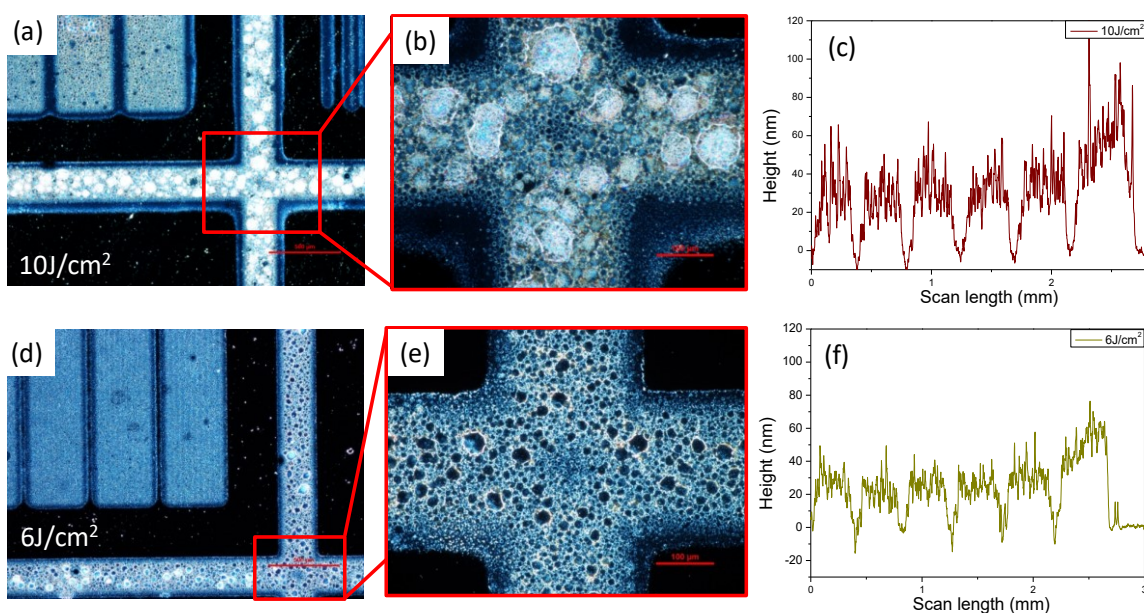


Figure 2-13. Azide modified $P(VDF-TrFE-CTFE)$ on silicon substrate patterned through a single photolithographic step, following Protocol (III) for 2 different UV doses, $6J/cm^2$ and $10J/cm^2$.

D. Effect of the Post exposure Baking (PEB) step and air drying

The next step was to add a post exposure baking step in our patterning process. That allowed us to lower the UV dose at the desired level ($2J/cm^2$), significantly decreasing the thickness loss to less than 40% of the initial thickness and greatly improving the patterning quality (**Figure 2-14**). At this step air drying of the films was also made possible in the end of the process.

Protocol (IV)

- 1) Spincoating 4% solution of azide modified polymer @ 1000 rpm
- 2) Soft baking @ 60°C for 5 min
- 3) Exposure @ different doses under nitrogen flow
- 4) Post exposure baking @ 60°C for 5 min
- 5) Developing with cyclopentanone @ RT for 1 min
- 6) Rinsing with isopropanol
- 7) Air drying

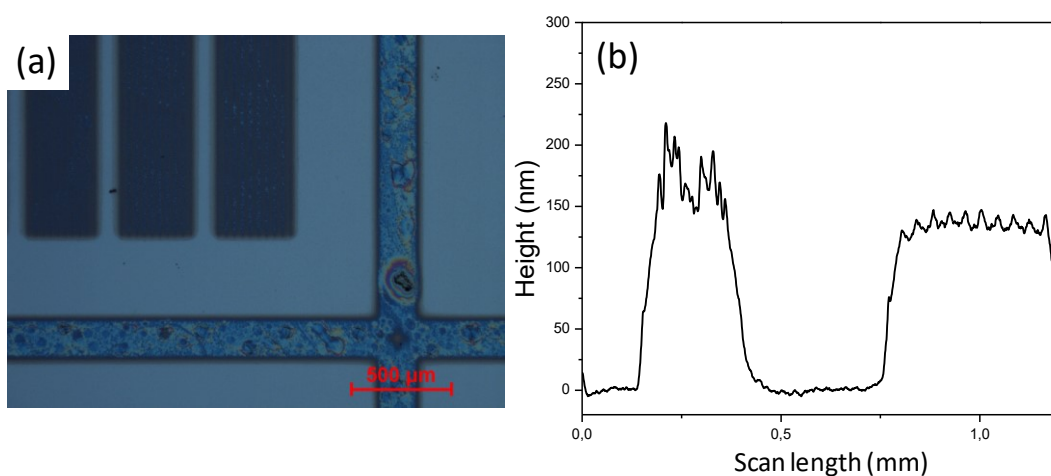


Figure 2-14. (a) Azide modified P(VDF-TrFE-CTFE) on silicon substrate patterned through a single photolithographic step, following protocol (IV). (b) Measurement of the film roughness using mechanical profilometer.

E. Effect of the Development in solvent/non-solvent blend

Although we had previously chosen cyclopentanone as the developing solvent that gives the best quality patterned films, the observed roughness of the films shown in **Figure 2-15 b** indicated that a softer development process could be beneficial for the patterning quality. Since the development time could not be further reduced, as it was already as low as 1 min, we tried to develop under milder conditions for the same time intervals, by blending the development solvent (cyclopentanone) with a bad solvent for the fluoropolymers (isopropanol). The first mixture used was 50/50 by volume and the results appeared to be very beneficial for the patterning quality (**Figure 2-15**) with the observed surface roughness being reduced as well (**Figure 2-15**).

Protocol (V)

- 1) Spincoating 4% solution of azide modified polymer @ 1000 rpm
- 2) Soft baking @ 60°C for 5 min
- 3) Exposure @ 2J/cm² under nitrogen flow
- 4) Post exposure baking @ 60°C for 5 min
- 5) Developing with mixture of isopropanol/cyclopentanone, 50/50 @ RT for 1 min
- 6) Rinsing with isopropanol
- 7) Air Drying

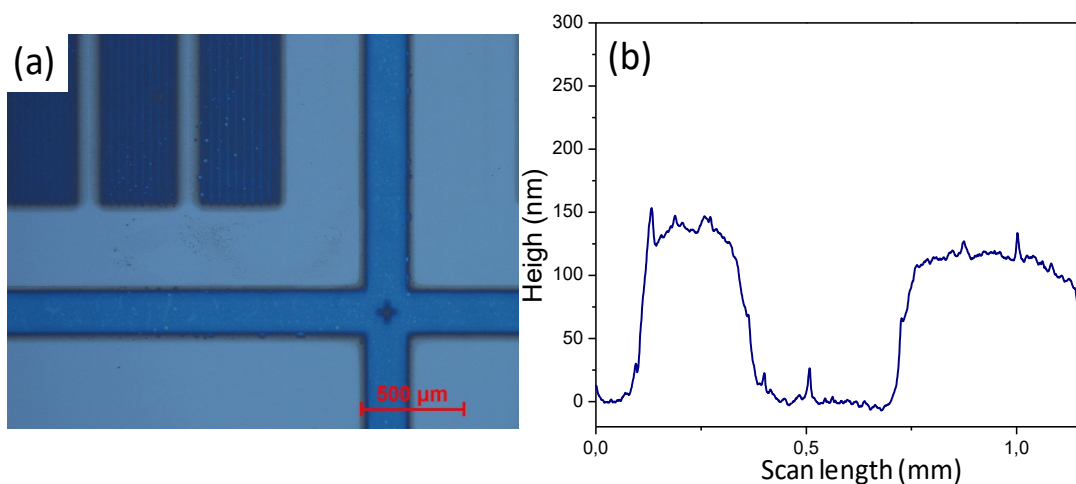


Figure 2-15. (a) Azide modified P(VDF-TrFE-CTFE) on silicon substrate patterned through a single photolithographic step, following protocol (V). (b) Measurement of the film roughness using mechanical profilometer.

In an attempt to obtain even smoother patterned films, the bad solvent ratio was further increased to 70/30, keeping all other parameters constant. The patterned films obtained with that protocol were extremely smooth with an average surface roughness less than 5 nm as accessed both by mechanical profilometry (**Figure 2-16b**) and a 30 μm AFM scan (**Figure 2-17**). The quality of the patterned films as appears in the optical microscope also appeared to be very good with no apparent defects and sharp edges (**Figure 2-16a**).

Protocol (VI)

- 1) Spincoating 4% solution of azide modified polymer @ 1000 rpm
- 2) Soft baking @ 60°C for 5 min
- 3) Exposure @ 2J/cm² under nitrogen flow
- 4) Post exposure baking @ 60°C for 5 min
- 5) Developing with mixture of isopropanol/cyclopentanone, 70/30 @ RT for 1 min
- 6) Rinsing with isopropanol
- 7) Air Drying

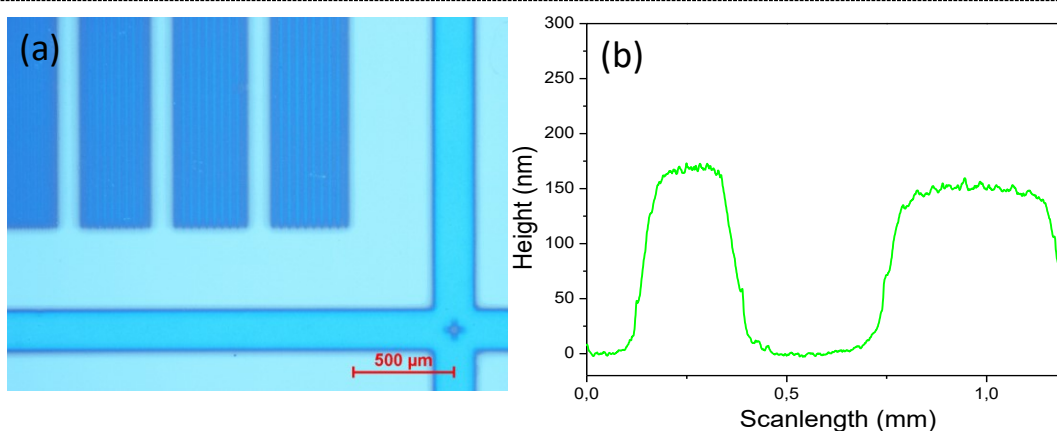


Figure 2-16. (a) Azide modified P(VDF-TrFE-CTFE) on silicon substrate patterned through a single photolithographic step, following protocol (VI). (b) Measurement of the film roughness using mechanical profilometer.

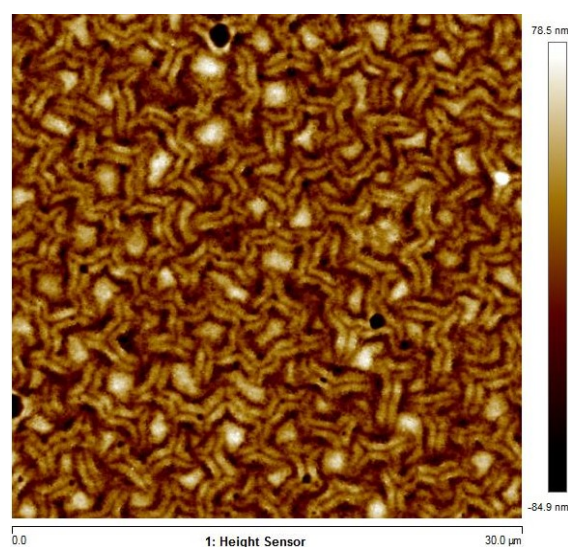
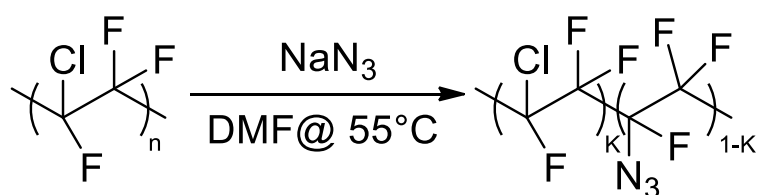


Figure 2-17. AFM image (height) of the patterned film of the azide containing P(VDF-TrFE-CTFE) terpolymer, following the optimized protocol (VI).

Excellent quality patterned films were obtained as shown in **Figure 2-16** at low UV dose after fine tuning all the protocol parameters.

2.2.5) Blank tests on PCTFE and P(VDF-TrFE)

To verify that the substitution during the azidation occurs only in the CTFE groups, two blank tests were performed. The former test was the reaction of PCTFE homopolymer with sodium azide, in which the reaction was successful, as a very intense band at 2100 cm^{-1} appeared, indicating the strong presence of azido groups (**Figure 2-18**). The reaction is shown in **Scheme 2-4**. This reaction was successful despite the very limited solubility of the PCTFE homopolymer in the used solvent (DMF).



Scheme 2-4. Azidation reaction of PCTFE homopolymer, in DMF at 55°C overnight, using 0.25 and 0.75 eq of sodium azide.

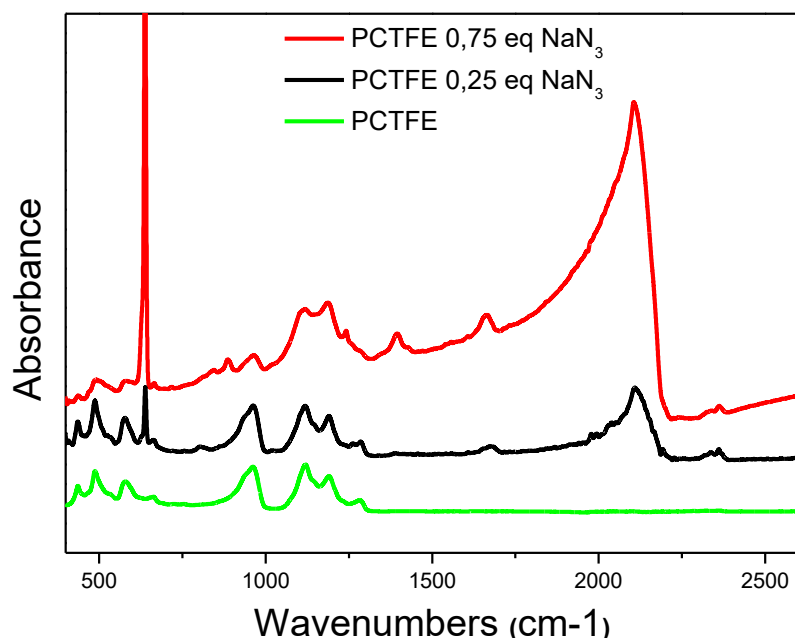
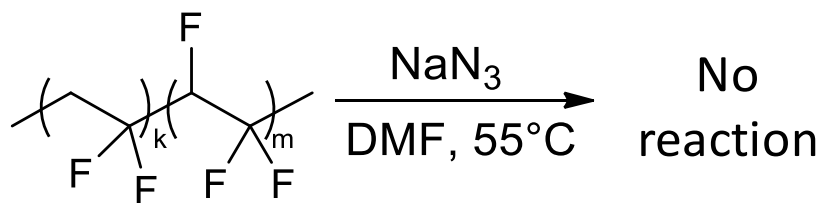


Figure 2-18. ATR-IR spectra of PCTFE before reaction with sodium azide (green) and after reaction with 0.25 eq of sodium azide (black) and 0.75 eq of sodium azide (red).

We also tested the reaction of P(VDF-TrFE) copolymer with sodium azide (see **Scheme 2-5**), in which no reaction took place, as no band correlated to the azido group appeared in the IR spectrum after the reaction (**Figure 2-19**).



Scheme 2-5. Azidation reaction attempt on P(VDF-TrFE) copolymer, in DMF at 55°C overnight, using 0.04 eq of sodium azide.

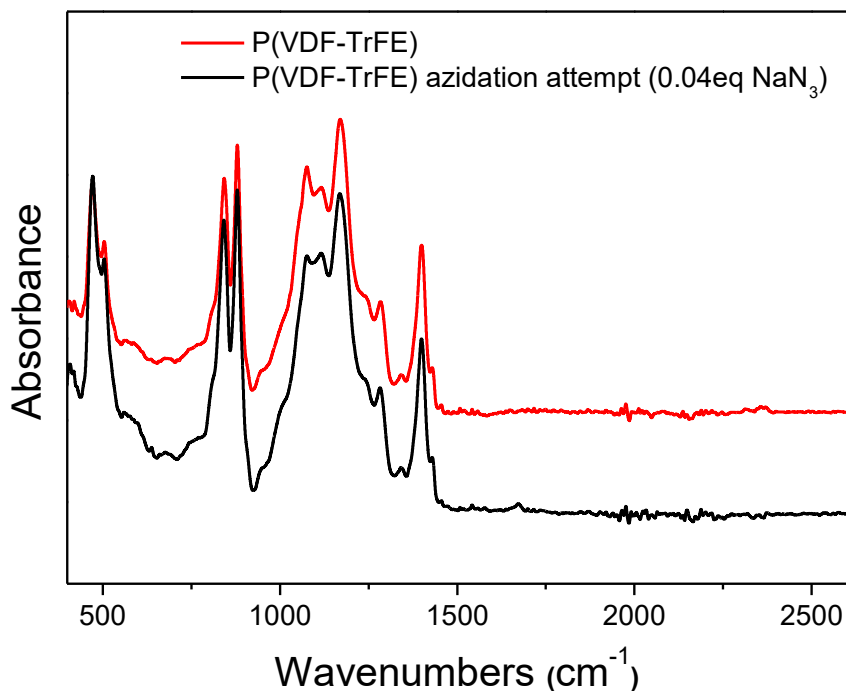


Figure 2-19. ATR-IR spectra of P(VDF-TrFE) (75/25 mol) before reaction with sodium azide (red) and after reaction with sodium azide (black)

The combination of the two attempts of azidation provides us with convincing evidence that the azidation reaction is selective to the CTFE groups alone, due to the nature of the chlorine, which behaves like a good leaving group.

2.2.6) Surface tension characterization

Contact angle measurements on the cross-linked and pristine polymers show a decrease of the dispersive/polar surface tension ratio from 16.9 of the pristine polymer down to 2.5 of the cross-linked polymer modified with 0.04 eq of NaN₃. That indicates that the adhesion of the cross-linked polymer should be better than the one of the pristine polymer on common substrates such as silicon and glass, as well as aluminium, which is used as the electrode. The contact angle measurement data are

presented in Table 2-3.

Table 2-3. Surface tensions of P(VDF-TrFE-CTFE) terpolymers modified with different amounts of sodium azide, compared to substrates such as glass and silicon and aluminium electrodes.

Modified polymer	Surface Tension (mN/m)	Dispersive Surface Tension (mN/m)	Polar Surface Tension (mN/m)	Dispersive/Polar ratio
Pristine terpolymer	35.4 ± 0.2	33.4 ± 0.2	2.0 ± 0.0	16.9
Terpolymer mod 0.04 eq NaN ₃	38.9 ± 0.2	32.8 ± 0.1	6.2 ± 0.1	5.3
Terpolymer mod 0.04 eq NaN ₃ - CL	36.4 ± 0.1	26.1 ± 0.0	10.3 ± 0.1	2.5
Terpolymer mod 0.8 eq NaN ₃	40.4 ± 0.2	32.0 ± 0.1	8.4 ± 0.1	3.8
Terpolymer mod 0.8 eq NaN ₃ - CL	41.8 ± 0.5	26.8 ± 0.2	15.0 ± 0.3	1.8
Silicon	64.4 ± 0.3	34.1 ± 0.1	30.3 ± 0.2	1.1
Glass	56.2 ± 0.2	31.7 ± 0.1	24.5 ± 0.1	1.3
Aluminium	64.9 ± 0.7	34.1 ± 0.4	30.8 ± 0.3	1.1

2.3) Experimental Part

Synthesis. A typical modification reaction was done using standard schlenk techniques. P(VDF-TrFE-CTFE) (61.9, 29.9, 8.2) (4 g, 4.5 mmol of CTFE) and NaN₃ (0.21 g, 3.2 mmol) were mixed and degassed in DMF (170 ml). The glass schlenk was sealed under argon and heated to 55°C in the dark for 16 hours. The solvent was then evaporated under reduced pressure and the polymer was washed with DI water and ethanol, re-dissolved in acetone and dialyzed (13 kDa membrane cutoff) to remove remaining traces of salt. Then it was dried in vacuum oven at 40°C for 12 hours.

Preparation of patterned thin films. A 4% wt solution of the modified polymer in cyclopentanone was spincoated on a silicon wafer at 500 rpm for 5 sec and then at 1000 rpm for 1 min, yielding a 250 nm thick film. The wafer was soft baked before exposure at 60°C for 5 min and subsequently cross-linked by UV light under nitrogen, using a photo-lithographic mask. Different UV doses were applied, varying from 0.5 to 20J/cm². Then, the film was post exposure baked at 60°C for 5 min. Finally, the

patterned film was developed in a blend of one-third cyclopentanone and two thirds isopropanol for 1 min. Subsequently, the wafer was rinsed with isopropanol and dried with compressed air.

2.4) Conclusions

Photopatternable fluoropolymers were synthesized by a single step grafting reaction of azido groups on commercially available P(VDF-TrFE-CTFE). The azide containing polymers were subsequently used in a photolithographic process as negative photoresists, yielding excellent quality films at low UV doses. In addition, the cross-linked polymers yield films with significantly lower roughness than the pristine ones, making them excellent candidates for gate dielectrics in OFETs. The dielectric and ferroelectric properties of the abovementioned polymers are discussed in detail in **Chapter 5**.

2.5) References

1. Breemen, A. J. J. M. v.; Putten, J. B. P. H. v. d.; Cai, R.; Reimann, K.; Marsman, A. W.; Willard, N.; Leeuw, D. M. d.; Gelinck, G. H., Photocrosslinking of ferroelectric polymers and its application in three-dimensional memory arrays. *Applied Physics Letters* **2011**, *98* (18), 183302.
2. Chen, X.-Z.; Li, Z.-W.; Cheng, Z.-X.; Zhang, J.-Z.; Shen, Q.-D.; Ge, H.-X.; Li, H.-T., Greatly Enhanced Energy Density and Patterned Films Induced by Photo Cross-Linking of Poly(vinylidene fluoride-chlorotrifluoroethylene). *Macromolecular Rapid Communications* **2011**, *32* (1), 94-99.
3. Bräse, S.; Gil, C.; Knepper, K.; Zimmermann, V., Organic Azides: An Exploding Diversity of a Unique Class of Compounds. *Angewandte Chemie International Edition* **2005**, *44* (33), 5188-5240.
4. Adhikari, J. M.; Gadinski, M. R.; Li, Q.; Sun, K. G.; Reyes-Martinez, M. A.; Iagodkine, E.; Briseno, A. L.; Jackson, T. N.; Wang, Q.; Gomez, E. D., Controlling Chain Conformations of High-k Fluoropolymer Dielectrics to Enhance Charge Mobilities in Rubrene Single-Crystal Field-Effect Transistors. *Advanced Materials* **2016**, *28* (45), 10095-10102.
5. Briseno, A. L.; Tseng, R. J.; Ling, M.-M.; Falcao, E. H. L.; Yang, Y.; Wudl, F.; Bao, Z., High-Performance Organic Single-Crystal Transistors on Flexible Substrates. *Advanced Materials* **2006**, *18* (17), 2320-2324.
6. Sundar, V. C.; Zaumseil, J.; Podzorov, V.; Menard, E.; Willett, R. L.; Someya, T.; Gershenson, M. E.; Rogers, J. A., Elastomeric transistor stamps: reversible probing of charge transport in organic crystals. *Science* **2004**, *303* (5664), 1644-6.
7. Bang, J.; Bae, J.; Löwenhielm, P.; Spiessberger, C.; Given-Beck, S. A.; Russell, T. P.; Hawker, C. J., Facile Routes to Patterned Surface Neutralization Layers for Block Copolymer Lithography. *Advanced Materials* **2007**, *19* (24), 4552-4557.
8. Reis Simas, E.; Kang, E. S. H.; Gassmann, A.; Katholing, E.; Janietz, S.; von Seggern, H., Cross-linkable random copolymers as dielectrics for low-voltage organic field-effect transistors. *Journal of Materials Chemistry C* **2015**, *3* (35), 9217-9223.
9. Albuszis, M.; Roth, P. J.; Pauer, W.; Moritz, H.-U., Two in one: use of azide functionality for controlled photo-crosslinking and click-modification of polymer microspheres. *Polymer Chemistry* **2016**, *7* (34), 5414-5425.
10. Soulestin, T.; Ladmiral, V.; Lannuzel, T.; Domingues Dos Santos, F.; Ameduri, B., Importance of Microstructure Control for Designing New Electroactive Terpolymers Based on Vinylidene Fluoride and Trifluoroethylene. *Macromolecules* **2015**, *48* (21), 7861-7871.
11. Roberts, M. E.; Queraltó, N.; Mannsfeld, S. C. B.; Reinecke, B. N.; Knoll, W.; Bao, Z., Cross-Linked Polymer Gate Dielectric Films for Low-Voltage Organic Transistors. *Chemistry of Materials* **2009**, *21* (11), 2292-2299.
12. Wang, C.; Lee, W.-Y.; Nakajima, R.; Mei, J.; Kim, D. H.; Bao, Z., Thiol-ene Cross-Linked Polymer Gate Dielectrics for Low-Voltage Organic Thin-Film Transistors. *Chemistry of Materials* **2013**, *25* (23), 4806-4812.
13. Yang, L.; Li, X.; Allahyarov, E.; Taylor, P. L.; Zhang, Q. M.; Zhu, L., Novel polymer ferroelectric behavior via crystal isomorphism and the nanoconfinement effect. *Polymer* **2013**, *54* (7), 1709-1728.
14. Zhang, Q. M.; Bharti, V.; Zhao, X., Giant Electrostriction and Relaxor Ferroelectric Behavior in Electron-Irradiated Poly(vinylidene fluoride-trifluoroethylene) Copolymer. *Science* **1998**, *280* (5372), 2101-2104.

Chapter 3

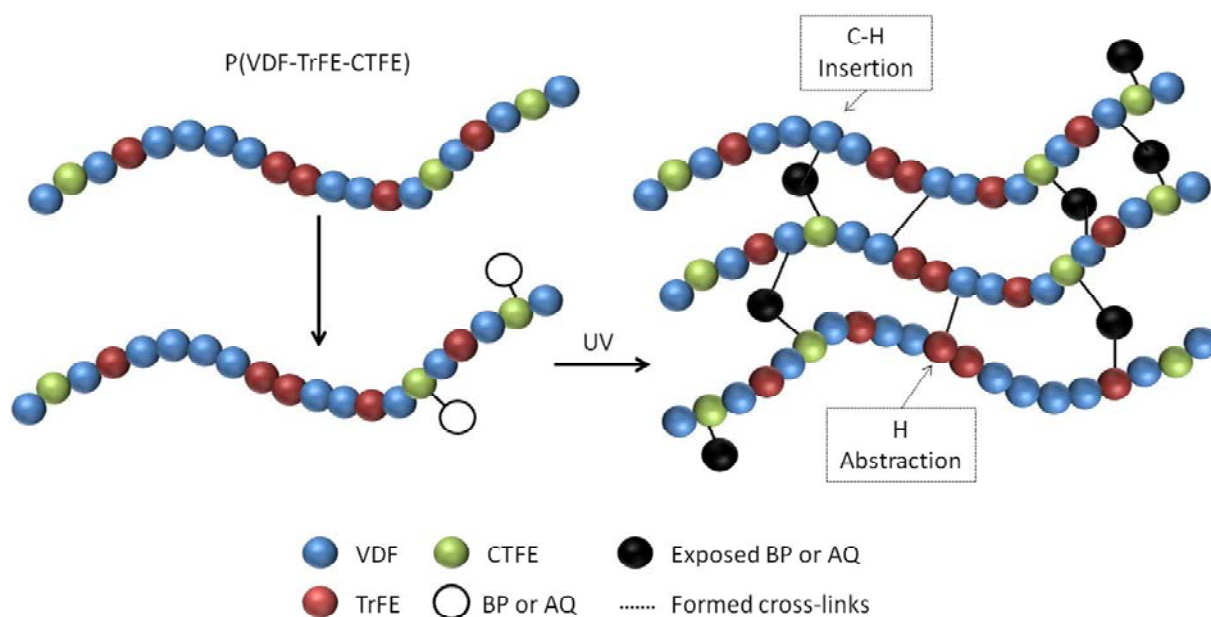
Chemical Modification of Fluoropolymers via Williamson Ether Synthesis

Chapter 3: Chemical modification of Fluoropolymers via Williamson Ether Synthesis

3.1) Introduction

In previous chapter, a facile way to induce photo-patternability to FEPs was presented, by introducing azide pendant groups directly on the fluoropolymer's backbone. Although this approach is quite inexpensive and straightforward, it presents some drawbacks regarding the polymer stability and the reduced dielectric constant (discussed in **Chapter 5**) in respect to the pristine terpolymer depending on the modification conditions. Another drawback of this method is its specificity, as it provides no freedom regarding the groups that can be grafted on the fluoropolymer. Thus, this chapter is about the quest for a new, more general method to modify fluoropolymers and induce photopatternability that allows the grafting of large variety of groups and would ideally solve some of the drawbacks inherited by the azide approach such as reduced dielectric constant and stability.

It has been recently reported in literature that polymers bearing pendent photosensitive groups such as benzophenone¹⁻² (BP) and anthraquinone³ (AQ) can be crosslinked upon irradiation with UV light and are thus suitable for photolithography and two photon crosslinking applications. This behavior seems similar to the azide functionalized polymers, especially when the mechanism of each reaction is considered. In the case of azide functionalized polymers nitrogen is released upon irradiation and the remaining nitrene acts as a free radical intermediate leading to the cross-linking through hydrogen abstraction and C-H insertion. Similarly polymers bearing benzophenone or anthraquinone groups, upon irradiation, form free radicals on the carbonylic carbon⁴ and the carbonylic oxygen³ respectively, doing similar C-H insertion and hydrogen abstraction reactions that lead to subsequent cross-linking (**Scheme 3-1**). Thus preparing fluorinated polymers with those pendent photosensitive groups would be a promising alternative to the azide approach. The way those fluoropolymers bearing side benzophenone and anthraquinone groups would cross-link upon UV irradiation is illustrated in **Scheme 3-1**.



Scheme 3-1. Schematic representation of photo-induced crosslinking of $P(\text{VDF-TrFE-CTFE})$ terpolymers bearing side photosensitive groups such as benzophenone (BP) and anthraquinone (AQ).

One way to synthesize such polymers, would be to start from the azide functionalized fluoropolymer and use Huisgen cycloaddition in order to click an alkyne functionalized derivative of the photosensitive group, similarly to literature reports⁴. Although this approach would be possible, it would require a two-step approach, one-step more than the azide approach. Another issue that makes this approach less attractive is the costly time consuming purification that would have to be performed to remove all copper residues in order for this polymer to be used in electronics.

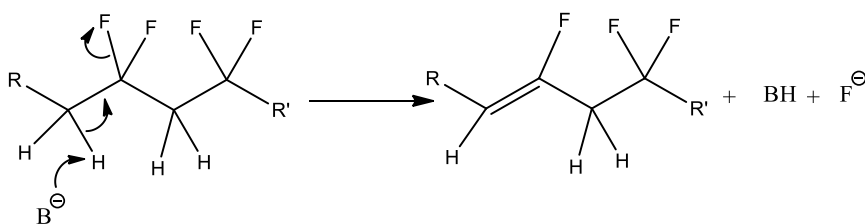
3.2) Results and Discussion

3.2.1) Chemical modification of $P(\text{VDF-TrFE-CTFE})$ (61.7/28.3/10) terpolymers

3.2.1.1) $P(\text{VDF-TrFE-CTFE})$ terpolymers functionalized with benzophenone groups

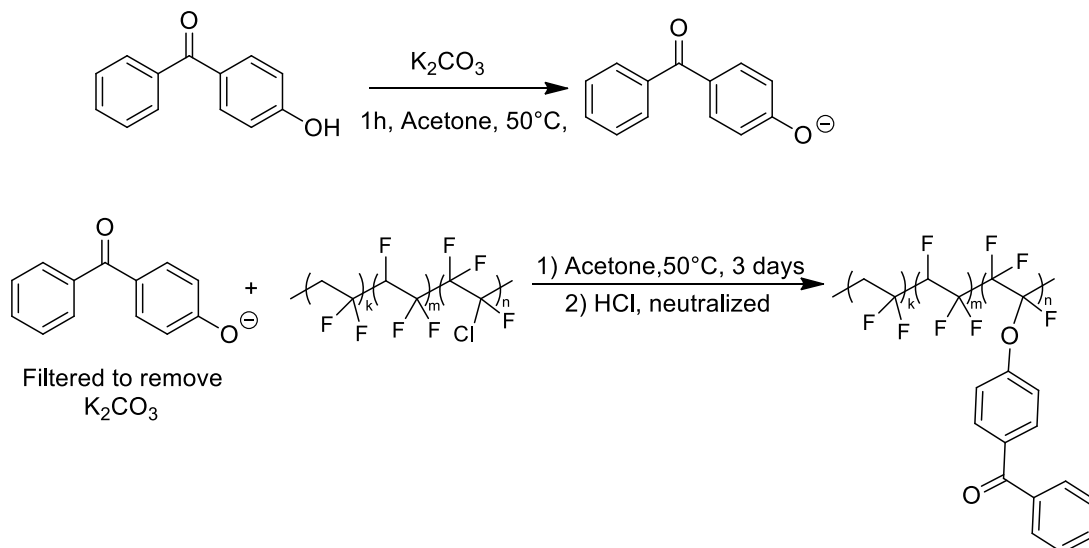
It has been reported in literature that hydroxyl benzophenone and anthraquinone derivatives can react with alkyl halides in the presence of a base⁵⁻⁶. Such reaction would proceed through $\text{S}_{\text{N}}2$ mechanism similar to the one of the azide substitution reaction. Main bottleneck for this approach is the use of a base, in order to activate the phenolic derivative, as bases are known to lead to dehydrofluorination⁷⁻⁸. In order to avoid the non desirable dehydrofluorination reaction, the standard reaction protocol

were blended together, we moved to a two-step protocol with the first step being the treatment of the phenolic derivative with the base and subsequent filtration in order for the phenoxide to react with the fluoropolymer in the absence of the initial base. Despite the fact that the base is filtered off, some dehydrofluorination can still be observed, as the phenoxide is itself a base, which can lead to elimination reactions. The dehydrofluorination reaction leading to backbone unsaturation is presented in **Scheme 3-2**.



Scheme 3-2. Elimination reaction of fluoropolymers in the presence of a base proceeding through an E2 mechanism and leading to unsaturation on the polymer backbone.

The first attempt was to modify the P(VDF-TrFE-CTFE) (61.7/28.3/10) with 4-hydroxybenzophenone. The targeted modification reaction is shown in **Scheme 3-3**.



Scheme 3-3. Grafting reaction of 4-hydroxy benzophenone on P(VDF-TrFE-CTFE) via a two-step process.

The reaction was monitored through attenuated total reflection infrared spectroscopy (ATR-IR) and as observed, peaks on the 1500-1800 wavenumbers regime start appearing which can be attributed amongst other things to the presence of carbonyl groups (**Figure 3-1a**). As the information obtained through the infrared spectroscopy does not allow us to draw conclusions on whether modification was

successful or not, since there is no information on whether this is a physical blend of benzophenone with the fluoropolymer or the targeted grafted polymer. So in order to investigate if the benzophenone moieties were successfully grafted on the fluoropolymer or not, size exclusion chromatography (SEC) was employed. More specifically, the product of the reaction was compared to the pristine fluoropolymers using two detectors. The first detector was a light scattering detector that would indicate any difference in the retention time due to the benzophenone modification, and as observed in **Figure 3-1b** there is no such apparent difference. However, the second detector is an ultraviolet detector (UV) and that is of much higher interest as the pristine terpolymer does not absorb in UV light. On the other hand, the benzophenone modified polymer does absorb in UV light, indicating that the modification reaction was successful and the UV absorption derives from the benzophenone pendant groups (**Figure 3-1c**).

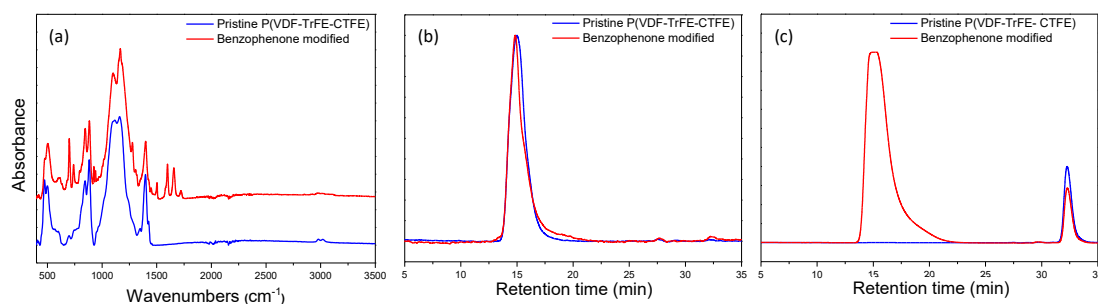


Figure 3-1. (a) FT-IR spectra of Pristine P(VDF-TrFE-CTFE) (blue) and benzophenone modified terpolymer as purified (red). (b) SEC in DMF, light scattering detector comparing the Pristine P(VDF-TrFE-CTFE) (blue) and the benzophenone modified terpolymer (red). (c) SEC in DMF, UV detector showing that the benzophenone modified terpolymer (red) absorbs in UV light, while the pristine P(VDF-TrFE-CTFE) doesn't.

In order to quantify the amount of benzophenone grafted, ¹H-NMR was employed (**Figure 3-2**). The appearance of the aromatic signals at 7-8 ppm confirms the above findings. Then, by comparing them to the integration of the vinylidene fluoride protons at 2.2-3.7 ppm, the trifluoroethylene protons at 4.7-5.7 ppm and the protons of the double bonds at 6-6.7 ppm we are able to quantify the amount of benzophenone grafted, which in this case equals to 6.5%, in respect to the total number of repeating units.

The above number was calculated by using the following equation.

$$\text{Modification degree} = \frac{\int_{7\text{ppm}}^{8\text{ppm}} \text{aromatic protons} / \text{number of protons per BP}}{\int_{4.7\text{ppm}}^{5.7\text{ppm}} \text{CHF of TrFE} + (\int_{2.2\text{ppm}}^{3.7\text{ppm}} \text{CH}_2 \text{ of VDF})/2 + (\int_{6\text{ppm}}^{6.7\text{ppm}} \text{CH of double bonds}) * 2}$$

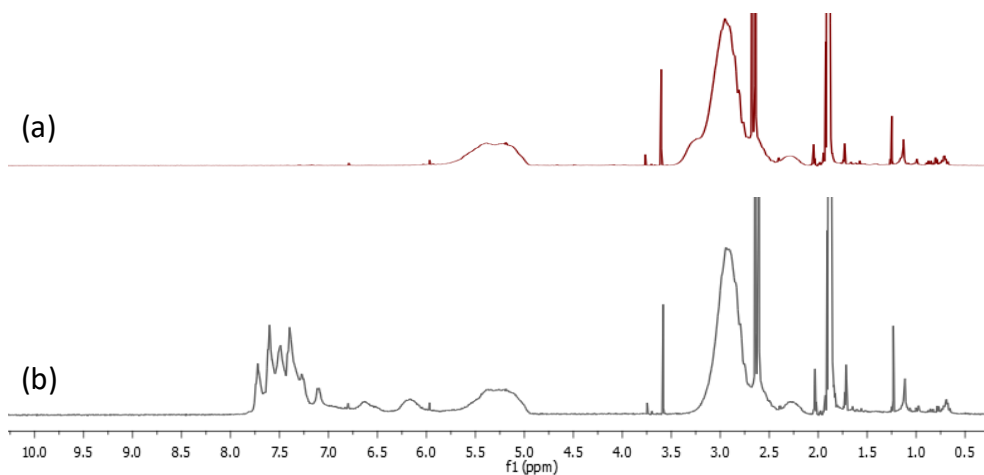


Figure 3-2. $^1\text{H-NMR}$ at 400 MHz of (a) the pristine terpolymer and (b) the benzophenone modified terpolymer which is estimated to be 6.5% in respect of the total number of the repeating units.

UV-Vis experiments were performed and the benzophenone modified polymer seems to have a broader red shifted UV absorption in comparison to the azide modified (**Figure 3-3**). That can be an important difference as in some cases that high energy deep UV light has to be avoided as it leads to degradation of some materials, such as the organic semiconductors.

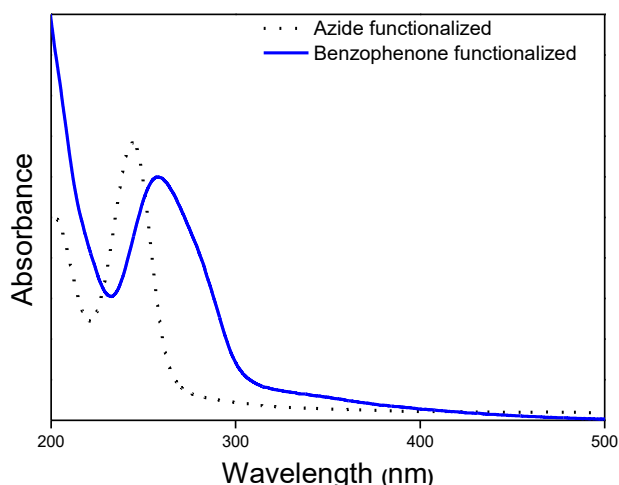
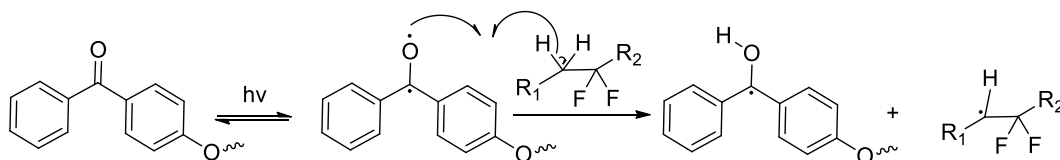


Figure 3-3. UV-Vis absorption spectra comparing the absorption of self standing films of the azide modified terpolymers to the absorption of the benzophenone modified P(VDF-TrFE-CTFE) terpolymers.

As mentioned above, one of the reasons that the benzophenone group was chosen is that it acts as a type II photoinitiator. Indeed, when polymers bearing the benzophenone chromophore get exposed to UV light, a triplet ketyl biradical is reversibly formed by transferring a non bonding electron from the carbonyl oxygen to the carbonyl π^* orbital, as described in **Scheme 3-4**⁹. If the biradical does not abstract a hydrogen from a neighboring molecule during its half-life, the benzophenone will return to its ground state and will be available for further excitation. However, if the ketyl biradical abstracts a hydrogen from a polymer chain, a new radical will be formed on that chain. Then, neighboring radicals can couple with each other leading to the formation of a C-C bond and a cross-linked polymer network, as illustrated in **Scheme 3-1**.



Scheme 3-4. Reversible excitation of the benzophenone moieties upon irradiation with UV light and reaction towards VDF units.

In order to investigate the effect that this new modification reaction has on the crystalline properties of the material differential scanning calorimetry was employed. As showed in **Figure 3-4** both the melting and crystallization peaks of the pristine terpolymer disappear after the modification reaction. Investigation of the consequences on the electric properties will be discussed later. Similar disappearance of the melting

and crystallization peaks has been previously reported in the case of terpolymers grafted with high amounts of azido groups.

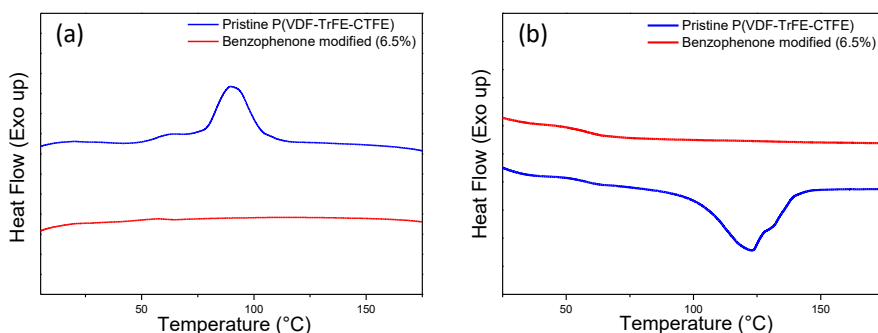


Figure 3-4. DSC thermograms with 10°C/min ramp, comparing the pristine terpolymer (blue) and the benzophenone modified terpolymer (red) during (a) the first cooling cycle and (b) the second heating cycle.

The motivation behind grafting the benzophenone groups on the fluoropolymer in the first place was to make it photo cross-linkable and thus compatible with photolithographic patterning techniques as a negative photoresist, in analogy to the azide modified polymers. Thus, a photolithographic patterning protocol had to be developed in order to pattern the benzophenone modified polymer through a single photolithographic step. Such protocol is shown below, with the patterned fluoropolymer film shown in **Figure 3-5**. The baking temperature required for the patterning of those polymers is much higher than the baking temperatures used in the case of the azide modified terpolymers (**Chapter 2**), indicating that the benzophenone modified polymers are much more stable at high temperatures.

Protocol

- 1) Spincoating of 4 % wt solution of P(VDF-TrFE-CTFE)-(BP 6.5%) @ 1000rpm
- 2) Soft baking @ 130°C for 5 min
- 3) Exposure @ 6J/cm² under N₂
- 4) Post exposure baking @ 130°C for 5 min
- 5) Developing with isopropanol/cyclopentanone (80/20) @ RT for 2 min
- 6) Rinsing with isopropanol
- 7) Air drying

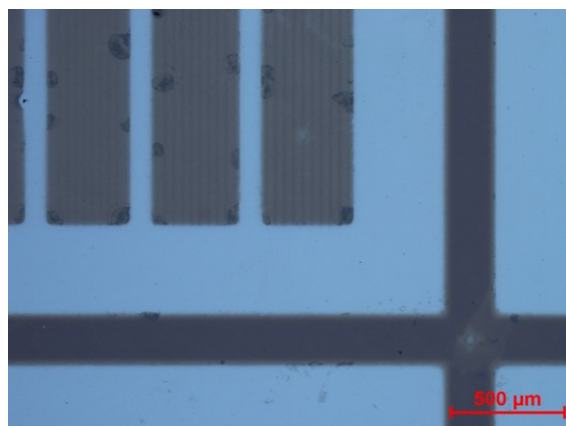


Figure 3-5. Optical microscope picture of patterned benzophenone modified P(VDF-TrFE-CTFE) terpolymer (6.5% benzophenone) on a silicon wafer.

Our first attempt to graft benzophenone groups on the CTFE group of fluoropolymers was successful, and those polymers appeared to act as negative photoresists, just like the azide modified polymers.

In order to investigate the effect of different benzophenone loadings on the properties of the fluoropolymer, polymers with different loadings were synthesized, by varying the reaction conditions, such as the feeding ratios or the reaction time. The different benzophenone loadings were assessed by $^1\text{H-NMR}$ (**Figure 3-6**). Polymers with a range of benzophenone loadings from 0.4 to 6.5% were synthesized. The VDF protons appear at 2.2 to 3.7 ppm, while the double bond protons appear at 6.7 ppm. The shoulder of the VDF peak at 3.4 ppm corresponds to the VDF-CTFE sequence. That shoulder disappears regardless of the modification degree, and it appears that for the (b) and (c) polymers the majority of the CTFE groups has been converted to double bonds (DB) through a dehydrochlorination reaction. All the $^1\text{H-NMR}$ data are summarized in **Table 3-1**.

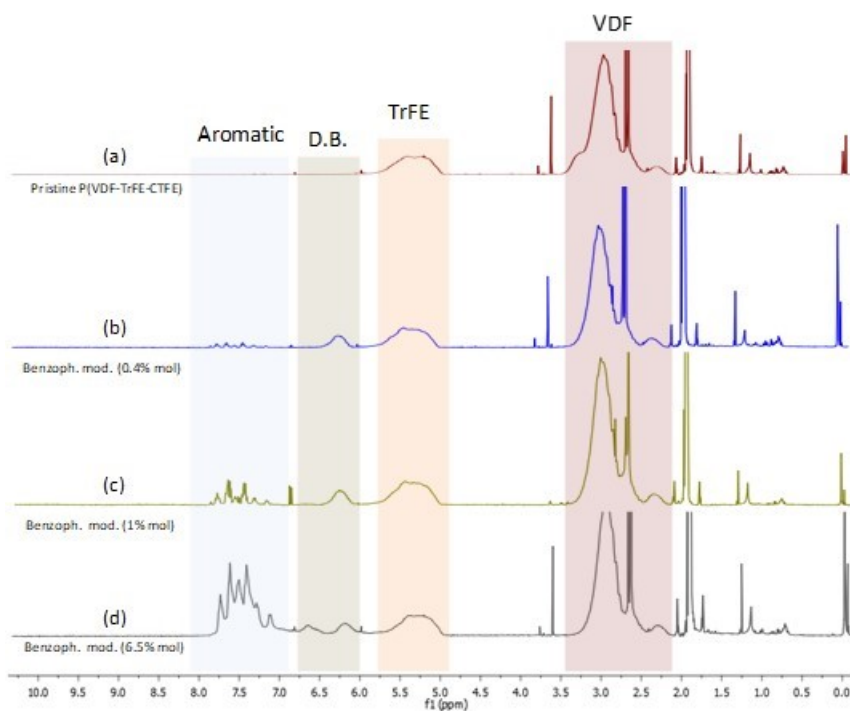


Figure 3-6. $^1\text{H-NMR}$ at 400 MHz of (a) the pristine terpolymer and (b) benzophenone modified terpolymer (0.4%), (c) benzophenone modified terpolymer (1%), (d) benzophenone modified terpolymer (6.5%), with DB = double bonds.

Table 3-1. Summary of the modification results of $P(\text{VDF-TrFE-CTFE})$ with 4-hydroxybenzophenone.

	Equivalents of benzophenone	Reaction time	TrFE (1 H) 4.7-5.7 ppm	Double bonds (1 H) 6-7 ppm	Aromatic (9 H) 7-8 ppm	Modification degree
(a)	0	0h	28.3	0%	0	0 %
(b)	0.3	4h	28.3	7.3%	3.7	0.4%
(c)	0.5	4h	28.3	7.1%	9.2	1%
(d)	0.5	3 days	28.3	18%	59	6.5%

Further characterization was performed by $^{19}\text{F-NMR}$. All synthesized polymers (b) to (d) started appearing peaks correlated to double bonds, confirming the above $^1\text{H-NMR}$ findings (**Figure 3-7**). The new peaks at -89.29 ppm, corresponding to the $(-\text{CF}_2\text{CH}=\text{CF}_2-)$ sequence and -120.72 ppm corresponding to the $(-\text{CF}_2\text{CH}=\text{CF}_2\text{CF}_2-)$ sequence confirm the insertion of unsaturation on the polymer backbone, although no useful information regarding the benzophenone insertion could be obtained via $^{19}\text{F-NMR}$.

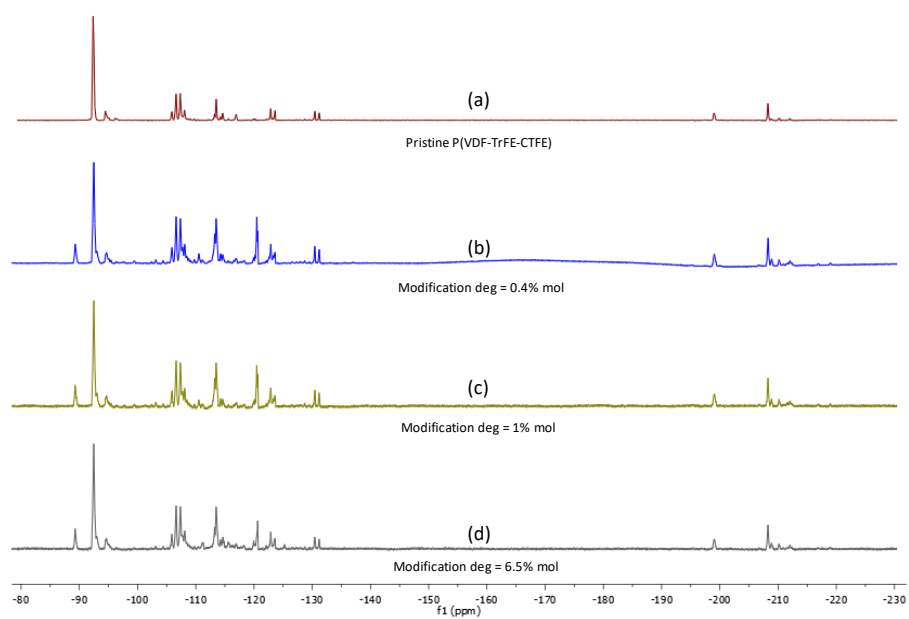


Figure 3-7. ^{19}F -NMR at 376,5 MHz of (a) the pristine terpolymer and (b) benzophenone modified terpolymer (0.4%), (c) benzophenone modified terpolymer (1%), (d) benzophenone modified terpolymer (6.5%).

Table 3-2. Assignment of ^{19}F -NMR signals as presented in literature¹⁰.

Sequence	Chemical Shift (ppm)
$-\text{CF}_2\text{CH}=\underline{\text{CF}}\text{CF}_2-$	-89.29
$-\text{CF}_2\text{CH}_2\underline{\text{CF}_2}\text{CH}_2\text{CF}_2-$	-92.36
$-\text{CHFCH}_2\underline{\text{CF}_2}\text{CH}_2\text{CF}_2-$	-94.45 to 95.27
$-\text{CF}_2\text{CFCl}\underline{\text{CF}_2}\text{CFClCF}_2-$	-106.05 to -107.82
$-\text{CF}_2\text{CH}_2\underline{\text{CF}_2}\text{CF}_2\text{CFCl}-$	-108.0 to -109.34
$-\text{CF}_2\text{CFCl}\underline{\text{CF}_2}\text{CFClCH}_2-$	-109.34 to -113.10
$-\text{CH}_2\text{CF}_2\underline{\text{CF}_2}\text{CF}=\text{CH}-$	-110.56 to -111.16
$-\text{CF}_2\text{CF}_2\text{CH}=\underline{\text{CF}}\text{CF}_2-$	-113.40
$-\text{CF}_2\text{CH}_2\underline{\text{CF}_2}\text{CF}_2\text{CHF}-$	-113.64
$-\text{CF}_2\text{CH}=\underline{\text{CF}}\text{CF}_2-$	-113.89
$-\text{CF}_2\text{CH}_2\underline{\text{CF}_2}\text{CF}_2\text{CH}_2-$	-114.27
$-\text{CH}_2\text{CF}_2\underline{\text{CF}_2}\text{CH}_2\text{CH}_2-$	-116.57
$-\text{CF}_2\text{CF}_2\text{CH}=\underline{\text{CF}}\text{CF}_2\text{CF}_2-$	-118.30
$-\text{CH}_2\text{CF}_2\underline{\text{CF}_2}\text{CFClCH}_2-$	-118.25 to -119.98
$-\text{CF}_2\text{CH}=\underline{\text{CF}}\text{CF}_2\text{CF}_2-$	-120.72
$-\text{CF}_2\text{CF}_2\underline{\text{CF}}\text{ClCH}_2\text{CF}_2-$	-120.35 to -123.32
$-\text{CF}_2\text{CHF}\underline{\text{CF}_2}\text{CHF}\text{CF}_2-$	-122.46 to -123.12
$\text{CF}_2\text{CHF}\underline{\text{CF}_2}\text{CHFCH}_2-$	-123.29 to -123.96
$-\text{CF}_2\text{CFCl}\underline{\text{CF}_2}\text{CHFCH}_2-$	-130.94
$-\text{CH}_2\text{CF}_2\underline{\text{CCl}}\text{F}\text{CF}_2\text{CH}_2-$	-131.34
$-\text{CF}_2\text{CF}_2\underline{\text{CHF}}\text{CH}_2\text{CF}_2-$	-198.72
$-\text{CH}_2\text{CF}_2\underline{\text{CHF}}\text{CF}_2\text{CH}_2-$	-212.50

The different benzophenone modified polymers were characterized by attenuated total reflection infrared spectroscopy (ATR FT-IR) (see **Figure 3-8**). The presence of the benzophenone groups leads to the appearance of peaks at 700-740, 920-935, 1500-1540, 1600-1660 cm^{-1} respectively. The peak at 1660 cm^{-1} which corresponds to the C=C stretching (formed double bonds), does not change drastically, which is in good accordance with the observed evolution of double bonds from ^1H -NMR presented in **Table 3-1**. On the other hand, the peaks at 1500-1540 increase in intensity again confirming the increase in benzophenone content observed by ^1H -NMR.

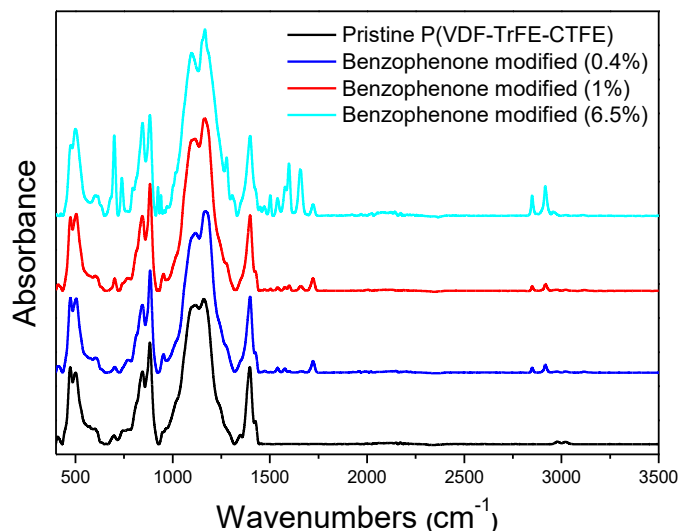


Figure 3-8. FT-IR spectra of P(VDF-TrFE-CTFE) modified with different amounts of benzophenone (ATR on films).

In order to confirm that the newly formed peaks are indeed due to the inserted benzophenone group, the FT-IR spectrum of the pristine 4-hydroxybenzophenone molecule is presented in **Figure 3-9**. Here it is also observed that the 4-hydroxybenzophenone shows a broad absorption above the 3000 cm⁻¹ that is characteristic of the hydroxy protons. It can be noted here that this broad absorption peak is not observed in any of the polymers of **Figure 3-8** confirming that no free 4-hydroxybenzophenone groups exist in the modified polymers.

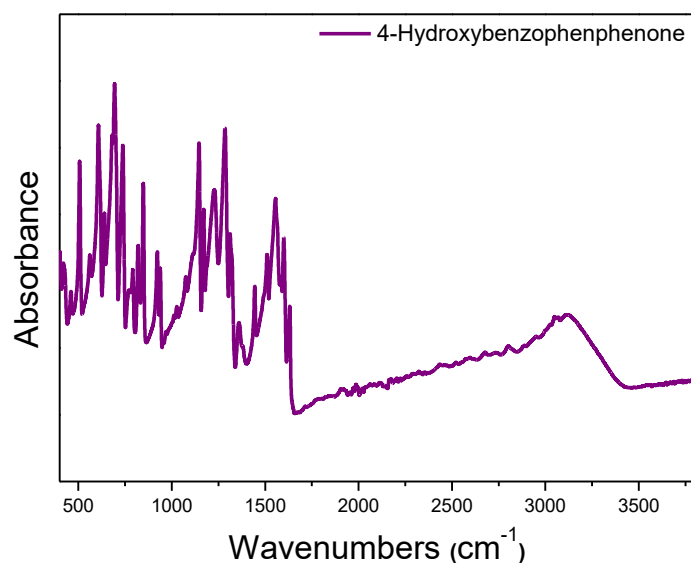


Figure 3-9. FT-IR spectra of 4-hydroxybenzophenone.

All the polymers mentioned above were characterized by differential scanning calorimetry (DSC). It appears that the polymers grafted with very small amounts of benzophenone (0.4%) show both melting and crystallization peaks in the same range as the pristine P(VDF-TrFE-CTFE). However, the crystallization peak of the modified terpolymer with 0.4% benzophenone is sharper, indicating smaller crystal size distribution as shown in **Figure 3-10**. The enthalpies calculated both by the melting and the crystallization peaks are lower in respect to the pristine terpolymer, indicating that the total crystallinity is lower. When the benzophenone loading reaches, 6.5% neither melting nor crystallization transitions appear, indicating that the polymer has lost its semicrystalline character. Both the calculated enthalpies and temperatures from the cooling and heating DSC ramps are shown in **Table 3-3**.

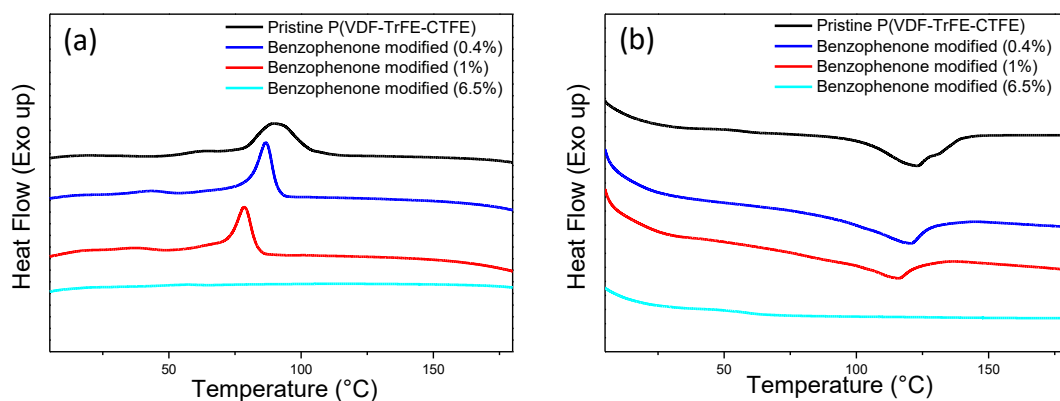


Figure 3-10. DSC thermograms with 10°C/min ramp, comparing the pristine terpolymer with terpolymers modified with different benzophenone loadings for the (a) first cooling cycle and (b) the second heating cycle (on polymer powders).

Table 3-3. Summary of the data derived from the DSC thermograms of benzophenone modified terpolymers.

	Melting		Crystallization	
	Temperature (°C)	Enthalpy (J/g)	Temperature (°C)	Enthalpy (J/g)
Pristine terpolymer	142°C	14	107°C	13
Benzophenone (0.4%)	131°C	8	93°C	12
Benzophenone (1%)	128°C	5	86°C	9
Benzophenone (6.5%)	-	-	-	-

In order to get a better understanding of the impact that the modification has on the crystalline properties of the terpolymer, simultaneous SAXS-WAXS experiments were performed on the pristine and benzophenone grafted terpolymers. All the X-ray characterizations were done in collaboration with PIMM, Arts et Metiers ParisTech, within the framework of the Industrial Chair Arkema (Arkema/CNRS/ANSAM-CNAM) and were performed by Dr. Sylvie Tencé-Girault. The 1D WAXS patterns obtained for the as cast terpolymers with different benzophenone contents are presented in **Figure 3-11**. In the case of the pristine polymer film, WAXS spectrum presents a symmetrical crystalline peak around 4.84 Å (**Figure 3-11a**). It can be fitted by one broad peak (orange peak), characteristic of the RFE phase. It corresponds to a combination of the (200) and (110) reflections. The position of the peak is shifted to higher 2θ with the incorporation of the benzophenone (**Figure 3-11b and c**), while its width is slightly reduced. This shift corresponds to a decrease of the interplanar distance after grafting, indicating that benzophenone is not incorporated in the crystal. Finally, at 1% benzophenone content, the crystallinity index remains largely unaffected by the modification, with a very slight increase for the very low benzophenone content. The appearance of the blue peak in **Figure 3-11c** indicates that a second population of crystals with lower interplanar distance appears.

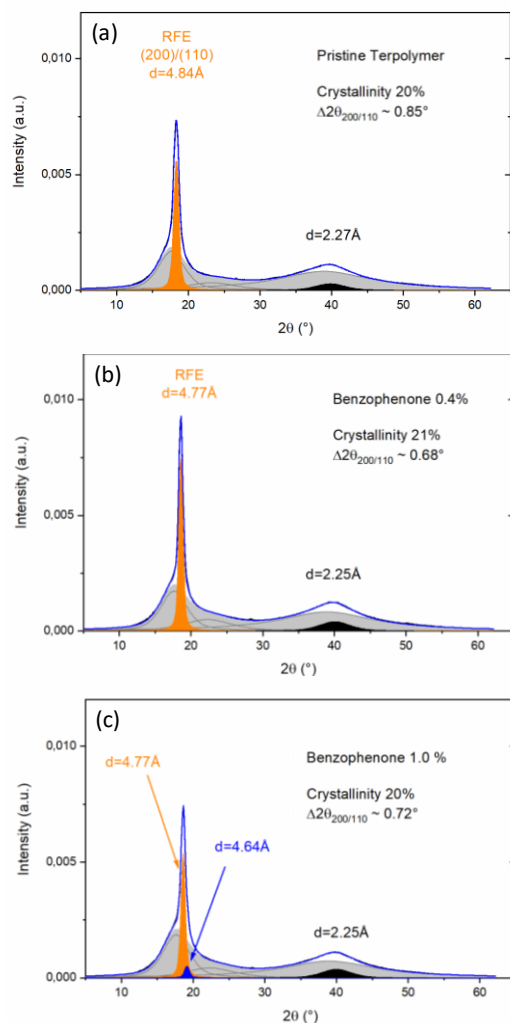


Figure 3-11. WAXS characterization of 100 μm self standing films of (a) the pristine P(VDF-TrFE-CTFE) terpolymer, (b) P(VDF-TrFE-CTFE) terpolymer with 0.4% benzophenone content, (c) P(VDF-TrFE-CTFE) terpolymer with 1% benzophenone content. (As cast films).

Similarly, WAXS characterization was performed in annealed self standing films of the benzophenone modified polymers. **Figure 3-12** shows the 1D WAXS pattern obtained after annealing the sample 1h at 110°C . As in the previous case, the characteristic peak of the RFE phase is observed. It should be noted that the crystallinity slightly improves upon thermal annealing, compared to the as cast samples.

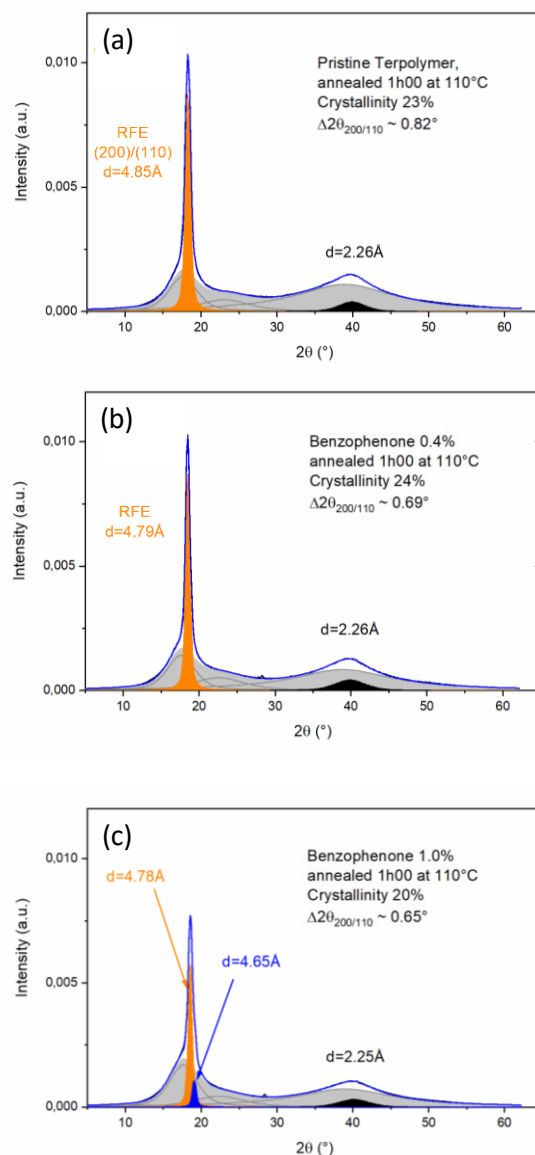


Figure 3-12. WAXS characterization of 100 μm self standing films of (a) the pristine P(VDF-TrFE-CTFE) terpolymer, (b) P(VDF-TrFE-CTFE) terpolymer with 0.4% benzophenone content, (c) P(VDF-TrFE-CTFE) terpolymer with 1% benzophenone content. (films annealed for 1h at 110°C).

SAXS experiments were also performed simultaneously to the WAXS experiments. The 1D SAXS patterns were obtained for both, pristine and functionalized polymers (Figure 3-13 and Figure 3-14). The Benzophenone functionalization induces a shift of the peak toward high q , indicating a decrease of the lamellar periodicity (L_p) from 300 Å for the pristine terpolymer to 250 Å and 210 Å respectively for the 0.4% and 1% grafted terpolymers. The introduction of the benzophenone moieties decrease the crystalline thickness, as the benzophenone group acts as defect, limiting the crystalline lamellae thickness and then decrease the lamellae periodicity.

After the subsequent thermal annealing SAXS patterns show well defined lamellar morphology with sharper peaks and the appearance of second and third order peaks

(Figure 3-14). Annealing induces a significant increase of L_P to 490 Å, 480 Å and 330 Å for the pristine terpolymer, the BP 0.4% and the BP1% respectively.

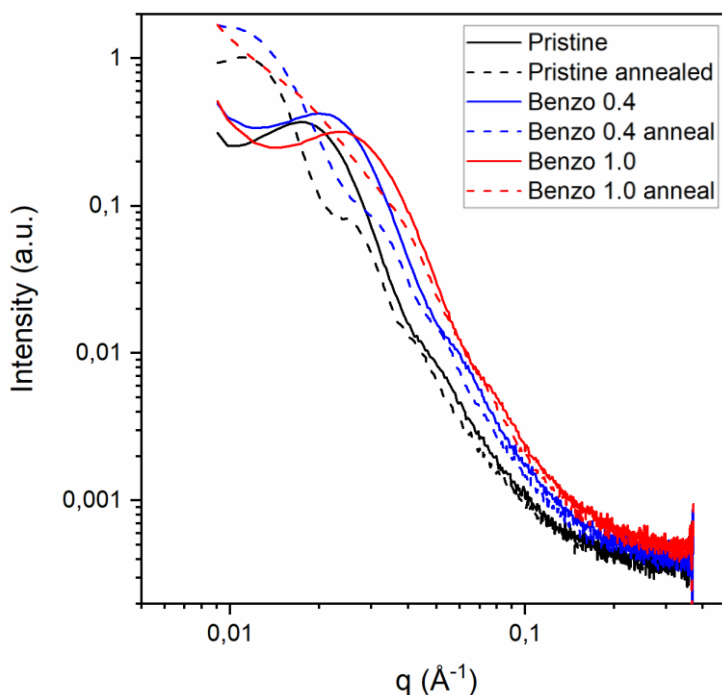


Figure 3-13. SAXS characterization of 100 μm self standing films of the pristine P(VDF-TrFE-CTFE) terpolymer (black), 0.4% benzophenone content (blue) and 1% benzophenone content (red). The continuous lines represent the as cast samples, and the dashed lines the samples annealed at 110°C for 1 h. $I(q)$ in logarithmic scale.

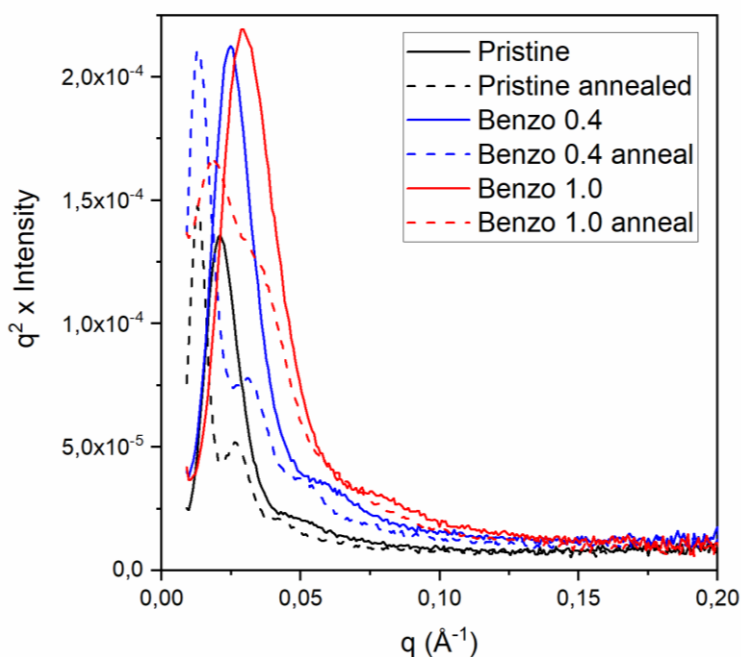


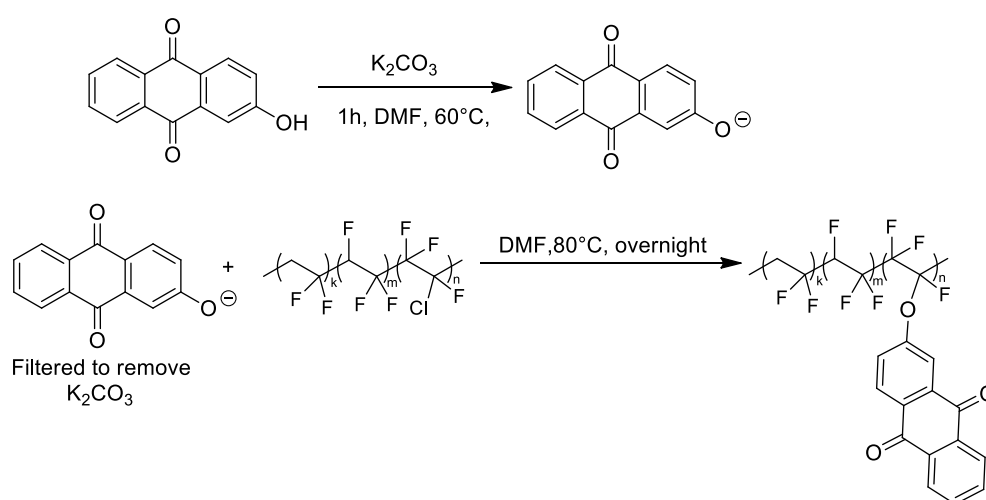
Figure 3-14. SAXS characterization of 100 μm self standing films of the pristine P(VDF-TrFE-CTFE) terpolymer (black), 0.4% benzophenone content (blue) and 1% benzophenone content (red). The continuous lines represent the as cast samples, and the dotted lines the samples annealed at 110°C for 1 h. Lorentz corrected spectra, $q^2 I(q)$.

By comparing the findings of both the WAXS and the SAXS experiments, we conclude that crystallinity and the crystalline lamellae stacking improve for very low benzophenone contents. That increase might be due to the presence of double bonds, while higher benzophenone contents leads the crystallinity to decrease.

These results on the BP modified fluoropolymers were compared with a simple blend between the pristine terpolymer and the 4-hydroxy benzophenone. In this case, it was not possible to get photo patternable fluoropolymers, highlighting the need for grafting the photoinitiator groups.

3.2.1.2) P(VDF-TrFE-CTFE) (61.7/28.3/10) terpolymers functionalized with anthraquinone groups

Similarly, to the benzophenone group, a large variety of aryl ketones can be used as photoinitiators and thus, initiate cross-linking upon irradiation. Such groups include among other anthraquinones and acetophenones. Indeed, polymers bearing pendant anthraquinone groups are also known to act as negative photoresists³. Thus, the same method previously applied to prepare benzophenone functionalized fluoropolymers, namely the Williamson ether synthesis could be also used to prepare fluoropolymers functionalized with the anthraquinone groups (**Scheme 3-5**).



Scheme 3-5. Grafting reaction of 2-hydroxy anthraquinone on P(VDF-TrFE-CTFE) via a two-step process.

Similarly to the previous case of terpolymers grafted with benzophenone (BP)

groups, in this case as well polymers with different anthraquinone (AQ) loadings were prepared by varying parameters such as the anthraquinone feeding ratio, the reaction conditions. All the prepared polymers were characterized by $^1\text{H-NMR}$ (**Figure 3-15**) in order to quantify the anthraquinone loading in each case. The loadings varied from 0.6% to 6% with respect to the total number of repeating units. The modification degrees were calculated using the same equation as in the case of the benzophenone modification. Here again shoulder of the VDF peak at 3.4 ppm corresponds to the VDF-CTFE sequence and since that shoulder disappears regardless of the modification degree, and it appears that for the (b) and (c) polymers the majority of the CTFE groups has been converted to double bonds through a dehydrochlorination reaction. All the $^1\text{H-NMR}$ data are summarized in **Table 3-4**.

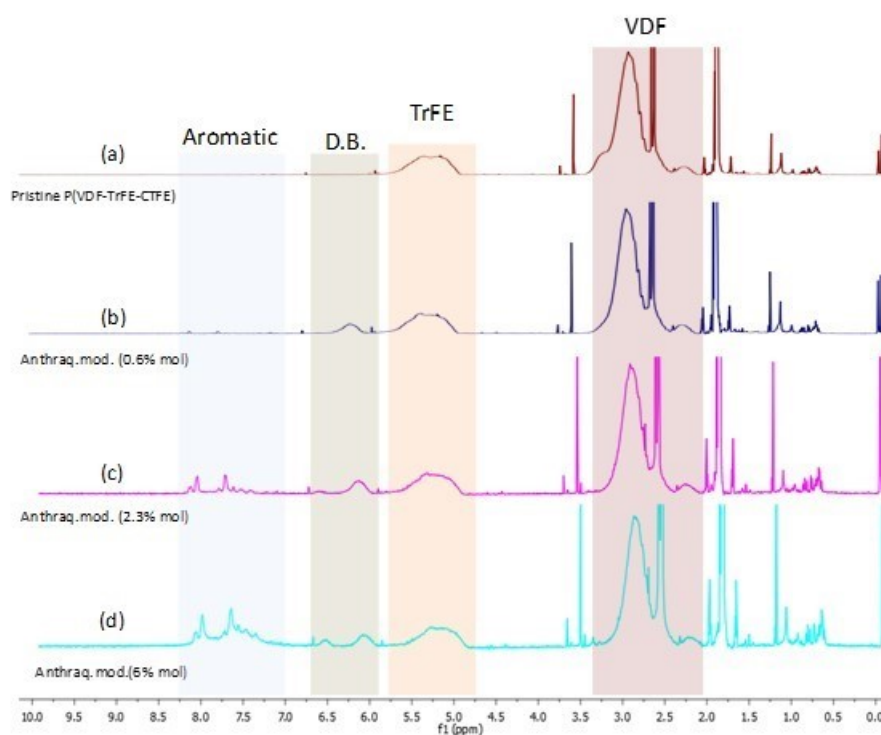


Figure 3-15. $^1\text{H-NMR}$ at 400 MHz of (a) the pristine terpolymer and (b) anthraquinone modified terpolymer (0.6%), (c) anthraquinone modified terpolymer (2.3%), (d) anthraquinone modified terpolymer (6%).

Table 3-4. Summary of the modification results of $P(\text{VDF-TrFE-CTFE})$ with 2-Hydroxyanthraquinone

	Equivalents of anthraquinone	Reaction time	TrFE (1 H) 4.7-5.7 ppm	Double bonds (1 H) 6-7 ppm	Aromatic (8 H) 7-8 ppm	Modification degree
(a)	0	0h	28.3	0%	0	0%

(b)	0.1	3 days	28.3	6.2%	4.4	0.6%
(c)	0.3	3 days	28.3	8.6%	18.4	2.3%
(d)	0.5	1 day	28.3	14.6%	46	6%

^{19}F -NMR was also used in this case and it clearly shows the appearance of the double bonds with the new peaks at -89.29ppm , corresponding to the $(-\text{CF}_2\text{CH}=\text{CFCF}_2-)$ sequence and -120.72 ppm corresponding to the $(-\text{CF}_2\text{CH}=\text{CFCF}_2\text{CF}_2-)$ sequence. However, the ^{19}F -NMR does not provide us with information concerning the inserted anthraquinone groups.

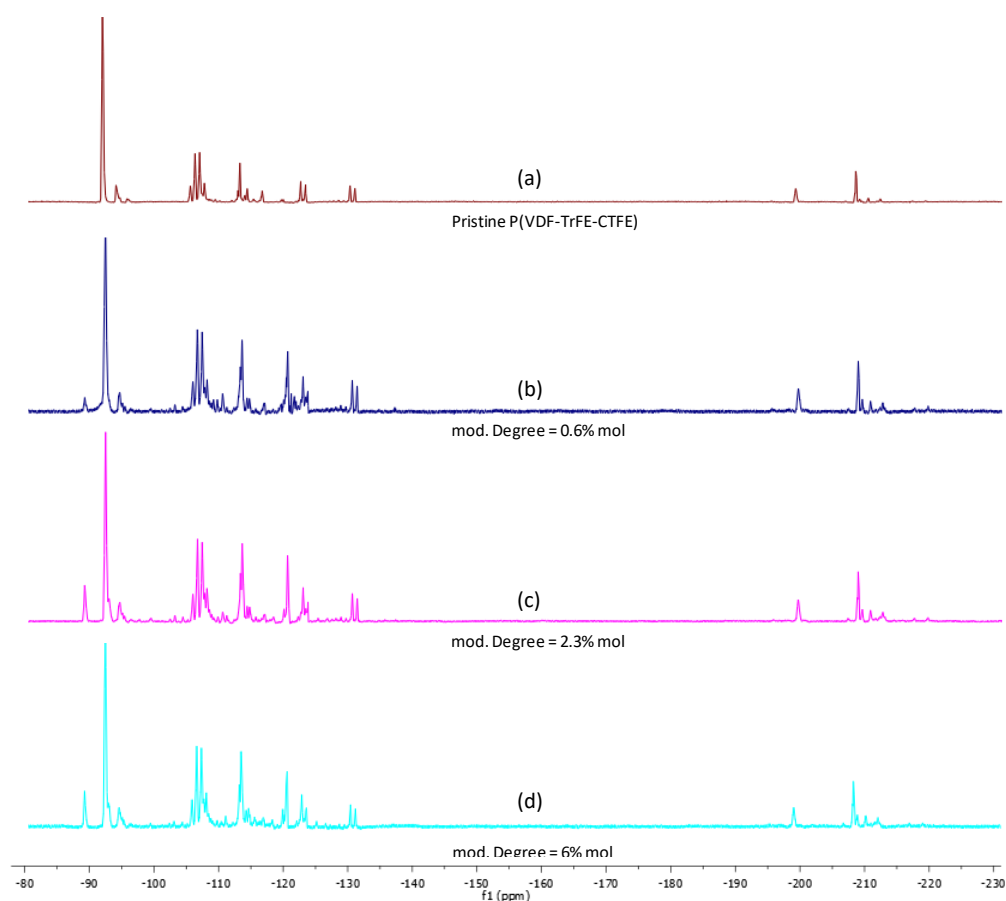


Figure 3-16. ^{19}F -NMR at 376,5 MHz of (a) the pristine terpolymer and (b) anthraquinone modified terpolymer (0.6%), (c) anthraquinone modified terpolymer (2.3%), (d) anthraquinone modified terpolymer (6%).

The different anthraquinone modified polymers were characterized by attenuated total reflection infrared spectroscopy as shown in **Figure 3-17**. The presence of the anthraquinone groups leads to the appearance of peaks at 710 , 945 , 1300 , 1590 cm^{-1} and 1680 cm^{-1} respectively, all increasing in intensity with increasing the anthraquinone content. On the other hand, a peak at 1720 cm^{-1} corresponding to the

C=C stretching also appears and does not vary much with increasing the anthraquinone content.

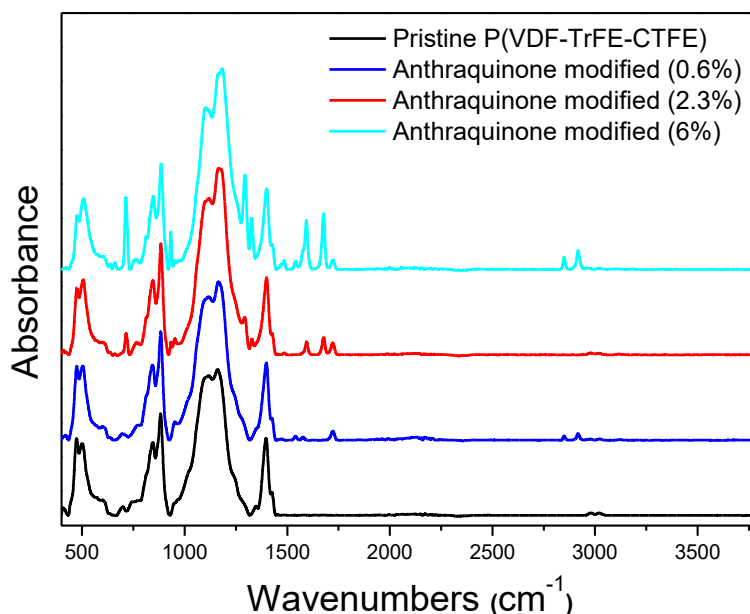


Figure 3-17. FT-IR spectra of P(VDF-TrFE-CTFE) modified with different amounts of anthraquinone.

In order to confirm that our attribution of the above mentioned peaks to the anthraquinone group was correct, the FT-IR spectra of the pristine 2-hydroxyanthraquinone were recorded and presented in **Figure 3-18**. There we see that the anthraquinone molecule strongly absorbs in 710, 945, 1300, 1590 cm⁻¹ as mentioned above. Furthermore, the absence of acidic protons in **Figure 3-17** further confirms the fact that all anthraquinone groups are grafted on the fluoropolymer backbone.

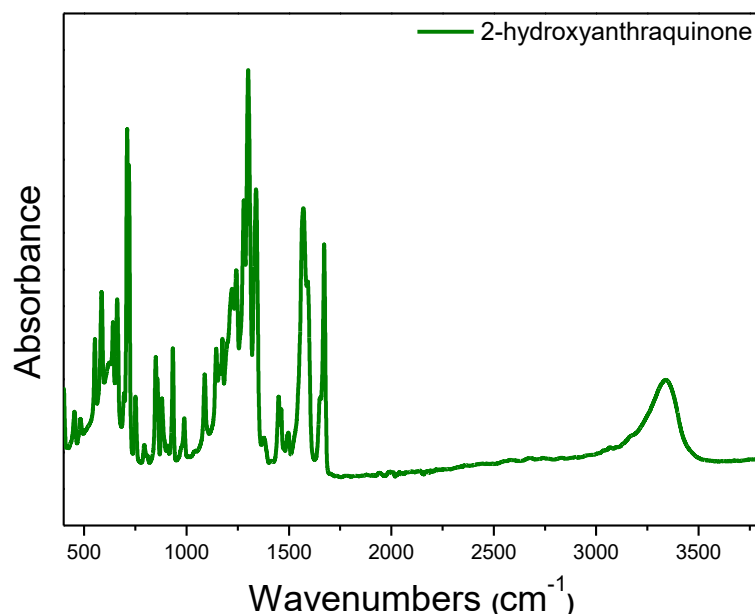


Figure 3-18. FT-IR spectra of 2-hydroxyanthraquinone.

Size exclusion chromatography equipped with a UV detector was also performed in order to confirm that the grafting with anthraquinone of the P(VDF-TrFE-CTFE) terpolymer was successful. As shown in **Figure 3-19**, the polymer grafted with anthraquinone absorbs in the UV, while the pristine does not, even though the two peaks are roughly similar in the LS detector.

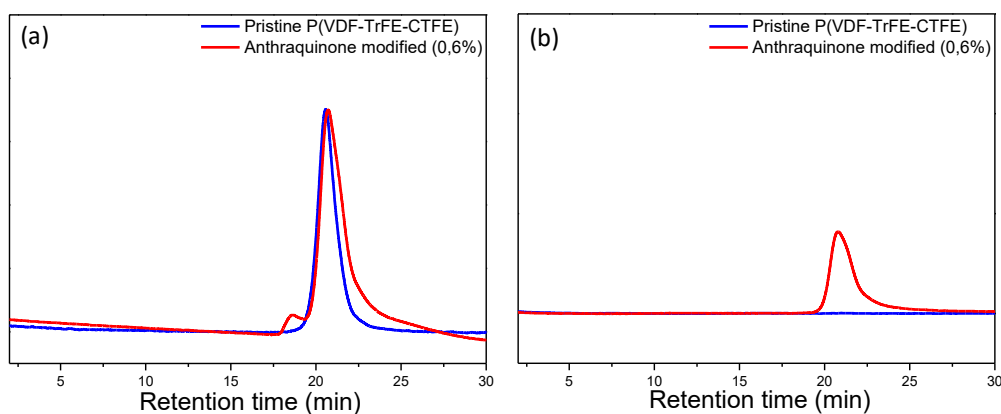


Figure 3-19. (a) SEC in DMF, light scattering detector comparing the Pristine P(VDF-TrFE-CTFE) (blue) and the anthraquinone modified terpolymer (0.6%, red). (b) SEC in DMF, UV detector showing that the anthraquinone modified terpolymer (red) absorbs in UV light, while the pristine P(VDF-TrFE-CTFE) doesn't.

Self-standing films of AQ modified terpolymers were also characterized by UV-Vis absorption spectroscopy and compared to their azide and BP counterparts. As shown in **Figure 3-20** the AQ modified terpolymer shows more pronounced shoulders in the near UV region between 300 and 400 nm.

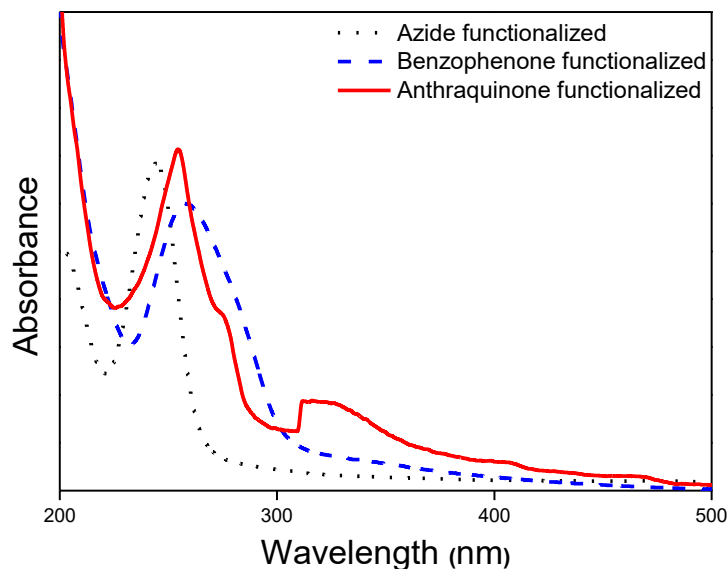


Figure 3-20. UV-Vis absorption spectra comparing the absorption of the azide modified terpolymers (black) to the absorption of the benzophenone (blue) and anthraquinone (red) modified terpolymers.

The thermal stability of the anthraquinone modified polymers was investigated via thermal gravimetric analysis under nitrogen atmosphere and a heating rate of 10°C/min. Here the anthraquinone modified polymers exhibit excellent thermal stability up to 400°C, like the pristine terpolymers (**Figure 3-21**). The increase in char residue over 500°C is indicative of the increase in aromatic grafting of the polymer.

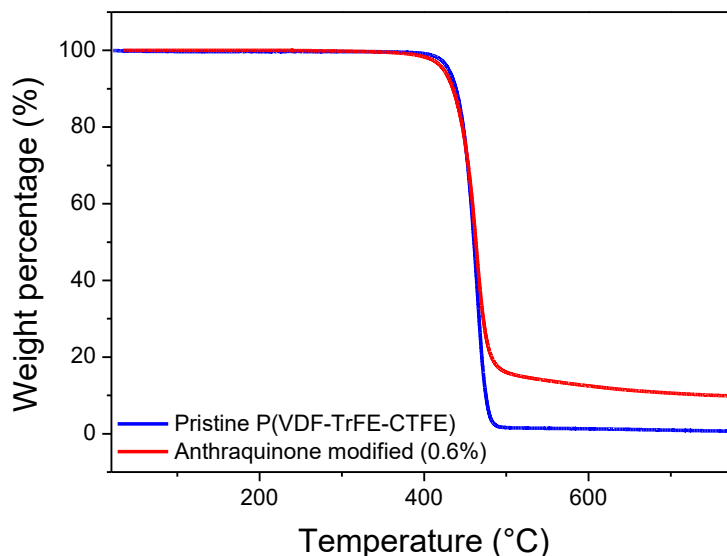


Figure 3-21. Thermal gravimetric analysis in nitrogen atmosphere and 10°C/min ramp comparing the thermal stability of the pristine terpolymer with the anthraquinone modified terpolymer.

The effect of the anthraquinone functionalization on the crystalline organization of the fluoropolymers was investigated by differential scanning calorimetry. The first heating ramp was used to erase thermal history and the first cooling and second heating ramps were recorded (**Figure 3-22**). The fluoropolymers grafted with 0.6% and 2.3% of anthraquinone groups show a sharper crystallization peak than the pristine terpolymer. The calculated enthalpies and crystallization from the thermograms are shown in **Table 3-5**.

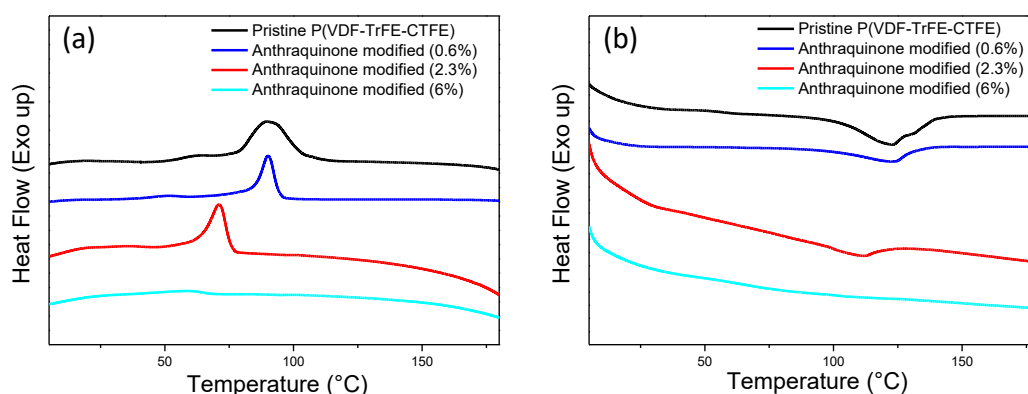


Figure 3-22. DSC thermograms with 10°C/min ramp, comparing the pristine terpolymer with terpolymers modified with different anthraquinone content for the (a) first cooling cycle and (b) the second heating cycle.

Table 3-5. Summary of the data derived from the DSC thermograms of anthraquinone modified terpolymers.

	Melting		Crystallization	
	Temperature (°C)	Enthalpy (J/g)	Temperature (°C)	Enthalpy (J/g)
Pristine terpolymer	142°C	14	107°C	13
Anthraquinone (0.6%)	137°C	10	97°C	12
Anthraquinone (2.3%)	125°C	3	78°C	7
Anthraquinone (6%)	-	-	69°C	0.9

Film morphology was also studied by AFM on the pristine and the AQ modified terpolymer. The modification degree seems to effect the crystalline domain size (**Figure 3-23**), which almost vanish for high AQ content, always in good agreement with the DSC data.

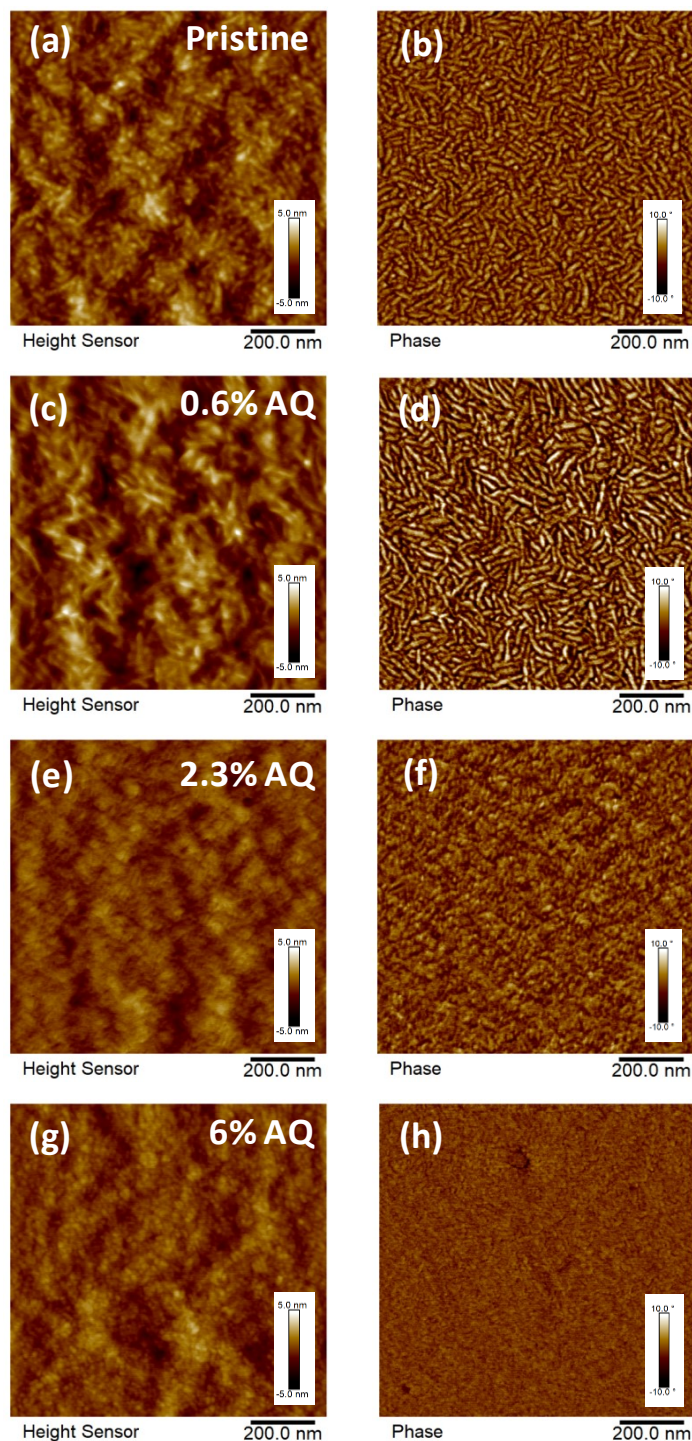


Figure 3-23. AFM images (height left and phase right) of as-cast films of the pristine and the anthraquinone modified P(VDF-TrFE-CTFE) terpolymers with various anthraquinone loadings.

Simultaneous SAXS-WAXS experiments were performed in order to investigate the impact of the anthraquinone modification on the crystalline organization of the terpolymer. Here again the spectra were recorded for terpolymers as cast and after an annealing step at 110°C for 1h. The 1D WAXS patterns obtained for the as cast terpolymers with different anthraquinone contents are presented in **Figure 3-24**.

Similarly to the case of benzophenone modified terpolymers, small amounts of anthraquinone seem to reduce the width of the peak corresponding to the PE phase with the total crystallinity slightly increasing. When the content of anthraquinone groups increases though, the peak characteristic of the RFE phase almost disappears and the total crystallinity decreases as well. The position of the peak is shifted to higher 2θ with the incorporation of AQ, corresponding to a decrease of interplanar distance upon grafting.

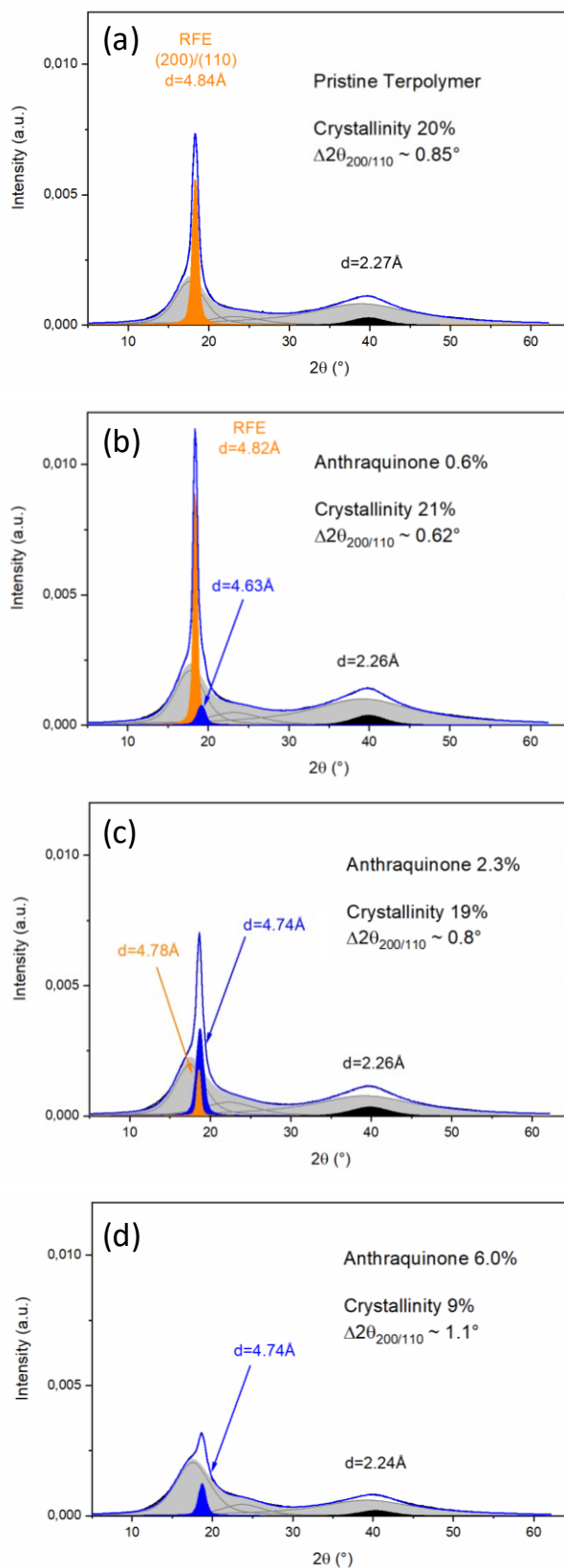


Figure 3-24. WAXS characterization of 100 μm self standing films of (a) the pristine P(VDF-TrFE-CTFE) terpolymer, (b) 0.6%, (c) 2.3% and (d) 6% anthraquinone content. (As cast films).

The self standing films of the annealed anthraquinone modified polymers were also

characterized by the same method. The WAXS patterns show an increase in the total crystallinity after annealing (**Figure 3-25**) for all the polymers except for the one with the highest anthraquinone content (**Figure 3-25d**), with that being most likely attributed to improper annealing conditions for the latter.

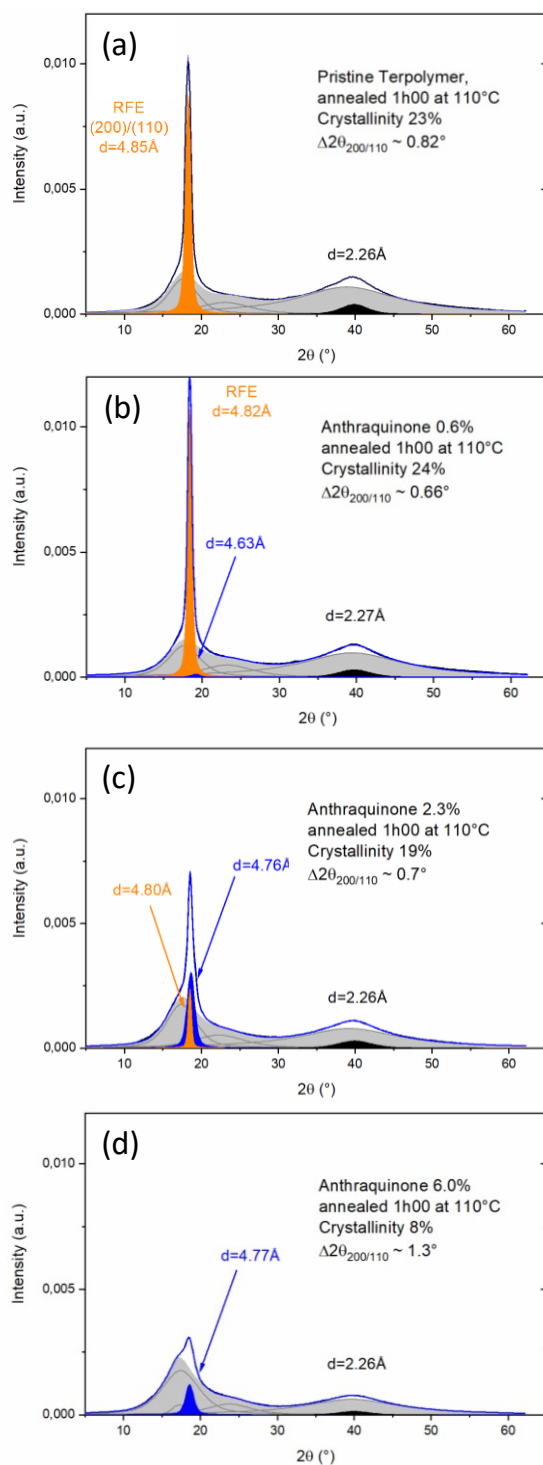


Figure 3-25. WAXS characterization of 100 μm self standing films of (a) the pristine P(VDF-TrFE-CTFE) terpolymer, (b) 0.6%, (c) 2.3% and (d) 6% anthraquinone content. (films annealed for 1h at 110°C).

The SAXS spectra were recorded simultaneously to the WAXS. The 1D SAXS patterns obtained for both, pristine and functionalized polymers are shown in **Figure 3-26** and **Figure 3-27**. After the subsequent thermal annealing SAXS patterns were indexed to a lamellar morphology. The annealing step causes the packing to improve, with sharper peaks at **Figure 3-27**. However the introduction of the anthraquinone groups decreases the crystalline thickness, as the anthraquinone group acts as defect, limiting the crystalline lamellae. The AQ functionalization induces a shift of the peak toward high q , indicating a decrease of the lamellar periodicity (LP) from 300 Å for the pristine terpolymer to 280 Å, 200 Å and 210 Å for the 0.6%, 2.3% and 6% AQ grafted terpolymers respectively. The introduction of the AQ moieties decrease the crystalline thickness, limiting the crystalline lamellae thickness as well and decrease the lamellae periodicity. However, the decrease was less pronounced, compared to the terpolymers grafted with the BP group.

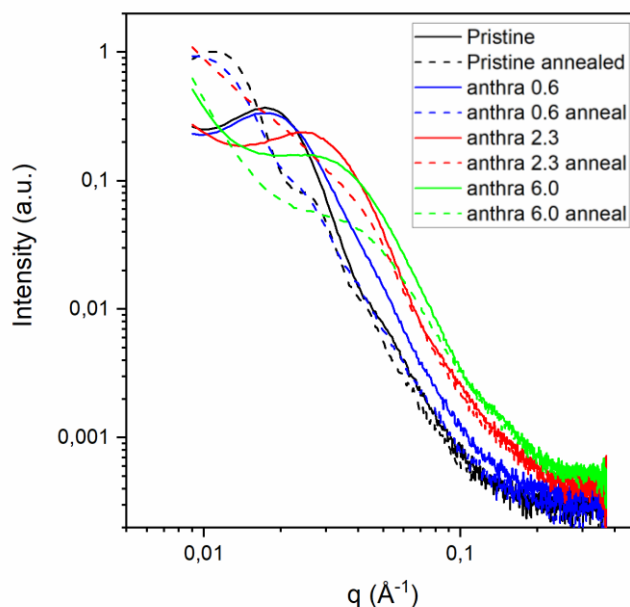


Figure 3-26. SAXS characterization of 100 μm self standing films of the pristine P(VDF-TrFE-CTFE) terpolymer (black), 0.6% anthraquinone (blue), 2.3% anthraquinone (red) and 6% anthraquinone (green). The continuous lines represent the as cast samples, and the dashed lines the samples annealed at 110°C for 1 h. $I(q)$ in logarithmic scale.

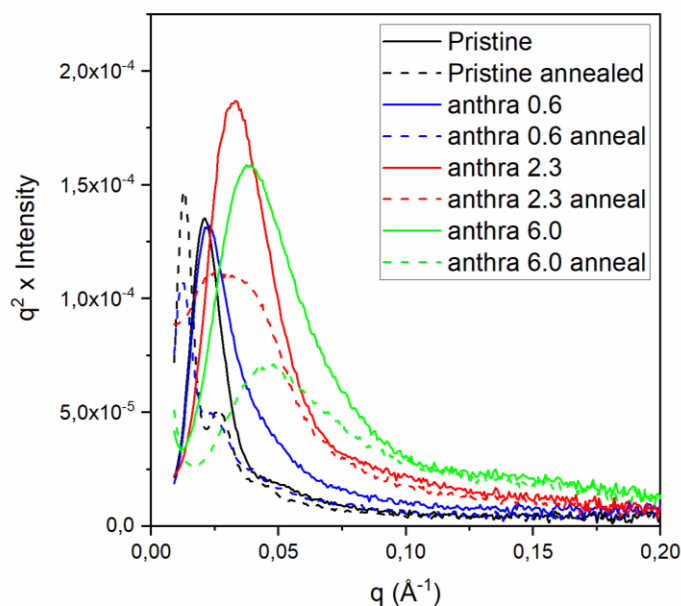


Figure 3-27. SAXS characterization of 100 μm self standing films of the pristine P(VDF-TrFE-CTFE) terpolymer (black), 0.6% anthraquinone (blue), 2.3% anthraquinone (red) and 6% anthraquinone (green). The continuous lines represent the as cast samples, and the dashed lines the samples annealed at 110°C for 1 h. Lorentz corrected spectra, $q^2 I(q)$.

By comparing the findings from the WAXS and the SAXS experiments, we observe that polymers grafted with small amounts of anthraquinone show improved crystallinity and lamellae stacking. That is most likely attributed to the double bonds which seem to be incorporated in the polymer crystal. On the other hand, when the anthraquinone content increases, the total crystallinity decreases as well, as the bulky anthraquinone groups are not incorporated in the polymer crystal.

An adapted photolithographic protocol was carried out, based on previous experience with the azide and BP modified terpolymers. Patterning was achieved at low UV dose and short irradiation time as shown in **Figure 3-28**.

Protocol

- 1) Spincoating 4 % wt solutions of P(VDF-TrFE-CTFE)-(AQ 0.6%) @1000rpm
- 2) Soft baking @ 250°C for 5 min
- 3) Exposure @ 2J/cm² under N₂
- 4) Post exposure baking @ 250°C for 5 min
- 5) Developing with isopropanol/cyclopentanone (66/33) @ RT for 1 min

6) Rinsing with isopropanol

7) Air drying

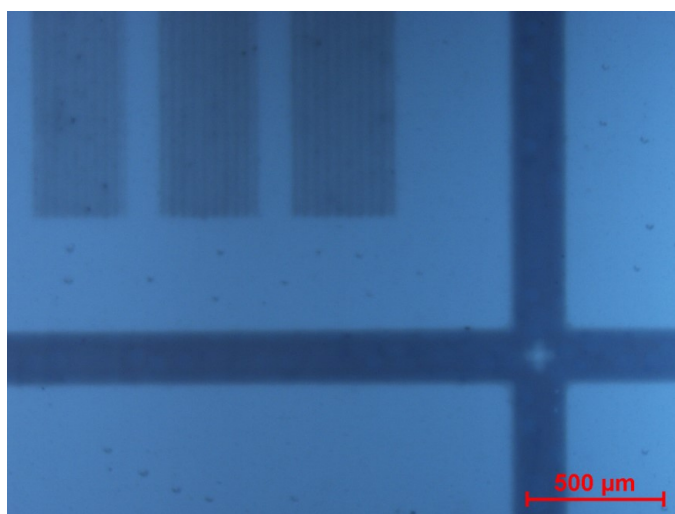
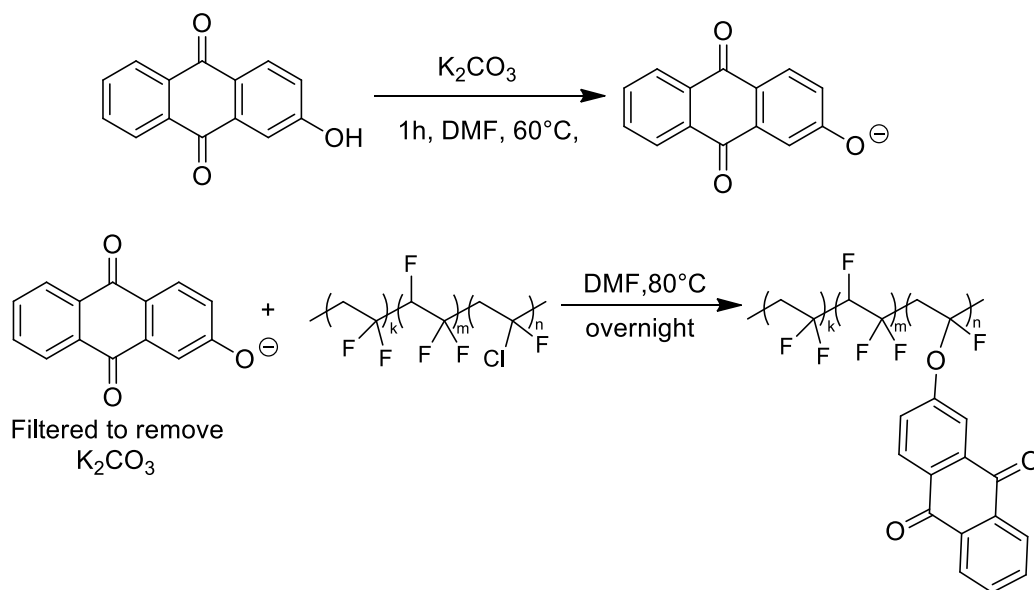


Figure 3-28. Optical microscope picture of patterned anthraquinone modified terpolymer (0.6%) on a silicon wafer.

3.2.2) Chemical modification of P(VDF-TrFE-CFE) terpolymers with anthraquinone groups

Polymer with similar relaxor-ferroelectric behavior to the P(VDF-TrFE-CFTE) is the P(VDF-TrFE-CFE). The modification reaction with anthraquinone was attempted in order to investigate the effect that this would have to the electric properties of the material and also to induce photo-patternability. The same two-step process was followed as in the case of P(VDF-TrFE-CTFE) terpolymers and the reaction is shown in **Scheme 3-6**.



Scheme 3-6. Grafting reaction of 2-hydroxy anthraquinone on P(VDF-TrFE-CFE) via a two-step process.

It was found that under mild modification conditions, low grafting content was obtained, varying from 0.02 to 0.5% compared to the total number of repeating units, while double bonds were also introduced to the polymer backbone (**Figure 3-29**). Those values have to be considered with caution, knowing that the resolution limits of the technique are reached. The double bond and anthraquinone contents on the P(VDF-TrFE-CFE) terpolymers are described in **Table 3-6**.

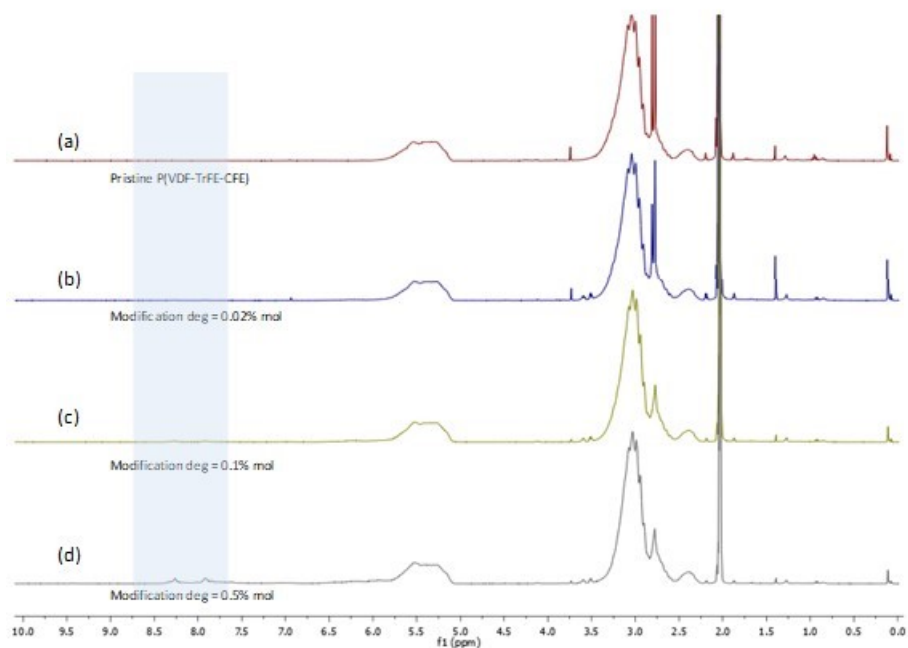


Figure 3-29. $^1\text{H-NMR}$ at 400 MHz of (a) the pristine terpolymer and (b) anthraquinone modified terpolymer (0.02%), (c) anthraquinone modified terpolymer (0.1%), (d) anthraquinone modified terpolymer (0.5%).

For clarity, the zone of interest from **Figure 3-29** is amplified in **Figure 3-30**.

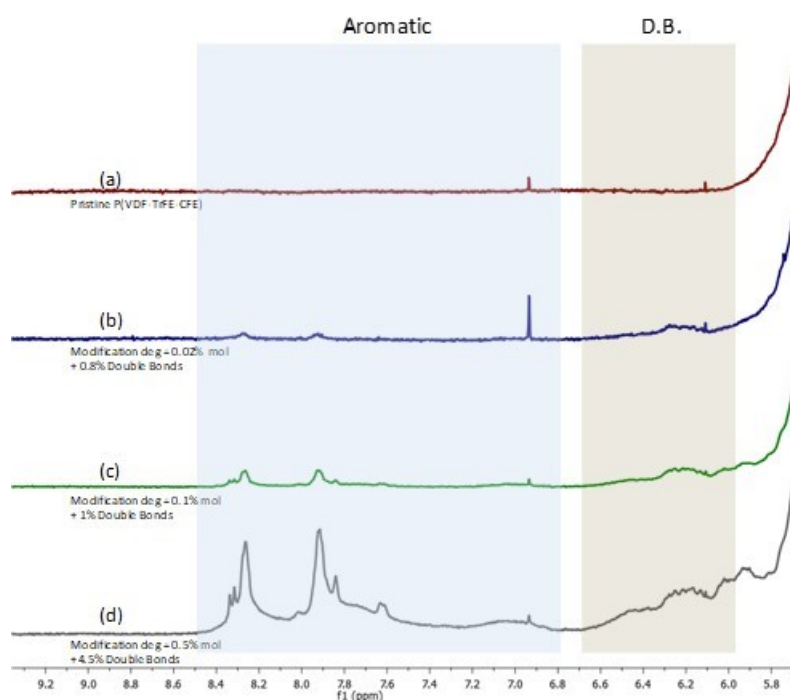
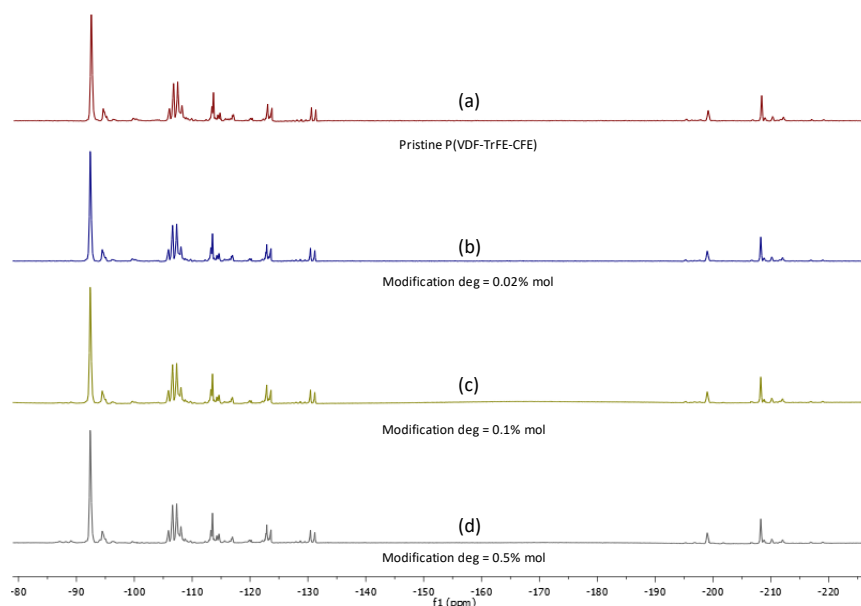


Figure 3-30. Amplification of $^1\text{H-NMR}$ from 5.7 to 9.4 ppm. $^1\text{H-NMR}$ at 400 MHz of (a) the pristine terpolymer and (b) anthraquinone modified terpolymer (0.02%), (c) anthraquinone modified terpolymer (0.1%), (d) anthraquinone modified terpolymer (0.5%).

Table 3-6. Summary of the modification results of P(VDF-TrFE-CFE) with 2-hydrxyanthraquinone, from ^1H NMR spectra.

	Equivalents of anthraquinone	Reaction time	TrFE (1 H) 4.7-5.7 ppm	Double bonds (1 H) 6-7 ppm	Aromatic (9 H) 7-8 ppm	Modification degree
(a)	0	0h	29.1	0%	0	0 %
(b)	0.05	1 day	29.1	0.8%	0.13	0.02%
(c)	0.1	1 day	29.1	1%	0.7	0.1%
(d)	0.2	1 day	29.1	4.5%	4.2	0.5%

The ^{19}F -NMR spectra of those polymers were also recorded and presented in **Figure 3-31**, however, no useful information could be derived from these spectra.

**Figure 3-31.** ^{19}F -NMR at 376,5 MHz of (a) the pristine terpolymer and (b) anthraquinone modified terpolymer (0.02%), (c) anthraquinone modified terpolymer (0.1%), (d) anthraquinone modified terpolymer (0.5%).

The different anthraquinone modified polymers were characterized by attenuated total reflection infrared spectroscopy as shown in **Figure 3-32**. The peaks at 710, 945, 1300, 1590 and 1680 cm^{-1} which correspond to the anthraquinone group and the one at 1720 cm^{-1} corresponding to the C=C stretching are again in this case barely visible for such low anthraquinone and double bond contents.

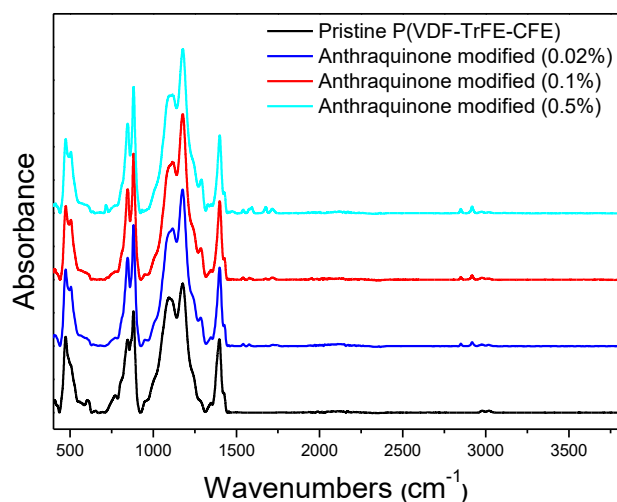


Figure 3-32. FT-IR ATR spectra of P(VDF-TrFE-CFE) modified with different amounts of benzophenone.

Despite the very low loadings though, the modification seems to have strong influence on the crystalline properties of those materials, as characterized by the DSC thermograms (**Figure 3-33**). The enthalpies of both the melting and the crystallization transitions seem to steadily decrease with increasing the anthraquinone and double bond content (**Table 3-7**).

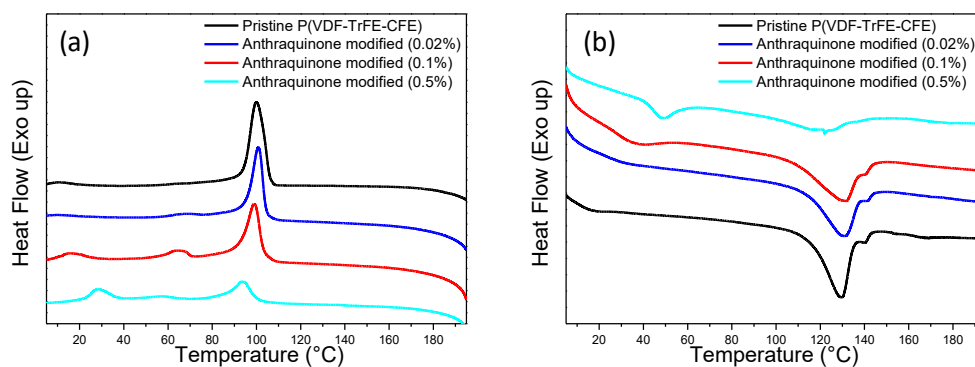


Figure 3-33. DSC thermograms with 10°C/min ramp, comparing the pristine terpolymer with terpolymers modified with different anthraquinone loadings for the (a) first cooling cycle and (b) the second heating cycle.

Table 3-7. Summary of the data derived from the DSC thermograms of anthraquinone modified P(VDF-TrFE-CFE) terpolymers.

	Melting		Crystallization	
	Temperature (°C)	Enthalpy (J/g)	Temperature (°C)	Enthalpy (J/g)
Pristine terpolymer	145°C	22	108	22
Anthraquinone (0.02%)	145°C	23	106	19
Anthraquinone (0.1%)	145°C	19	105	15
Anthraquinone (0.5%)	142°C	14	100	10

The dielectric and electroactive properties of some of those polymers appear to be very interesting and they will be extensively discussed in **Chapter 5**.

3.2.3) Chemical modification of P(VDF-TrFE) copolymers

Amongst Fluorinated Electroactive Polymers, the ferroelectric P(VDF-TrFE) copolymer is of permanent importance. Devices can be fabricated with this copolymer, through a great variety of techniques such as inkjet¹² and screen printing or alternative techniques such as nano imprint¹³⁻¹⁴. Even photolithography has been demonstrated to be used for the structuring of P(VDF-TrFE),¹⁵ however in this case, similarly to the case of P(VDF-CTFE) structured by photolithography, a very expensive and potentially explosive bisazide photoinitiator was used as an additive to the fluoropolymer, making it very difficult for this technique to reach industrial scale. Thus a need emerges for the development of a scalable method that would make P(VDF-TrFE) compatible with photolithography.

Ideally, the copolymers could be grafted with photosensitive groups similarly to the terpolymers which would make them crosslink upon irradiation with UV light. The main bottleneck for this to be realized is the absence of the CTFE groups on the copolymers and thus the lack of the chlorine groups which are the good leaving groups allowing the SN2 reaction to happen. Indeed, in previous chapter the grafting of P(VDF-TrFE) with azide groups was attempted without any success. That was attributed mainly to the fact that the fluorine groups of P(VDF-TrFE) are not nearly as good leaving groups as the chlorine groups of P(VDF-TrFE-CTFE). However it's widely known in literature that P(VDF-TrFE) can undergo elimination reactions in the presence of base¹⁶. That indicates that the fluorines of the P(VDF-TrFE) act as leaving

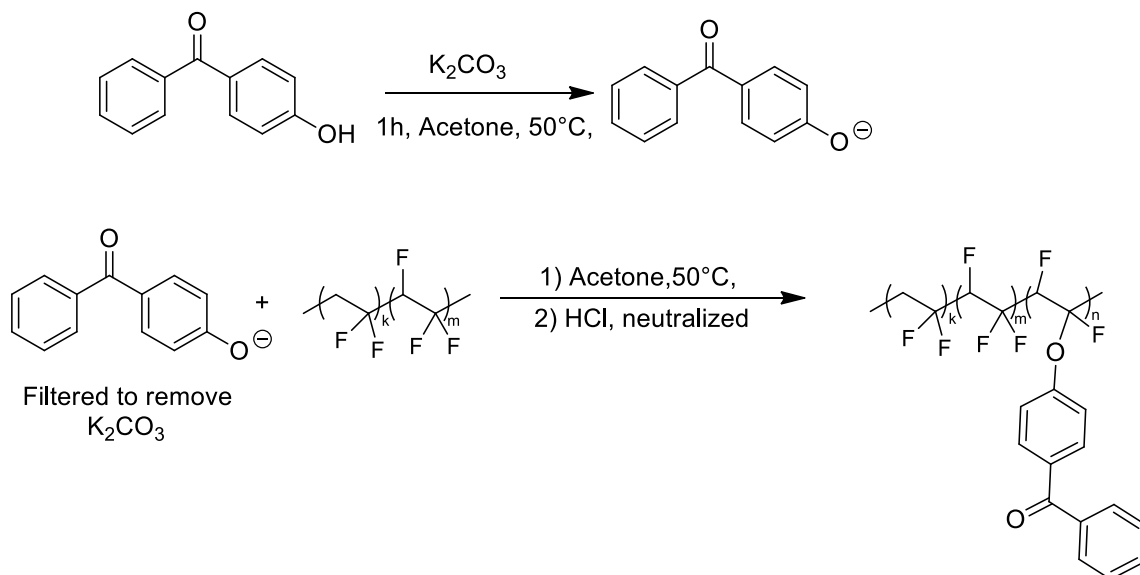
groups under certain circumstances.

It has to be noted here that phenoxides have been demonstrated to react with non halogenated fluoropolymers, as explained in the introductory chapter, and that was attributed to the dehydrofluorination reaction leading to the double bonds formation on the fluoropolymer backbone followed by a Michael addition of the phenoxide on the double bonds.

That fact opens up the possibility to extend the modification methods presented previously to the ferroelectric P(VDF-TrFE). That method allowed the grafting of fluorinated polymers through a Williamson ether synthesis approach and has been proven very efficient for the grafting of fluoropolymers containing the CTFE group. Now the question rises whether this same method could be extended to P(VDF-TrFE) as well.

3.2.3.1) P(VDF-TrFE) (75/25) copolymers functionalized with benzophenone groups

The grafting of the ferroelectric P(VDF-TrFE) with benzophenone groups was attempted under the same conditions used for the grafting of benzophenone on P(VDF-TrFE-CTFE) The detailed reaction is shown in detail in **Scheme 3-7**.



Scheme 3-7. Grafting reaction of 4-hydroxy benzophenone on P(VDF-TrFE) via a two-step process, according to Williamson Ether Synthesis route.

The different benzophenone modified copolymers were characterized by attenuated total reflection infrared spectroscopy (ATR FT-IR) as shown in **Figure 3-33**. The presence of the benzophenone and the double bond groups leads to the appearance of

peaks at 700-740, 920-935, 1500-1540, 1600-1660 cm^{-1} respectively. That combined with the fact that no peaks of acidic proton appear in the FT-IR spectra, indicates the success of the grafting reaction on the P(VDF-TrFE) copolymer. Reaction conditions and benzophenone feeding ratios were studied in order to control the grafting percentage of benzophenone.

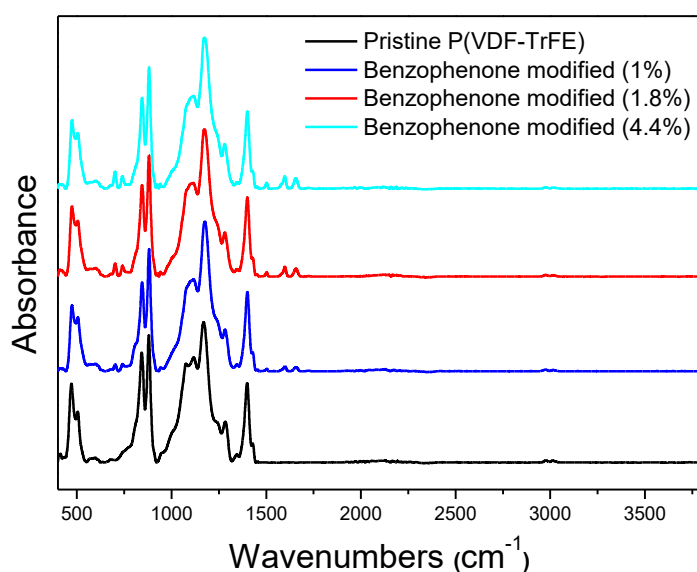


Figure 3-33. FT-IR spectra of P(VDF-TrFE) modified with different benzophenone content.

Indeed, by comparing the UV and LS detectors, we were able to confirm that P(VDF-TrFE) has been successfully grafted with a chromophore group i.e. BP (see **Figure 3-34**).

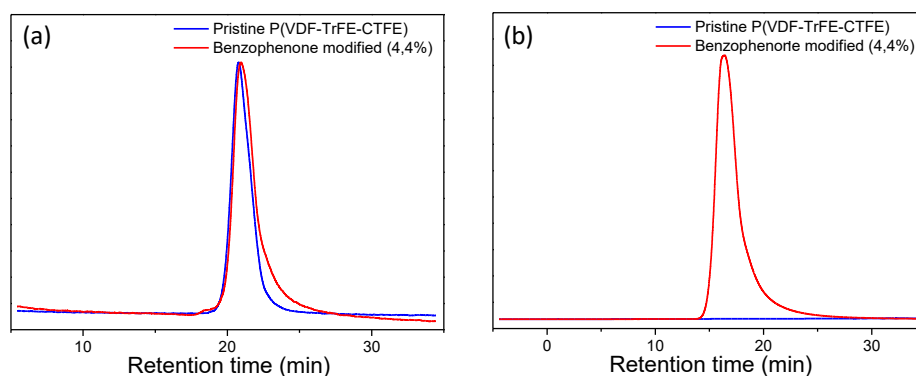


Figure 3-34. Size exclusion chromatography of the pristine copolymer and the benzophenone modified copolymer observing (a) the RI detector and (b) the UV detector.

Since the modification reaction was successful, copolymers with different

benzophenone loadings were prepared by varying the modification reaction conditions such as the benzophenone feeding ratio, reaction time etc. The benzophenone loadings of the different prepared copolymers was quantified using ^1H and ^{19}F NMR presented in **Figures 3-35** and **Figure 3-36**, while the calculated double bond and benzophenone loadings are presented in **Table 3-8**. The way that the double bond and benzophenone contents were calculated was identical to the previous cases, where the integrations of the signals corresponding to double bond and aromatic protons were compared to the integration of signals corresponding to the VDF and TrFE protons.

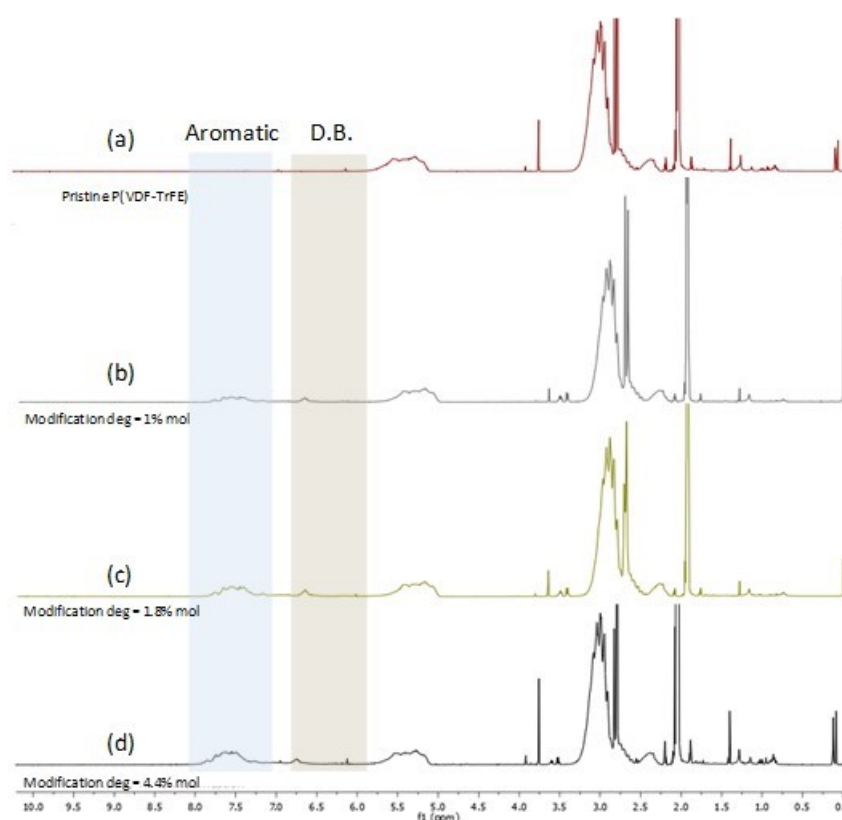


Figure 3-35. ^1H -NMR at 400 MHz of (a) the pristine copolymer and (b) benzophenone modified copolymer (1%), (c) benzophenone modified copolymer (1.8%), (d) benzophenone modified copolymer (4.4%).

Table 3-8. Summary of the modification results of $P(\text{VDF-TrFE})$ with 4-hydroxybenzophenone from ^1H NMR data.

	Equivalents of benzophenone	Reaction time	TrFE (1 H) 4.7-5.7 ppm	Double bonds (1 H) 6-7 ppm	Aromatic (9 H) 7-8 ppm	Modification degree
(a)	0	0 days	28.3	0%	0	1 %
(b)	0.3	1 day	28.3	2.8%	9	1.8%
(c)	0.5	1 day	28.3	3.6%	16.2	1%

(d)	0.4	3 days	28.3	8.3%	31	4.4%
-----	-----	--------	------	------	----	------

As mentioned above, the benzophenone modified copolymers were characterized with ^{19}F -NMR, however the spectra do not provide us with much information since the differences are not apparent upon modification (**Figure 3-36**).

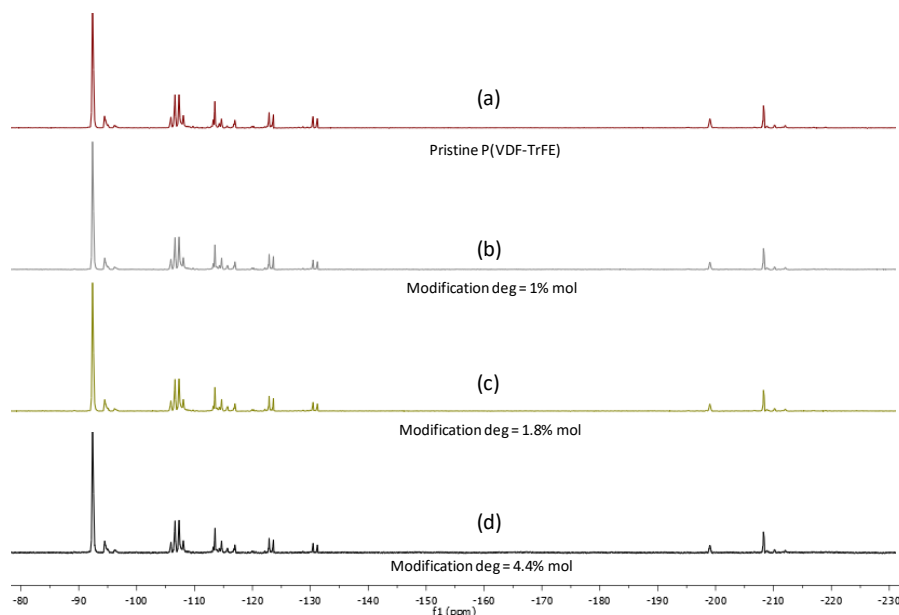


Figure 3-36. ^{19}F -NMR at 376,5 MHz of (a) the pristine copolymer and (b) benzophenone modified copolymer (1%), (c) benzophenone modified copolymer (1.8%), (d) benzophenone modified copolymer (4.4%).

The DSC thermograms of the benzophenone modified copolymers were compared to the pristine P(VDF-TrFE) copolymer (**Figure 3-37**), where the impact of the modification reaction is more significant. The Curie, the melting and crystallization transitions have been influenced by the modification. Starting by the effect of the modification on the melting and the crystallization, decreasing melting temperature and melting enthalpies are observed with increasing the benzophenone and double bond contents. That is indicative of smaller crystalline domains of the ferroelectric polymer as well as lower overall crystallinity, with potentially detrimental effect on the ferroelectric properties (discussed in **Chapter 5**). On the other hand the curie transition is also affected by the modification. Although the curie temperature does not shift, the modified polymers present a single curie peak, indicative of a single crystalline phase¹⁷, while the pristine P(VDF-TrFE) polymer presents a multiple curie transition peak.

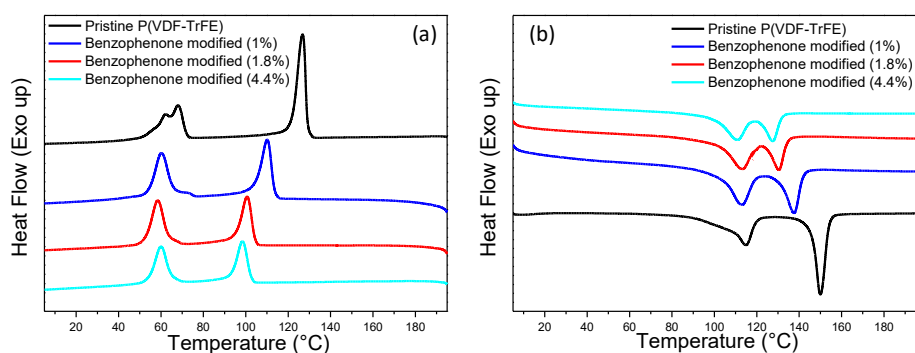


Figure 3-37. DSC thermograms with 10°C/min ramp, comparing the pristine copolymer with copolymers modified with different benzophenone contents for the (a) first cooling cycle and (b) the second heating cycle.

The data from the Curie (**Figure 3-37a**) and the melting (**Figure 3-37b**) transitions are summarized in **Table 3-9**.

Table 3-9. Summary of the data derived from the DSC thermograms of benzophenone modified copolymers.

Sample	Curie		Melting	
	Temperature (°C)	Enthalpy (J/g)	Temperature (°C)	Enthalpy (J/g)
Pristine copolymer	68°C	20.7J/g	157°C	26.5J/g
Benzophenone (1%)	60°C	14.7	144°C	12J/g
Benzophenone (1.8%)	58°C	14.9J/g	138°C	7.7J/g
Benzophenone (4.4%)	60°C	14J/g	134°C	7J/g

An attempt was made to pattern the benzophenone modified P(VDF-TrFE) polymers through a photolithographic process using the modified polymer as the negative photoresist. That was made possible and such patterned film is shown in **Figure 3-38**. However the quality of the patterned film is poor, since the protocol is not optimized. The followed protocol is presented below.

Protocol

- 1) Spincoating of 4 % wt solution of P(VDF-TrFE)-(BP4.4%) @ 1000rpm
- 2) Soft baking @ 125°C for 5 min
- 3) Exposure @ 6J/cm² under N₂
- 4) Post exposure baking @ 110°C for 5 min
- 5) Developing with acetone @ RT for 1 min
- 6) Rinsing with isopropanol
- 7) Air drying

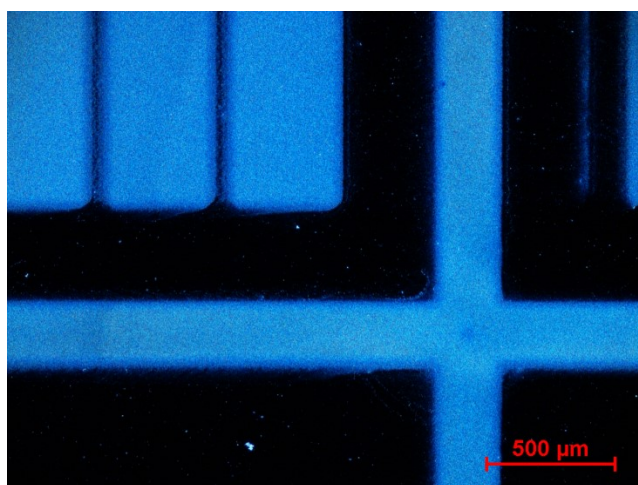
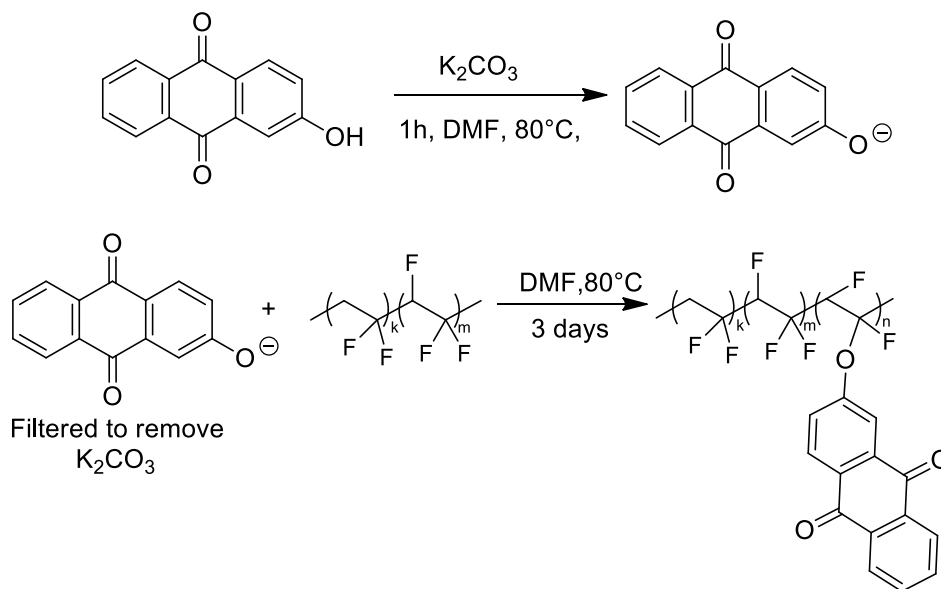


Figure 3-38. Optical microscope picture of patterned benzophenone modified P(VDF-TrFE) copolymer on a silicon wafer.

3.2.3.2 P(VDF-TrFE) copolymers functionalized with anthraquinone groups

An attempt to attach anthraquinone moieties on P(VDF-TrFE) copolymers was also performed, following the Williamson ether synthesis approach (see **Scheme 3-8**).



Scheme 3-8. Grafting reaction of 2-hydroxy anthraquinone on P(VDF-TrFE) via a two-step process, following the Williamson ether synthesis route.

Copolymers with different anthraquinone and double bond content were synthesized by varying the reaction conditions and the different products were characterized by 1H (**Figure 3-39**) and ^{19}F (**Figure 3-40**) NMR and the data derived from the 1H -NMR spectra are presented in **Table 3-10**.

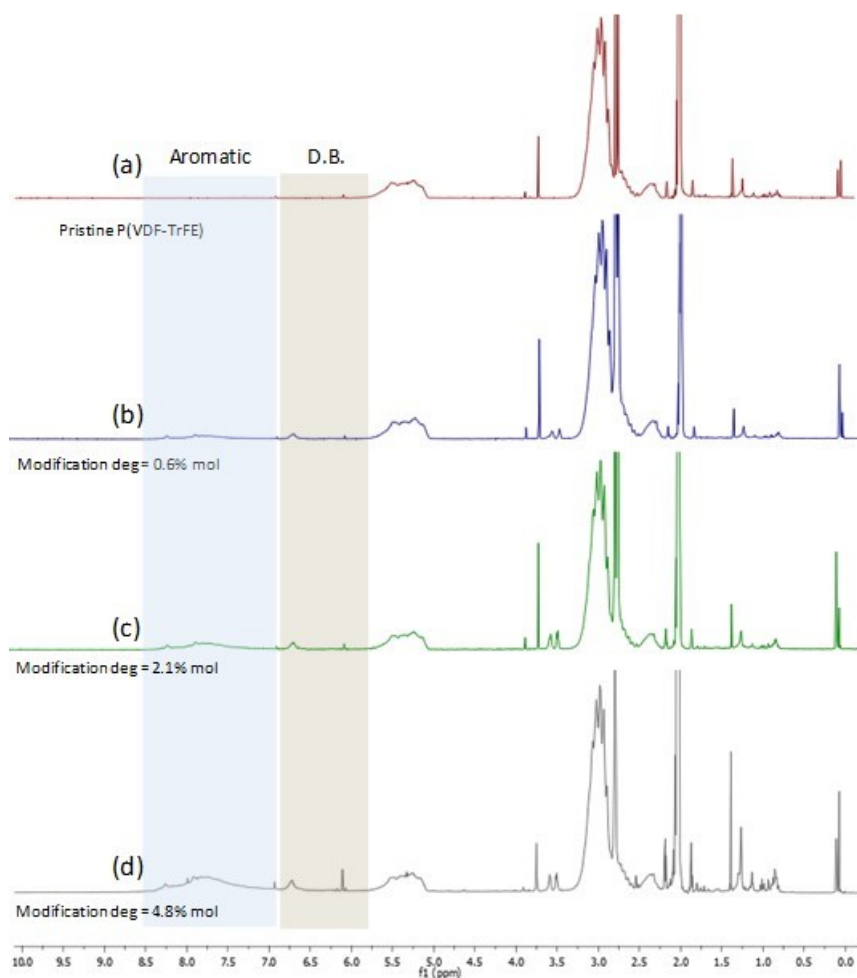


Figure 3-39. $^1\text{H-NMR}$ at 400 MHz of (a) the pristine copolymer and (b) anthraquinone modified copolymer (0.6%), (c) anthraquinone modified copolymer (2.1%), (d) anthraquinone modified copolymer (4.8%).

Table 3-10. Summary of the modification results of P(VDF-TrFE) with 2-hydroxyanthraquinone, from $^1\text{H NMR}$ spectra.

	Equivalents of anthraquinone	Reaction time	TrFE (1 H) 4.7-5.7 ppm	Double bonds (1 H) 6-7 ppm	Aromatic (8 H) 7-8 ppm	Modification degree
(a)	0	0h	25	0%	0	0 %
(b)	0.05	1 day	25	1.1%	4.4	0.6%
(c)	0.1	3days	25	3.3%	15.0	2.1%
(d)	0.4	3 days	25	5.6%	34.4	4.8%

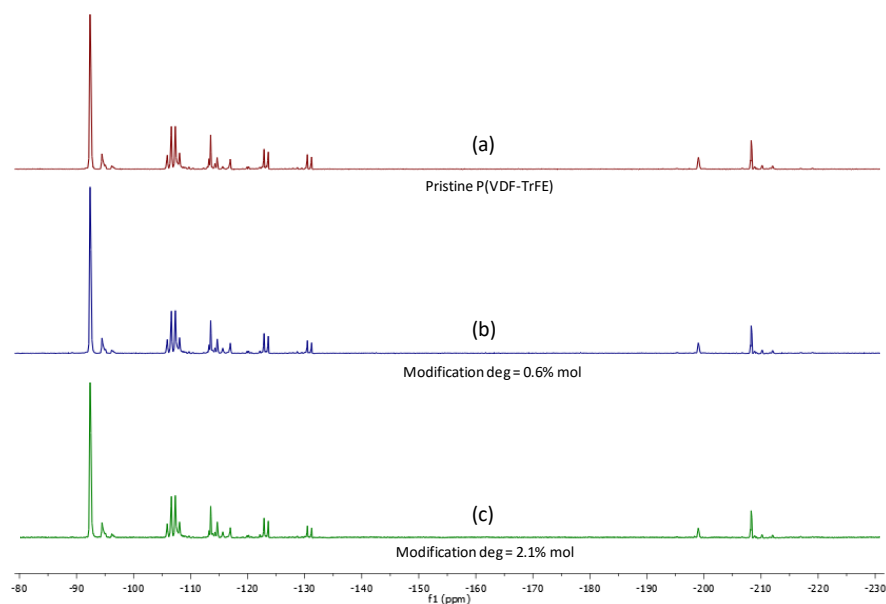


Figure 3-40. ^{19}F -NMR at 376,5 MHz of (a) the pristine copolymer and (b) anthraquinone modified copolymer (0.6%), (c) anthraquinone modified copolymer (2.1%).

The products of the modification reaction were also characterized by FT-IR in reflexion mode and the spectra are presented in **Figure 3-41**. The presence of the anthraquinone groups was observed by the appearance of peaks at 710, 945, 1300, 1590 cm^{-1} and 1680 cm^{-1} respectively, all increasing in intensity with increasing anthraquinone loading. On the other hand, a peak at 1720 cm^{-1} corresponding to the C=C stretching also appears.

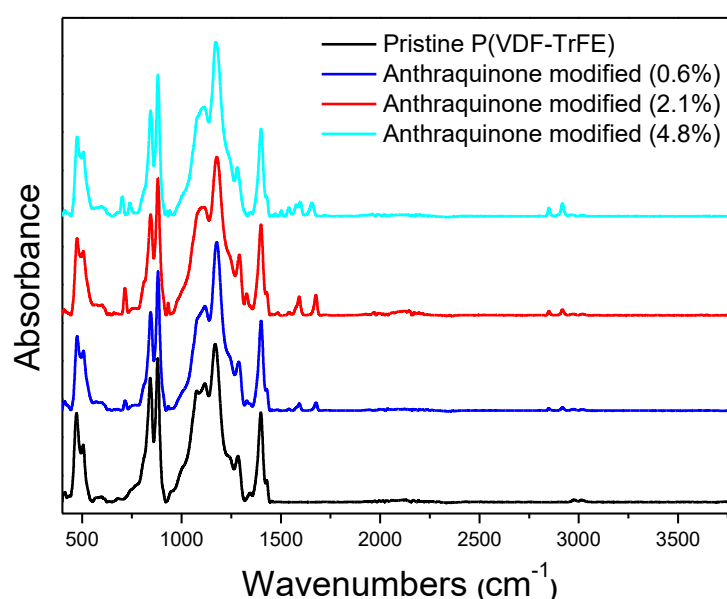


Figure 3-41. ATR of P(VDF-TrFE) modified with different anthraquinone content, as determined by ^1H NMR.

The DSC thermograms of the anthraquinone modified copolymers were recorded and presented in **Figure 3-42**. Similarly to their benzophenone modified counterparts, here again the Curie, the melting and the crystallization transitions have been influenced by the modification in a similar way. The curie and melting temperatures and enthalpies are summarized in **Table 3-11**.

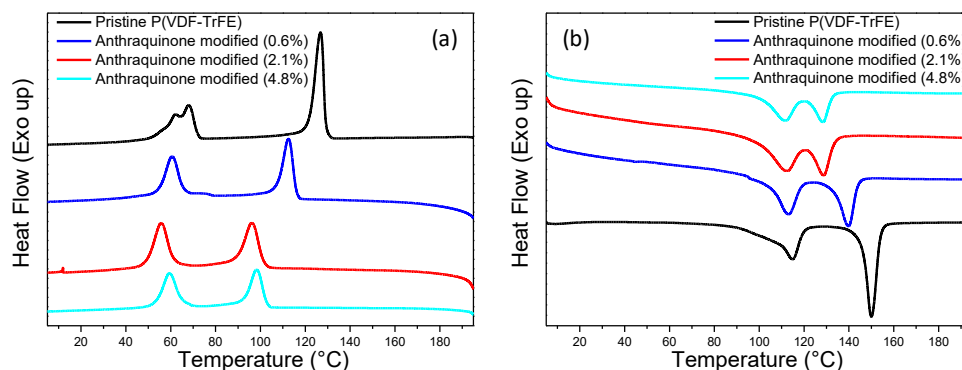


Figure 3-42. DSC thermograms with 10°C/min ramp, comparing the pristine copolymer with copolymers modified with different anthraquinone content for the (a) first cooling cycle and (b) the second heating cycle.

Table 3-11. Summary of the data derived from the DSC thermograms of anthraquinone modified P(VDF-TrFE) copolymers.

	Curie		Melting	
	Temperature (°C)	Enthalpy (J/g)	Temperature (°C)	Enthalpy (J/g)
Pristine copolymer	68°C	20.7J/g	157°C	26.5 J/g
Anthraquinone (0.6%)	60.5°C	15J/g	147°C	14.3J/g
Anthraquinone (2.1%)	56°C	13J/g	137°C	6.7J/g
Anthraquinone (4.8%)	59.3°C	14J/g	135°C	7.2 J/g

The anthraquinone modified P(VDF-TrFE) copolymers were also used as negative photoresists in a photolithographic patterning process following the protocol mentioned below. The protocol was not optimized, however patterning was possible, with a cross-polar microscope picture of the patterned film being showed in **Figure 3-43**.

Protocol

- 1) Spincoating of 4 % wt solution of P(VDF-TrFE)-(AQ4.8%) @ 1000rpm
- 2) Soft baking @ 110°C for 5 min
- 3) Exposure @ 3J/cm² under N₂
- 4) Post exposure baking @ 110°C for 5 min
- 5) Developing with cyclopentanone @ RT for 1 min
- 6) Rinsing with isopropanol
- 7) Air drying

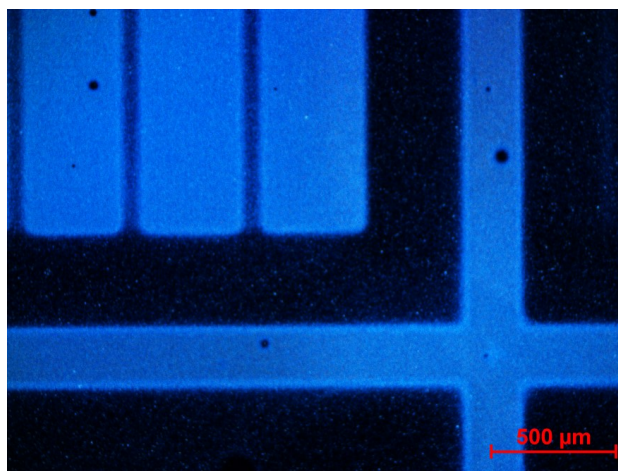


Figure 3-43. Optical microscope picture of patterned benzophenone modified copolymer on a silicon wafer.

3.3) Experimental Part

3.3.1) Chemical modification of Fluoropolymers

Typical modification reactions were performed using standard schlenk techniques.

4-hydroxy benzophenone grafting reaction on P(VDF-TrFE-CTFE) (61.7/28.3/10): (1g) of terpolymer was dissolved in 25 ml of acetone in a 50ml glass schlenk ampoule. 4-hydroxy benzophenone (0.8g, 4.0mmol) and potassium carbonate (0.7g, 5.6 mmol) were mixed in acetone (15 ml). The glass schlenk was sealed under argon and heated to 60°C in the dark for 1 hour. Then, the second solution was filtered and added to the first in order to remove the excess of the base. The glass ampoule was sealed and left in the dark at 60°C for 16 hours to react. Few drops of condensed HCl were added after the end of the reaction and the polymer was precipitated in water and washed with water, ethanol and chloroform for several hours to remove any impurities. Then it was

dried in vacuum oven at 40°C for 12 hours.

2-hydroxy anthraquinone grafting reaction on P(VDF-TrFE-CTFE) (61.7/28.3/10): (5g) of terpolymer were dissolved in 100ml of dimethyl formamide (DMF) in a 250ml glass schlenk ampoule. 2-hydroxy anthraquinone (1.4g, 6.4mmol) and potassium carbonate (1.32, 9.6 mmol) were mixed in dimethyl formamide (DMF) (100 ml). The glass schlenk was sealed under argon and heated to 80°C in the dark for 1 hour. Then, the second solution was filtered and added to the first in order to remove the excess of the base. The glass ampoule was sealed and left in the dark at 80°C for 16 hours to react. The polymer was precipitated in water and then washed with water, ethanol and chloroform for several hours to remove any impurities. Then it was dried in vacuum oven at 40°C for 12 hours.

2-hydroxy anthraquinone grafting reaction on P(VDF-TrFE-CFE) (68.2/29.1/7.1): (3g) of terpolymer were dissolved in 50ml of dimethyl formamide (DMF) in a 250ml glass schlenk ampoule. 2-hydroxy anthraquinone (1.9g, 8.5mmol) and potassium carbonate (1.75 g, 12.8 mmol) were mixed in dimethyl formamide (DMF) (100 ml). The glass schlenk was sealed under argon and heated to 80°C in the dark for 1 hour. Then, the second solution was filtered and added to the first in order to remove the excess of the base. The glass ampoule was sealed and left in the dark at 80°C for 16 hours to react. The polymer was precipitated in water and then washed with water, ethanol and chloroform for several hours to remove any impurities. Then it was dried in vacuum oven at 40°C for 12 hours.

4-hydroxy benzophenone grafting reaction on P(VDF-TrFE) (75/25): (2g) of copolymer were dissolved in 80 ml of acetone in a 250ml glass schlenk ampoule. 4-hydroxy benzophenone (1.3 g, 5.9 mmol) and potassium carbonate (1.2 g, 8.8 mmol) were mixed in acetone (20 ml). The glass schlenk was sealed under argon and heated to 60°C in the dark for 1 hour. Then, the second solution was filtered and added to the first in order to remove the excess of the base. The glass ampoule was sealed and left in the dark at 60°C for 16 hours to react. Few drops of condensed HCl were added after the end of the reaction and the polymer was precipitated in water and washed with water, ethanol and chloroform for several hours to remove any impurities. Then it was dried in vacuum oven at 40°C for 12 hours.

2-hydroxy anthraquinone grafting reaction on P(VDF-TrFE) (75/25): (2g) of colymer were dissolved in 80ml of dimethyl formamide (DMF) in a 250 ml glass schlenk ampoule. 2-hydroxy anthraquinone (1.3 g, 5.9 mmol) and potassium carbonate (1.2 g,

8.8 mmol) were mixed in dimethyl formamide (DMF) (20 ml). The glass schlenk was sealed under argon and heated to 80°C in the dark for 1 hour. Then, the second solution was filtered and added to the first in order to remove the excess of the base. The glass ampoule was sealed and left in the dark at 80°C for 16 hours to react. The polymer was precipitated in water and then washed with water, ethanol and chloroform for several hours to remove any impurities. Then it was dried in vacuum oven at 40°C for 12 hours.

3.3.2) Preparation of patterned thin films via photolithography

Benzophenone containing P(VDF-TrFE-CTFE): A 4% wt solution of the benzophenone modified polymer (4.4%) in cyclopentanone was spincoated on a silicon wafer at 500 rpm for 5 sec and then at 1000 rpm for 1 min, yielding a 250 nm thick film. The wafer was soft baked before exposure at 130°C for 5 min and subsequently cross-linked by UV light under nitrogen, using a photo-lithographic mask. The applied UV dose was 6 J/cm². Then, the film was post exposure baked at 130°C for 5 min. Finally, the patterned film was developed in a blend of one fifth cyclopentanone and four fifths isopropanol for 1 min. Subsequently, the wafer was rinsed with isopropanol and dried with compressed air.

Anthraquinone containing P(VDF-TrFE-CTFE): A 4% wt solution of the anthraquinone modified polymer (0.6%) in cyclopentanone was spincoated on a silicon wafer at 500 rpm for 5 sec and then at 1000 rpm for 1 min, yielding a 250 nm thick film. The wafer was soft baked before exposure at 250°C for 5 min and subsequently cross-linked by UV light under nitrogen, using a photo-lithographic mask. The applied UV dose was 3 J/cm². Then, the film was post exposure baked at 250°C for 5 min. Finally, the patterned film was developed in a blend of one fifth cyclopentanone and four fifths isopropanol for 1 min. Subsequently, the wafer was rinsed with isopropanol and dried with compressed air.

Benzophenone containing P(VDF-TrFE): A 4% wt solution of the benzophenone modified polymer (4.4%) in cyclopentanone was spincoated on a silicon wafer at 500 rpm for 5 sec and then at 1000 rpm for 1 min, yielding a 250 nm thick film. The wafer was soft baked before exposure at 125°C for 5 min and subsequently cross-linked by UV light under nitrogen, using a photo-lithographic mask. The applied UV dose was 6 J/cm². Then, the film was post exposure baked at 110°C for 5 min. Finally, the

patterned film was developed in a acetone for 1 min. Subsequently, the wafer was rinsed with isopropanol and dried with compressed air.

Anthraquinone containing P(VDF-TrFE): A 4% wt solution of the anthraquinone modified polymer (4.8%) in cyclopentanone was spincoated on a silicon wafer at 500 rpm for 5 sec and then at 1000 rpm for 1 min, yielding a 250 nm thick film. The wafer was soft baked before exposure at 110°C for 5 min and subsequently cross-linked by UV light under nitrogen, using a photo-lithographic mask. The applied UV dose was 3 J/cm². Then, the film was post exposure baked at 110°C for 5 min. Finally, the patterned film was developed in cyclopentanone for 1 min. Subsequently, the wafer was rinsed with isopropanol and dried with compressed air.

3.4) Conclusions

A general method allowing for introduction of additional functionality to FEPs was developed. The relaxor-ferroelectric polymers P(VDF-TrFE-CTFE) and P(VDF-TrFE-CFE), as well as the ferroelectric P(VDF-TrFE) were functionalized with photoinitiator groups via a simple etherification reaction and the produced photo cross-linkable polymers which could be used as negative photoresists in photolithographic patterning processes. Despite this method being used in this context primarily to induce photopatternability and tune the electroactive properties of FEPs, it's by no means limited to such use, as it allows for freedom regarding both the grafted group and the fluorinated polymer on which it can be applied. The electroactive and dielectric properties of all the polymers mentioned in this Chapter are discussed in detail in **Chapter 5**. As mentioned above, the developed pathway, leads to the formation of double bonds, as a side product of the grafting reaction. In order to investigate the impact that double bonds alone have on the electroactive properties of FEPs, **Chapter 4** is entirely devoted to the synthesis of FEPs bearing only double bonds and no other functional group.

3.5) References

1. Lin, A. A.; Sastri, V. R.; Tesoro, G.; Reiser, A.; Eachus, R., On the crosslinking mechanism of benzophenone-containing polyimides. *Macromolecules* **1988**, *21* (4), 1165-1169.
2. Kim, J.; Hanna, J. A.; Byun, M.; Santangelo, C. D.; Hayward, R. C., Designing responsive buckled surfaces by halftone gel lithography. *Science* **2012**, *335* (6073), 1201-5.
3. Schwärzle, D.; Hou, X.; Prucker, O.; Rühle, J., Polymer Microstructures through Two-Photon Crosslinking. *Advanced Materials* **2017**, *29* (39), 1703469.
4. Temel, G.; Aydogan, B.; Arsu, N.; Yagci, Y., Synthesis and Characterization of One-Component Polymeric Photoinitiator by Simultaneous Double Click Reactions and Its Use in Photoinduced Free Radical Polymerization. *Macromolecules* **2009**, *42* (16), 6098-6106.
5. Ren, Y.; Lee, S.; Christensen, J. M.; Plotnikov, N. V.; Burgess, M.; Martínez, T. J.; Dlott, D. D.; Moore, J. S., Pressure-Induced Neutral-to-Ionic Transition in an Amorphous Organic Material. *Chemistry of Materials* **2016**, *28* (18), 6446-6449.
6. Virkar, A.; Ling, M.-M.; Locklin, J.; Bao, Z., Oligothiophene based organic semiconductors with cross-linkable benzophenone moieties. *Synthetic Metals* **2008**, *158* (21), 958-963.
7. Tan, S.; Hu, X.; Ding, S.; Zhang, Z.; Li, H.; Yang, L., Significantly improving dielectric and energy storage properties via uniaxially stretching crosslinked P(VDF-co-TrFE) films. *Journal of Materials Chemistry A* **2013**, *1* (35), 10353-10361.
8. Tan, S.; Li, J.; Gao, G.; Li, H.; Zhang, Z., Synthesis of fluoropolymer containing tunable unsaturation by a controlled dehydrochlorination of P(VDF-co-CTFE) and its curing for high performance rubber applications. *Journal of Materials Chemistry* **2012**, *22* (35), 18496-18504.
9. Preston, G. W.; Wilson, A. J., Photo-induced covalent cross-linking for the analysis of biomolecular interactions. *Chemical Society Reviews* **2013**, *42* (8), 3289-3301.
10. Soulestin, T.; Ladmiral, V.; Lannuzel, T.; Domingues Dos Santos, F.; Ameduri, B., Importance of Microstructure Control for Designing New Electroactive Terpolymers Based on Vinylidene Fluoride and Trifluoroethylene. *Macromolecules* **2015**, *48* (21), 7861-7871.
11. Ma, R.; Zhang, Z.; Tong, K.; Huber, D.; Kornbluh, R.; Ju, Y. S.; Pei, Q., Highly efficient electrocaloric cooling with electrostatic actuation. *Science* **2017**, *357* (6356), 1130-1134.
12. Thuau, D.; Kallitsis, K.; Dos Santos, F. D.; Hadziioannou, G., All inkjet-printed piezoelectric electronic devices: energy generators, sensors and actuators. *Journal of Materials Chemistry C* **2017**, *5* (38), 9963-9966.
13. Cai, R.; Antohe, V.-A.; Hu, Z.; Nysten, B.; Piraux, L.; Jonas, A. M., Multiferroic Nanopatterned Hybrid Material with Room-Temperature Magnetic Switching of the Electric Polarization. *Advanced Materials* **2017**, *29* (6), 1604604.
14. Hu, Z.; Tian, M.; Nysten, B.; Jonas, A. M., Regular arrays of highly ordered ferroelectric polymer nanostructures for non-volatile low-voltage memories. *Nature Materials* **2008**, *8*, 62.
15. Breemen, A. J. J. M. v.; Putten, J. B. P. H. v. d.; Cai, R.; Reimann, K.; Marsman, A. W.; Willard, N.; Leeuw, D. M. d.; Gelinck, G. H., Photocrosslinking of ferroelectric polymers and its application in three-dimensional memory arrays. *Applied Physics Letters* **2011**, *98* (18), 183302.
16. Kim, Y.; Hong, S.; Oh, S.; Choi, Y.-Y.; Choi, H.; No, K. S., *The Effects of an Alkaline Treatment on the Ferroelectric Properties of Poly(vinylidene fluoride trifluoroethylene) Films*. 2015; Vol. 11, p 586-591.
17. Kim, K. J.; Kim, G. B.; Vanlencia, C. L.; Rabolt, J. F., Curie transition, ferroelectric crystal structure, and ferroelectricity of a VDF/TrFE(75/25) copolymer 1. The effect of the consecutive annealing in the ferroelectric state on curie transition and ferroelectric crystal structure. *Journal of Polymer Science Part B: Polymer Physics* **1994**, *32* (15), 2435-2444.

Chapter 4

Unsaturation containing Fluoropolymers

Chapter 4: Unsaturation containing Fluoropolymers

4.1) Introduction

In the two previous chapters, methods to introduce functional groups on fluoropolymers were presented. However, both the presented methods created unsaturation on the fluoropolymer's backbone as side product of the functionalization reaction. Therefore, the scope of this chapter is to evaluate the impact of the controllably introduced unsaturation on the electric properties of various FEPs (*e.g.* P(VDF-TrFE-CTFE), P(VDF-TrFE-CFE) and P(VDF-TrFE)). Although the creation of unsaturation on fluoropolymers is already documented¹⁻², its effect on the electroactive properties of FEPs has only recently been reported³⁻⁴. More specifically it has been reported that once unsaturation is created on the ferroelectric P(VDF-TrFE) copolymer, the polymer's behavior changes to antiferroelectric, but when the polymer is annealed at high temperature, the initial ferroelectric character of the polymer is reobtained³.

The second report, concerns the introduction of unsaturation on PVDF homopolymer and as reported, unsaturation seems to favor the β -phase crystallization and thus improved ferroelectric properties of the PVDF homopolymer approaching the behavior of the ferroelectric P(VDF-TrFE) copolymer.

We therefore wanted to investigate the impact of the double bonds on the fluoropolymers we have used in the context of this work. To do so, different contents of double bonds were introduced in fluoropolymers such as the P(VDF-TrFE-CTFE) and the P(VDF-TrFE-CFE) terpolymer, as well as the ferroelectric P(VDF-TrFE) copolymer.

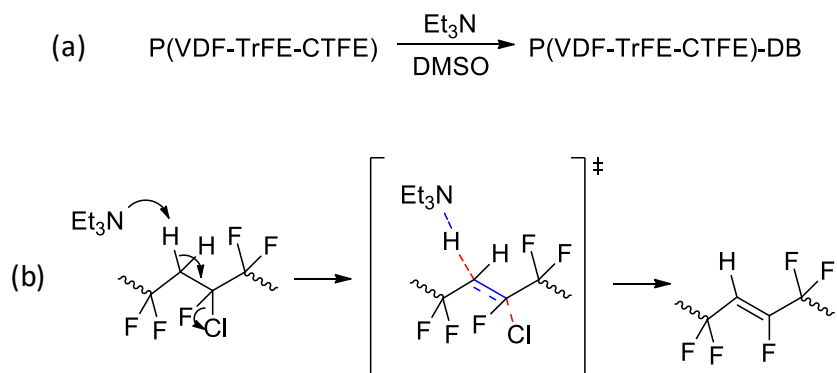
4.2) Results and Discussion

4.2.1) P(VDF-TrFE-CTFE) terpolymers containing unsaturation

Those P(VDF-TrFE-CTFE) terpolymers are commercially available in different monomers' compositions. These differences in composition give rise to different electroactive responses. In the context of this work, two different compositions of P(VDF-TrFE-CTFE) terpolymers were used. The first composition used was (61.9/29.9/8.2), while the second composition was (61.7/28.3/10), (VDF/TrFE/CTFE) respectively.

4.2.1.1) P(VDF-TrFE-CTFE) (61.9/29.9/8.2)

The introduction of unsaturation was carried out by treatment of the terpolymer with a weak base such as triethylamine. The reaction proceeded under mild conditions and is described in **Scheme 4-1a**. Since the dehydrochlorination reaction cannot occur on the CTFE unit itself, since no α protons exist, it has to occur in a sequence which brings protons to α position in respect to the chlorine group of the CTFE. Such sequence is the VDF-CTFE (H-T) as described in **Scheme 4-1b**. The fact that dehydrochlorination occurs in this sequence will be discussed below.



Scheme 4-1. (a) Dehydrochlorination reaction of P(VDF-TrFE-CTFE) upon treatment with triethylamine (DB=Double Bond); (b) Nucleophilic attack of triethylamine on a VDF-CTFE sequence, leading to the formation of unsaturation via an E2 pathway.

Terpolymers treated under different conditions with triethylamine were characterized by $^1\text{H-NMR}$, which are shown in **Figure 4-1**. The double bond content (compared to the total number of repeating units) was then quantified for each polymer by comparing the integration of double bond protons (6.0-6.7 ppm) to the

VDF (2.2-3.7 ppm) and TrFE (4.7-5.7 ppm) protons respectively.

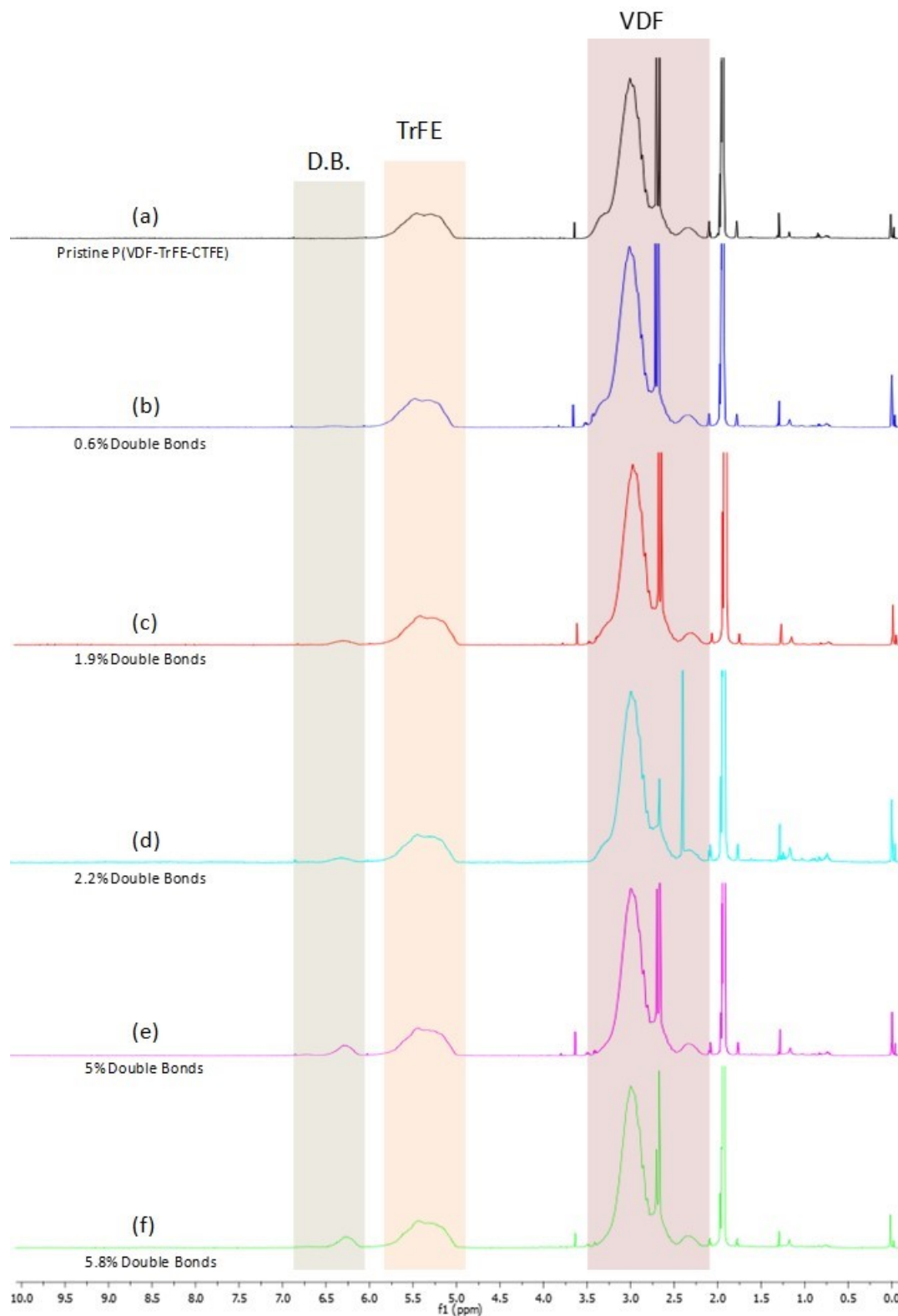


Figure 4-1. $^1\text{H-NMR}$ at 400 MHz (acetone- d_6) of (a) the pristine P(VDF-TrFE-CTFE) terpolymer and (b) P(VDF-TrFE-CTFE) terpolymer with estimated 0.6% of double bonds, (c) P(VDF-TrFE-CTFE) terpolymer with estimated 1.9% of double bonds, (d) P(VDF-TrFE-CTFE) terpolymer with estimated 2.2% of double bonds, (e) P(VDF-TrFE-CTFE) terpolymer with estimated 5% of double bonds, (f) P(VDF-TrFE-CTFE) terpolymer with estimated 5.8% of double bonds.

The equation used for the calculation of the double bond content of each terpolymer is presented below, while the calculated double bond contents are presented in **Table 4-1** along with the reaction conditions used in each case.

$$\text{DB content} = \frac{\int_{6\text{ppm}}^{6.7\text{ppm}} \text{CH of double bonds})}{\int_{4.7\text{ppm}}^{5.7\text{ppm}} \text{CHF of TrFE} + (\int_{2.2\text{ppm}}^{3.7\text{ppm}} \text{CH}_2 \text{ of VDF})/2 + (\int_{6\text{ppm}}^{6.7\text{ppm}} \text{CH of double bonds}) * 2}$$

A range of double bond contents varying from 0.6% to 5.8% was obtained as shown in **Table 4-1**.

Table 4-1. Summary of the treatment results of P(VDF-TrFE-CTFE) with triethylamine under different reaction conditions. The equivalents of Et₃N are calculated in respect to the total number of repeating units.

	Equivalents of Et ₃ N	Reaction time	Reaction temperature	Double bonds (1 H) 6-7 ppm
(a)	-	-	-	0%
(b)	0.3	2h	20°C	0.6%
(c)	0.3	4h	40°C	1.9%
(d)	0.3	4h	50°C	2.2%
(e)	0.6	4h	40°C	5%
(f)	0.9	4h	40°C	5.8%

¹H-NMR was the only technique used for the quantification of the double bond content in each polymer. The obtained results are considered a good proxy to the real double bond content, however dehydrochlorination can occur in sequences that do not involve protons on the double bonds. Such sequence could be the TrFE-CTFE leading to the formation of double bonds with no protons on them (-CF₂CF=CFCF₂-). Therefore, it is likely that the method we used to quantify the double bond content slightly underestimates the real value.

Further characterization was done by ¹⁹F-NMR. The new signals at -89.29 ppm, corresponding to the (-CF₂CH=CFCF₂-) sequence and -120.72 ppm corresponding to the (-CF₂CH=CFCF₂CF₂-) sequence, which are more apparent in materials (e) and (f) of **Figure 4-2** confirm the insertion of unsaturation on the polymer backbone.

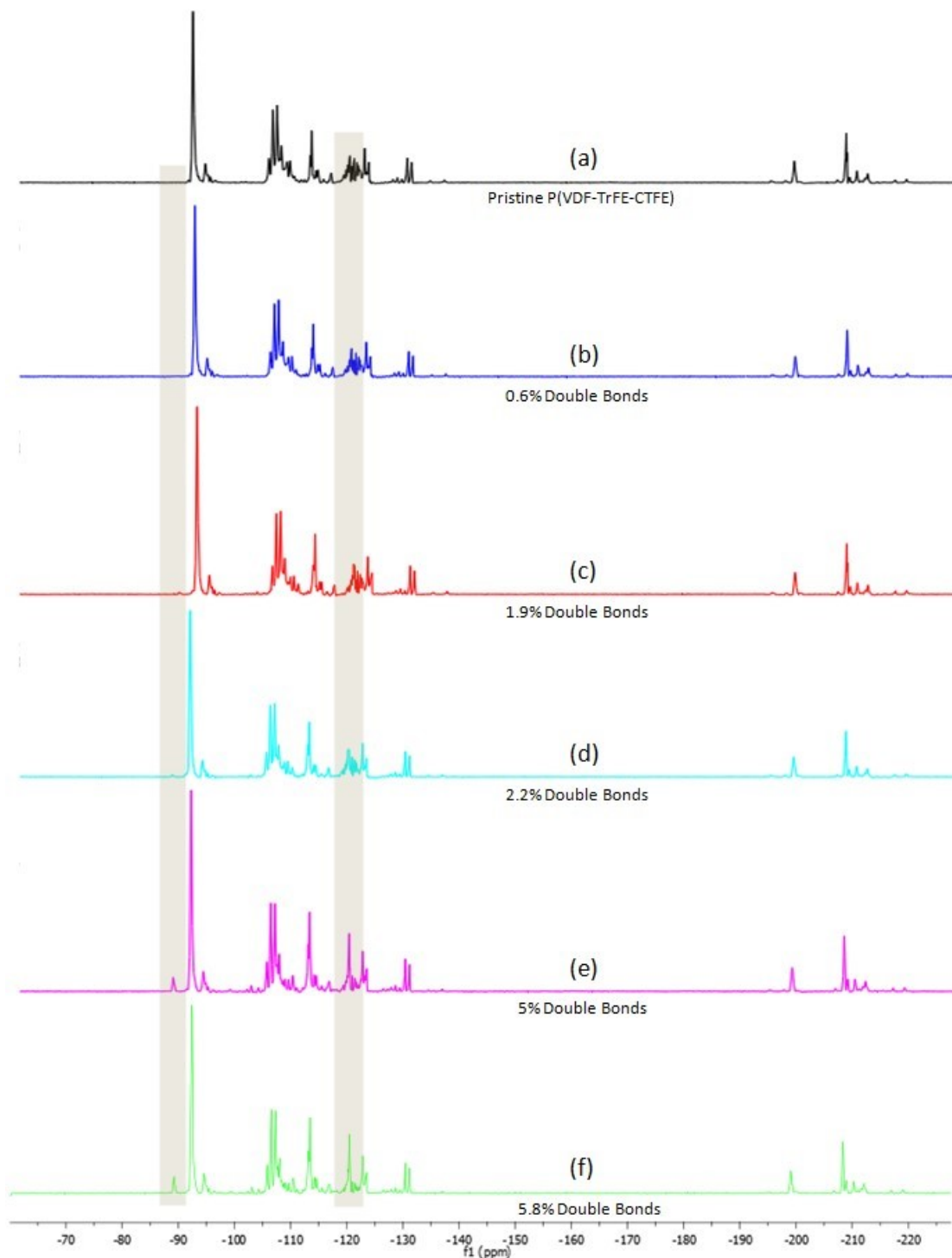


Figure 4-2. ^{19}F -NMR at 376,5 MHz (acetone- d_6) of (a) the pristine P(VDF-TrFE-CTFE) terpolymer and (b) P(VDF-TrFE-CTFE) terpolymer with estimated 0.6% of double bonds, (c) P(VDF-TrFE-CTFE) terpolymer with estimated 1.9% of double bonds, (d) P(VDF-TrFE-CTFE) terpolymer with estimated 2.2% of double bonds, (e) P(VDF-TrFE-CTFE) terpolymer with estimated 5% of double bonds, (f) P(VDF-TrFE-CTFE) terpolymer with estimated 5.8% of double bonds.

The different terpolymers containing various ratio of double bonds were characterized by attenuated total reflection infrared spectroscopy (ATR FT-IR) and are shown in **Figure 4-3**. The main band appearing in the polymers treated with base is the C=C stretching band at 1720cm^{-1} .

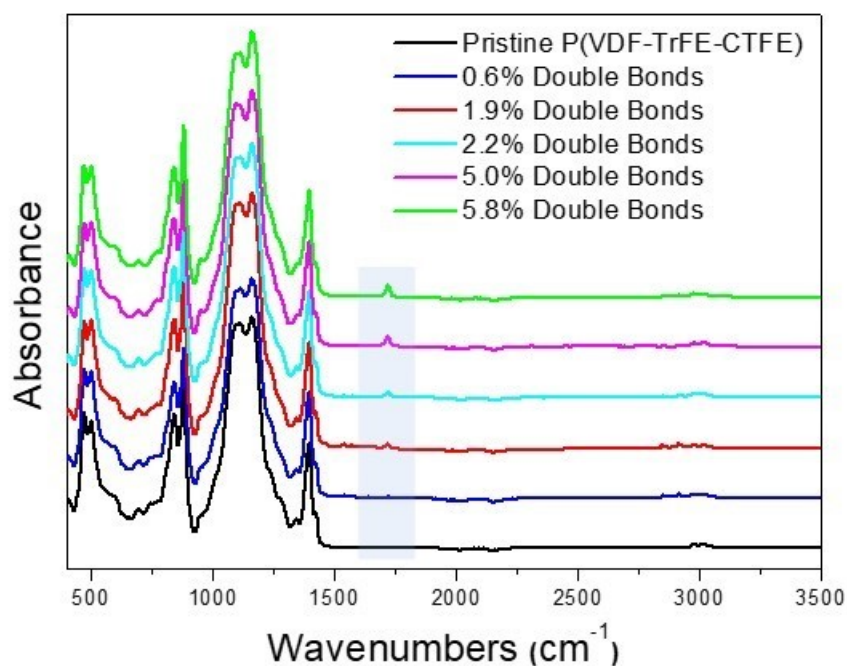


Figure 4-3. FT-IR (ATR) spectra of P(VDF-TrFE-CTFE) with different amounts of introduced double bonds.

The Raman spectra of the double bond containing P(VDF-TrFE-CTFE) terpolymers with 1.9% and 5.8% respectively, as well as the pristine terpolymer were recorded (**Figure 4-4**). The disappearance of the C-Cl band at 600-700 cm^{-1} is much more evident compared to the FT-IR spectra. In addition, the C=C stretching band at 1720 cm^{-1} , corresponding to the newly formed double bonds is also more pronounced in the Raman spectra.

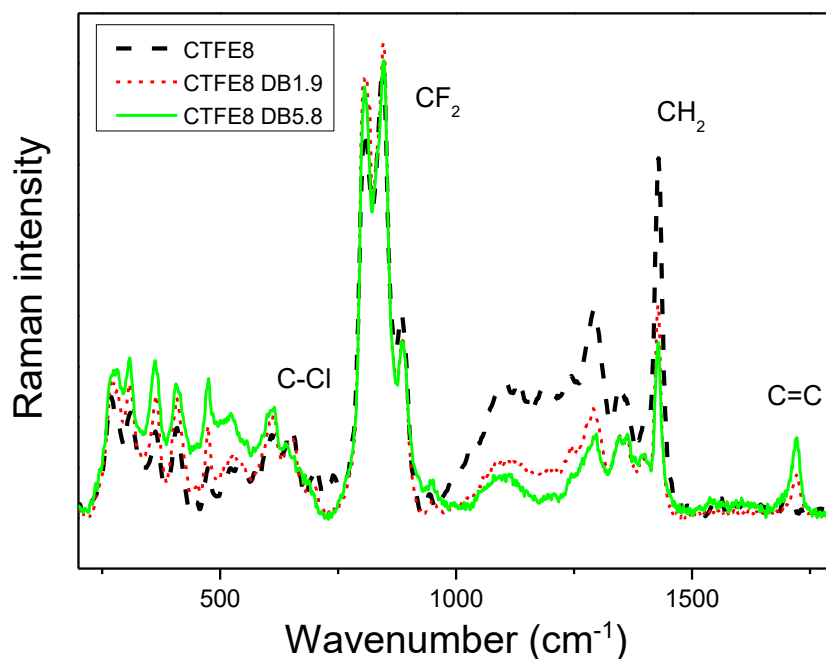


Figure 4-4. Raman spectra of the pristine P(VDF-TrFE-CTFE) (black) compared to the double bond containing terpolymer (1.9%) and (5%) respectively.

Optical images of the P(VDF-TrFE-CTFE) terpolymers with different double bond contents are shown in **Figure 4-5**, where the slight coloring of the polymers with increasing the double bond content can be observed.

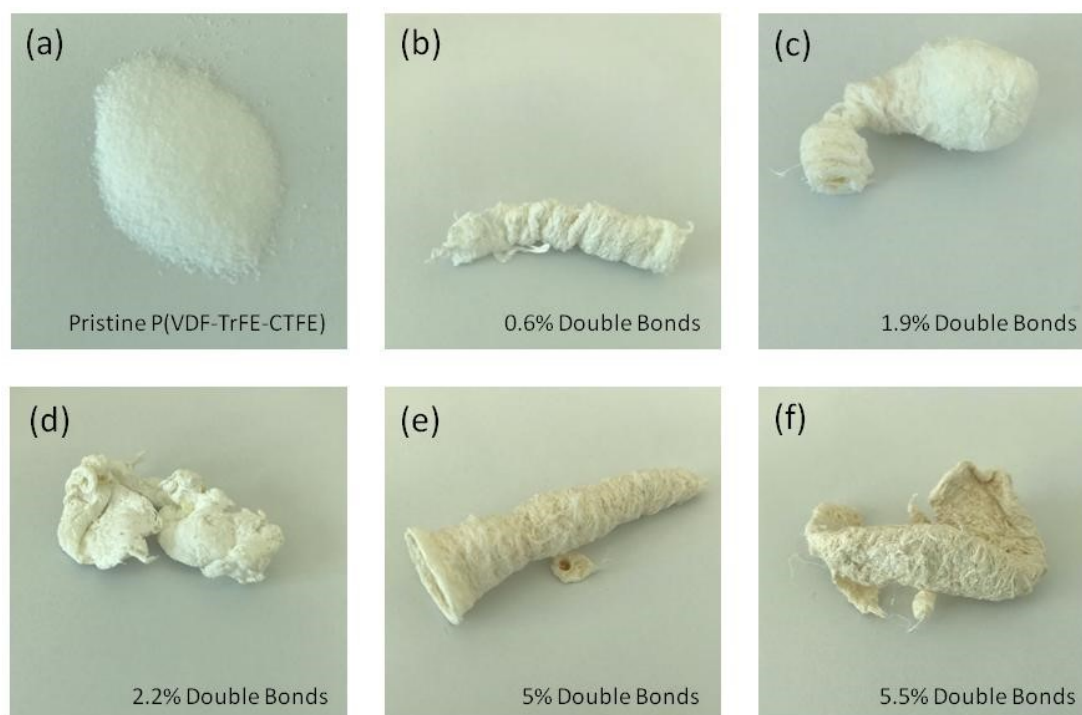


Figure 4-5. Photographs of (a) the pristine P(VDF-TrFE-CTFE) terpolymer and (b) P(VDF-TrFE-CTFE) terpolymer with estimated 0.6% of double bonds, (c) P(VDF-TrFE-CTFE) terpolymer with estimated 1.9% of double bonds, (d) P(VDF-TrFE-CTFE) terpolymer with estimated 2.2% of double bonds, (e) P(VDF-TrFE-CTFE) terpolymer with estimated 5% of double bonds, (f) P(VDF-TrFE-CTFE) terpolymer with estimated 5.8% of double bonds.

All the polymers mentioned above were characterized by differential scanning calorimetry (DSC), with the thermograms shown in **Figure 4-6** and the data derived from them being summarized in **Table 4-2**.

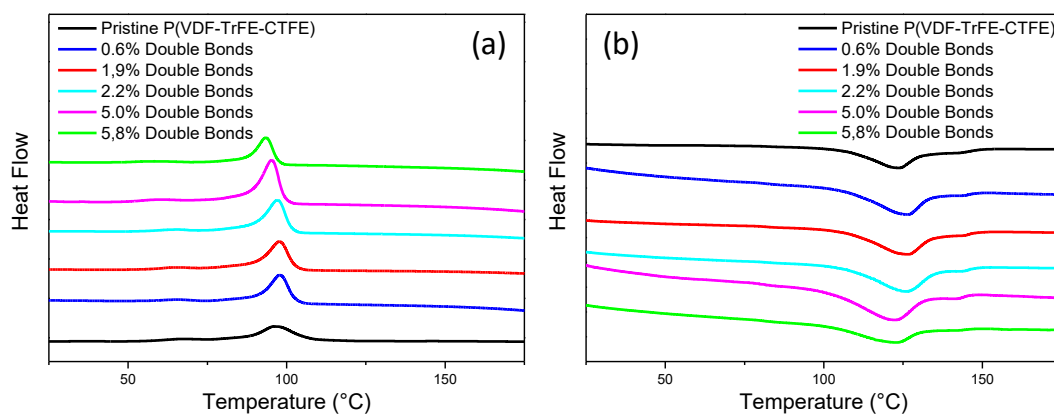


Figure 4-6. DSC thermograms with 10°C/min ramp, comparing P(VDF-TrFE-CTFE) terpolymers with different double bond contents. (a) first cooling cycle and (b) the second heating cycle.

In order to better understand the DSC data all crystallization and melting peaks are overlapped in **Figure 4-7**. Therefore the impact of the double bonds becomes much more apparent. From those graphs, the crystallization and melting temperatures are calculated as follows. The crystallization temperature is considered the temperature at the onset of the crystallization peak. On the other hand the melting temperature is considered the temperature at the end of the melting peak, where all crystals are molten. The calculated temperatures in that sense are summarized in **Table 4-2** alongside with the calculated enthalpies. It has to be noted though, that all calculated enthalpy values in this example or in any other example cannot be considered very precise as they were calculated from a single experiment.

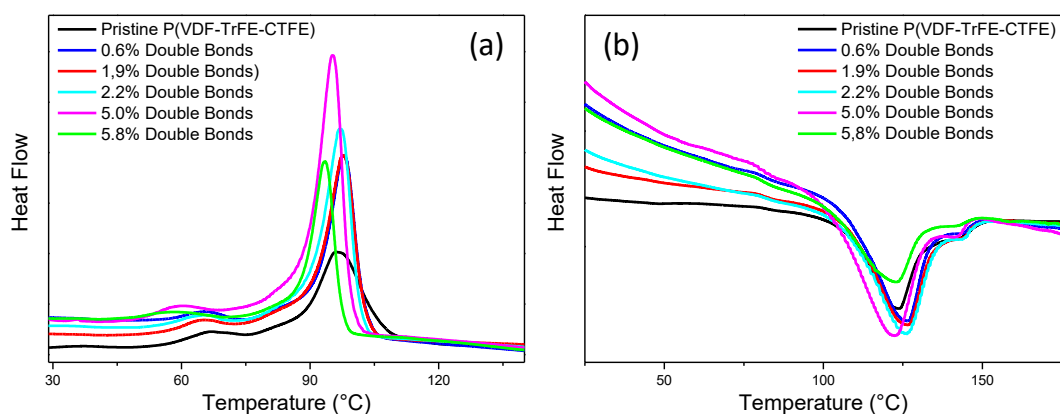


Figure 4-7. Overlapped crystallization (first cooling) and melting (second heating) peaks from Figure 4-6.

Table 4-2. Summary of the data derived from the DSC thermograms of P(VDF-TrFE-CTFE) terpolymers with different double bond contents.

	Melting		Crystallization	
	Temperature (°C)	Enthalpy (J/g)	Temperature (°C)	Enthalpy (J/g)
Pristine terpolymer	153°C	16	107°C	18
0.6% Double Bonds	150°C	18	103°C	14
1.9% Double Bonds	152°C	17	103°C	17
2.2% Double Bonds	152°C	17	102°C	17
5% Double Bonds	149°C	16	99°C	13
5.8% Double Bonds	149°C	14	97°C	13

It looks that the introduction of double bonds affects the crystallization much more than the melting. The melting temperatures do not seem to follow any particular trend. However the crystallization temperatures seemed to evolve with increasing the double bond content. That evolution is plotted in **Figure 4-8**, where the crystallization temperature seems to steadily decrease with increasing the double bond content.

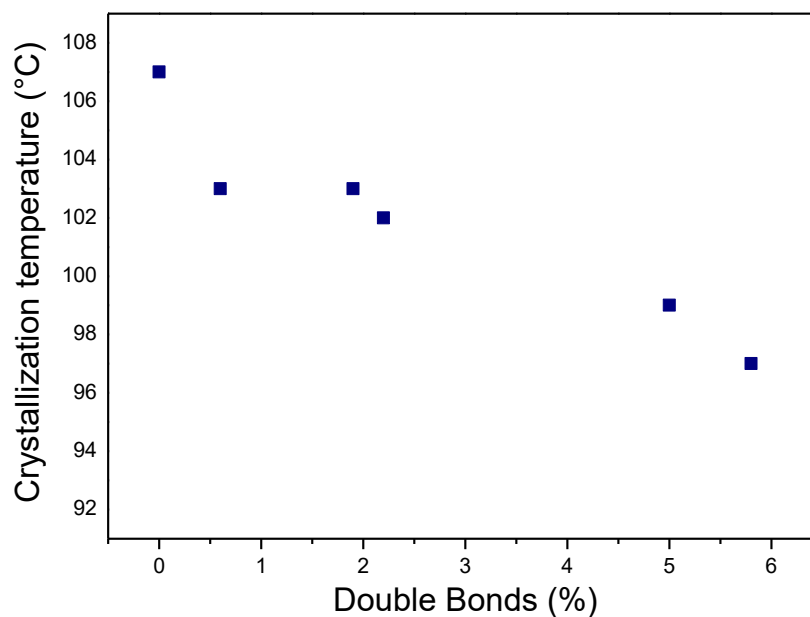


Figure 4-8. Onset of the crystallization peak plotted against the double bond content as estimated from $^1\text{H-NMR}$.

The thermal stability of the functionalized polymers was also investigated. To do so, the P(VDF-TrFE-CTFE) terpolymer containing the highest double bond content was drop casted to yield 4 films, to which different annealing protocols were applied. The first film was kept as cast in room temperature without any annealing, while the other three films were annealed for 1 hour, 5 hours and 3 days respectively at 110°C. Then all the films were characterized with different methods in order to investigate the stability of double bonds in annealing conditions. It has to be noted here that a typical annealing protocol for such polymers is 110°C for 1hour. The four films were peeled off from the glass substrate and submitted to FT-IR spectroscopy, shown in **Figure 4-9**. The band at 1720 cm^{-1} (assigned to double bonds) can still be observed even after three days of annealing, indicating that the double bonds are quite stable at high temperatures.

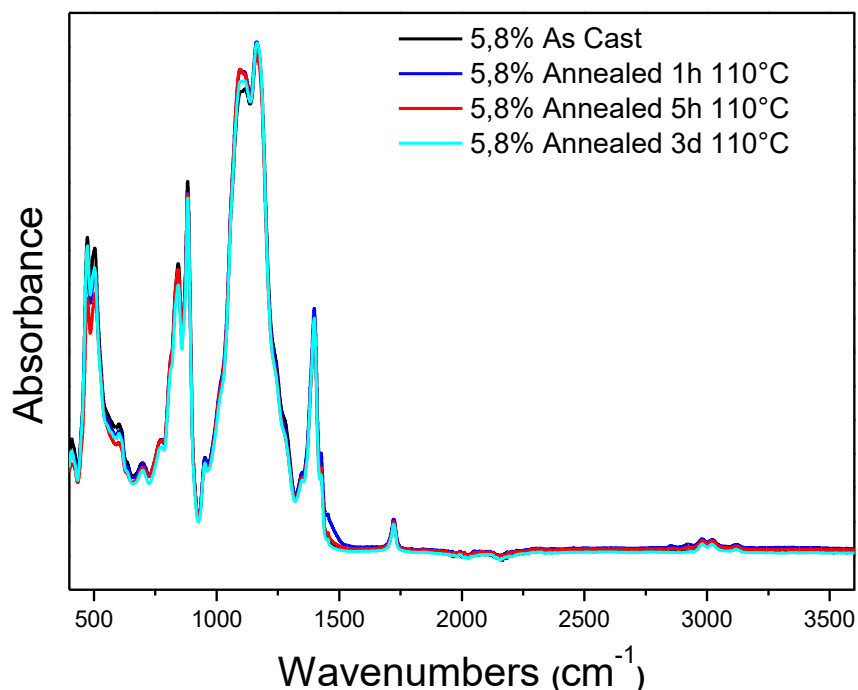


Figure 4-9. ATR FT-IR spectra of P(VDF-TrFE-CTFE) containing 5.8% double bonds, annealed for different time intervals @ 110°C.

Solubility tests were also performed to all four films and they were all found to be soluble in common solvents such as acetone and cyclopentanone which indicated that no extensive cross-linking has occurred during the annealing. Since all polymers were soluble, ¹H-NMR was performed for all of them in order to quantify the exact double bond content. The spectra are shown in **Figure 4-10** and the data are summarized in **Table 4-3**. As observed from the ¹H-NMR during the typical annealing conditions (1h, 110°C) no reduction of the double bond content can be observed, while a small decrease is observed for longer annealing time intervals.

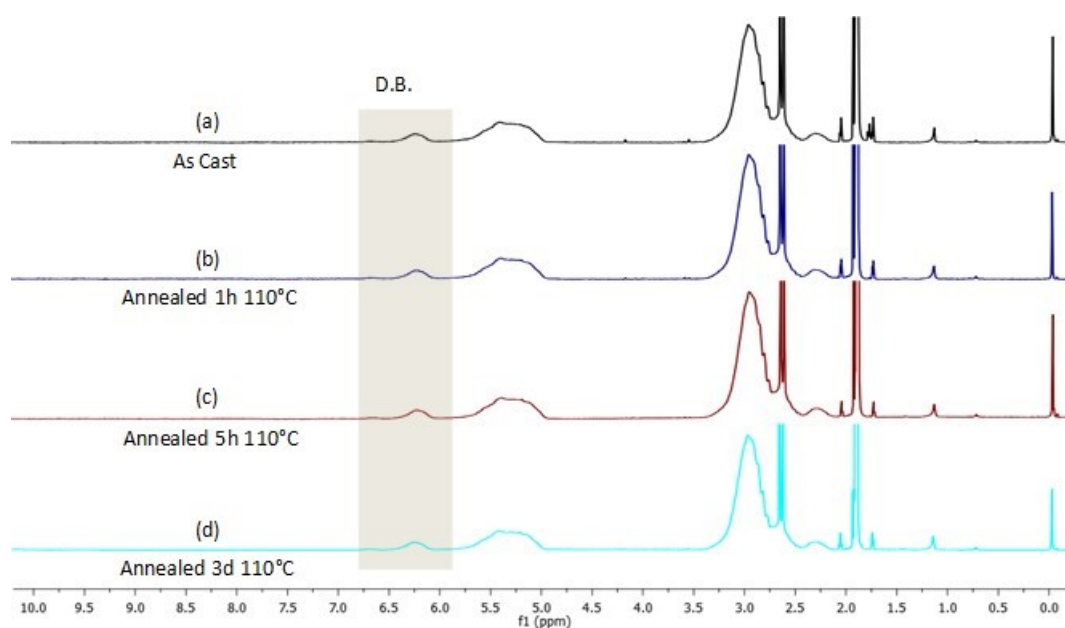


Figure 4-10. $^1\text{H-NMR}$ at 400 MHz (acetone- d_6) of $\text{P}(\text{VDF-TrFE-CTFE})$ (5.8% DB) (a) As cast, (b) annealed 1h @ 110°C, (c) annealed 5h @ 110°C, (d) annealed 3d @ 110°C.

Table 4-3. Summary of $^1\text{H-NMR}$ data of $\text{P}(\text{VDF-TrFE-CTFE})$ (5.8% DB) annealed for different time intervals.

	Annealing temperature	Annealing time	Double bonds (1 H) 6-7 ppm
(a)	110°C	-	5.8%
(b)	110°C	1h	5.8%
(c)	110°C	5h	5.4%
(d)	110°C	72h	4.5%

$^{19}\text{F-NMR}$ was also performed in the polymers treated with different thermal protocols, with the spectra being shown in **Figure 4-11**.

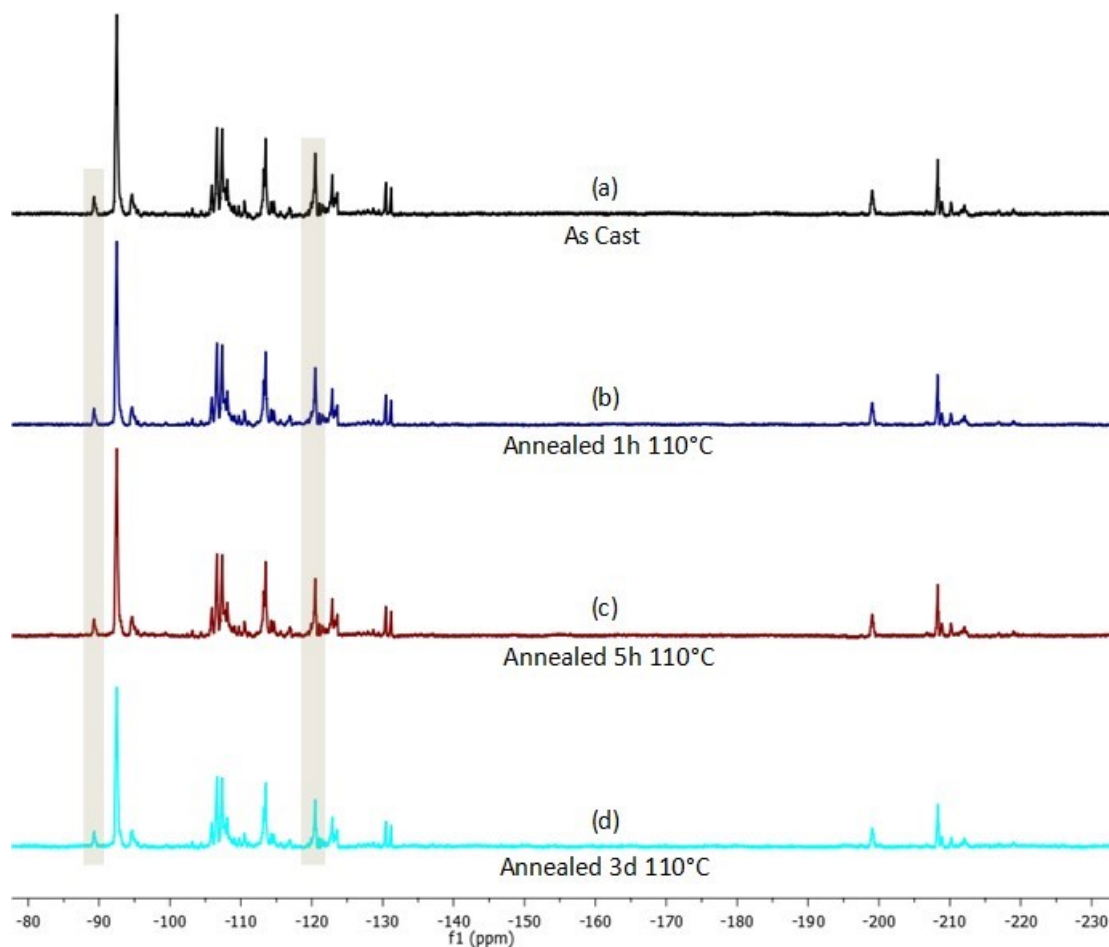


Figure 4-11. ^{19}F -NMR at 376,5 MHz (acetone- d_6) of P(VDF-TrFE-CTFE) (5.8% DB) (a) As cast, (b) annealed 1h @ 110°C, (c) annealed 5h @ 110°C, (d) annealed 3d @ 110°C.

4.2.1.2) P(VDF-TrFE-CTFE) (61.7/28.3/10)

This terpolymer was subjected to the same protocol as before using trimethylamine. The different polymers were characterized by the same techniques as above. First, ^1H -NMR was performed and is shown in **Figure 4-12**. One of the polymers obtained had a very low double bond content (0.7%) while the two other polymers had very similar double bond contents close to 4.5%. Both the modification conditions and the double bond contents are summarized in **Table 4-4**.

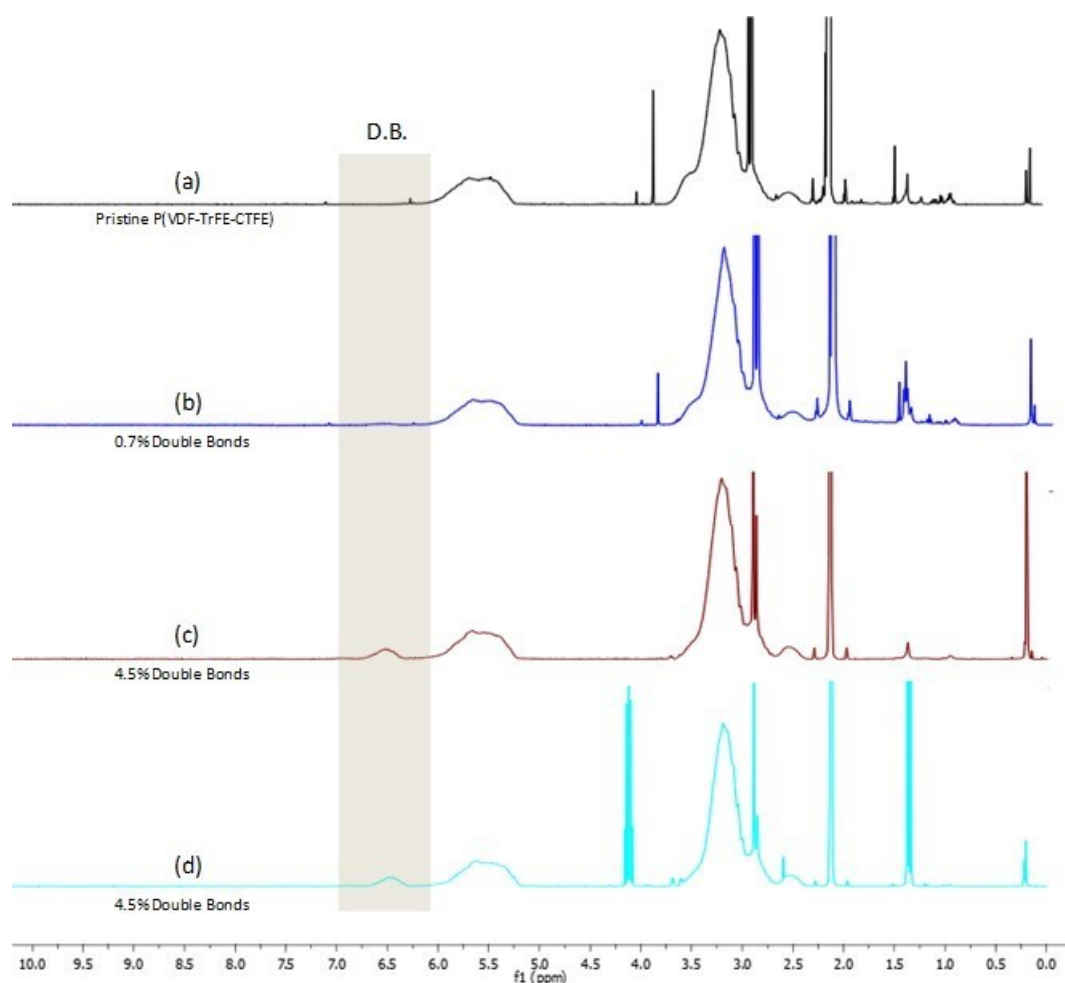


Figure 4-12. $^1\text{H-NMR}$ at 400 MHz (acetone- d_6) of (a) the pristine P(VDF-TrFE-CTFE) terpolymer and (b) P(VDF-TrFE-CTFE) terpolymer with estimated 0.7% of double bonds, (c) P(VDF-TrFE-CTFE) terpolymer with estimated 4.5% of double bonds and (d) P(VDF-TrFE-CTFE) terpolymer with estimated 4.5% of double bonds.

Table 4-4. Summary of the results of P(VDF-TrFE-CTFE) treated with triethylamine under different reaction conditions. The triethylamine equivalents are calculated compared to the total number of repeating units.

	Equivalents of Et_3N	Reaction time	Reaction temperature	Double bonds (1 H) 6-7 ppm
(a)	-	-	-	0%
(b)	10	24 h	20°C	0.7%
(c)	0.75	4h	50°C	4.5%
(d)	1.7	4h	50°C	4.5%

The $^{19}\text{F-NMR}$ spectra also showed the appearance of signals which are characteristic of the double bonds, such as the -89.29 ppm signal, corresponding to the $(-\text{CF}_2\text{CH}=\underline{\text{CF}}\text{CF}_2-)$ sequence and -120.72 ppm signal corresponding to the $(-\text{CF}_2\text{CH}=\underline{\text{CF}}\text{CF}_2\text{CF}_2-)$ sequence (**Figure 4-13**).

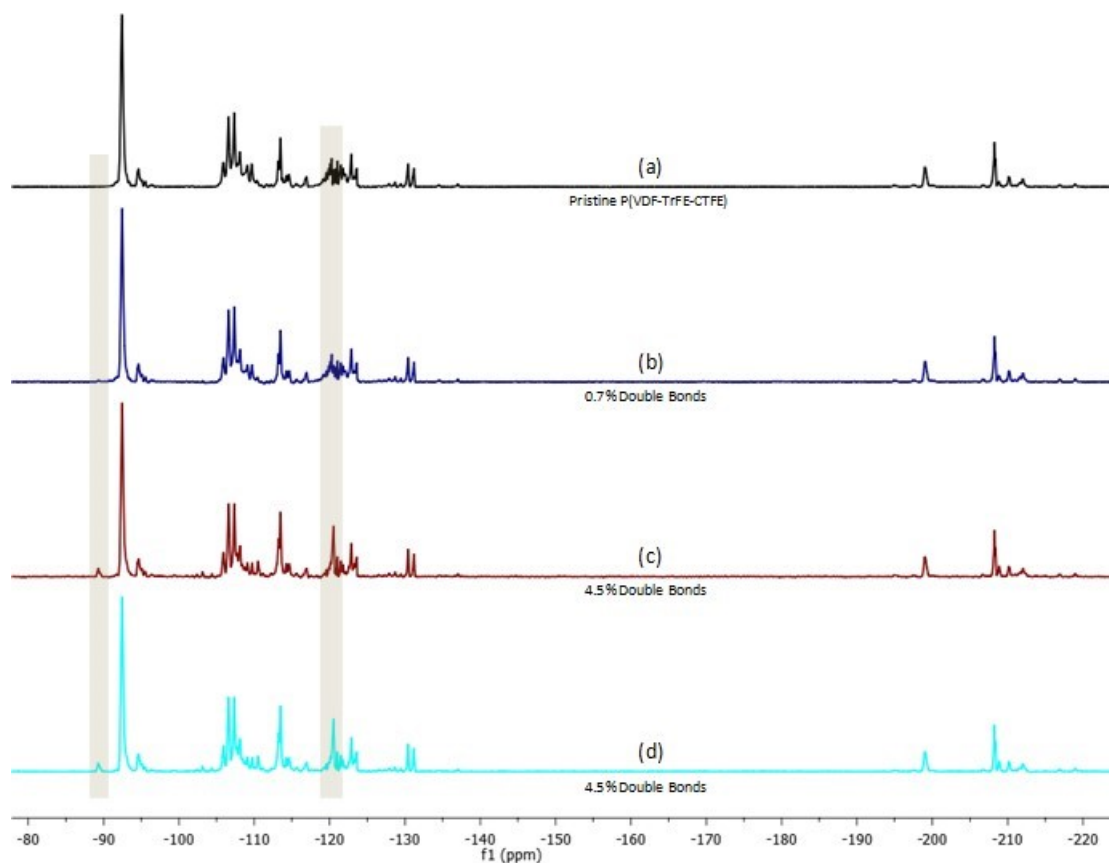


Figure 4-13. ^{19}F -NMR at 376,5 MHz (acetone- d_6) of (a) the pristine P(VDF-TrFE-CTFE) terpolymer and (b) P(VDF-TrFE-CTFE) terpolymer with estimated 0.7% of double bonds, (c) P(VDF-TrFE-CTFE) terpolymer with estimated 4.5% of double bonds and (d) P(VDF-TrFE-CTFE) terpolymer with estimated 4.5% of double bonds.

The different modified P(VDF-TrFE-CTFE) terpolymers were also characterized by attenuated total reflection infrared spectroscopy (ATR FT-IR) as shown in **Figure 4-14**. The main band appearing in the polymers treated with base is the C=C stretching band at 1720cm^{-1} .

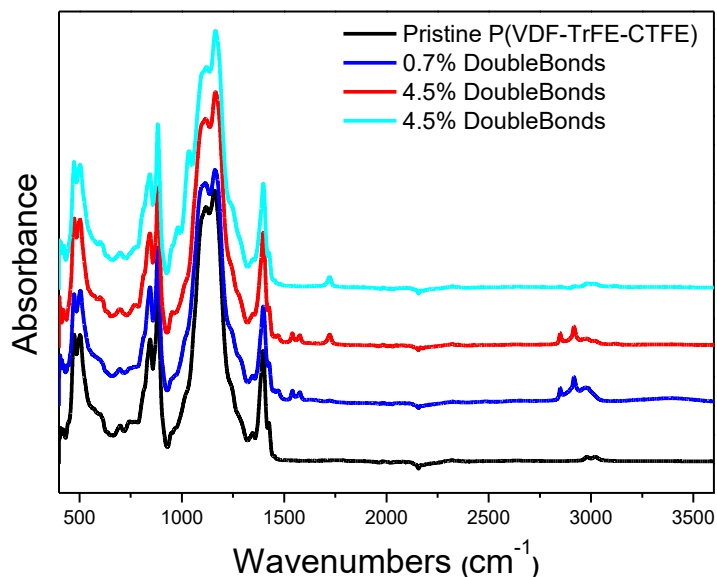


Figure 4-14. ATR FT-IR spectra of $P(\text{VDF-TrFE-CTFE})$ with different amounts of introduced double bonds as estimated from $^1\text{H NMR}$.

All the different modified terpolymers were characterized by differential scanning calorimetry (DSC), with the thermograms shown in **Figure 4-15** and the data gathered in **Table 4-5**.

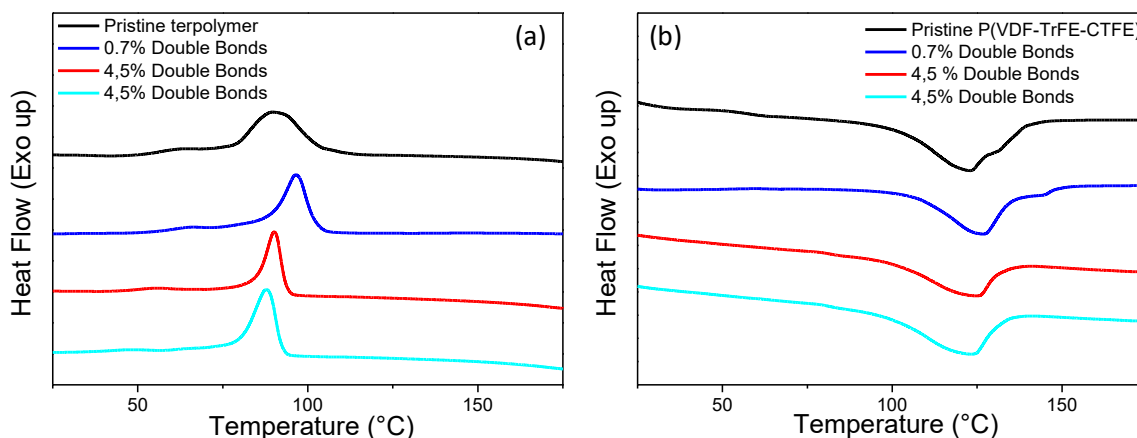
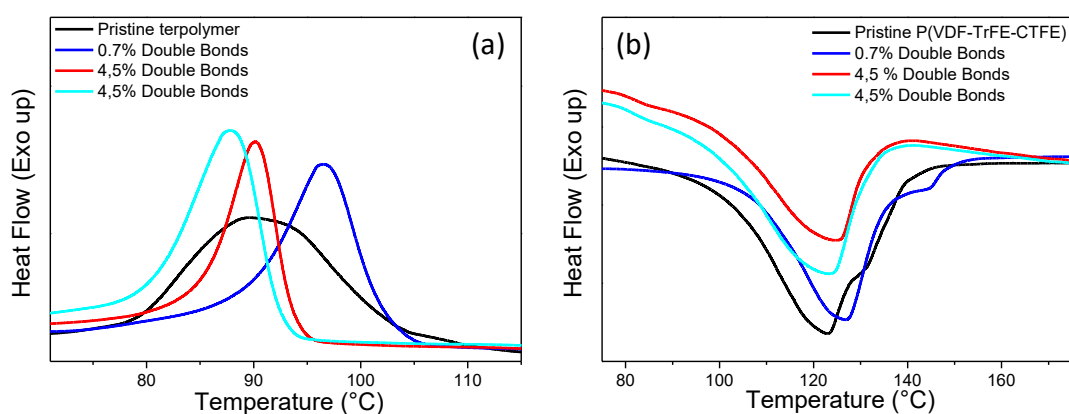


Figure 4-15. DSC thermograms with $10^\circ\text{C}/\text{min}$ ramp, comparing $P(\text{VDF-TrFE-CTFE})$ terpolymers with different double bond contents. (a) first cooling cycle and (b) the second heating cycle.

Table 4-5. Summary of the data derived from the DSC thermograms of P(VDF-TrFE-CTFE) terpolymers with different double bond contents.

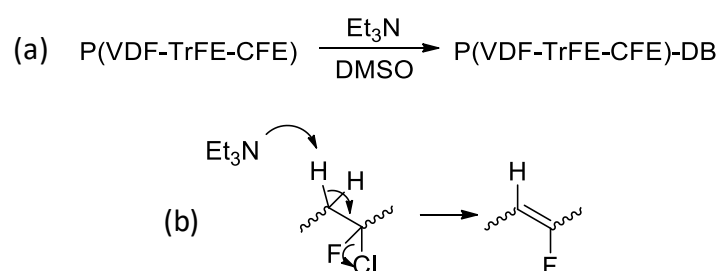
	Melting		Crystallization	
	Temperature (°C)	Enthalpy (J/g)	Temperature (°C)	Enthalpy (J/g)
Pristine terpolymer	148°C	14	110°C	13
0.7% Double Bonds	156°C	17	107°C	20
4.5% Double Bonds	140°C	17	97°C	17
4.5% Double Bonds	139°C	15	96°C	14

For better comparison, the transitions' peaks were overlapped (see **Figure 4-16**). The polymers seem to follow similar trends as before regarding their crystallization behavior, with temperature decreasing as double bond content increases. Nevertheless, these data should be taken with caution due to the number of samples and the low degree of modification.

**Figure 4-16.** Overlapped crystallization (first cooling) and melting (second heating) peaks from **Figure 4-15**.

4.2.2) P(VDF-TrFE-CFE) terpolymers containing unsaturation

The second class of FEPs that have been used in the context of this work are the CFE containing terpolymers, which are particularly interesting for specific kinds of devices. Following the same methodology as above, unsaturation was introduced in CFE containing terpolymers using triethylamine (see **Scheme 4-2**). Unlike CTFE groups, CFE groups bear α protons with respect to the chlorine on the monomer unit and thus the creation of unsaturations does not require any particular sequence of monomers **Scheme 4-2b**.



Scheme 4-2. (a) Dehydrochlorination reaction of P(VDF-TrFE-CFE) upon treatment with triethylamine. (b) Nucleophilic attack of triethylamine on the CFE unit, leading to the formation of unsaturation via an E2 pathway.

The CFE containing terpolymers treated under different conditions with triethylamine were characterized by $^1\text{H-NMR}$ with the spectra being shown in **Figure 4-17**. Although no double bond signals can be observed in **Figure 4-17** they could be observed after amplification of the area assigned to double bonds as shown in **Figure 4-18**. The data derived from the $^1\text{H-NMR}$ spectra are gathered in **Table 4-6** along with the reaction conditions.

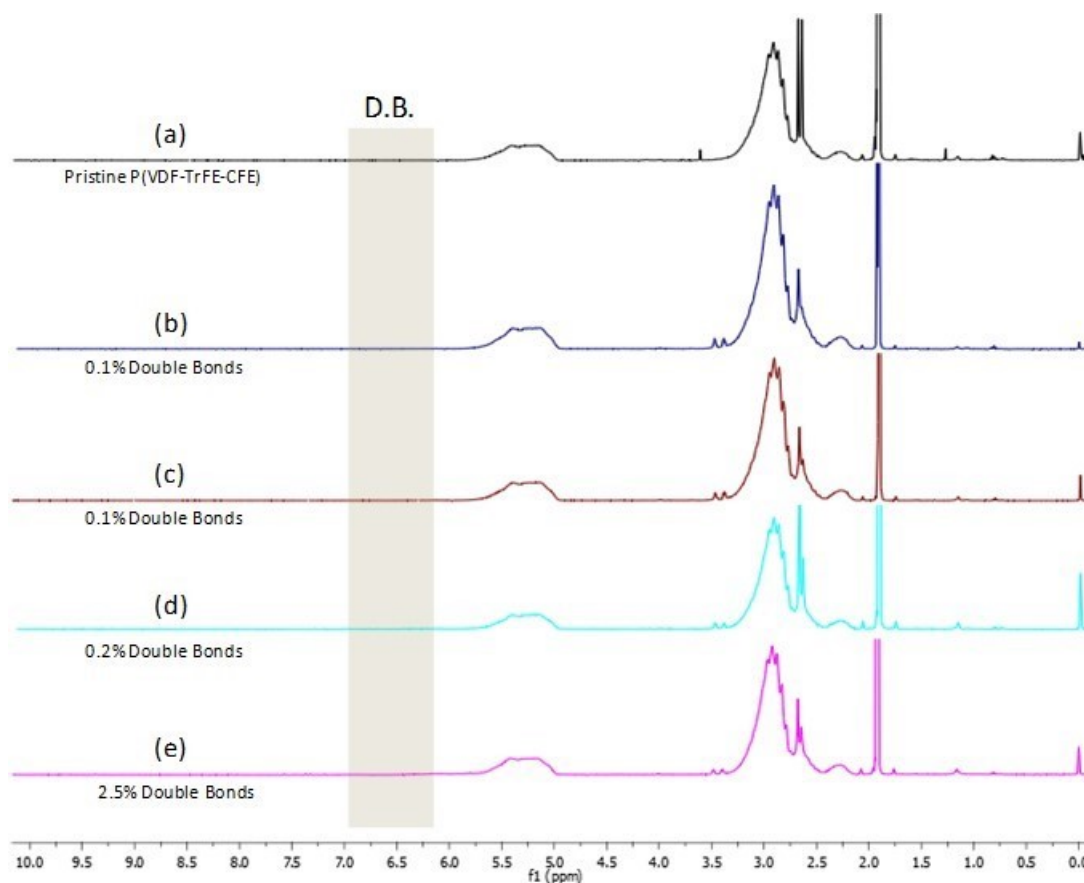


Figure 4-17. $^1\text{H-NMR}$ at 400 MHz (acetone-d_6) of (a) the pristine P(VDF-TrFE-CFE) terpolymer and (b) P(VDF-TrFE-CFE) terpolymer with estimated 0.1% of double bonds, (c) P(VDF-TrFE-CFE) terpolymer with estimated 0.1% of double bonds, (d) P(VDF-TrFE-CFE) terpolymer with estimated 0.2% of double bonds, (e) P(VDF-TrFE-CFE) terpolymer with estimated 2.5% of double bonds.

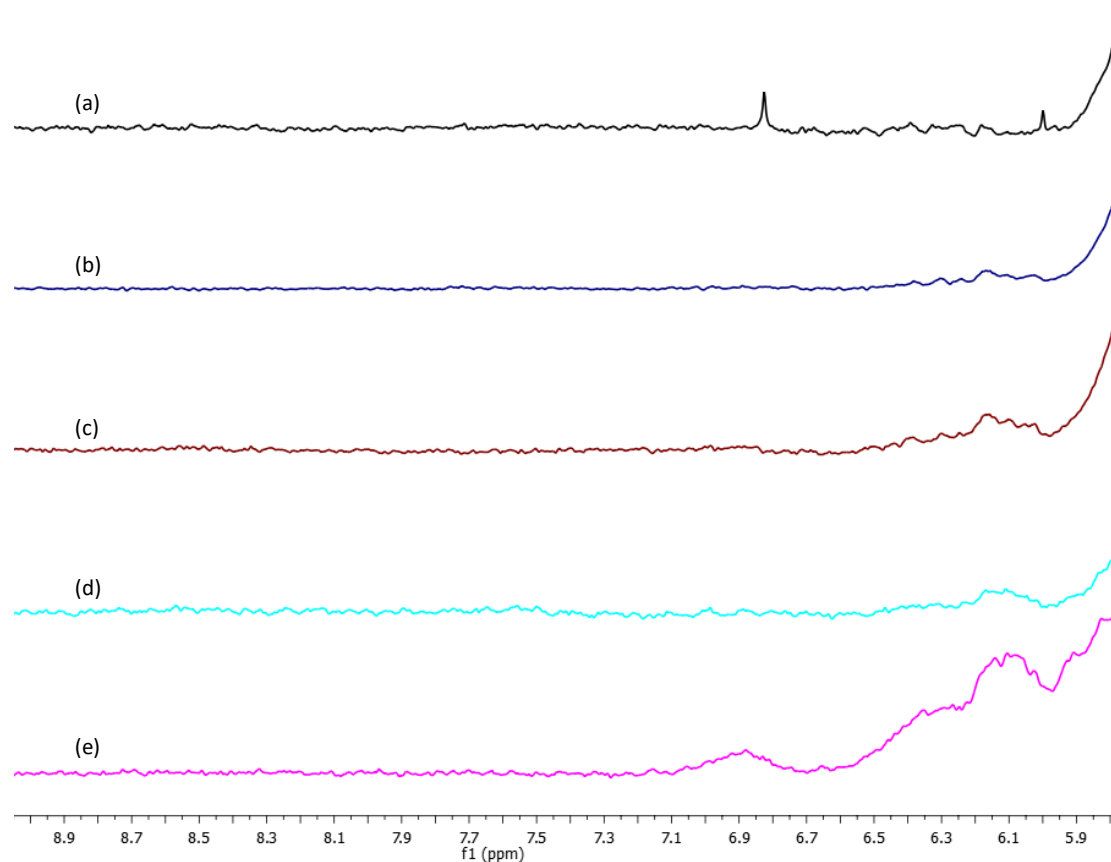


Figure 4-18. Amplification of **Figure 4-17** in the assigned double bonds area. $^1\text{H-NMR}$ at 400 MHz (acetone- d_6) of (a) the pristine P(VDF-TrFE-CFE) terpolymer and (b) P(VDF-TrFE-CFE) terpolymer with estimated 0.1% of double bonds, (c) P(VDF-TrFE-CFE) terpolymer with estimated 0.1% of double bonds, (d) P(VDF-TrFE-CFE) terpolymer with estimated 0.2% of double bonds, (e) P(VDF-TrFE-CFE) terpolymer with estimated 2.5% of double bonds.

Table 4-6. Summary of the treatment results of P(VDF-TrFE-CFE) with triethylamine under different reaction conditions. The equivalents of Et_3N are calculated in respect to the total number of repeating units.

	Equivalents of Et_3N	Reaction time	Reaction temperature	Double bonds (1 H) 6-7 ppm
(a)	-	-	-	0%
(b)	0.1	4 h	40°C	0.1%
(c)	0.2	4h	40°C	0.1%
(d)	0.35	8h	40°C	0.2%
(e)	0.65	24h	40°C	2.5%

$^{19}\text{F-NMR}$ was also performed in the double bond containing the P(VDF-TrFE-CFE) terpolymer and the spectra are presented in **Figure 4-19**.

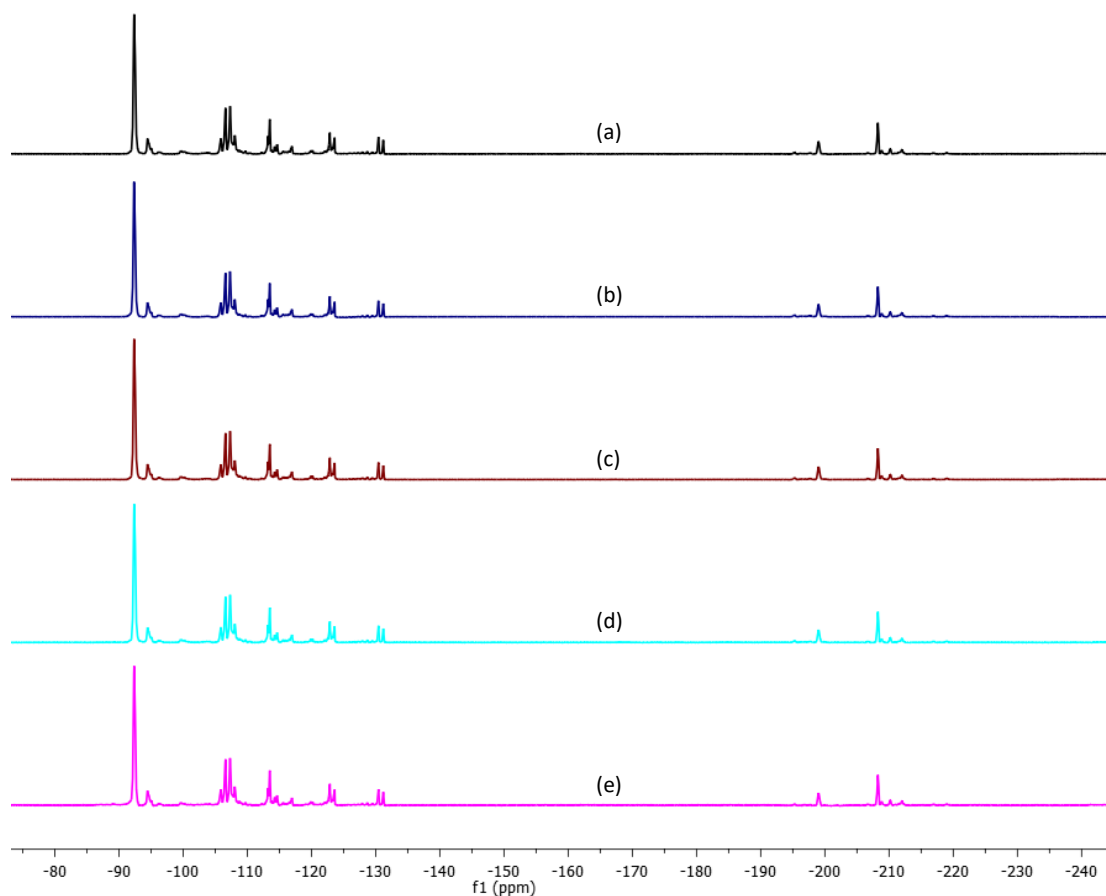


Figure 4-19. ^{19}F -NMR at 376,5 MHz (acetone- d_6) of (a) the pristine P(VDF-TrFE-CFE) terpolymer and (b) P(VDF-TrFE-CFE) terpolymer with estimated 0.1% of double bonds, (c) P(VDF-TrFE-CFE) terpolymer with estimated 0.1% of double bonds, (d) P(VDF-TrFE-CFE) terpolymer with estimated 0.2% of double bonds, (e) P(VDF-TrFE-CFE) terpolymer with estimated 2.5% of double bonds.

Assignment of double bonds signals was also difficult via FTIR spectroscopy, as shown in **Figure 4-20**.

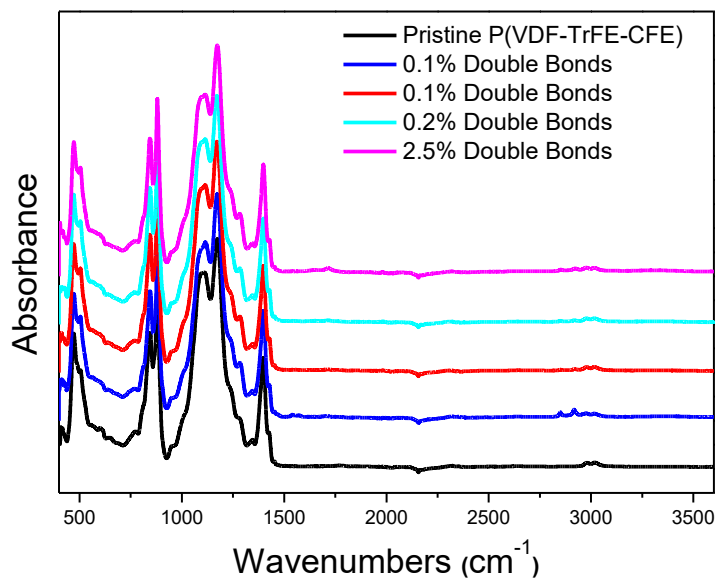


Figure 4-20. ATR FT-IR spectra of P(VDF-TrFE-CFE) with different amounts of introduced double bonds as estimated from NMR.

Pictures of the P(VDF-TrFE-CFE) terpolymers with different double bond contents are presented in **Figure 4-21**. It appears that with increasing the double bond content the polymers become "brownish", with the terpolymer with 2.5% double bond content having a brownish color, probably due to the presence of conjugated double bonds (**Figure 4-21**).

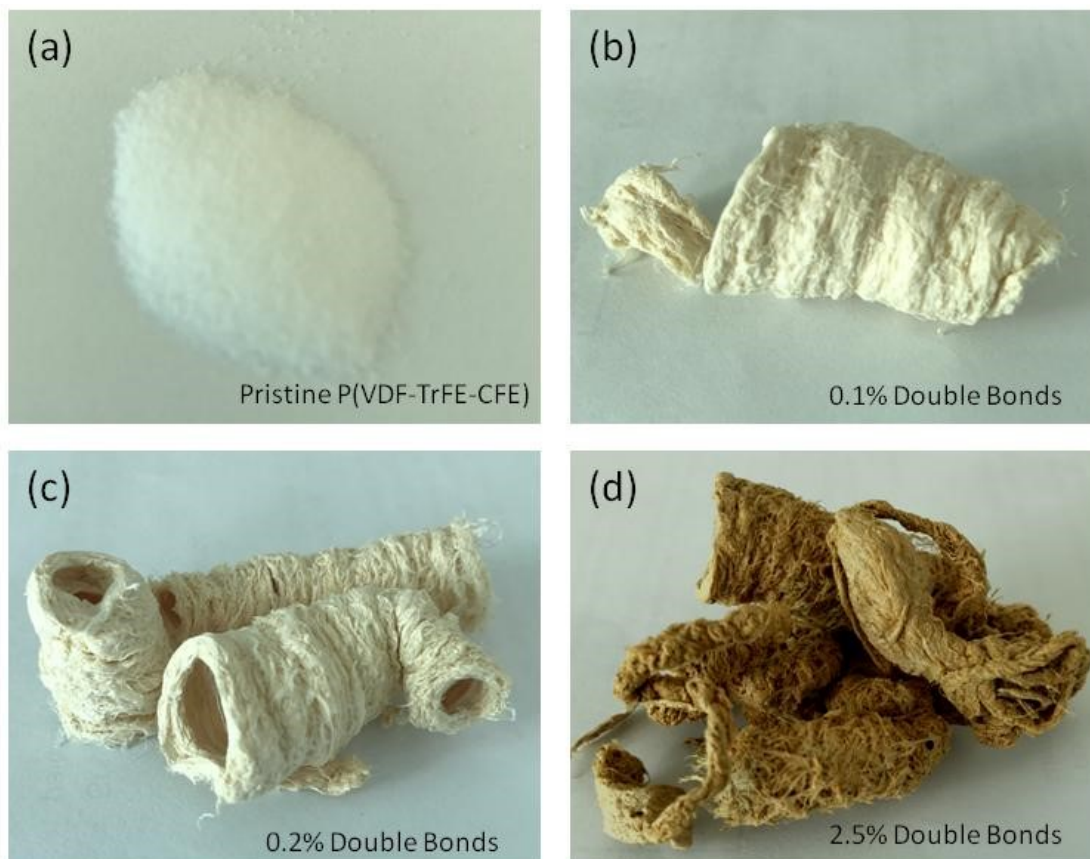


Figure 4-21. Photographs of (a) the pristine $P(\text{VDF-TrFE-CFE})$ terpolymer and (b) $P(\text{VDF-TrFE-CFE})$ terpolymer with estimated 0.1% of double bonds, (c) $P(\text{VDF-TrFE-CFE})$ terpolymer with estimated 0.2% of double bonds, (d) $P(\text{VDF-TrFE-CFE})$ terpolymer with estimated 2.5% of double bonds.

The DSC thermograms are presented in **Figure 4-22** and the corresponding data are gathered in **Table 4-7**. The introduction of double bonds impacts both the melting and the crystallization transitions. Furthermore, the terpolymer containing 2.5% double bonds presents a second peak in the first cooling ramp at about 65°C (**Figure 4-22a**), which resembles to the Curie transition peak of the ferroelectric polymers.

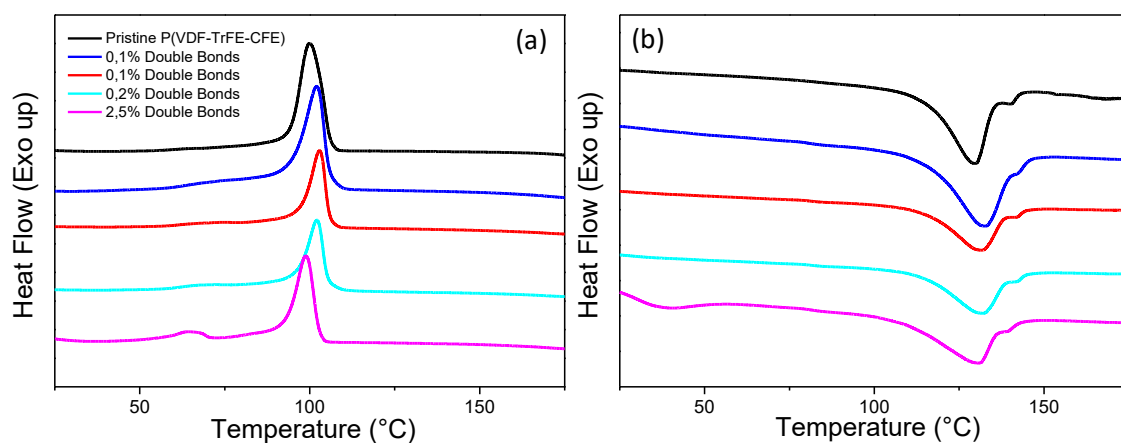


Figure 4-22. DSC thermograms with 10°C/min ramp, comparing *P(VDF-TrFE-CFE)* terpolymers with different double bond contents. (a) first cooling cycle and (b) the second heating cycle.

Table 4-7. Data derived from the DSC thermograms of *P(VDF-TrFE-CFE)* terpolymers with different double bond contents as estimated from ^1H NMR.

	Melting		Crystallization	
	Temperature (°C)	Enthalpy (J/g)	Temperature (°C)	Enthalpy (J/g)
Pristine CFE	144°C	24	110°C	25
0.1% DB	148°C	24	113°C	22
0.1% DB	144°C	21	111°C	22
0.2% DB	145°C	21	112°C	21
2.5% DB	144°C	17	107°C	14

For better comparison, the melting and crystallization peaks of the thermograms are overlapped for all modified P(VDF-TrFE-CFE) terpolymers and presented in **Figure 4-23**. No clear trend can be observed contrarily to the previous case of P(VDF-TrFE-CTFE).

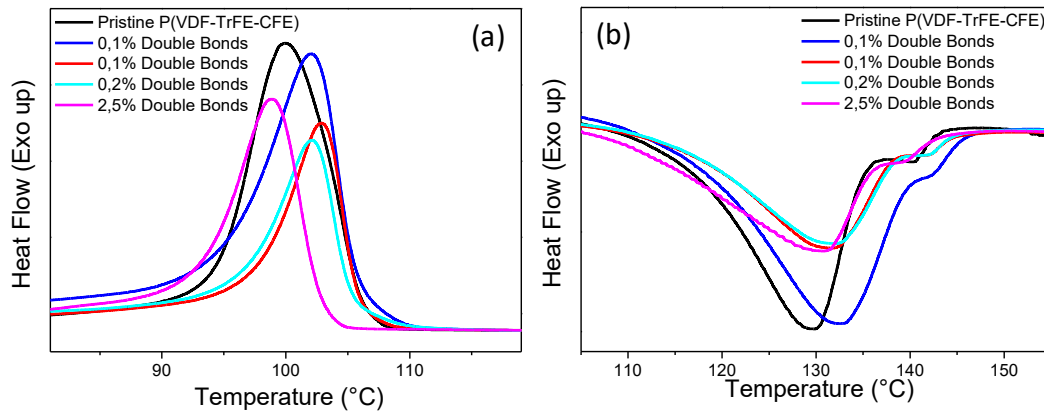
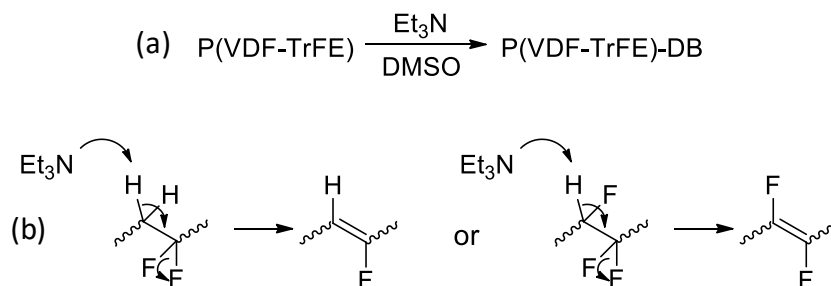


Figure 4-23. Overlapped crystallization (first cooling) and melting (second heating) peaks from **Figure 4-22**.

The electroactive and dielectric properties of those materials will be discussed in detail in **Chapter 5**.

4.2.3) P(VDF-TrFE) copolymers containing unsaturation

The copolymers were subjected to a similar protocol using a treatment with triethylamine giving rise in this case to dehydrofluorination. In both cases, the dehydrofluorination of VDF and TrFE units is possible, as they have α protons (see in **Scheme 4-3b**).



Scheme 4-3. (a) Dehydrofluorination reaction of P(VDF-TrFE) upon treatment with triethylamine. (b) Nucleophilic attack of triethylamine on the VDF or the TrFE unit, leading to the formation of unsaturation via an E2 pathway.

The copolymers treated under different conditions with triethylamine were characterized by $^1\text{H-NMR}$ with the spectra being shown in **Figure 4-24**. Since the signals attributed to the double bonds are very hard to distinguish in the whole spectrum (**Figure 4-24**) an amplification of the area of interest is presented in **Figure 4-25**, where the signals attributed to the double bond protons are much more visible. All the data derived from the $^1\text{H-NMR}$ are summarized in **Figure 4-24**. It has to be noted that all the obtained double bond contents were very low, below 1% which is mostly due to the very mild conditions use. In case higher double bond contents are desired, the reaction conditions have to be adjusted accordingly. Again these data should be taken with caution due to uncertainty of measurements on $^1\text{H NMR}$ spectra.

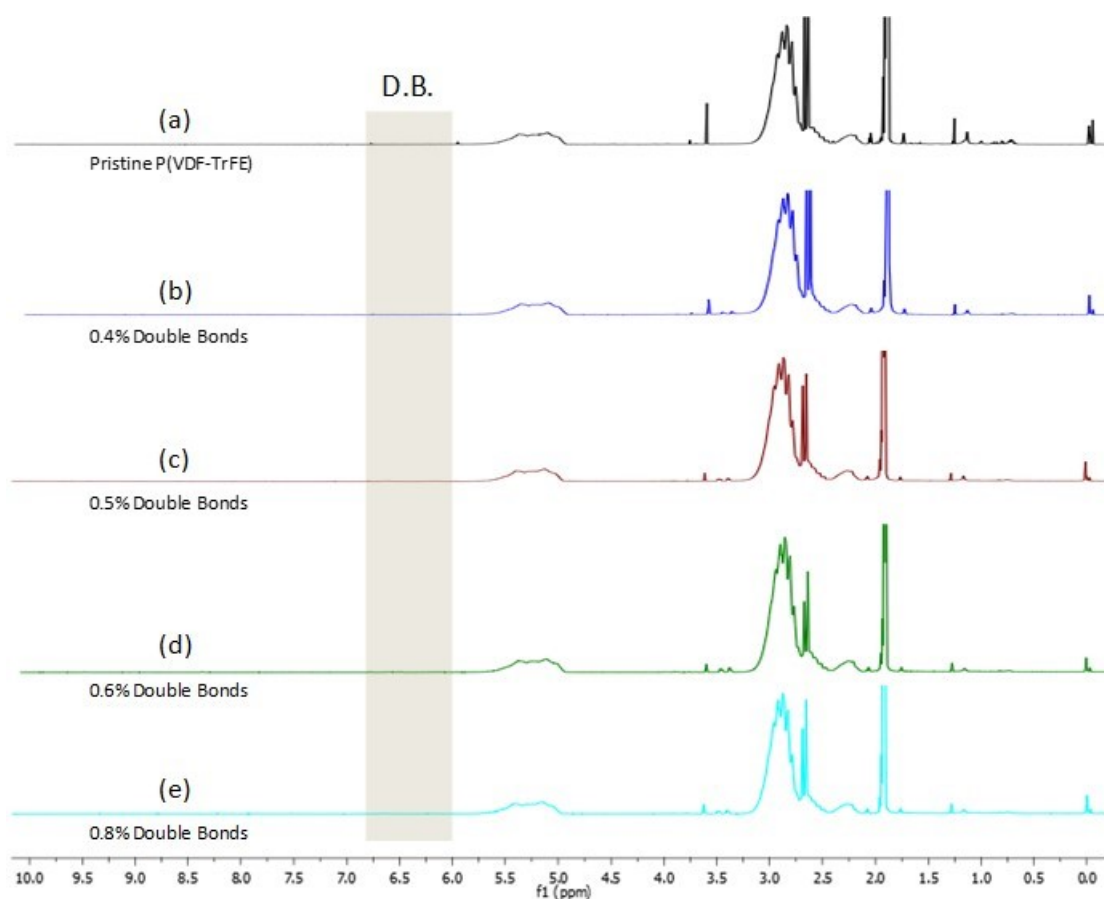


Figure 4-24. $^1\text{H-NMR}$ at 400 MHz (acetone- d_6) of (a) the pristine P(VDF-TrFE) copolymer and (b) P(VDF-TrFE) copolymer with estimated 0.4% of double bonds, (c) P(VDF-TrFE) copolymer with estimated 0.5% of double bonds, (d) P(VDF-TrFE) copolymer with estimated 0.6% of double bonds, (e) P(VDF-TrFE) copolymer with estimated 0.8% of double bonds.

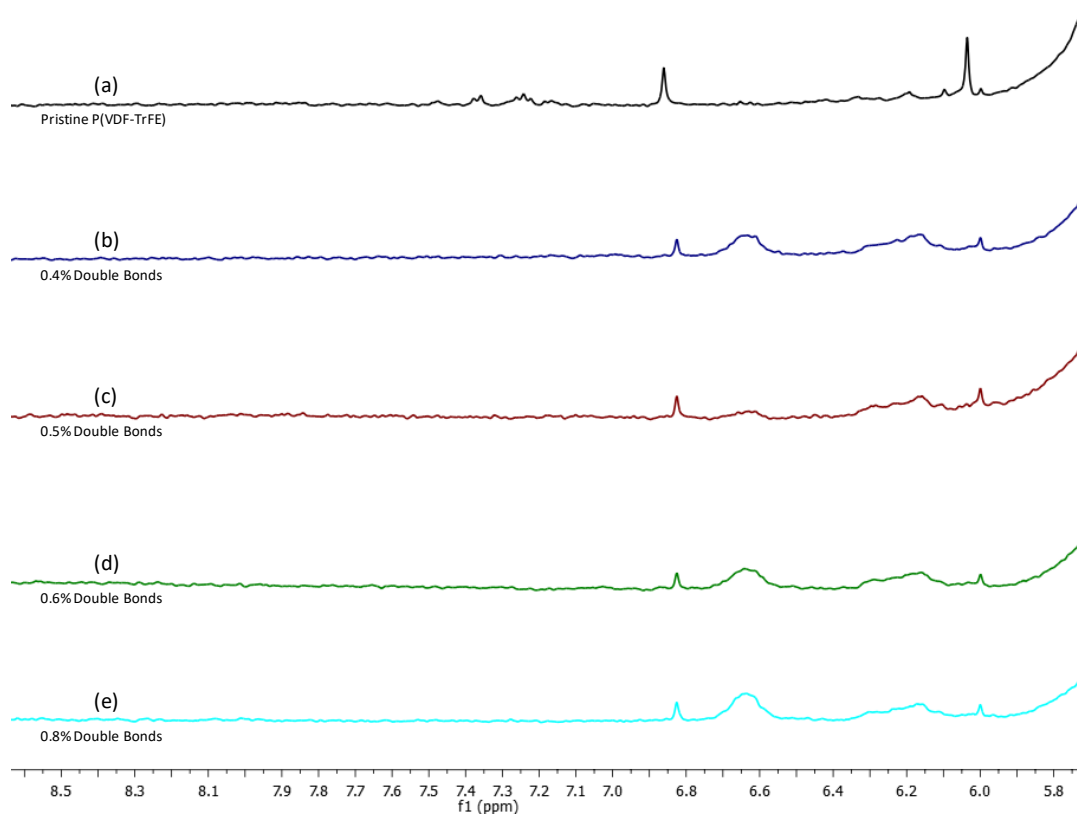


Figure 4-25. Amplification of area assigned to double bonds protons (a) the pristine P(VDF-TrFE) copolymer and (b) P(VDF-TrFE) copolymer with estimated 0.4% of double bonds, (c) P(VDF-TrFE) copolymer with estimated 0.5% of double bonds,, (d) P(VDF-TrFE) copolymer with estimated 0.6% of double bonds, (e) P(VDF-TrFE) copolymer with estimated 0.8% of double bonds.

Table 4-8. Summary of the treatment results of P(VDF-TrFE) with triethylamine under different reaction conditions. The equivalents of Et₃N are calculated in respect to the total number of repeating units.

	Equivalents of Et ₃ N	Reaction time	Reaction temperature	Double bonds (1 H) 6-7 ppm
(a)	-	-	-	0%
(b)	0.3	2 h	50°C	0.4%
(c)	0.7	2 h	50°C	0.6%
(d)	0.9	2 h	50°C	0.7%
(e)	1.2	2 h	50°C	0.8%

Similarly to ¹H NMR, it was difficult to detect double bonds signals by ¹⁹F-NMR spectroscopy as shown in **Figure 4-26**. Nevertheless, signals @ -89 ppm, from the (-CF₂CH=CFCF₂CF₂-) sequence could be observed (as shown in **Figure 4-27**) confirming the formation of few double bonds in these conditions. It is also in accord with the double bond formation's mechanism which is favored in the case of chlorine substituted electroactive fluorinated copolymers.

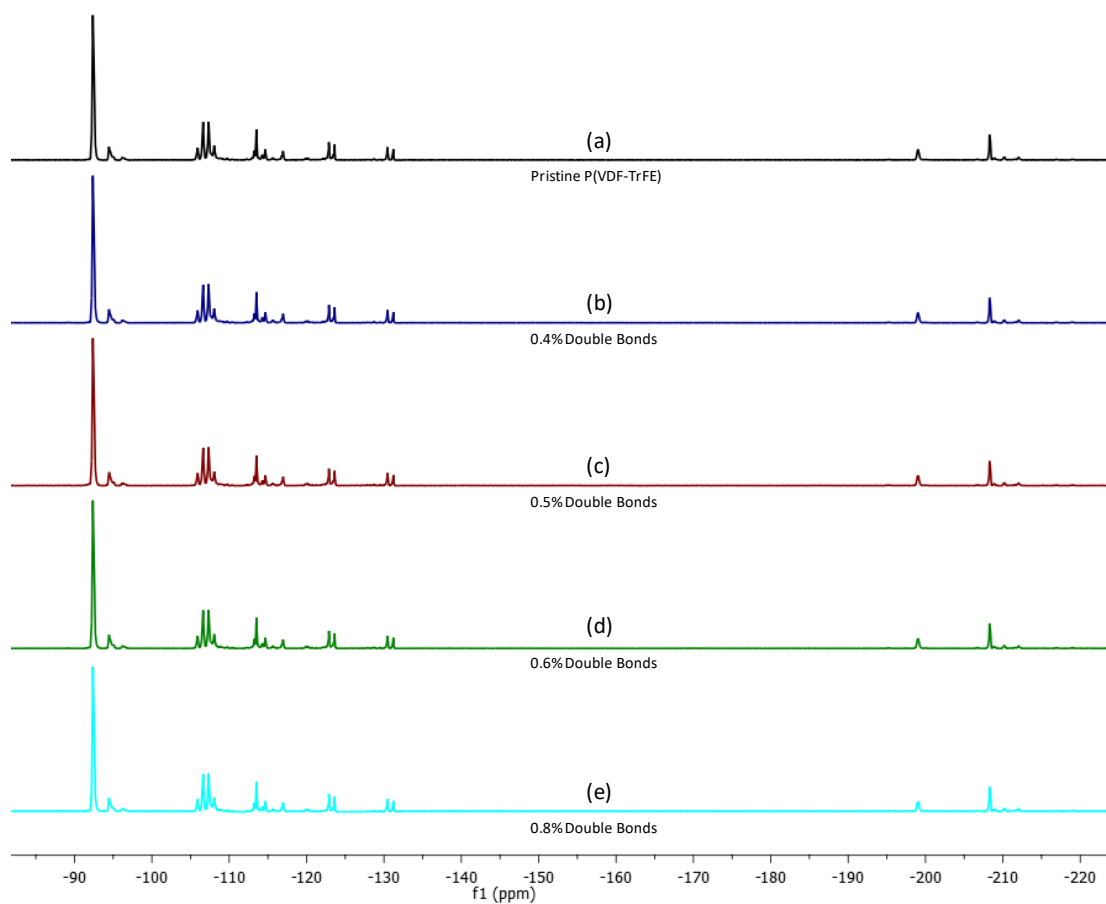


Figure 4-26. ^{19}F -NMR at 376,5 MHz (acetone- d_6) of (a) the pristine P(VDF-TrFE) copolymer and (b) P(VDF-TrFE) copolymer with estimated 0.4% of double bonds, (c) P(VDF-TrFE) copolymer with estimated 0.5% of double bonds, (d) P(VDF-TrFE) copolymer with estimated 0.6% of double bonds, (e) P(VDF-TrFE) copolymer with estimated 0.8% of double bonds.

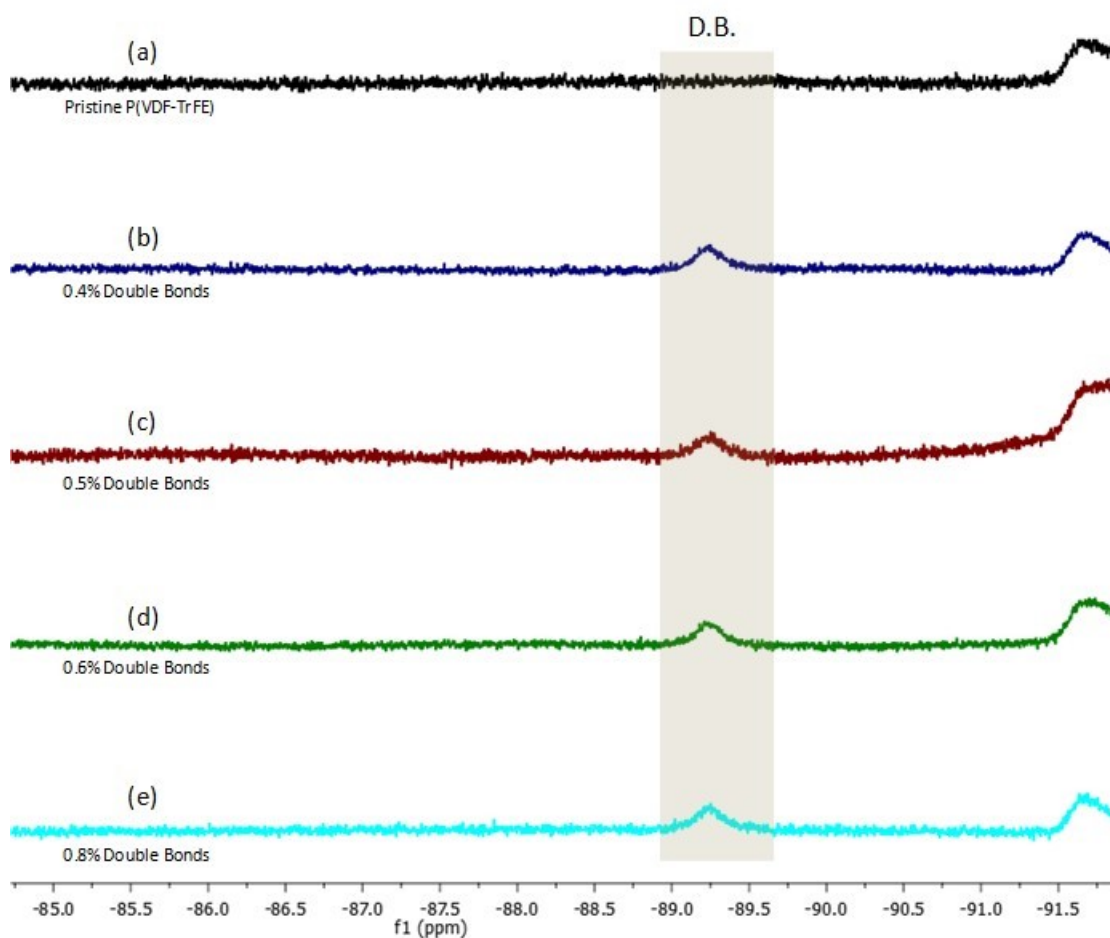


Figure 4-27. Amplification of **Figure 4-26** in the area where double bonds are assigned. of (a) the pristine P(VDF-TrFE) copolymer and (b) P(VDF-TrFE) copolymer with estimated 0.4% of double bonds, (c) P(VDF-TrFE) copolymer with estimated 0.5% of double bonds, (d) P(VDF-TrFE) copolymer with estimated 0.6% of double bonds, (e) P(VDF-TrFE) copolymer with estimated 0.8% of double bonds.

As shown in **Figure 4-27** (FTIR analysis of modified copolymer), no signal of double bond could be detected.

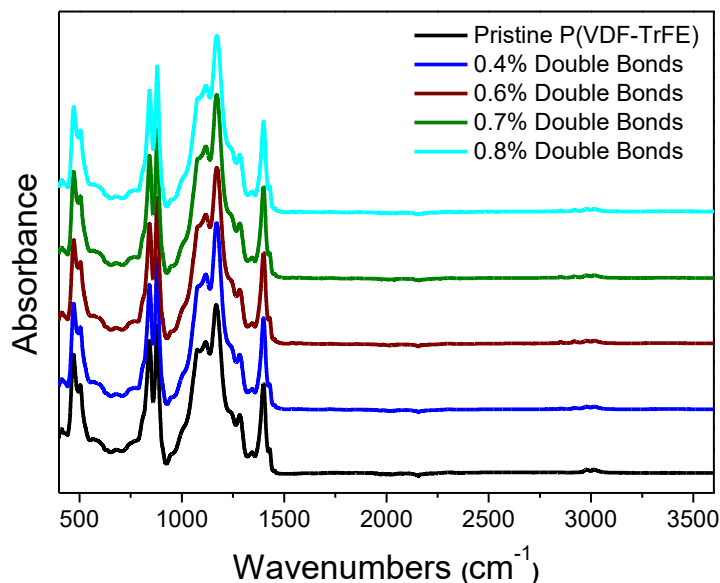


Figure 4-28. ATR FT-IR spectra of P(VDF-TrFE) with low content (<1%) of double bonds as estimated from ^1H NMR.

4.3) Experimental part

Modification of P(VDF-TrFE-CTFE) (61.9/29.9/8.2): (5g) of terpolymer were dissolved in 100 ml of Dimethyl sulfoxide (DMSO) in a 250ml round bottom flask. After solubilization, triethylamine (2.9g, 28 mmol) was added and left under stirring for 4 hours at 50°C. The polymer was then precipitated in water, collected, dried and dissolved in acetone to be reprecipitated in a mixture of water/ethanol (60/40). Finally the polymer was collected, immersed in water and ethanol and finally dried under reduced pressure at 40°C overnight.

Modification of P(VDF-TrFE-CTFE) (61.7/28.3/10): (0.5g) of terpolymer was dissolved in 10 ml of Dimethyl sulfoxide (DMSO) in a 25ml round bottom flask. After solubilization, triethylamine (0.4g, 4 mmol) was added and the reaction was left under stirring for 4 hours at 50°C. Then the polymer was precipitated in water. The polymer was collected, dried and dissolved in acetone to be reprecipitated in a mixture of water/ethanol (60/40). Finally the polymer was collected, immersed in water and ethanol and finally dried under reduced pressure at 40°C overnight.

Modification of P(VDF-TrFE-CFE) (68.2/29.1/7.2): (2.5g) of terpolymer were dissolved in 50 ml of Dimethyl sulfoxide (DMSO) in a 100ml round bottom flask. After solubilization, triethylamine (1.1g, 11 mmol) was added and left under stirring for 4 hours at 40°C. The polymer was then precipitated in water, collected, dried and

dissolved in acetone to be reprecipitated in a mixture of water/ethanol (60/40). Finally the polymer was collected, immersed in water and ethanol and finally dried under reduced pressure at 40°C overnight.

Modification of P(VDF-TrFE) (75/25): (2.5g) of copolymer were dissolved in 50 ml of Dimethyl sulfoxide (DMSO) in a 100ml round bottom flask. After solubilization, triethylamine (1.1g, 11 mmol) was added and the reaction was left under stirring for 4 hours at 50°C. Then the polymer was precipitated in water. The polymer was collected, dried and dissolved in acetone to be reprecipitated in a mixture of water/ethanol (60/40). Finally the polymer was collected, immersed in water and ethanol and finally dried under reduced pressure at 40°C overnight.

4.4) Conclusions

Unsaturation was successfully introduced in all the different kinds of fluorinated electroactive polymers used in the context of this thesis, such as the relaxor ferroelectric P(VDF-TrFE-CTFE) and P(VDF-TrFE-CFE) terpolymers as well as the ferroelectric P(VDF-TrFE) copolymer. It can be introduced either by dehydrochlorination or dehydrofluorination, even if the latter is less efficient. That was achieved through a straightforward treatment of the polymers with a weak base such as triethylamine. The impact of the double bonds content on the electroactive properties will be discussed in more details in Chapter 5.

4.5) References

1. Li, J.; Tan, S.; Ding, S.; Li, H.; Yang, L.; Zhang, Z., High-field antiferroelectric behaviour and minimized energy loss in poly(vinylidene-co-trifluoroethylene)-graft-poly(ethyl methacrylate) for energy storage application. *Journal of Materials Chemistry* **2012**, *22* (44), 23468-23476.
2. Soulestin, T.; Ladmiral, V.; Dos Santos, F. D.; Améduri, B., Vinylidene fluoride- and trifluoroethylene-containing fluorinated electroactive copolymers. How does chemistry impact properties? *Progress in Polymer Science* **2017**, *72*, 16-60.
3. Zhang, Y.; Tan, S.; Wang, J.; Wang, X.; Zhu, W.; Zhang, Z., Regulating Dielectric and Ferroelectric Properties of Poly (vinylidene fluoride-trifluoroethylene) with Inner CH= CH Bonds. *Polymers* **2018**, *10* (3), 339.
4. Sodano, H. A., Ferroelectric polymers from dehydrofluorinated PVDF. **2019**: US 2018230249A1.

Chapter 5

Electronic Properties and Devices

Chapter 5: Electronic Properties and Devices

5.1) Introduction

While the three previous chapters were devoted to the chemical modification of FEPs for their further integration in devices, there was no mention of the impact of functionalization on their electroactive properties. This will be the topic of this chapter by evaluating for instance ferroelectric or dielectric characteristics of modified copo- and terpolymers as function of the degree of chemical modification. Increased performance was observed in certain cases, as discussed in detail in the current chapter.

5.2) Results and discussion

5.2.1) Electronic properties of P(VDF-TrFE-CTFE) terpolymers with pendent Azido groups

First the ferroelectric response of the azide modified polymers after thermal cross-linking was compared to the ferroelectric response of the pristine terpolymer at room temperature as shown in **Figure 5-1**. It was found that the azide modified polymers maintained the desired relaxor-ferroelectric character of the pristine P(VDF-TrFE-CTFE). However, some differences became apparent. First, the double hysteresis loop (DHL), characteristic of the physical pinning caused by the bulky CTFE group on the pristine terpolymer becomes a narrow single hysteresis loop (SHL) on the azide modified terpolymer, characteristic of permanent chemical pinning caused by the cross-linking sites. The physical pinning caused by the bulkier CTFE groups ceases to exist, when the electric field becomes high enough, as the dipoles start switching due to the polarity of the CTFE group. That phenomenon gives rise to field induced hysteresis during the relaxor-ferroelectric (RFE) to ferroelectric (FE) transition. On the other hand, on the cross-linked polymer this kind of field induced hysteresis is eliminated. That can be explained by the permanent chemical pinning effect that cross-linking has to the terpolymer crystals¹. Similar behavior has been reported in literature for electron beam irradiated P(VDF-TrFE)². It was also observed that while the polymer modified with 0.06 eq NaN₃ showed a slim hysteresis loop **Figure 5-1** which is a sign for a good relaxor-ferroelectric behavior, the polymer modified with

0.04 eq NaN_3 showed deteriorated relaxor-ferroelectric properties with a much broader current peak and a more open hysteresis loop. Although this difference may seem odd at this point, it will be much better understood at the end of this chapter, where we are going to discuss the effect that double bonds can have on relaxor-ferroelectric polymers.

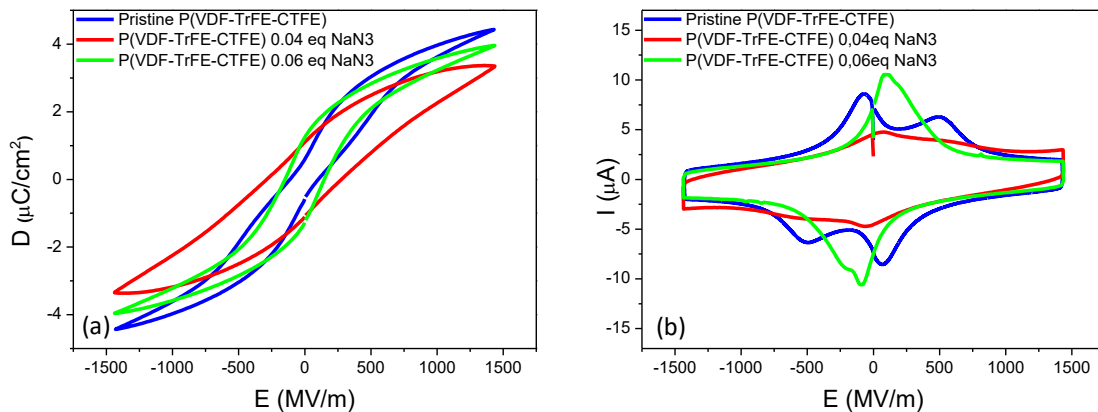


Figure 5-1. Ferroelectric testing at 20°C and 10Hz of the pristine terpolymer P(VDF-TrFE-CTFE) compared with terpolymer modified with different amounts of sodium azide, measuring the (a) Displacement and (b) the current as a function of applied electric field.

Broadband dielectric spectroscopy was used to investigate the effect of azide modification on the dielectric properties of the terpolymers. The azide modified terpolymers exhibit high- k and low loss across the studied temperature and frequency range, e.g. $\epsilon'_r = 25$ at 20°C and 1kHz (**Figure 5-2a**). Those values are nevertheless lower compared to the pristine terpolymer ($\epsilon'_r = 34$ at 20°C and 1kHz) (**Figure 5-2a**). However, they are to the best of our knowledge the highest dielectric constant values reported to date for photo patternable polymers³. It has to be noted that those values are further decreased with varying the sodium azide feeding ratio, similarly to the ferroelectric properties shown in **Figure 5-1**.

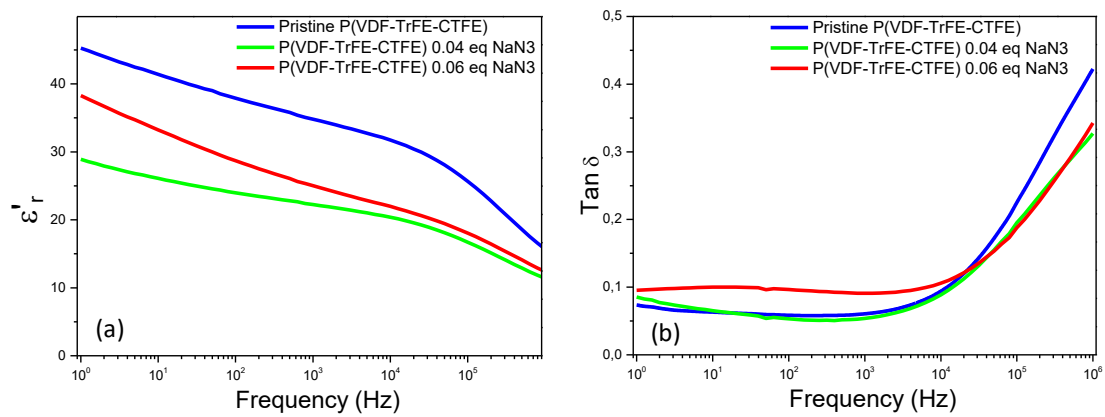


Figure 5-2. Broadband dielectric spectroscopy at 20°C of the pristine terpolymer P(VDF-TrFE-CTFE) compared with terpolymers modified with different amounts of sodium azide measuring (a) the real part of the relative permittivity and (b) the dielectric loss as a function of frequency.

The azide modified polymers have their dielectric constant peak at the same temperature as the pristine terpolymer (**Figure 5-3**) but the ϵ'_r values are reduced across the temperature and frequency range. The degree to which the dielectric properties get influenced from the azide modification and the subsequent cross-linking step greatly depend on the reaction conditions.

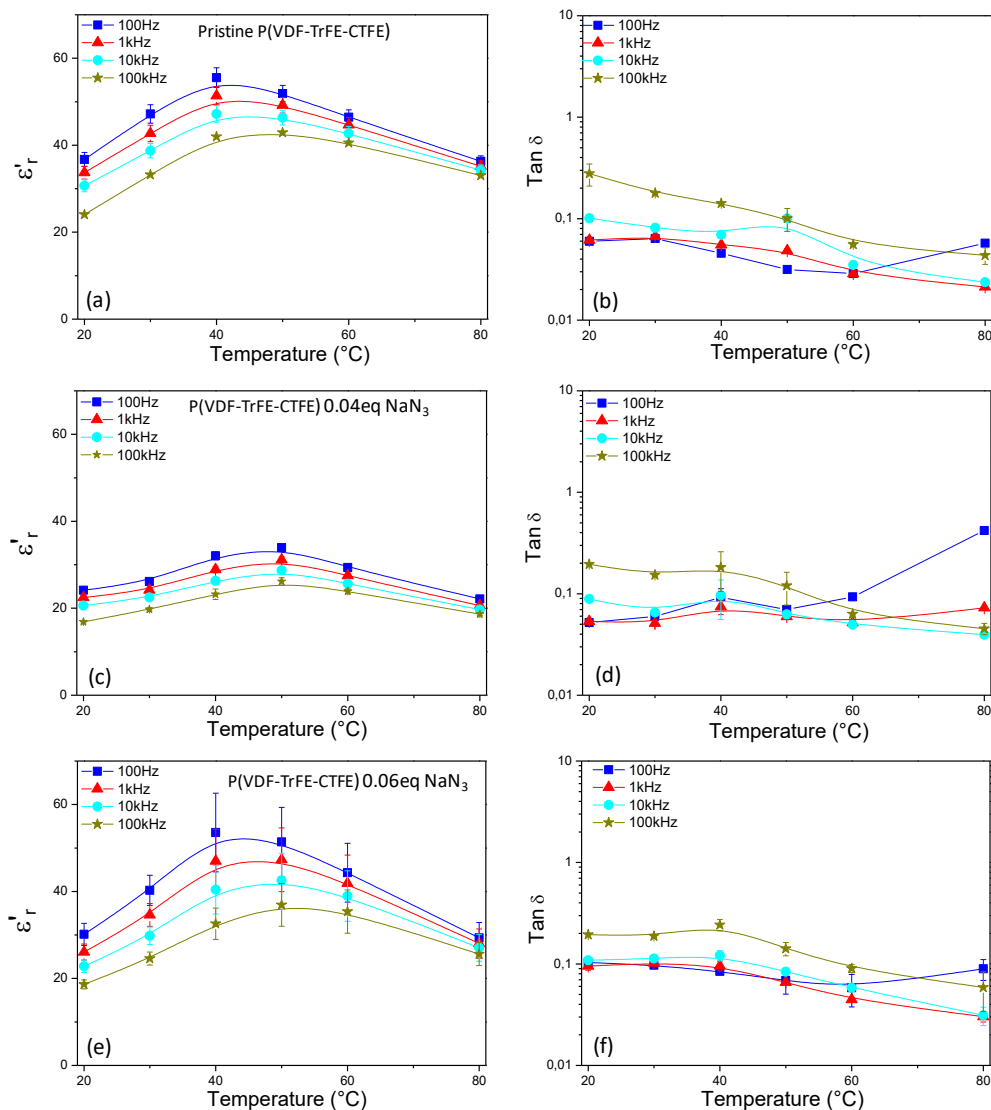


Figure 5-3. Broadband dielectric spectroscopy as a function of temperature comparing the pristine P(VDF-TrFE-CTFE) with the modified with 0.04 and 0.06eq of NaN_3 respectively. The real part of the relative permittivity from 20°C to 80°C for different frequencies (left). And the dielectric loss from 20°C to 80°C for different frequencies (right).

In addition, ϵ'_r of the pristine and modified polymers at 1 kHz were plotted on the same graph and presented in **Figure 5-4**.

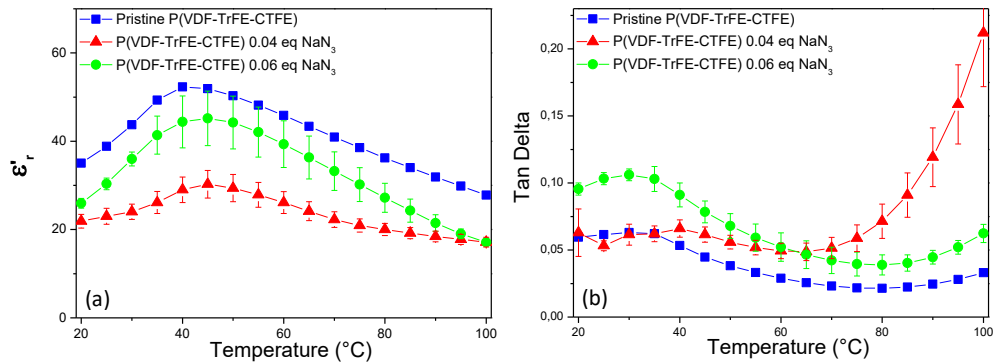


Figure 5-4. Broadband dielectric spectroscopy as a function of temperature comparing the pristine P(VDF-TrFE-CTFE) with the modified with 0.04 and 0.06 eq of NaN₃ at 1kHz frequency. The real part of the relative permittivity (left), and the dielectric loss (right).

The broadband dielectric spectroscopy measurements show that similarly to the ferroelectric properties, the azide modification affects the dielectric properties, with the decrease being more severe for the polymers modified with 0.04 eq of sodium azide, despite the lower azide content.

5.2.2) Electronic properties of P(VDF-TrFE-CTFE) terpolymers with pendent benzophenone groups

All materials were characterized in three different states, namely as cast, as annealed and finally as exposed to UV light and then annealed.

Starting with the as cast films, the real part of the relative permittivity (ϵ'_r) at 1 kHz as a function of temperature for terpolymers grafted with different amounts of benzophenone (BP) was assessed (**Figure 5-5**). It was observed that low amounts of grafted benzophenone (0.4 and 1%) showed improved performance in terms of dielectric properties, while increasing the benzophenone content leads to deteriorated dielectric properties.

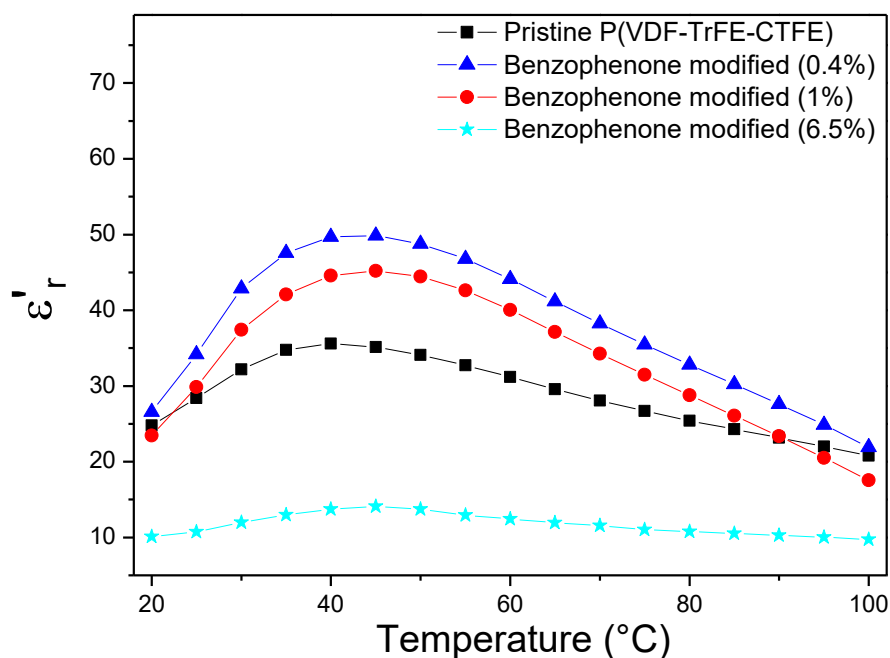


Figure 5-5. Broadband dielectric spectroscopy as a function of temperature comparing the real part of the relative permittivity of the pristine P(VDF-TrFE-CTFE) with the benzophenone modified terpolymers with different benzophenone loadings (1kHz, as cast films).

The ferroelectric properties of the benzophenone modified polymers were also characterized at 10Hz at a moderately high field (**Figure 5-6**). Similarly to the dielectric properties, the ferroelectric properties of the materials follow the same trend, with increased displacement values for the polymers with low benzophenone content and decreased values, when the benzophenone content increases.

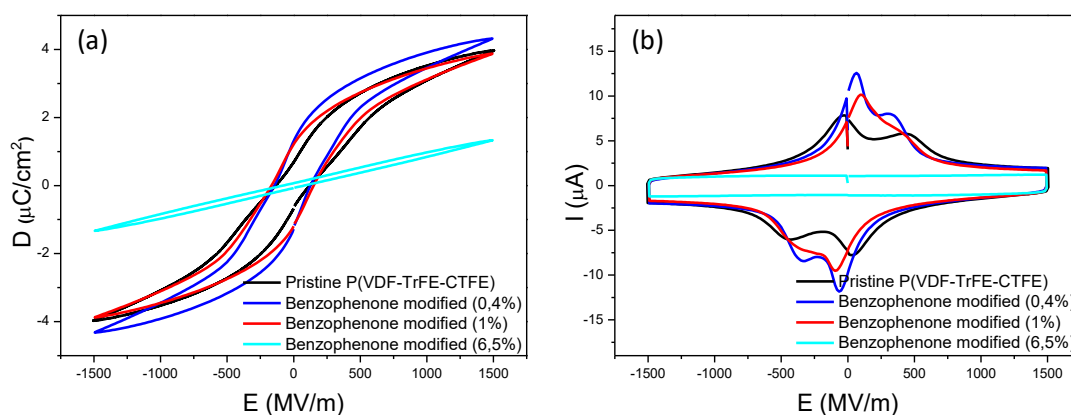


Figure 5-6. Ferroelectric testing at 20°C and 10Hz of the pristine terpolymer P(VDF-TrFE-CTFE) compared with terpolymer grafted with different amounts of benzophenone (BP), measuring the (a) Displacement and (b) the current as a function of applied electric field (as cast films).

The polymers were then similarly characterized after annealing at 110°C for 1h. The real part of the relative permittivity is presented in **Figure 5-7**, where the dielectric properties are slightly improved for all the polymers with respect to the as-cast samples.

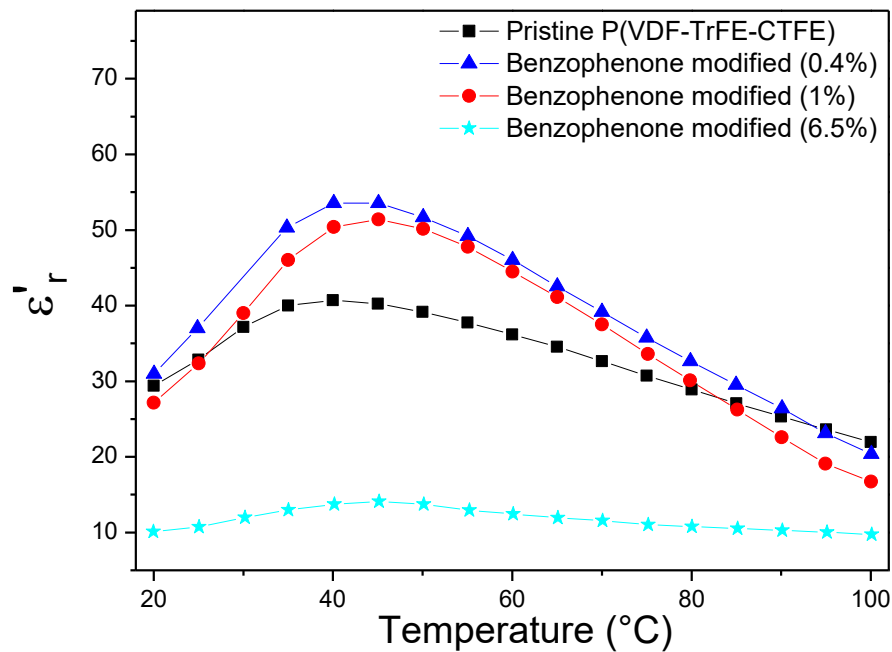


Figure 5-7. Broadband dielectric spectroscopy as a function of temperature comparing the real part of the relative permittivity of the pristine P(VDF-TrFE-CTFE) with the benzophenone modified terpolymers with different benzophenone loadings (1kHz, annealed films).

The benzophenone containing terpolymers, showed a small single hysteresis loop behavior (SHL), which is normally an indicator of chemical pinning induced by cross-linking sites⁴ (**Figure 5-8**). However, the fact that SHL is observed even at the as cast films (**Figure 5-6**), where no cross-linking had occurred is a strong indicator that the SHL behavior is due to the strong physical pinning induced by the bulky and highly polar benzophenone group, preventing the field induced hysteresis caused by the relaxor-ferroelectric (RFE) to ferroelectric (FE) transition, observed in the pristine terpolymers⁵.

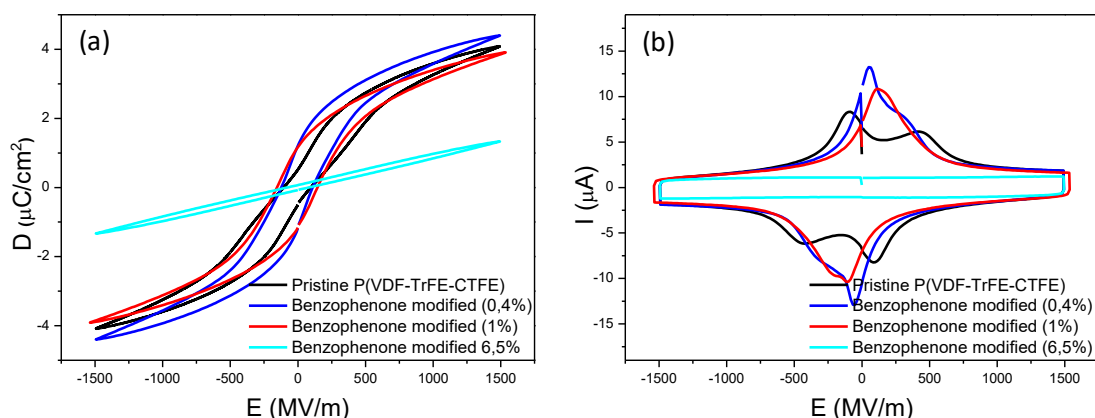


Figure 5-8. Ferroelectric testing at 20°C and 10Hz of the pristine terpolymer $P(\text{VDF-TrFE-CTFE})$ compared with terpolymer grafted with different amounts of benzophenone (BP), measuring the (a) Displacement and (b) the current as a function of applied electric field (annealed films, 110°C 1h).

The polymers were also characterized via broadband dielectric spectroscopy after being exposed to UV light and thus cross-linked. The most pronounced difference between the UV exposed polymers and the pristine ones is that the temperature of the dielectric permittivity peak shifts towards a higher regime, while the permittivity decreases for the polymer grafted with 1% of benzophenone, when the polymer grafted with 0.4% of benzophenone shows no apparent decrease in permittivity (Figure 5-9).

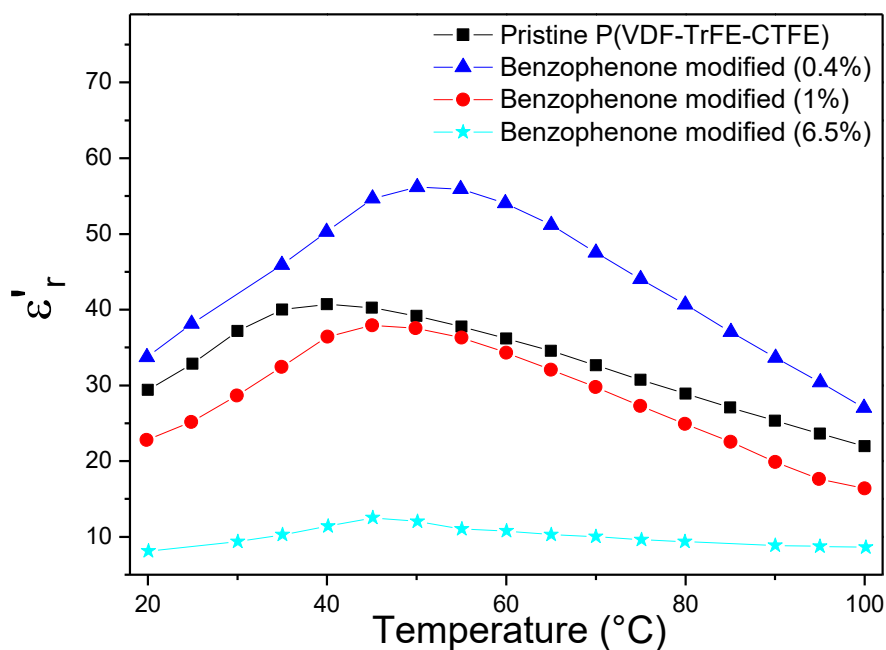


Figure 5-9. Broadband dielectric spectroscopy as a function of temperature comparing the real part of the relative permittivity of the pristine $P(\text{VDF-TrFE-CTFE})$ with the benzophenone modified

terpolymers with different benzophenone loadings (1kHz, exposed to UV (6J/cm²) light and then annealed 1h 110°C).

The data obtained from the broadband dielectric spectroscopy experiments at 1kHz for all three states (as cast, annealed, exposed + annealed) are summarized in **Table 5-1**.

Table 5-1. Summary of the data obtained by broadband dielectric spectroscopy at 1kHz for the benzophenone containing P(VDF-TrFE-CTFE) terpolymers.

	As cast		Annealed		Exposed + Annealed	
	Peak temperature (°C)	Dielectric constant (peak, 1kHz)	Peak temperature (°C)	Dielectric constant (peak, 1kHz)	Peak temperature (°C)	Dielectric constant (peak, 1kHz)
Pristine terpolymer	40°C	36	40°C	41	-	-
Benzophenone (0.4%)	45°C	50	42°C	54	47°C	55
Benzophenone (1%)	45°C	45	45°C	52	42°C	37
Benzophenone (6.5%)	45°C	14	45°C	14	45°C	13

From the abovementioned results it is concluded that the benzophenone modification at low BP contents positively influences the dielectric properties of the materials with as much as 30% increase in dielectric constant for the annealed samples. Even after exposure to UV light, the dielectric low BP content polymers exhibit dielectric constant comparable or even higher than the pristine terpolymer.

5.2.3) Electronic properties of P(VDF-TrFE-CTFE) terpolymers with pendent anthraquinone groups

The P(VDF-TrFE-CTFE) terpolymers grafted with anthraquinone groups were also characterized in the same three different states (as cast, annealed, exposed + annealed) as their benzophenone counterparts.

In order to investigate the impact that the different anthraquinone-modified polymers have on the dielectric properties, all polymers were characterized by broadband dielectric spectroscopy, from 20°C to 100°C and frequency 1 kHz. For the as cast films, the polymer with the lowest anthraquinone content (0.6%) shows greatly enhanced dielectric constant with respect to the pristine polymer, while all the polymers modified with higher amounts of anthraquinone present reduced dielectric

constant, in comparison to the pristine terpolymer (**Figure 5-10**).

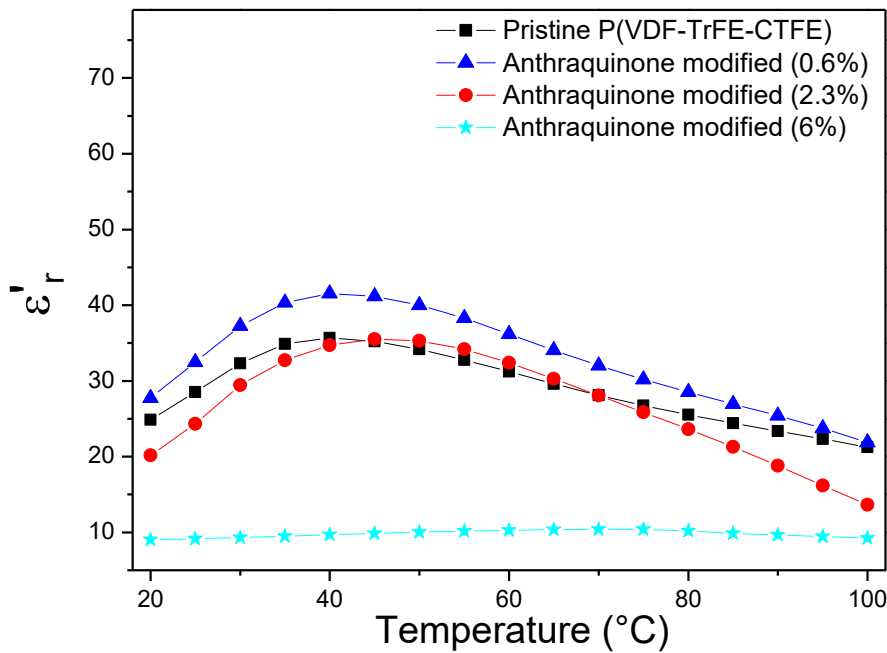


Figure 5-10. Broadband dielectric spectroscopy as a function of temperature comparing the real part of the relative permittivity of the pristine P(VDF-TrFE-CTFE) with the anthraquinone modified terpolymers with different anthraquinone grafting (1kHz, As cast films).

Similar evolution was followed with the ferroelectric properties of the polymer, with the polymer containing 0.6% of anthraquinone, exhibiting slightly increased displacement, while the terpolymers with higher anthraquinone content show decreased displacement at any given electric field.

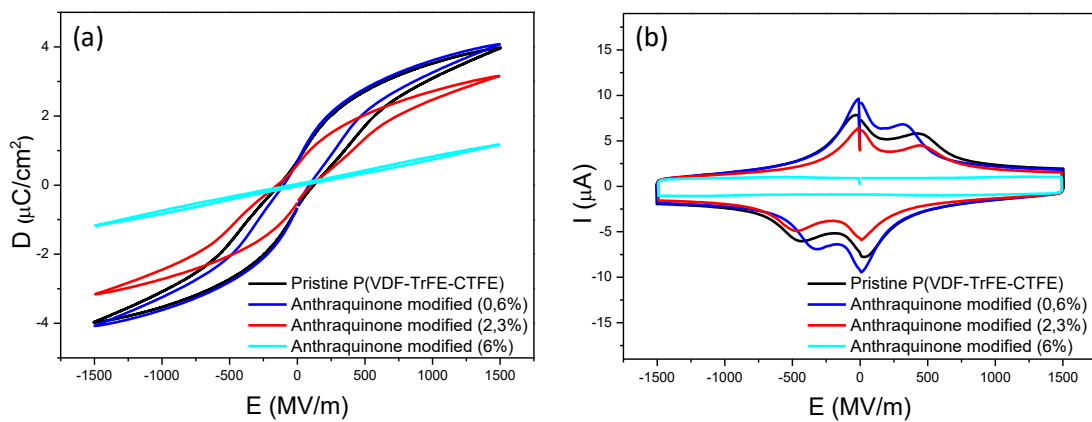


Figure 5-11. Ferroelectric testing at 20°C and 10Hz of the pristine terpolymer P(VDF-TrFE-CTFE) compared with terpolymer grafted with different amounts of anthraquinone (AQ), measuring the (a) Displacement and (b) the current as a function of applied electric field (as cast films).

The highest observed enhancement in dielectric properties occurred for the annealed (not exposed) anthraquinone (0.6%) polymer, where a 60% increase in relative permittivity was observed at the peak temperature (40°C), with the relative permittivity up to 65 compared to 40 for the pristine polymer. The annealing step was shown to improve the dielectric properties of all films. However, the largest improvement was again observed for the 0.6% anthraquinone-modified terpolymer, as shown in **Figure 5-12**. Such an improvement in the dielectric properties of FEPs has never been reported in literature. Only a few reports, to the best of our knowledge mention a considerable increase in the dielectric constant of FEPs and concern the mixing of FEPs with plasticizers⁶⁻⁷. However the increased dielectric constant in these cases is observed only at the very low frequency range (<1Hz), while the improvement in our case is observed across the frequency range.

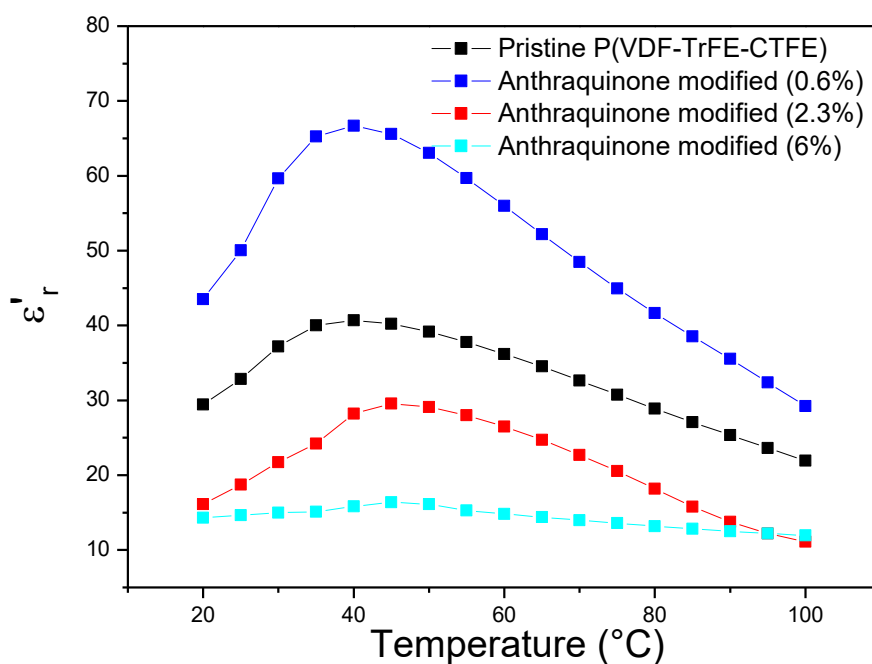


Figure 5-12. Broadband dielectric spectroscopy as a function of temperature comparing the real part of the relative permittivity of the pristine P(VDF-TrFE-CTFE) with the anthraquinone modified terpolymers with different anthraquinone degree of grafting (1kHz, annealed films, 110°C 1h).

The ferroelectric testing of the above mentioned polymers, showed that even after the annealing step the anthraquinone modified polymers maintained their DHL behavior in contrast to the benzophenone modified terpolymers (**Figure 5-13**). The annealing step does not appear to have an important impact on the ferroelectric properties of any of those polymers.

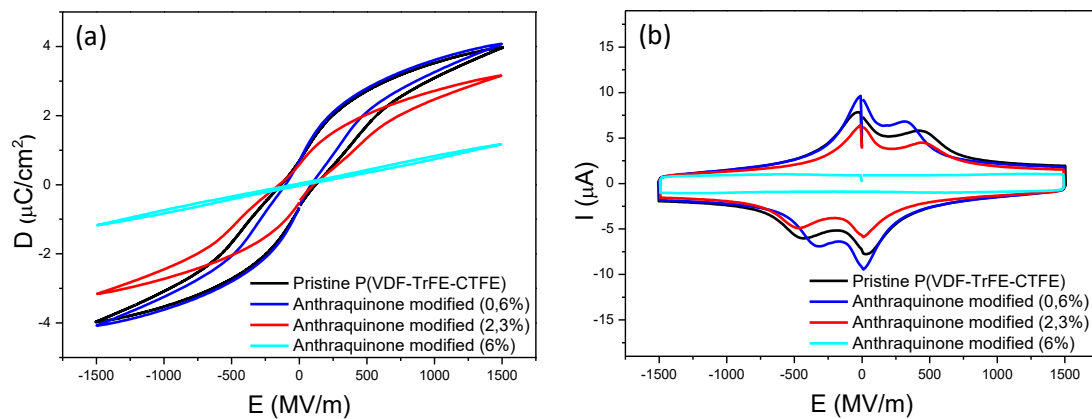


Figure 5-13. Ferroelectric testing at 20°C and 10Hz of the pristine terpolymer P(VDF-TrFE-CTFE) compared with terpolymer grafted with different amounts of anthraquinone (AQ), measuring the (a) Displacement and (b) the current as a function of applied electric field (annealed films, 110°C 1h).

The final stage at which the anthraquinone modified P(VDF-TrFE-CTFE) terpolymers were characterized was after exposure to $3\text{J}/\text{cm}^2$ of UV light and subsequent annealing at 110°C for 1h. The impact of the UV exposure to the dielectric properties was detrimental for all the polymers (**Figure 5-14**), however, the polymer with the lowest anthraquinone content (0.6%) still exhibited improved dielectric properties compared to the pristine terpolymer. Therefore, the positive impact on the electroactive properties induced by the double bonds, was reduced but not totally eliminated by the photo-induced cross-linking.

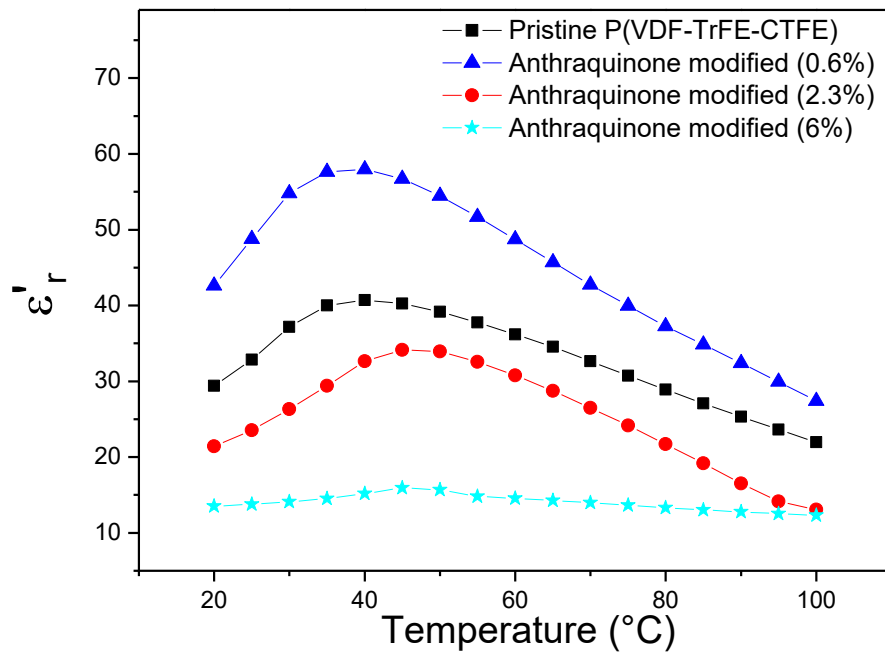


Figure 5-14. Broadband dielectric spectroscopy as a function of temperature comparing the real part of the relative permittivity of the pristine P(VDF-TrFE-CTFE) with the anthraquinone modified terpolymers with different anthraquinone degree of grafting (1kHz, exposed to UV light (6J/cm²) and then annealed 1h 110°C).

A summary of the data derived from the broadband dielectric spectroscopy of the anthraquinone modified polymers characterized in the three different stages (*i.e.* as cast, annealed, and after UV exposure/annealing) is presented in **Table 5-2**.

Table 5-3. Summary of the data obtained by broadband dielectric spectroscopy at 1kHz for the anthraquinone containing P(VDF-TrFE-CTFE) terpolymers.

	As cast		Annealed		Exposed + Annealed	
	Peak temperature (°C)	Dielectric constant (peak, 1kHz)	Peak temperature (°C)	Dielectric constant (peak, 1kHz)	Peak temperature (°C)	Dielectric constant (peak, 1kHz)
Pristine terpolymer	40°C	36	40°C	41	-	-
Anthraquinone (0.6%)	40°C	42	40°C	65	40°C	58
Anthraquinone (2.3%)	45°C	36	45°C	27	45°C	34
Anthraquinone (6%)	70	10	45°C	15	45°C	16

From the abovementioned results on the anthraquinone grafted P(VDF-TrFE-CTFE) terpolymers it is shown that improved dielectric properties can be obtained for the low anthraquinone content especially for the annealed samples. The permittivity can

increase up to 60% for the terpolymer containing 0.6% AQ. The photo-induced cross-linking is shown to reduce the dielectric performance of all materials, but the best ones can outperform the pristine P(VDF-TrFE-CTFE) terpolymer even when photo cross-linked.

5.2.4) Electronic properties of P(VDF-TrFE-CFE) terpolymers with pendent anthraquinone groups

The same modification reaction with anthraquinone was applied on the P(VDF-TrFE-CFE) terpolymers. The electric properties of the modified polymers were characterized after annealing at 110°C for 1h. The impact on the dielectric properties was investigated by broadband dielectric spectroscopy, from 20°C to 100°C and frequency 1 kHz. As shown in **Figure 5-15** the impact of the modification on the dielectric properties is quite different compared to the P(VDF-TrFE-CTFE) terpolymers. Here, instead of increasing the relative permittivity with low modification contents, the peak shifts to higher temperatures and the values of the permittivity are rather reduced.

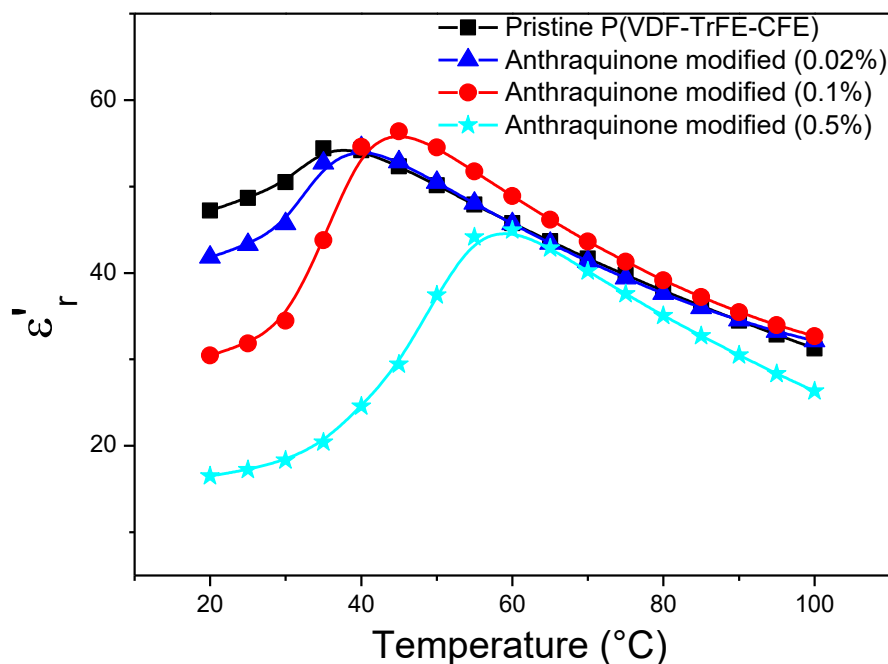


Figure 5-15. Broadband dielectric spectroscopy as a function of temperature comparing the real part of the relative permittivity of the pristine P(VDF-TrFE-CFE) with the anthraquinone modified terpolymers with different anthraquinone degree of grafting (1kHz, annealed films, 110°C 1h).

The ferroelectric response of the P(VDF-TrFE-CFE) terpolymers modified with

different amounts of anthraquinone was investigated at a frequency of 10Hz (**Figure 5-16**). For the low anthraquinone contents (0.5%), the polymers show increased displacement at any given field, while with increasing the anthraquinone (and double bond) content the polymer gains more ferroelectric character.

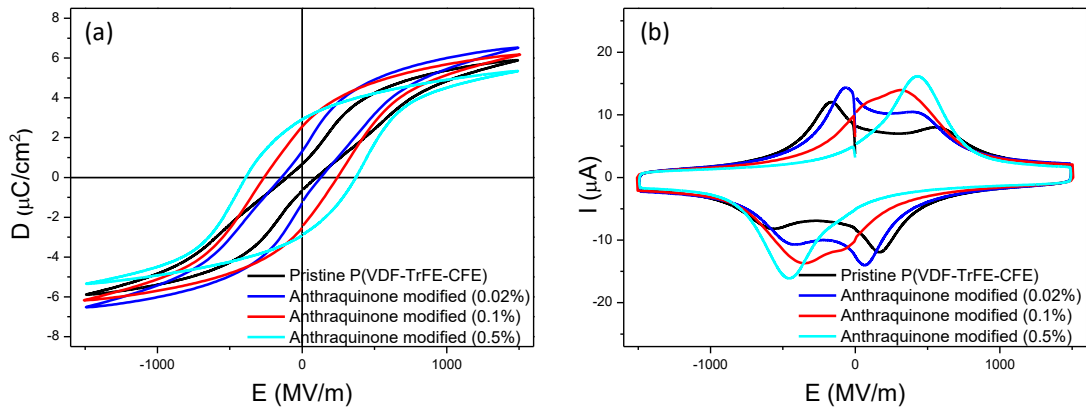


Figure 5-16. Ferroelectric testing at 20°C and 10Hz of the pristine terpolymer P(VDF-TrFE-CFE) compared with terpolymer grafted with different amounts of anthraquinone (AQ), measuring the (a) Displacement and (b) the current as a function of applied electric field (annealed films, 110°C 1h).

In order to better observe how the anthraquinone modified P(VDF-TrFE-CTFE) terpolymer with sufficiently high anthraquinone (and double bond) content is turned into a ferroelectric material, the hysteresis loop at low frequency (0.1Hz) is presented in **Figure 5-17**. The polymer shows proper ferroelectric behavior with a remnant displacement equal to $4\mu\text{C}/\text{cm}^2$.

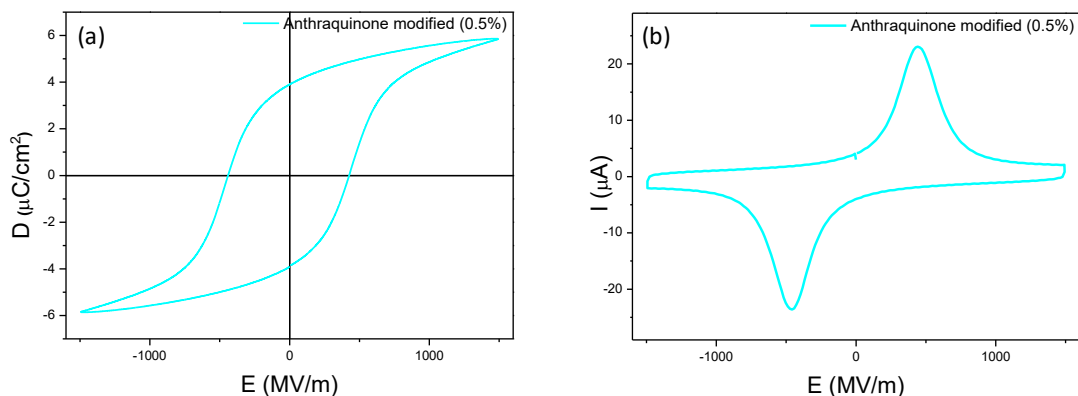


Figure 5-17. Ferroelectric testing at 20°C and 0.1Hz of the pristine terpolymer P(VDF-TrFE-CFE) compared with terpolymer grafted with 0.5% of anthraquinone (AQ), measuring the (a) Displacement and (b) the current as a function of applied electric field (annealed films, 110°C 1h).

Therefore, the anthraquinone modification appeared to have a very different impact on the P(VDF-TrFE-CFE) terpolymer compared to the P(VDF-TrFE-CTFE). In this case instead of an increase of the dielectric properties, the relaxor-ferroelectric

material is transformed to ferroelectric.

5.2.5) Electronic properties of P(VDF-TrFE) copolymers with pendent benzophenone groups

Both the benzophenone and the anthraquinone modifications were also applied in the ferroelectric P(VDF-TrFE) copolymers. The ferroelectric properties of which were characterized in as cast films, as well as films annealed for 30 minutes. However since polymers with different modification content had different melting and crystallization temperatures annealing all the films at the same temperature would not be optimal. We therefore chose to anneal all films on the onset of their melting peaks as assessed by differential scanning calorimetry.

Starting with the ferroelectric evaluation of not annealed P(VDF-TrFE) copolymers modified with benzophenone groups. The hysteresis loops as well as the current as a function of the applied electric field are displayed in **Figure 5-18**, where increasing the benzophenone content is shown to decrease the ferroelectric response of the polymers with simultaneous reduction of the remnant and saturation displacement and increase in the coercive field.

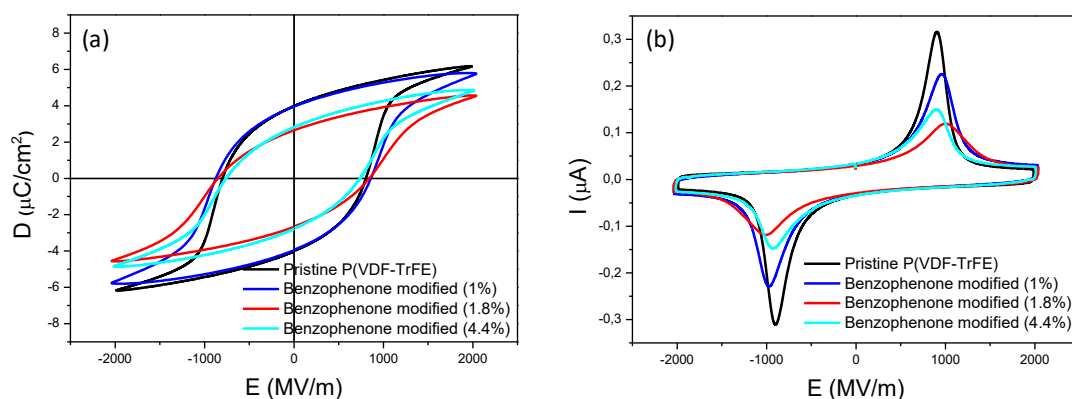


Figure 5-18. Ferroelectric behavior at 20°C and 0.1Hz comparing the pristine copolymer P(VDF-TrFE) with the benzophenone (BP) modified copolymers with different amounts of benzophenone. (a) Displacement as a function of electric field and (b) current as a function of electric field (as cast films).

Then all polymers were annealed for 30 minutes at the onset of their melting peaks as characterized by DSC. The hysteresis loops and the I-E curves are shown in **Figure 5-19**, where the decrease in ferroelectric response with increasing the benzophenone content becomes more apparent. However even at the highest modification degree (4.4%), the copolymer maintains its ferroelectric behavior, while being both thermally and photochemically cross-linkable.

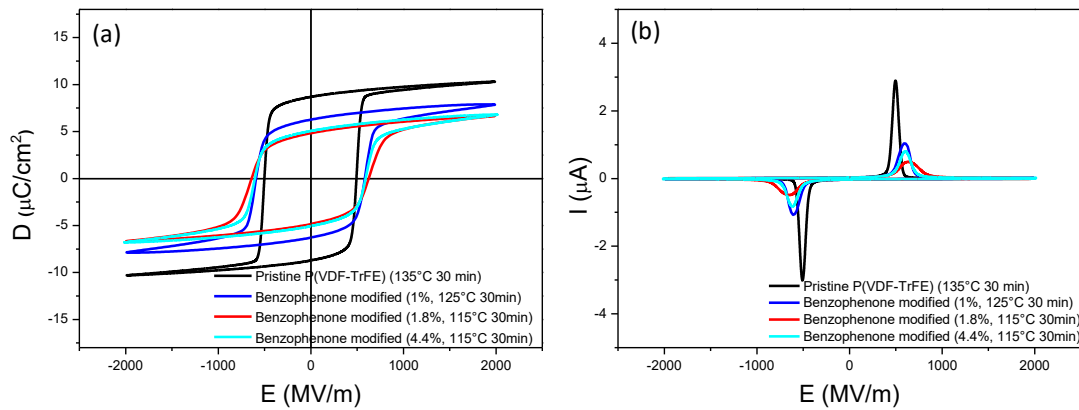


Figure 5-19. Ferroelectric evaluation at 20°C and 0.1Hz comparing the pristine copolymer P(VDF-TrFE) with the benzophenone (BP) modified copolymers with different amounts of benzophenone. (a) Displacement as a function of electric field and (b) current as a function of electric field. All the polymers are annealed on the onset of their melting for 30 min.

The data derived from the hysteresis loops for P(VDF-TrFE) copolymers modified with different benzophenone contents are summarized in **Table 5-4**.

Table 5-4. Summary of the data obtained by broadband dielectric spectroscopy at 1kHz for the benzophenone containing P(VDF-TrFE) copolymers.

Sample	As cast			Annealed	
	Remnant Displacement ($\mu\text{C}/\text{cm}^2$)	Saturation Displacement ($\mu\text{C}/\text{cm}^2$)	Dielectric constant @ 1kHz	Remnant Displacement ($\mu\text{C}/\text{cm}^2$)	Saturation Displacement ($\mu\text{C}/\text{cm}^2$)
Pristine copolymer	4.0	6.2	11.7	8.7	10.3
Benzophenone (1%)	4.0	5.77	10.3	6.2	7.9
Benzophenone (1.8%)	2.7	4.6	10.5	4.8	6.7
Benzophenone (4.4%)	2.8	4.9	10.0	4.9	6.8

Broadband dielectric spectroscopy at 20°C was performed on the annealed films. A slight decrease in relative permittivity (**Figure 5-20a**) was observed, while the dielectric loss remained almost identical regardless of the modification degree **Figure 5-20b**.

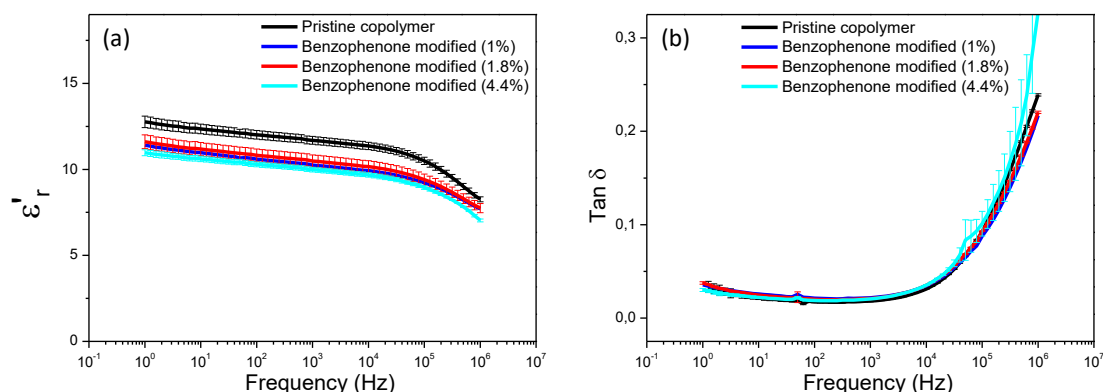


Figure 5-20. Broadband dielectric spectroscopy at room temperature comparing (a) the real part of the relative permittivity as a function of frequency and (b) the dielectric loss as a function of frequency of the pristine P(VDF-TrFE) with the benzophenone modified terpolymers with different benzophenone loadings.

The ferroelectric properties of some of the benzophenone modified copolymers were also characterized after exposure to $6\text{J}/\text{cm}^2$ of UV light and subsequent annealing at the onset of their melting. Even after the exposure the polymers maintained their ferroelectric character with no apparent changes (**Figure 5-21**).

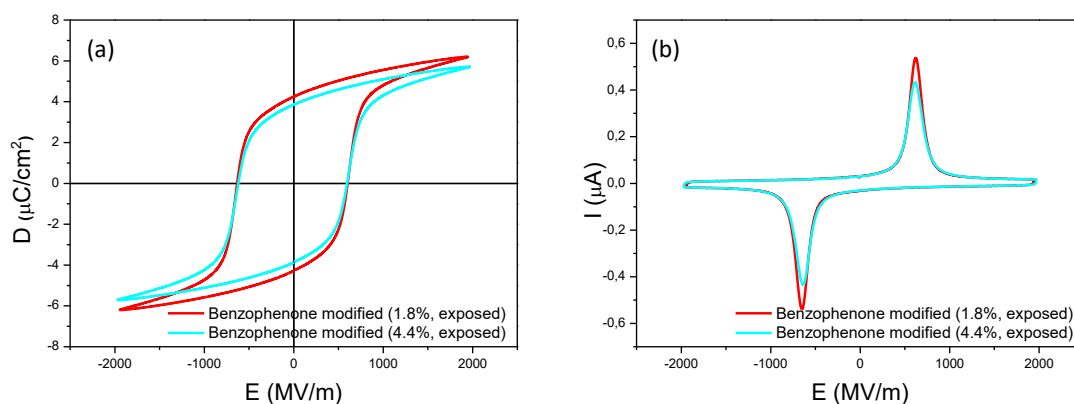


Figure 5-21. Ferroelectric testing at 20°C and 0.1Hz comparing the pristine copolymer P(VDF-TrFE) with the benzophenone (BP) modified copolymers with different amounts of benzophenone. (a) Displacement as a function of electric field and (b) current as a function of electric field. All the polymers are exposed at $6\text{J}/\text{cm}^2$ and then annealed on the onset of their melting for 30 min.

Films of the copolymer with 4.4% benzophenone content were also exposed to UV light ($6\text{J}/\text{cm}^2$) and then developed in cyclopentanone (1min) before being annealed at 135°C for 30 minutes. That experiment was to confirm that the patterned films (after exposure and development) maintained their ferroelectric character (see in **Figure 5-22**).

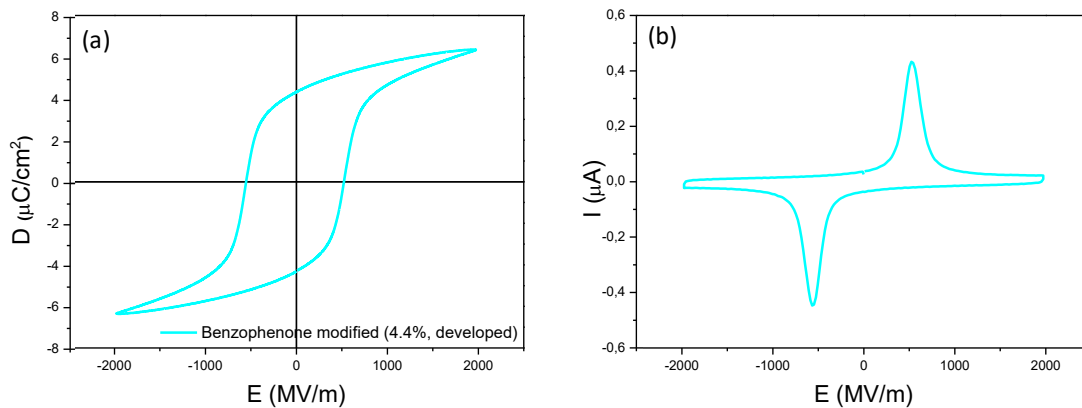


Figure 5-22. Ferroelectric testing at 20°C and 0.1Hz of the ~~the~~ benzophenone (BP) modified copolymers with 4.4% benzophenone. (a) Displacement as a function of electric field and (b) current as a function of electric field. The film is exposed at 6J/cm² and then developed in cyclopentanone for 1 min before being annealed on the onset of their melting for 30 min.

Since the differences between the not exposed, the exposed and the developed films are very subtle, we plotted them on the same graphs in order to observe the evolution of the properties with changing the treatment. Exposure to UV light seemed to have detrimental effects on the ferroelectric properties, both regarding the displacement (**Figure 5-23 a**) and also the coercive field (**Figure 5-23 b**). The fact that exposure to UV light caused deteriorated ferroelectric properties could come from limited chain mobility (along with dipole mobility) after photo-induced cross-linking. When the films are developed in cyclopentanone after the exposure step, the ferroelectric properties seem to improve compared to the non developed films (**Figure 5-23 black**).

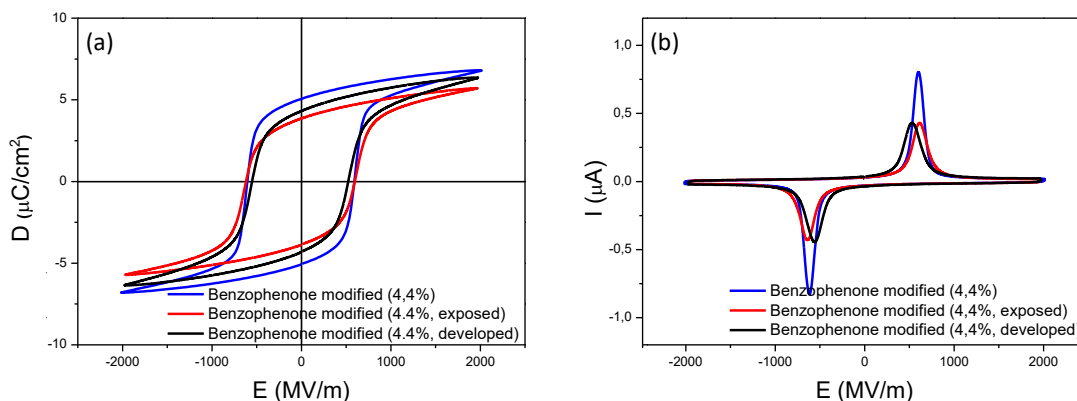


Figure 5-23. Ferroelectric testing at 20°C and 0.1Hz of the benzophenone (BP) modified copolymers with 4.4% benzophenone. (a) Displacement as a function of electric field and (b) current as a function of electric field. Comparison between non-exposed films, exposed at 6J/cm² and finally exposed and developed in cyclopentanone.

Therefore, the benzophenone modification negatively impacts the ferroelectric properties of the P(VDF-TrFE) copolymer. However, especially when the modification

degree is low the polymers maintain good ferroelectric properties even when cross-linked (and developed).

5.2.6) Electronic properties of P(VDF-TrFE) copolymers with pendent anthraquinone groups

The ferroelectric properties of films of the P(VDF-TrFE) copolymer modified with anthraquinone groups were also investigated. The ferroelectric properties of the non-annealed films are shown in **Figure 5-24**.

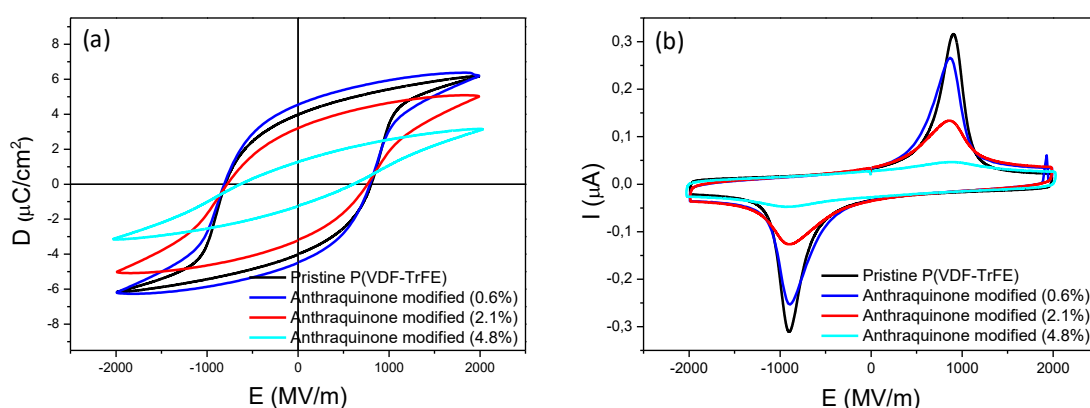


Figure 5-24. Ferroelectric testing at 20°C and 0.1Hz comparing the pristine copolymer P(VDF-TrFE) with the anthraquinone (AQ) modified copolymers with different amounts of anthraquinone. (a) Displacement as a function of electric field and (b) current as a function of electric field (as cast films).

Then, the films of the anthraquinone modified copolymers with different anthraquinone contents were annealed at the onset of their melting peaks, as characterized by differential scanning calorimetry. After the annealing steps, the ferroelectric properties of the polymers seem to constantly decrease with increasing the anthraquinone content. That was observed both for the displacement (remnant and saturation) which is shown in **Figure 5-25a** which steadily decreases with increasing the anthraquinone content but also the coercive field which steadily increases (**Figure 5-25b**).

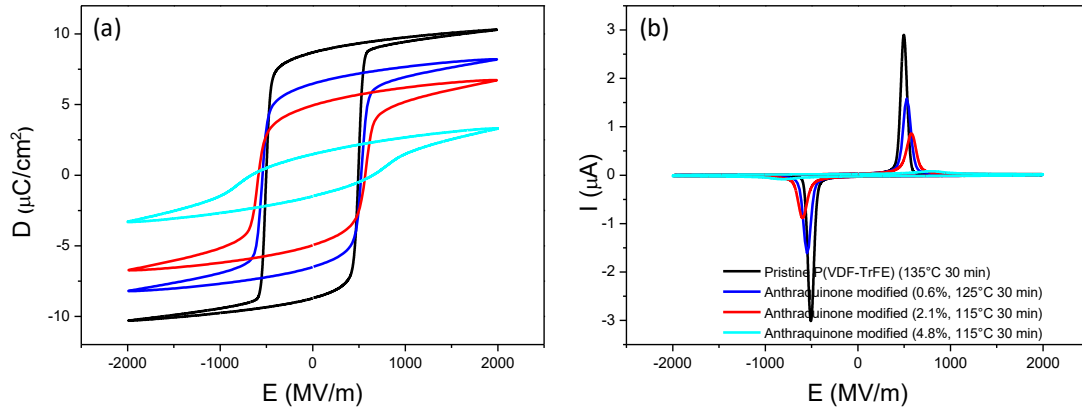


Figure 5-25. Ferroelectric testing at 20°C and 0.1Hz comparing the pristine copolymer $P(\text{VDF-TrFE})$ with the anthraquinone (AQ) modified copolymers with different amounts of anthraquinone. (a) Displacement as a function of electric field and (b) current as a function of electric field (all the films are annealed on the onset of their melting for 30 min).

The data regarding the remnant and saturation displacement for the $P(\text{VDF-TrFE})$ films modified with different amounts of anthraquinone are summarized in **Table 5-5**.

Table 5-5. Summary of the data obtained by broadband dielectric spectroscopy at 1kHz for the anthraquinone containing $P(\text{VDF-TrFE})$ copolymers.

Sample	Not annealed			Annealed	
	Remnant Displacement ($\mu\text{C}/\text{cm}^2$)	Saturation Displacement ($\mu\text{C}/\text{cm}^2$)	Dielectric constant @ 1kHz	Remnant Displacement ($\mu\text{C}/\text{cm}^2$)	Saturation Displacement ($\mu\text{C}/\text{cm}^2$)
Pristine copolymer	4.6	6.3	11.7	8.7	10.3
Anthraquinone (0.6%)	4.0	6.2	11.9	6.5	8.2
Anthraquinone (2.1%)	3.2	5.0	10.9	5.0	6.7
Anthraquinone (4.8%)	1.3	3.2	9.6	1.5	3.3

Broadband dielectric spectroscopy was performed on the annealed samples at room temperature. The anthraquinone modified copolymers showed some reduction in relative permittivity (**Figure 5-26**), depending on the anthraquinone content.

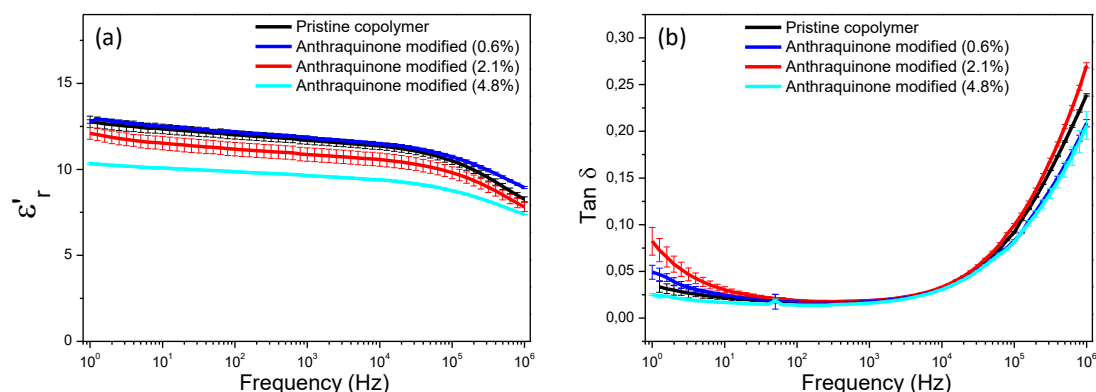


Figure 5-26. Broadband dielectric spectroscopy at room temperature comparing (a) the real part of the relative permittivity as a function of frequency and (b) the dielectric loss as a function of frequency of the pristine P(VDF-TrFE) with the anthraquinone modified terpolymers with different anthraquinone (AQ) loadings.

After exposure to UV light the ferroelectric properties of copolymers with different anthraquinone contents were recorded and are presented in **Figure 5-27**.

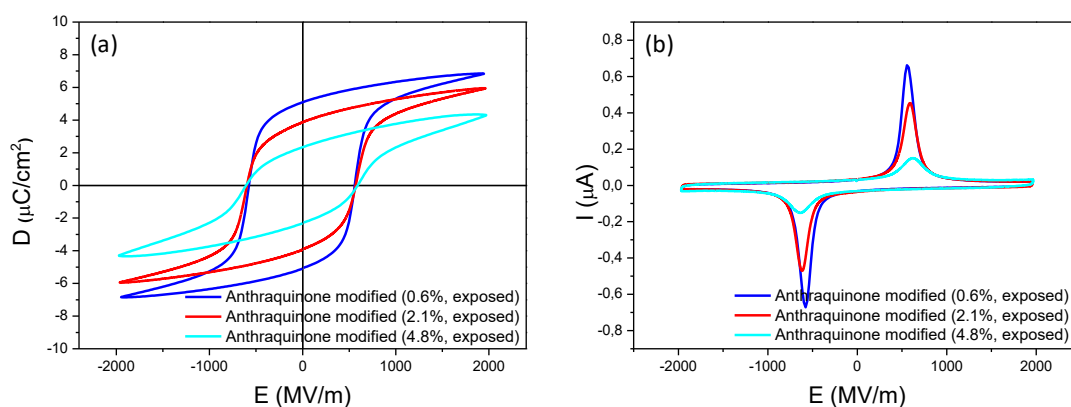


Figure 5-27. Ferroelectric testing at 20°C and 0.1Hz comparing the P(VDF-TrFE) modified with different amounts of anthraquinone (AQ). (a) Displacement as a function of electric field and (b) current as a function of electric field (exposed to 3J/cm², annealed on the onset of their melting for 30 min).

The final stage at which the anthraquinone modified copolymers were characterized was after development at cyclopentanone for 1 minute and subsequent annealing at the onset of the melting for 30 minutes. The hysteresis loops are shown in **Figure 5-28**.

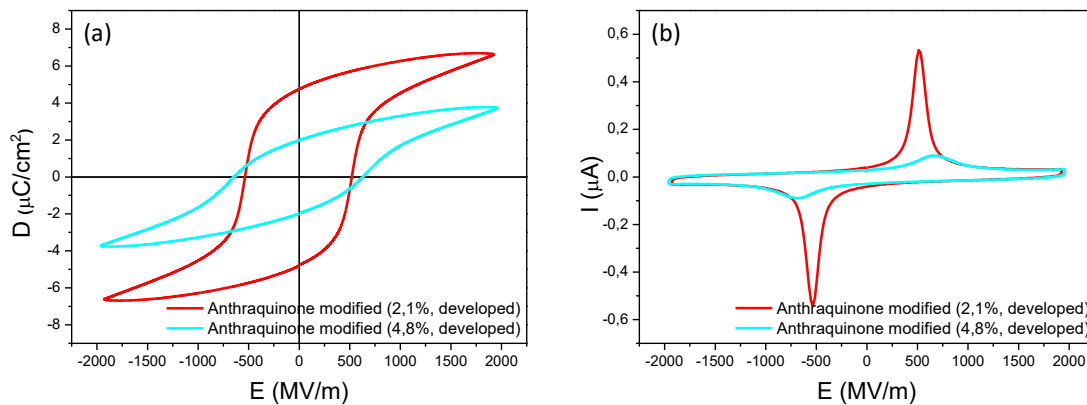


Figure 5-28. Ferroelectric testing at 20°C and 0.1Hz comparing the $P(\text{VDF-TrFE})$ modified with different amounts of anthraquinone (AQ). (a) Displacement as a function of electric field and (b) current as a function of electric field. (Exposed to $3\text{J}/\text{cm}^2$, developed and annealed on the onset of their melting for 30 min.)

In order to better understand the impact of the exposure and the subsequent annealing on the properties, the ferroelectric characterization of the copolymer with 2.1% anthraquinone content is shown after the three different kinds of treatment (Figure 5-29). Similarly to the copolymer modified with benzophenone (Figure 5-23), exposure seems to impact negatively the ferroelectric properties, while the development step seems to help recover the lost performance.

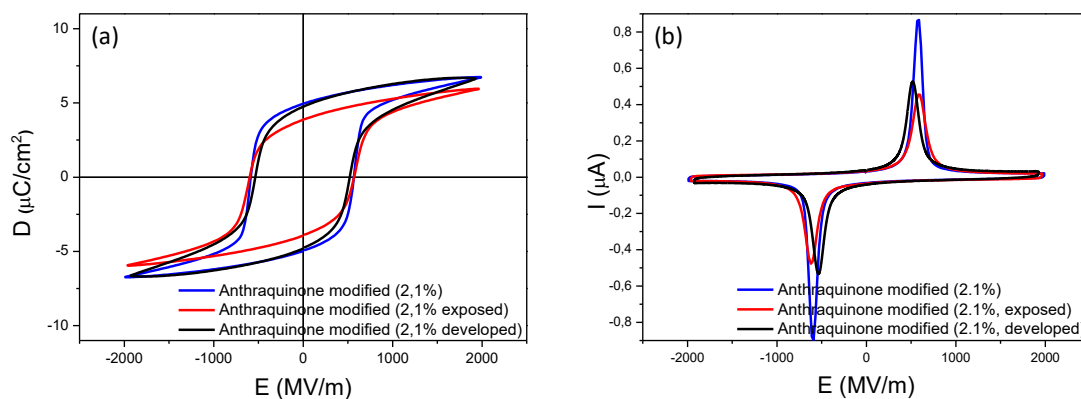


Figure 5-29. Ferroelectric testing at 20°C and 0.1Hz comparing the $P(\text{VDF-TrFE})$ modified with 2.1% of anthraquinone (AQ). (a) Displacement as a function of electric field and (b) current as a function of electric field. (Blue annealed, red exposed, black exposed + developed).

5.2.7) Electronic properties of $P(\text{VDF-TrFE-CTFE})$ terpolymers with intrachain double bonds

It is noteworthy that the above studied materials were composed of both inner double bonds and pendant functional groups such as azido, benzophenone and

anthraquinone. In order to try discriminating the role of each moiety, the electronic properties of P(VDF-TrFE-CTFE) terpolymer bearing only double bonds were characterized. The polymer films were characterized directly after casting as well as after annealing. The broadband dielectric spectroscopy of the as cast films at 1kHz and temperatures ranging from 20 to 100°C is shown in **Figure 5-30**. No improvement in terms of dielectric constant is observed for the as cast films as shown in **Figure 5-30a**, while the double bond containing films show increased dielectric loss with respect to the pristine terpolymer (**Figure 5-30b**).

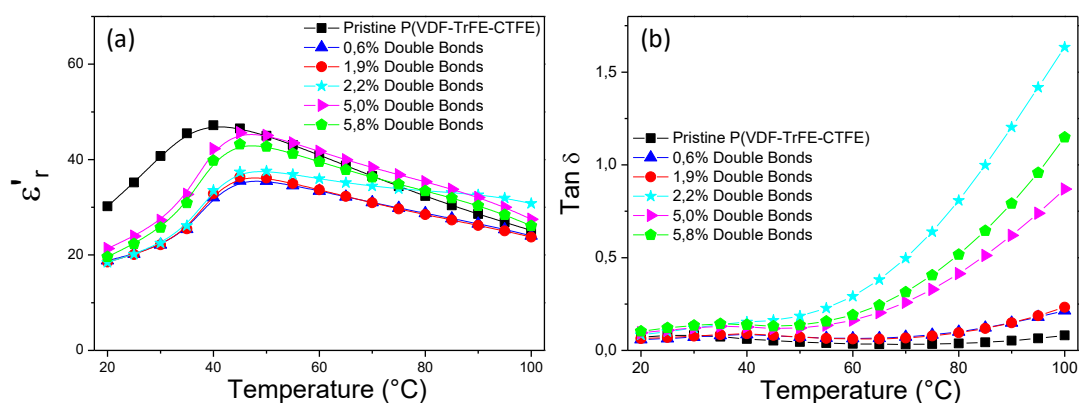


Figure 5-30. Broadband dielectric spectroscopy as a function of temperature comparing the real part of the relative permittivity of the pristine P(VDF-TrFE-CTFE) with the double bond containing terpolymers with different double bond contents (1kHz, as cast).

From the ferroelectric testing of the as cast films, it is confirmed that high double bond contents causes leakage current to increase (**Figure 5-31**). That is expressed both with the opening of the hysteresis loop for the terpolymers bearing more than 1.9% double bonds (**Figure 5-31a**) but also with the vertical shifting of the current at the high field regime (**Figure 5-31b**).

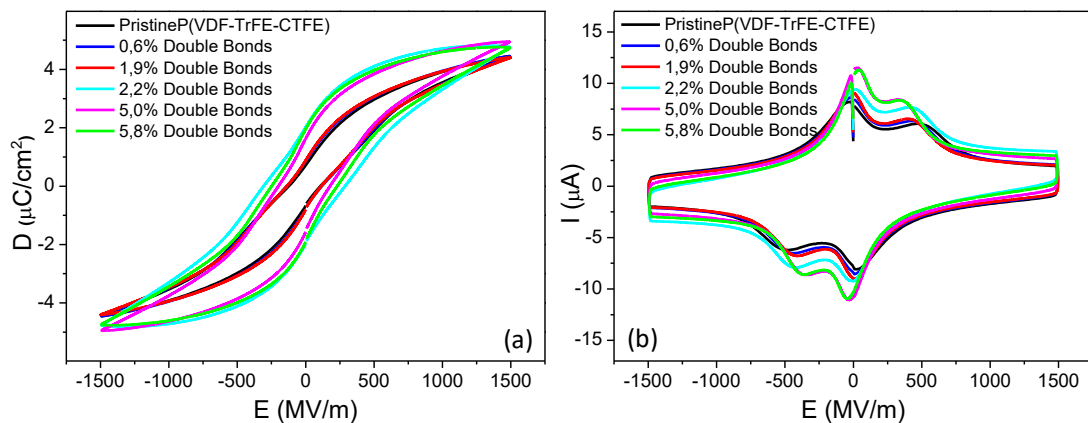


Figure 5-31. Ferroelectric testing at 20°C and 10 Hz comparing the P(VDF-TrFE-CTFE) terpolymer with different double bond contents. (a) Displacement as a function of electric field and (b) current as a function of electric field (as cast).

Films of the same terpolymers were characterized after an annealing step at 110°C for 1h. Both the dielectric and the ferroelectric response of the annealed films were recorded. Contrarily to the as cast films, after annealing the polymers showed improved dielectric properties with respect to the pristine polymer as shown in **Figure 5-32a**. Thus, increasing the double bond content seems to rise the relative permittivity with as much as 35% increase for the polymer bearing 5% of double bonds. The dielectric loss on the other hand increases as well with increasing the double bond content **Figure 5-32b**.

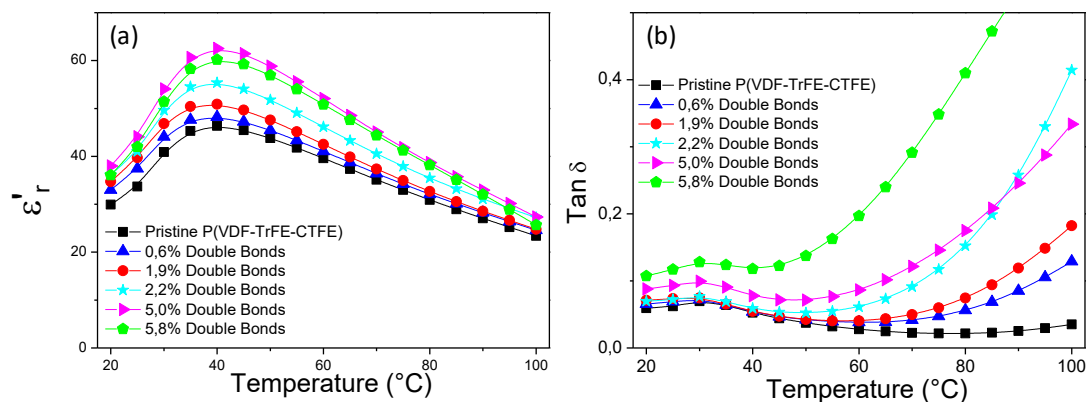


Figure 5-32. Broadband dielectric spectroscopy as a function of temperature comparing the real part of the relative permittivity of the pristine P(VDF-TrFE-CTFE) with the double bond containing terpolymers with different double bond contents (1kHz, annealed 1h 110°C).

The ferroelectric properties of the annealed films show improvement as well, with no signs of leakage current for all the polymers except for the one with the highest double bond content (**Figure 5-33**). The displacement at any given field seems to increase as well (see magnification in **Figure 5-34**).

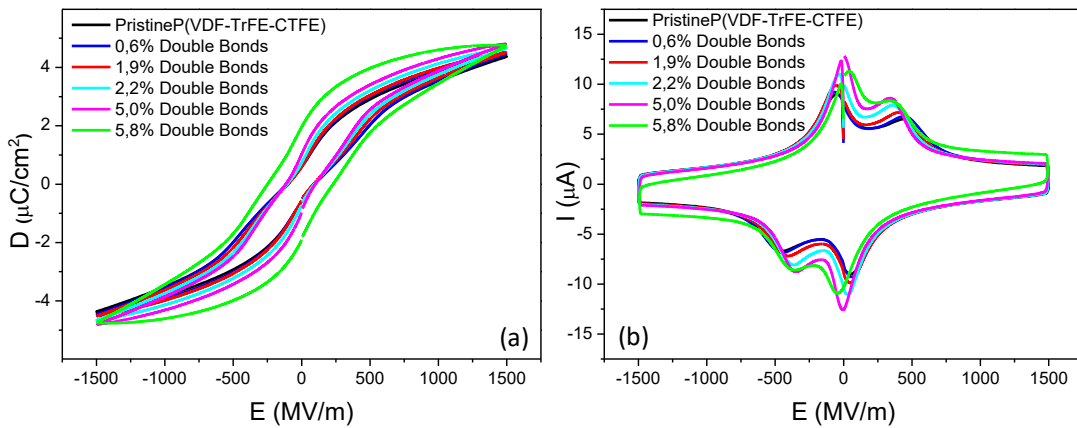


Figure 5-33. Ferroelectric testing at 20°C and 10 Hz comparing the P(VDF-TrFE-CTFE) terpolymer with different double bond contents. (a) Displacement as a function of electric field and (b) current as a function of electric field (annealed 1h 110°C).

As shown in **Figure 5-34**, the displacement at any given field increases as the double bond content increases, with the exception of the terpolymer containing 5.8% double bonds, which has also the highest dielectric loss.

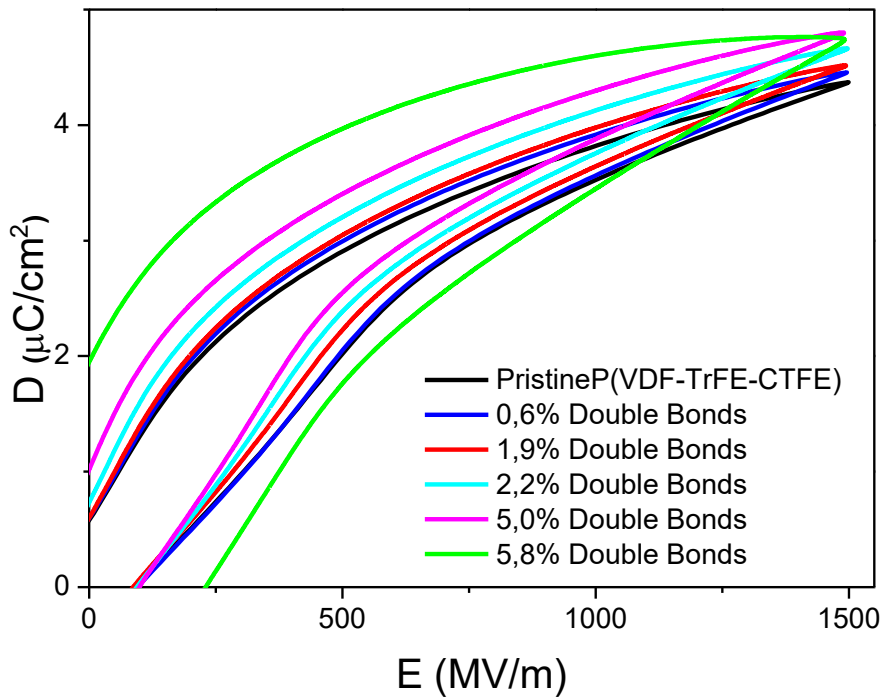


Figure 5-34. Amplification of **Figure 5-33**, showing the ferroelectric testing at 20°C and 10 Hz comparing the P(VDF-TrFE-CTFE) terpolymer with different double bond contents. (a) Displacement as a function of electric field and (b) current as a function of electric field (annealed 1h 110°C).

The dielectric spectroscopy data before and after annealing, are summarized in **Table 5-6**.

Table 5-6. Summary of the data obtained by broadband dielectric spectroscopy at 1kHz for the double bond containing P(VDF-TrFE-CTFE) terpolymers on both as cast and annealed films.

	As cast		Annealed	
	Peak temperature (°C)	Dielectric constant (peak, 1kHz)	Peak temperature (°C)	Dielectric constant (peak, 1kHz)
Pristine terpolymer	40°C	47	40°C	46
0.6% DB	45°C	36	40°C	48
1.9% DB	45°C	36	40°C	51
2.2% DB	50°C	38	40°C	55
5.0% DB	45°C	46	40°C	63
5.8% DB	45°C	43	40°C	60

The improved dielectric constant of the double bond containing terpolymers in combination with their improved displacement makes them excellent candidates for electrocaloric cooling devices.

5.2.8) Electronic properties of P(VDF-TrFE) copolymers with intrachain double bonds

In **Chapter 4** the introduction of double bonds on the P(VDF-TrFE) copolymer was attempted, however all the modified copolymers contained less than 1% double bonds. Their ferroelectric properties were nevertheless characterized in as cast films (**Figure 5-35**), as well as films annealed @135°C for 30min (**Figure 5-36**). The ferroelectric response of the as cast double bond containing copolymers remained largely unaffected (**Figure 5-35**) with no observed changes neither regarding the displacement, nor the current.

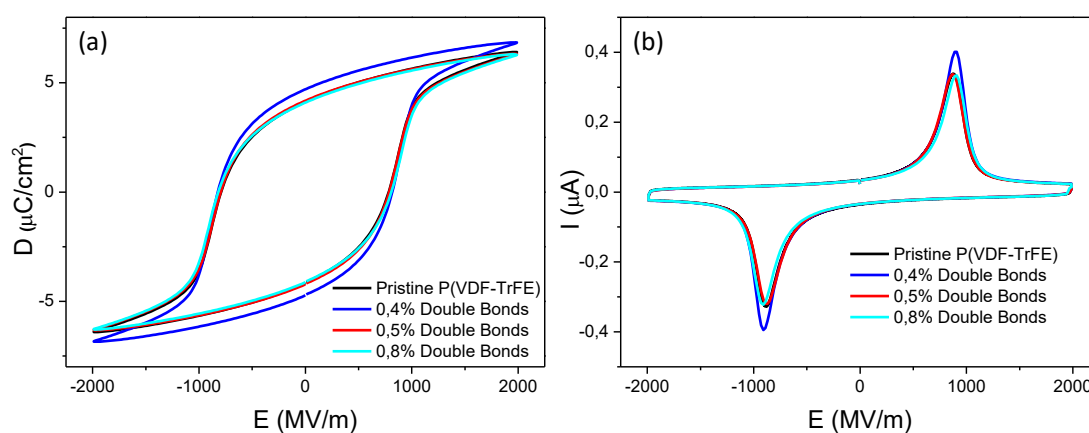


Figure 5-35. Ferroelectric testing at 20°C and 0.1 Hz comparing the P(VDF-TrFE) terpolymer with different double bond contents. (a) Displacement as a function of electric field and (b) current as a function of electric field (as cast films).

Similar behavior was observed in the annealed films, where the ferroelectric response of all the double bond containing copolymers was identical (**Figure 5-36**).

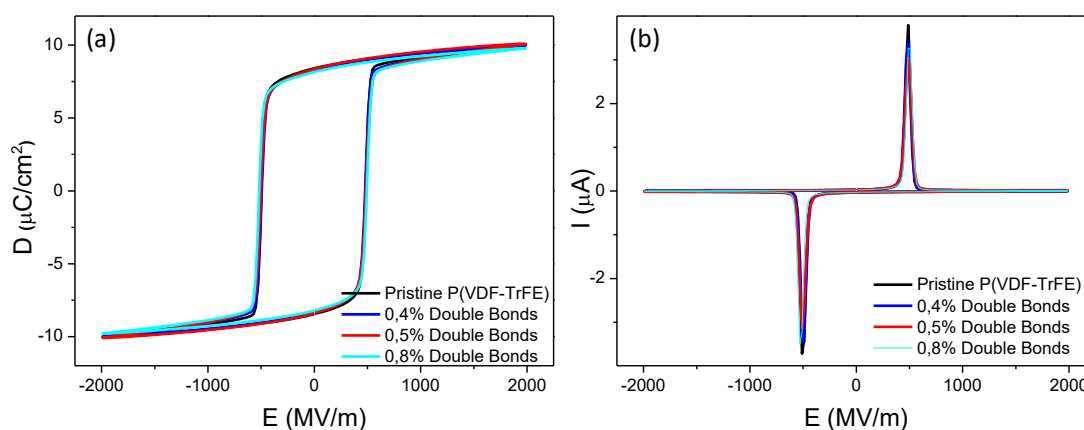


Figure 5-36. Ferroelectric testing at 20°C and 0.1 Hz comparing the P(VDF-TrFE) terpolymer with different double bond contents. (a) Displacement as a function of electric field and (b) current as a function of electric field (annealed 30 min 135°C).

5.3) Experimental part

Device fabrication. The metal-dielectric-metal devices were fabricated as follows. Glass substrates were cleaned and sonicated in acetone and isopropanol for 15 min. Then a layer of aluminum (80 nm) was evaporated as the bottom electrode using a thermal evaporator at a pressure of 1.10^{-6} mbar. Subsequently a 10% (wt) solution polymer dielectric layer was spincoated at 500 rpm for 5 sec and then 1000 rpm for 1 min. An aluminum top electrode (80 nm) was evaporated, creating a metal-insulator-metal device area of 2 mm². The devices were annealed at 110°C for 1 h and slowly cooled down to room temperature.

5.4) Conclusions

This chapter presented the electronic characterization of all the polymers synthesized in the context of this thesis. The azide containing terpolymers showed slightly deteriorated electroactive properties when compared to the pristine terpolymer. On the other hand, the terpolymers grafted with benzophenone and anthraquinone groups showed improved electroactive properties, when grafted with low amounts of photoinitiator (PI), with as much as 60% improvement in some of the cases. Reduced electroactive properties were observed, when the polymers grafted with higher photoinitiator amounts. The impact of the same types of modification on the P(VDF-TrFE-CFE) terpolymer was very different than the P(VDF-TrFE-CTFE), as instead of an improvement on the dielectric properties, the relaxor-ferroelectric terpolymer was transformed into ferroelectric after the modification. The P(VDF-TrFE) copolymers on the other hand showed reduced electroactive properties for all photoinitiator contents. However, the fact that the polymers mentioned above maintain either ferroelectric or relaxor-ferroelectric properties even after cross-linking (thermal or photochemical) is a great advantage for two main reasons. The first reason is that direct photolithographic patterning of such materials is possible as shown in **Chapter 3**. The second and even more important reason though, is that after cross-linking the electroactive layer becomes orthogonal to all solvents, which can be a great advantage for the fabrication of multilayer devices with conventional printing techniques. Finally, the introduction of double bonds was shown to have a very positive impact on the electroactive properties of the terpolymers providing us with a new way to enhance the electroactive properties of FEPs and to discriminate between

the role of photoinitiators and inner double bonds in our study.

5.4)References

1. Yang, L.; Li, X.; Allahyarov, E.; Taylor, P. L.; Zhang, Q. M.; Zhu, L., Novel polymer ferroelectric behavior via crystal isomorphism and the nanoconfinement effect. *Polymer* **2013**, *54* (7), 1709-1728.
2. Zhang, Q. M.; Bharti, V.; Zhao, X., Giant Electrostriction and Relaxor Ferroelectric Behavior in Electron-Irradiated Poly(vinylidene fluoride-trifluoroethylene) Copolymer. *Science* **1998**, *280* (5372), 2101-2104.
3. Adhikari, J. M.; Gadinski, M. R.; Li, Q.; Sun, K. G.; Reyes-Martinez, M. A.; Iagodkine, E.; Briseno, A. L.; Jackson, T. N.; Wang, Q.; Gomez, E. D., Controlling Chain Conformations of High-k Fluoropolymer Dielectrics to Enhance Charge Mobilities in Rubrene Single-Crystal Field-Effect Transistors. *Advanced Materials* **2016**, *28* (45), 10095-10102.
4. Chu, B.; Zhou, X.; Ren, K.; Neese, B.; Lin, M.; Wang, Q.; Bauer, F.; Zhang, Q. M., A Dielectric Polymer with High Electric Energy Density and Fast Discharge Speed. *Science* **2006**, *313* (5785), 334-336.
5. Gadinski, M. R.; Li, Q.; Zhang, G.; Zhang, X.; Wang, Q., Understanding of Relaxor Ferroelectric Behavior of Poly(vinylidene fluoride-trifluoroethylene-chlorotrifluoroethylene) Terpolymers. *Macromolecules* **2015**, *48* (8), 2731-2739.
6. Yin, X.; Liu, Q.; Galineau, J.; Cottinet, P.-J.; Guyomar, D.; Capsal, J.-F., Enhanced electromechanical performances in plasticizer modified electrostrictive polymers. *European Polymer Journal* **2016**, *76*, 88-98.
7. Della Schiava, N.; Le, M.-Q.; Galineau, J.; Domingues Dos Santos, F.; Cottinet, P.-J.; Capsal, J.-F., Influence of Plasticizers on the Electromechanical Behavior of a P(VDF-TrFE-CTFE) Terpolymer: Toward a High Performance of Electrostrictive Blends. *Journal of Polymer Science Part B: Polymer Physics* **2017**, *55* (4), 355-369.

Chapter 6

Conclusions and Perspectives

Chapter 6: Conclusions and Perspectives

6.1) Conclusions

This thesis was devoted to the development of chemical methods enabling the modification of Fluorinated Electroactive Polymers (FEPs) for photolithographic patterning applications. Our first approach, described in **Chapter 2**, was to introduce azido groups on the relaxor-ferroelectric P(VDF-TrFE-CTFE) terpolymer backbone. That was achieved thanks to the presence of chlorine groups (CTFE subunits) acting as good leaving groups in a nucleophilic substitution pathway (S_N2 reaction) with sodium azide. The presence of azido groups renders the terpolymers cross-linkable upon irradiation with UV light that could then be directly patterned as negative photoresists in a conventional photolithography process. Photo-patterned films of excellent quality were obtained through this method at low UV dose (2 J/cm^2).

In **Chapter 3**, a more general methodology for the introduction of different functional groups on fluoropolymers was presented. Indeed the Williamson ether synthesis route was efficiently used to bring various functionalities via hydroxy-functional photoactive molecules (*e.g.* benzophenone (BP) and anthraquinone (AQ)). More importantly this route doesn't involve necessarily the presence of chlorine atoms and can be applied to copolymers as well. Thus, hydroxy derivatives of benzophenone and anthraquinone photoinitiators were successfully grafted on different kinds of FEPs, including the relaxor-ferroelectric P(VDF-TrFE-CTFE) and P(VDF-TrFE-CFE) terpolymers along with the ferroelectric P(VDF-TrFE) copolymer. The BP and AQ functionalized materials facilitated crosslinking upon UV irradiation. However, it is noteworthy that such chemical modification led to double bond subunits along the polymers backbone via dehydrochlorination or dehydrofluorination. The effect of such unsaturation on the polymer materials was studied in more detail in **Chapter 4**. In fact, in this case only double bonds were purposely introduced after treatment of the different FEPs with a weak base, *i.e.* triethylamine.

Finally, **Chapter 5** was devoted to electric characterizations of all materials developed in **Chapters 2 to 4**. First, the azide modified P(VDF-TrFE-CTFE) (**Chapter 2**) showed a high dielectric constant of about 21 (at 20°C and 1 kHz) which makes those polymers the highest k photo-patternable polymers obtained to date.

Nevertheless, dielectric properties of the azide modified polymers were slightly reduced when compared to the pristine P(VDF-TrFE-CTFE) terpolymers, whose dielectric constant is 34 under same conditions. The P(VDF-TrFE-CTFE) terpolymers grafted both with BP and AQ groups, which are discussed in **Chapter 3**, showed very different behavior when it came to their electronic properties. When the terpolymers were grafted with low amounts of the photoinitiator (either BP or AQ), their dielectric constant increase. The latter could be attributed to a slight increase in total polymer crystallinity, as characterized by WAXS, as well as an improvement in lamellae organization as characterized by SAXS. Nevertheless, an upper content limit was observed where the properties started diminishing. When the same photoinitiator groups were grafted on the P(VDF-TrFE) copolymer, the effect on the electroactive properties was universally negative. Nevertheless, the polymers maintained their ferroelectric character even after being solvent developed. Last, electronic properties of FEPs (*e.g.* P(VDF-TrFE-CTFE) and P(VDF-TrFE-CFE)) bearing only double bonds on their backbone (**Chapter 4**) were discussed. In both cases, the presence of unsaturation (depending on the content) has positive impact on properties such as displacement and dielectric constant.

6.2) Perspectives

The materials developed in this work can tackle a very broad range of applications. For instance, the best performing materials, in terms of displacement and dielectric constant, were integrated in electronic devices, where improved performance was observed.

As an extension to the chemical modification via the Williamson reaction pathway, we believe that it is not limited to FEPS neither to photoactive pendant molecules such as AQ or BP. For instance, in the same manner PEO side chains have been integrated on FEPs backbone giving rise to very interesting materials for polymer electrolyte solid state batteries. Other pendant moieties were also investigated with good promise in the field of conductive materials (*e.g.* FEP/PEDOT hybrid materials).

Patents

- 1) Crosslinkable electroactive fluorinated polymers (WO2019/016454 A1)
- 2) Manufacturing films by crosslinking electroactive fluoropolymers (WO2019/016453 A1)
- 3) Composition for a electroactive ink for inkjet printing (WO 2018/215341 A1)

Publications

- 1) Thuau, D.; Kallitsis, K.; Dos Santos, F. D.; Hadziioannou, G., All inkjet-printed piezoelectric electronic devices: energy generators, sensors and actuators. *Journal of Materials Chemistry C* **2017**, 5 (38), 9963-9966.
- 2) Kallitsis, K.; Thuau, D.; Soulestin, T.; Brochon, C.; Cloutet, E.; Dos Santos, F. D.; Hadziioannou, G., Photopatternable High-k Fluoropolymer Dielectrics bearing pendent Azido groups. *Macromolecules* **2019**, 52 (15), 5769-5776